

156

AFWAL-TR-80-2037

(2) **LEVEL** DT 4046 3

ADA 087427

CAPACITORS FOR AIRCRAFT HIGH POWER

DR. ROBERT D. PARKER

TECHNOLOGY SUPPORT DIVISION

ELECTRO-OPTICAL AND DATA SYSTEMS GROUP

AEROSPACE GROUPS

HUGHES AIRCRAFT COMPANY

CULVER CITY, CALIFORNIA 90230

APRIL 1980

TECHNICAL REPORT AFWAL-TR-80-2037

Final Report for Period May 1975 — October 1979

Approved for public release; distribution unlimited.

DDC FILE COPY

AERO PROPULSION LABORATORY
AIR FORCE WRIGHT AERONAUTICAL LABORATORY
AIR FORCE SYSTEMS COMMAND
WRIGHT-PATTERSON AIR FORCE BASE, OHIO 45433

DTIC
ELECTE
S AUG 4 1980
A

80 8 1 093

NOTICE

When Government drawings, specifications, or other data are used for any purpose other than in connection with a definitely related Government procurement operation, the United States Government thereby incurs no responsibility nor any obligation whatsoever; and the fact that the Government may have formulated, furnished, or in any way supplied the said drawings, specifications, or other data, is not to be regarded by implication or otherwise as in any manner licensing the holder or any other person or corporation, or conveying any rights or permission to manufacture, use, or sell any patented invention that may be related thereto.

This report has been reviewed by the Office of Public Affairs (ASD/PA) and is releasable to the National Technical Information Service (NTIS). At NTIS, it will be available to the general public, including foreign nations.

This technical report has been reviewed and is approved for publication.

Michael P. Dougherty

Project Engineer

B.L. McFadden

B.L. MCFADDEN
Acting Chief, Power Systems Branch
Aerospace Power Division

FOR THE COMMANDER

Robert R. Barthelemy

ROBERT R. BARTHELEMY
Acting Chief, Aerospace Power Division
Aero Propulsion Laboratory

If your address has changed, or if you wish to be removed from our mailing list, or if the addressee is no longer employed by your organization please notify AFWAL/POOS-2, W-PAFB, OH 45433 to help us maintain a current mailing list.

Copies of this report should not be returned unless return is required by security considerations, contractual obligations, or notice on a specific document.

SECURITY CLASSIFICATION OF THIS PAGE (When Data Entered)

19 REPORT DOCUMENTATION PAGE		READ INSTRUCTIONS BEFORE COMPLETING FORM	
1. REPORT NUMBER AFWAL TR-80-2037	2. GOVT ACCESSION NO.	3. RECIPIENT'S CATALOG NUMBER	
4. TITLE (and Subtitle) Capacitors For Aircraft High Power	5. TYPE OF REPORT & PERIOD COVERED Technical Final <i>rept.</i> May 1975 - Oct 1979		
6. AUTHOR(s) Dr Robert D. Parker	7. CONTRACT OR GRANT NUMBER(s) F33615-75-C-2021		
8. PERFORMING ORGANIZATION NAME AND ADDRESS Hughes Aircraft Company Culver City, CA 90230	9. PROGRAM ELEMENT, PROJECT, TASK AREA & WORK UNIT NUMBERS 3145 32-17		
10. CONTROLLING OFFICE NAME AND ADDRESS Aero Propulsion Laboratory AF Wright Aeronautical Laboratories (AFSC) Wright-Patterson AFB OH 45433	11. REPORT DATE Apr 1980		
12. MONITORING AGENCY NAME & ADDRESS (if different from Controlling Office)	13. NUMBER OF PAGES 248		
	14. SECURITY CLASS. (of this report) Unclassified		
15. DECLASSIFICATION/DOWNGRADING SCHEDULE			
16. DISTRIBUTION STATEMENT (of this Report) Approved for public release; distribution unlimited.			
17. DISTRIBUTION STATEMENT (of the abstract entered in Block 20, if different from Report)			
18. SUPPLEMENTARY NOTES			
19. KEY WORDS (Continue on reverse side if necessary and identify by block number) Capacitors Pulse Discharge Pulse Forming Networks Pulsed Capacitors Energy Storage Dielectric Systems Pulse Power			
20. ABSTRACT (Continue on reverse side if necessary and identify by block number) This report describes an experimental exploratory development program conducted by Hughes Aircraft Company to develop reliable light weight pulse discharge capacitors for airborne application. The specific duty was a 1 minute burst every 2 hours, and both low (50pps) and high (300pps) repetition rate service was to be considered. The energy density goals were 400 to 1100 J/kg with a 20 μ s capacitor current pulse width. A five layer polysulfone/kraft paper dielectric was selected for high			

DD FORM 1 JAN 73 1473 EDITION OF 1 NOV 65 IS OBSOLETE

SECURITY CLASSIFICATION OF THIS PAGE (When Data Entered)

411286

mt

pulse forming network

rate service, while polyvinylidene fluoride/kraft paper was chosen for the low rate service. Both mineral oil and dioctylphthalate fluids were used. Tension-controlled winding was used to eliminate failure-producing wrinkles and folds. Reduced temperature drying further reduced wrinkles. Special filtration, purification, and cleaning produced very high resistivity fluids free from particles. A highly-instrumented test bay accurately simulated a PFN environment and allowed detailed and accurate testing. The best single section high rate results were 550 J/kg at $10^5 - 10^6$ shot life at double the specified duty, while the best low rate results were slightly higher. Case weight minimization was studied, and three prototype lightweight cases were built. Several techniques for smoothing rough capacitor foils were examined, and a flame technique was selected as being most easily implemented. Problems of terminating extended foils were examined, and a flame-spray method selected as most practical.

Three types of complete capacitors were built, all for high rate service. The first two were both 2.2 μ F 15 kV, and showed package energy densities of 46 J/kg and 169 J/kg. The third unit was rated 1.1 μ F at 30 kV, and employed the same construction as the 169 J/kg unit. Two different PFNs were assembled and tested, one a 6 section 15 kV 20 μ S type E, and the other a 4 section 30 kV 10 μ S type E.

Accession For	
NTIS GAAI	<input checked="" type="checkbox"/>
DDC TAB	<input type="checkbox"/>
Unannounced	<input type="checkbox"/>
Justification	
By	
Distribution/	
Availability Codes	
Dist	Avail and/or special
A	

FOREWORD

This is the final report of a pulse capacitor development program supported by the Aero Propulsion Laboratory at Wright-Patterson Air Force Base, Ohio, under contract F33615-75-C-2021, Project 3145, Task 32, Work Unit 17. The program was monitored by Mr. Michael P. Dougherty of the Power Systems Branch. The Program Manager at Hughes was Dr. Robert D. Parker.

The majority of the work described herein was conducted by the Hughes Aircraft Company at its Culver City, California facility. The flame spraying and electron beam welding discussed in Section 13 were performed by shops in the Culver City area. The final pulse testing described in Sections 10 and 16 was carried out at the High Power Laboratory of the Rome Air Development Center, Griffiss Air Force Base, New York.

Robert D. Gourlay designed the pulse test instrumentation, including the load and the waveshape control, and conducted some of the pulse tests. Clarence Stroope, Watson Kilbourne, and Don McWilliams assisted Mr. Gourlay. Ronald V. DeLong designed and fabricated much of the corona test instrumentation, as well as the automatic sequencer for the pulse test equipment. Ernest R. Haberland, assisted by Mr. Kilbourne, was responsible for the winder design. Mr. Haberland, assisted by Harry Ashe, designed and fabricated the final pulse test power supply. Robert S. Buritz and Edward G. Wong fabricated capacitors and consulted on capacitor design. Mr. Buritz, Mr. Kilbourne, James H. Holley, and H. Haydostian developed lightweight capacitor cases. Ronald L. Williams developed extended foil terminations and assisted in the foil edge work. Thermal analyses were performed by Peter F. Taylor and Herbert Rifkin. Donald C. Smith designed the oil filtration and filling system, and consulted on contamination control. Richard Holbrook and Norman Bilow consulted on material properties

and chemical compatibility. James J. Erickson performed many of the failure analyses and operated the scanning electron microscope.

Many helpful suggestions were provided by Ed Bullwinkel and Richard Taylor of the Schweitzer Division of Kimberly-Clark. The advice and consultation of James O'Loughlin of the Air Force Weapons Laboratory and Richard J. Verga of the Aero Propulsion Laboratory were very valuable. Mr. Bobby Gray of the Air Force High Power Laboratory at the Rome Air Development Center furnished the facilities and assistance for the full PFN tests, as well as many helpful comments.

TABLE OF CONTENTS

1.0	INTRODUCTION	1
2.0	DIELECTRIC MATERIALS SELECTION	5
2.1	Introduction	5
2.2	Dielectric Films	6
2.3	Foils	14
2.4	Dielectric Papers and Fluids	15
2.4.1	Dielectric Papers	16
2.4.2	Dielectric Fluids	22
2.4.3	Paper-Fluid Combinations	36
2.5	Conclusion	50
2.5.1	Films	50
2.5.2	Paper-Oil Combinations	50
2.5.3	Foil	51
3.0	PAD DESIGN	53
3.1	Energy Density	53
3.2	Layer Design Concepts	55
3.3	Field Balance	56
3.4	Materials	57
3.5	Layer Designs	57
4.0	WRINKLE-FREE PADS	59
4.1	Winding Wrinkle-Free Pads	59
4.2	Drying Capacitor Pads	67
4.3	Capacitor Impregnation	68
4.4	Pad Test Configuration	71
4.5	Pad Test Circuits	72
4.5.1	Analysis	72
4.5.2	Pulse Test Apparatus	73

CONTENTS (Continued)

4.6	Corona Test Activity	77
4.7	Pulse Test Results	81
4.7.1	Summary	81
4.7.2	Introduction	82
4.7.3	Test Data	83
4.7.4	Failure Mechanisms	89
5.0	CAPACITOR DESIGNS	95
5.1	Part Number 014	95
5.1.1	Layer Design and Number of Pads	95
5.1.2	Packaging Design	97
5.1.3	Design Weight Summary	101
5.2	Part Number 026	101
5.2.1	Layer Design and Number of Pads	101
5.2.2	Packaging Design	102
5.2.3	Design Weight Summary	102
6.0	CAPACITOR FABRICATION AND TEST	105
6.1	Capacitor Fabrication	105
6.1.1	Winding and Termination	105
6.1.2	Drying and Impregnation	108
6.1.3	Acceptance Data	110
6.2	Capacitor Test	110
6.2.1	Test Stand Modifications	112
6.2.2	Test Results	112
6.2.3	Failures and Failure Analysis	115
6.2.4	Connector Tests	120
7.0	HEAT SINK/COOLING TRADE-OFF INVESTIGATION	121
7.1	Summary	121
7.2	Introduction	122
7.3	Results	127
7.4	Conclusions	133
7.5	Experimental	134
8.0	PFN OPERATING ENVIRONMENT	137
8.1	PFN Design	137
8.2	Computer Modelling	139
8.3	Design of Test Apparatus	141

CONTENTS (Continued)

9.0	RELIABILITY AND MAINTAINABILITY ANALYSIS	143
10.0	PULSE FORMING NETWORK	145
10.1	PFN Construction	145
10.1.1	Capacitor Inductance	145
10.1.2	Design Considerations	146
10.1.3	Coil Construction	147
10.2	PFN Checkout	147
10.3	PFN Test	147
10.3.1	Set-up	147
10.3.2	Tests and Results	149
11.0	FOIL EDGE INVESTIGATION	153
11.1	Foil Edge Treatment	153
11.1.1	Processing Limitation	156
11.1.2	Process Evaluation	156
11.1.3	Corona Testing	160
11.1.4	Conclusions	160
11.2	Capacitor Weight Minimization	161
12.0	CASE WEIGHT MINIMIZATION	165
12.1	Metal Cases	165
12.2	Plastic Cases	169
12.2.1	Summary	169
12.2.2	Fabrication Procedure	169
12.2.3	Testing	170
12.2.4	Results and Discussion	170
13.0	EXTENDED FOIL TERMINATION	173
13.1	Selection of Techniques	173
13.2	Contact Resistance Tests	174
13.3	Capacitor Pulse Tests	175
13.4	Conclusions	180
14.0	CAPACITOR DESIGN	183
14.1	Layer Design and Number of Pads	183

CONTENTS (Continued)

15.0	PFN DESIGN AND FABRICATION	187
15.1	Capacitor Fabrication	187
15.2	PFN Coil Design	187
15.3	Enclosure	187
16.0	PFN TEST	193
16.1	Capacitor Hi-Pot and Conditioning	193
16.2	PFN Test	195
17.0	CONCLUSIONS	197
APPENDIX A	STATEMENT OF WORK CAPACITORS FOR AIRCRAFT HIGH POWER	199
APPENDIX B	WINDER DRAWINGS	211
APPENDIX C	OPERATING INSTRUCTIONS OIL IMPREGNATION SYSTEM	243

LIST OF ILLUSTRATIONS

Figure		Page
1	Dissipation Factor Versus Temperature of Various Films at 10^5 Cycles	8
2	Typical Test Device Used in Paper and Paper-Fluid Evaluations	18
3	Test Samples Used in PCB-Al Foil Reaction Tests	27
4	Test Sample Used in Paper-Fluid Electrical Properties Determinations	37
5	Split Mandrel	60
6	Typical Friction Brake	61
7	Capacitor Winder Friction Brake Tension Characteristics .	62
8	Single Web Servo Control	63
9	Revised Winder Web Paths	64
10	Rear of Modified Winder	65
11	Operator Position-Modified Winder	66
12(a)	Wound-Flat Stack	69
12(b)	Wrinkled Dielectric Stack	69
12(c)	Special Drying	69
13	Fluid Process Cycle	70
14	Test Pad Assembly and Can	71
15	Test Pad Detail	72
16	PFN Capacitor Current Waveform	74
17	Discharge Current Waveform	75
18	Pulse Tester Simplified Circuit	76
19	High Power Load Components	76

LIST OF ILLUSTRATIONS (Continued)

Figure		Page
20	High Voltage Section of Pulse Test	77
21	Pulse Test Load and Contactors	78
22	Pulse Test Controls	78
23	Corona Test Circuit	79
24	Corona Test Resonator	80
25	Biased Corona Test Waveform	80
26	Corona Test System	81
27	Glass-Encased Capacitor for Observing Section Motion ...	83
28	Top of Reusable Can Showing Thermocouple Lead Wires for External Temperature Measurement	87
29	Tab Breakdown Mechanism	90
30(a)	Polysulfone Edge Damage	92
30(b)	Polysulfone Edge Damage	93
31	Corona Damage Edge of Foil	94
32	Internal Schematic, P/N 014	97
33	Case for P/N 014	98
34	Packaging Design, P/N 014	100
35	Case for P/N 026 (Lightweight Stainless)	103
36	Constant Tension Winder	106
37	Packaging of 026 Unit	108
38	Pulse Capacitors 014 (Left) and 026 (Right), 2.2 μ F 15 kV	110
39	Capacitor Pulser Block Diagram	113
40	Twin 1.1 μ F Capacitor for Pulser Check-Out	114
41	Edge Failure in 026 Unit, S/N 2	117
42	Discoloration of Dielectric Near Tab, 026 Unit S/N 2 ...	117
43	Cross Section of Tab-Termination	118
44	Holes in Aluminum Foil, 026 Unit S/N 2	119
45	Connector Pulse Test Capacitor	120

LIST OF ILLUSTRATIONS (Continued)

Figure		Page
46	Polysulfone Capacitor - Schematic and Model	124
47	Kapton Capacitor - Schematic and Model	125
48	Capacitor Study (Both Runs, 1 Minute On 1 Hour Off)	130
49	Capacitor Study (1 Minute On - 1 Hour Off)	131
50	Capacitor Study (1 Minute On - 2 Hours Off)	132
51	Capacitor Study (1 Minute On - 1 Hour Off)	132
52	Capacitor Study (Last Four Hours)	133
53	Capacitor Study (1 Minute On - 2 Hours Off)	134
54	Capacitor Study (1 Minute On, 2 Hours Off With and Without Beryllium Oxide Top and Bottom Plates)	135
55	Type E PFN Schematic	137
56	Typical Type E PFN Application	138
57	Schematic of Current and Voltage, PFN Capacitor	138
58	ESR and Harmonic Discharge Current	140
59	20 μ S Capacitor Current Waveform	142
60	Capacitor Inductance Measuring Arrangement	146
61	PFN Coil Construction	148
62	Diagram of Test Setup	149
63	Untreated 1/4 Mil Foil	154
64	Treated Foil Edge	155
65	Foil Edge Corona Test Fixture	155
66	Laser Cut Foil Edge	158
67	Spark Erosion Treated Foil Edge	159
68	Field Enhancement Factor f Vs Thickness Ratio, For Cylindrical Foil Edges	162
69	Quality Parameter For Foil Edge Effect	164
70	Case for P/N 026 (lightweight stainless)	166
71	Capacitor P/N 026 Utilizing Very Lightweight Stainless Steel Case	167
72	Case for P/N 036 (Lightweight Stainless)	168
73	Lightweight Plastic Case With 014-Type Capacitor Inside	171

LIST OF ILLUSTRATIONS (Continued)

Figure		Page
74	Termination Test Device, Cross Section	174
75	Typical Terminations	176
76	Termination Microsections	178
77	EB Weld, Torn Loose	179
78	Babbitt Termination	179
79	Electron Beam Cut in Dielectric	182
80	Internal Packaging, P/N 036	188
81	Capacitor P/N 036, 1.1 μ F 30kV	189
82	PFN Coil Schematic	190
83	PFN Enclosure	191
84	Capacitor With Case Rupture	194
85	Drive Disc-Capacitor Winder	211
86	Controller - Capacitor Winder	212
87	Mounting Bracket - Torquer Brake, Capacitor Winder . .	214
88	Cabinet Assembly - Capacitor Winder	215
89	Roller Assembly	217
90	Torque Spring	218
91	Dial Clamp	219
92	Adapter	220
93	Shaft	221
94	Bearing Shaft	222
95	Bolt	223
96	Spacer	224
97	Mounting Plate	225
98	Plate	226
99	Spring Drum	227
100	Spindle	228
101	Support Shaft	229
102	Drive Shaft	230
103	Drive Bushing	231
104	Spindle Drive Assembly	232

LIST OF ILLUSTRATIONS (Continued)

Figure		Page
105	Adjusting Wheel	233
106	Spacer	234
107	Mounting Plate	235
108	Plate	236
109	Tensioning Device, Capacitor Winder Electronic CKT . .	237
110	Flat Mandrel Drive	238
111	Stirup	239
112	Wedge	240
113	Torque Motor Drive Spindle Assembly	241
114	Tension Arm Assembly	242
115	Schematic Oil Impregnation System	248

LIST OF TABLES

Table		Page
1	Dielectric Properties of Candidate Films	10
2	Dissipation Factors as a Function of Frequency for Four Candidate Films at 25° and 150°C	11
3	Dielectric Constants as a Function of Frequency for Four Candidate Films at 25° and 150°C	11
4	Physical Properties of Candidate Capacitor Films	12
5	Maximum Energy Storage Densities of Dielectric Films . .	13
6	Chemical Compatibilities of Candidate Dielectric Films and Fluids	13
7	Properties of Candidate Capacitor Foils	15
8	Effects of Methanol Extraction on the Capacitance and Dissipation of Capacitor Papers	20
9	Capacitance and Dissipation Factor as a Function of Frequency for Candidate Papers - Measured at 23°C . . .	21
10	Properties of Candidate Fluids	24
11	Aluminum Foil - PCB (Inerteen 100-42) Compatibility Test Results	28
12	A Comparison of Column Length on the Purification of DOP (Purified Grade) With Al ₂ O ₃	31
13	Effects of Multiple Passes Through an Al ₂ O ₃ Column of the Purity of DOP (Eastman)	32
14	Purification of Plasticizer Grade DOP Using Al ₂ O ₃	33
15	Electrical Properties of Candidate Fluids at 23°C	34
16	Electrical Measurements of DOP Impregnated Papers at 23°C	39
17	Electrical Measurements of DOP Impregnated Papers Measured at 150°C	40

LIST OF TABLES (Continued)

Table		Page
18	Electrical Measurements of Mineral Oil Impregnated Papers Measured at 23°C	41
19	Electrical Measurements of Mineral Oil Impregnated Papers Measured at 150°C	42
20	Electrical Measurements of PCB Impregnated Papers Measured at 23°C	43
21	Electrical Measurements of PCB Impregnated Papers Measured at 150°C	44
22	Electrical Measurement of Silicone Oil Impregnated Papers Measured at 23°C	45
23	Electrical Measurements of Silicone Oil Impregnated Papers Measured at 150°C	46
24	Effects of 168 Hours, 150°C Exposure on the Electrical Properties of Paper-Oil Combinations	49
25	Typical Energy Density	55
26	Layer Designs	58
27	Pulse Test Summary	58
28	Capacitor Current Spectrum	73
29	Initial Tests	84
30	High Density Layer Designs	86
31	High Energy Density Tests	88
32	Energy Density	90
33	High Rate Layer Design Energy Densities at 5 kV	96
34	Calculated Fields for P/N 014	97
35	Weight of Capacitor Parts, P/N 014	101
36	Field Balance for P/N 014 and 026	102
37	Weight of Capacitor Parts, P/N 026	102
38	Winding Data, 014 and 026	107
39	Final Measurements, Part Number 014	111
40	Acceptance Data, Part Number 026	111
41	Analysis of Acceptance Test Data	112
42	Pulse Test Summary, Part Number 014	115
43	Pulse Test Summary, Part Number 026	116

LIST OF TABLES (Continued)

Table		Page
44	Capacitor Configuration, Nodes, and Connectors	123
45	Physical Constants	126
46	Capacitor Hotspot Temperatures - First 16 Cases	128
47	Temperature Rises for Modified Nodal Models	129
48	Capacitor Current Spectrum	139
49	Capacitor Current Spectrum, 20 μ S PFN Output.	140
50	Failure Rate Data.	143
51	Capacitor Inductance Data	146
52	012 PFN Testing Summary.	150
53	PFN Data with 1 026 Capacitor	151
54	C ₆ Case Temperature Data	151
55	Corona Inception Voltage, Foil Edges	160
56	Plastic Case Distension Measurement	172
57	Extended Foil Contact Resistance Tests	177
58	Pulse Test of Terminations	181
59	Field Balance Comparisons	184
60	Trade-Off Weight Penalties	184
61	Winding Data P/N 036	185
62	P/N 036 Acceptance Data.	190
63	PFN Coil Parameters	190
64	Final Data, P/N 036	196

1.0 INTRODUCTION

Present design concepts for a variety of space and airborne systems depend upon the emission of electromagnetic energy in intermittent trains of short pulses. One of the most feasible methods for storing power supply energy over relatively long periods and transferring it to the tube or other active element over relatively short periods is the pulse-forming network, which is composed of capacitors and inductors. Unfortunately, the size and weight of the capacitors so employed make the design of an appropriately mobile energy delivery system extremely difficult.

Some effort has been devoted in the past to the development of small, light-weight pulse-discharge capacitors. An energy density of 210 J/kg (95 J/lb) at 2.5 kV was achieved by Rice, using a patented metallized electrode configuration on a dielectric composed of polyethylene terephthalate coated with cellulose acetate. A pulse-service energy density of 310 J/kg (141 J/lb) at 50 kV was produced by Hoffman and Ferrante, using an unspecified paper/plastic/mineral oil dielectric tested at undisclosed discharge width and repetition rates. In an effort to develop airborne components, Hoffman was able to reach 480 J/kg (218 J/lb) at a few pulses per second, and 264 J/kg (120 J/lb) at moderate repetition rates. These capacitors, which employed a variety of common capacitor materials, were tested in an undisclosed electrical environment. In a similar program, capacitors that demonstrated 10^5 pulse life were made at 110 J/kg (50 J/lb) and 167 J/kg (76 J/lb). The lower density components were tested at repetition rates up to 250 pps in 60 second bursts, while the higher density components were run at rates up to 125 pps in 30 second bursts.

The intrinsic dielectric strengths of the films available for use in capacitors range from 3.1 MV/cm (8 kV/mil) to 5.9 MV/cm (15 kV/mil), so it appears that energy densities in the range 1100 J/kg (500 J/lb) to 3850 J/kg (1750 J/lb) ought to be possible. Since these numbers are far in excess of those reported in the literature, it is pertinent to ask the reason for the large difference.

Two problems faced in achieving higher energy densities are electrical breakdown and thermal failure. Some capacitors used for pulsed-energy storage fail because corona arising in manufacturing anomalies or materials defects eventually punctures the insulation, resulting in a shorted unit. The second failure results from dissipation of relatively large amounts of power in a poorly-cooled volume. This can take the form of thermal runaway, insulation failure because of very great local hot-spot temperatures, or excessive thermal expansion. This last failure mode is sometimes quite dramatic; the capacitor case suddenly ruptures from the internal pressure.

To develop small light pulse service capacitors, it is important to understand the failure mechanisms of wound liquid-impregnated capacitors and to design components which eliminate or control them. This was the approach adopted for this program. As many known mechanisms as possible were eliminated in the initial designs. Then, each design was tested to failure and analyzed to determine the failure mechanisms. The next design was made in such a way as to eliminate the newly discovered problem.

This report presents a section on each of the fifteen program tasks. These tasks were:

- Dielectric System Selection
- Pad (Section) Design
- Wrinkle Free Capacitor Pads
- Capacitor Designs
- Capacitor Fabrication and Test
- Heat Sink/Cooling Trade-off Investigation
- PFN Operating Environment
- Reliability and Maintainability
- Pulse Forming Networks

- Foil Edge Investigation
- Case Weight Minimization
- Extended Foil Termination
- Capacitor Design
- PFN Design and Fabrication
- PFN Test

All but the last four of these tasks were concerned with the development of a capacitor technology for the following service regime:

Current pulse width, per capacitor:	20 μ S
Pulse repetition rate:	: 300/s
Capacitance	: 2.2 μ F
Pulse voltage	: 15 kV

The last four tasks were concerned with the design of capacitors and a PFN to the following specifications:

PFN pulse width	: 10 μ S
Pulse repetition rate	: 90 to 150/s
Stored energy	: 2 kJ
Number of sections	: 4
Network type	: E (modified)
Pulse Voltage	: 30 kV

Knowledgeable readers will recognize that there is a great difference between the specifications for the last four tasks and those for the rest of the program.

A complete statement of work for the entire program is found in Appendix A.

2.0 DIELECTRIC MATERIALS SELECTION

2.1 INTRODUCTION

These studies and evaluations were undertaken for the purpose of selecting the materials of construction for high energy density pulse discharge capacitors. The basic objectives here were the selection of those combinations of materials which yield the maximum energy storage per unit mass, have minimal or low electrical loss, and would be compatible with the operating environments known and anticipated for such devices. The materials evaluated included films, foils, papers and fluids.

The film and foil selections for evaluation were made on the basis of an analysis of those fundamental properties which would determine their behavior within the device. Their compatibility with the other materials of construction was established on the basis of known solubilities, chemical reactivities and previous experimental evaluations. With the exception of the aluminum-chlorinated biphenyl, no experimental work was performed on the film and foil combinations.

Unlike the films and foils, the papers and fluids investigation was largely experimental. Experimentation and testing here was deemed necessary because of several factors. First, there is not existent sufficient fundamental property information on the candidate papers and fluids, either singly or in combination. Secondly, the electrical losses in fluids, and also in certain papers, are very dependent upon the processing and purification; hence, the results reported by any investigator are of value only if the sample preparation is given. The importance of processing will be seen in this work when comparing "as-received" and "processed" material

properties. Further, the paper-fluid combination is a complex dielectric system whose properties can only be determined experimentally. Since certain of the dielectric combinations investigated here were not found in the literature, their properties needed to be determined. Finally, the property measurements of all combinations under similar conditions provides a common and controlled base from which the comparisons and final selections can be made. In addition to these factors it was desired to establish the high temperature aging characteristics of certain combinations, again requiring experimental determinations.

The following sections summarize the material selection for each material type and the results of the paper-fluid aging evaluation. The final section provides recommendations for various material combinations including the energy storage density and electrical loss characteristics.

2.2 DIELECTRIC FILMS

As stated previously, the primary objective of this program was to develop a high energy density capacitor capable of operating at high PRF and severe duty cycles. In this regard, the dielectric film will play a major role. The achievement of the goals will be primarily determined by the properties of the dielectric films used.

The significant properties of a film which will determine its behavior in the device include:

- Critical field strength
- Dielectric constant
- Density
- Dielectric loss
- Temperature limits
- Chemical reactivity

The first three properties establish the energy storage density (D_E), as given by the relationship

$$D_E = \frac{1}{2} \frac{\epsilon' E^2}{\rho_m}$$

where ϵ' is the complex permittivity, E is the critical field strength, and ρ_m is the density. From this relationship it is obvious that the maximum energy storage density is achieved by materials having high dielectric constants (permittivities), large critical field strengths and low densities. With these as the only requirements the solution to the problem would be relatively simple -- tabulate the film properties, calculate the energy storage density, and the film having the highest value is the preferred material.

The problem of selection becomes more complicated when the final three properties are introduced. Consider the electrical loss, represented by the dissipation factor, shown in Figure 1 for several materials. Loss is important in two aspects. It appears as heat which, if not dissipated, results in temperature increases which, if unchecked, will result in catastrophic failure. Even when controlled, temperature increases generally lower the energy storage capacity. This results because increased temperatures produce lower dielectric constants (in almost all cases), and lower critical field strengths. With respect to energy density, the lower the operating temperature, the higher is the density. Losses, if appreciable, could require active cooling within the device or pose limitations on PRF and/or duty cycle. Active cooling might actually reduce the energy storage density since such additions do not contribute to energy storage, but do increase the weight.

The second area of concern for electric loss is the overall efficiency of the system. The energy requirements for the device, including the losses, must be supplied by an external source. As the losses increase, there is a corresponding increase on the external power requirements, resulting in lower overall efficiency.

For the films the electrical loss at 300 Hz and 50 kHz was included with the energy density in making the final selection. In the absence of a clear relationship between the energy density and loss, selection was, in part, a matter of judgment.

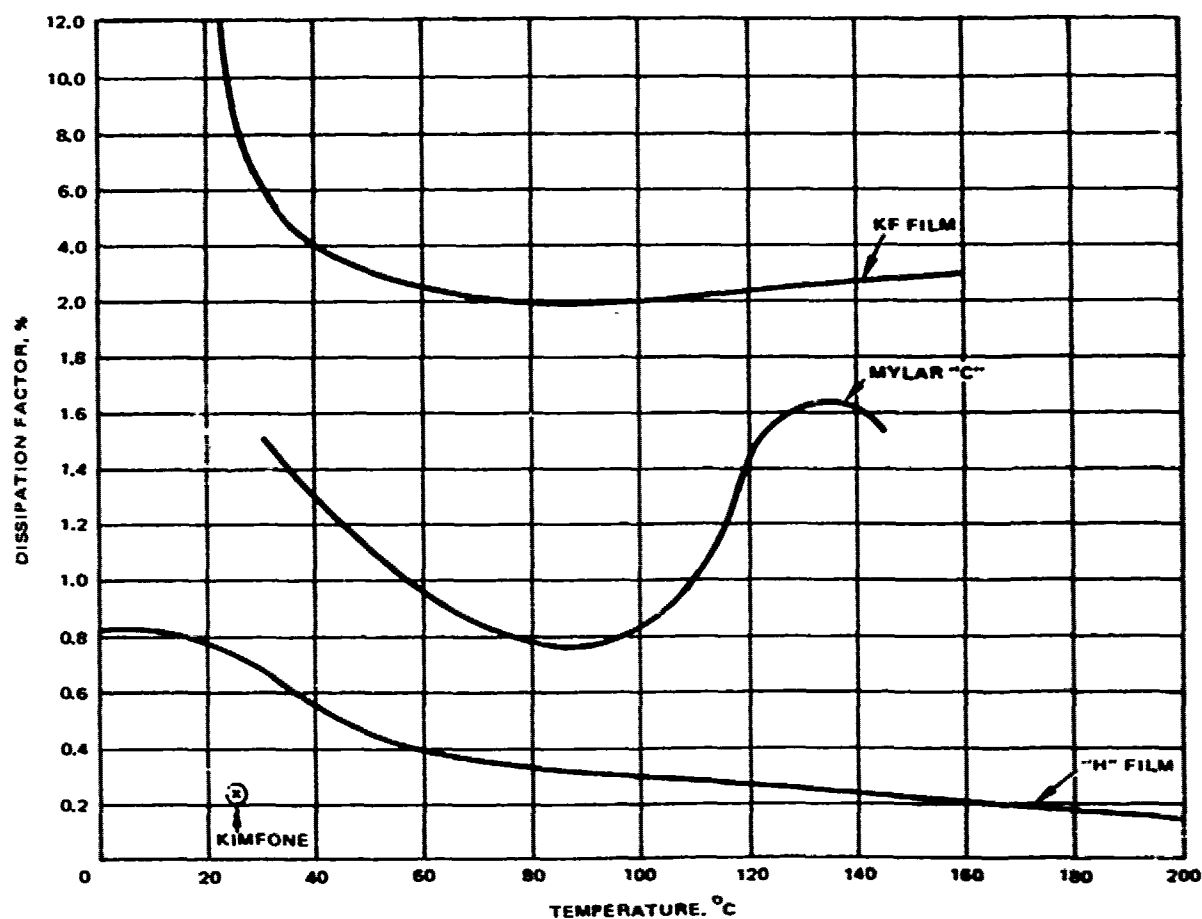


Figure 1. Dissipation factor versus temperature of various films at 10^5 cycles.

Chemical reactivity and temperature limits are also criteria used in the selection processes. The upper temperature limit for films in this selection was placed at 150°C. To be a final candidate, the film must (a) be capable of operating at this temperature while maintaining its designed energy storage, (b) not experience excessive electrical loss and (c) be compatible with the other materials of constructions. Compatibility here refers to the absence of chemical reactions which could adversely affect the operating characteristics of the device.

Seven candidate films were compared applying these general requirements. These were:

- Polycarbonate
- Poly(ethylene terephthalate)
- Polyimide
- Polypropylene
- Polysulfone
- Polyvinylfluoride
- Polyvinylidene fluoride

The properties of these materials used in these evaluations are presented in Tables 1 through 4.

Based on properties of these seven films and the requirements of the capacitors to be constructed from them, three of the films were selected as candidates for device fabrication — (1) polyvinylidene fluoride, (2) polyimide, and (3) polysulfone.

When compared in terms of energy storage density the polyimide and the polysulfone rank the highest having potential energy storage densities of 1.08 and 0.96 joules/gram. The energy storage capacity for each of the candidates is given in Table 5. It should be noted that these values are maximum values based on energy storage at the critical field strength of films, at nominal thicknesses of 0.5 to 1 mil.

In terms of electrical loss at high frequency, the polyvinylidene fluoride exhibits a larger change with temperature than any of the other films. At 10^5 Hz, the room temperature dissipation factor is 12%, but this value falls to about 2% at 80°C. Properly exploited in design, this property can be

TABLE 1. DIELECTRIC PROPERTIES OF CANDIDATE FILMS

Dielectric Film	Electrical							
	Dielectric Constant			Dissipation Factor			Volume Resistivity (ohm-cm)	Electrical Breakdown Strength (volts RMS/mil)
	1 MHz			1 MHz				
	1 kHz	100 kHz	1 MHz	1 kHz	100 kHz	1 MHz		
Polyvinylidene fluoride (Kure: a KF)	10.7	9.5	7.5	0.015	0.1	0.16	1.5×10^{15}	4500 at 1/2 mil
Polyimide (Kapton H)	3.7	3.5	3.5	0.002	0.008	0.010	1×10^{18}	7800 at 1 mil
Polysulfone (Kimfone)	3.1	3.0	3.0	0.001	0.002	0.003	5×10^{16}	7500 at 1 mil
Polyester (Mylar C)	3.3	3.2	3.0	0.005	0.016	0.016	1×10^{18}	10,500 at 1/2 mil 7,500 at 1 mil
Polycarbonate (Kimfol)	2.8	2.7	2.7	0.0008	0.002	0.003	2×10^{17}	7000 at 1 mil
Polytetra-fluoroethylene Teflon TFE	2.1	2.1	2.1	<0.0002	<0.0002	<0.0002	1×10^{19}	2000 at 1 mil
Polypropylene	2.2	2.2	2.2	<0.0005	<0.0005	<0.0005	1×10^{17}	4000 at 1 mil

TABLE 2. DISSIPATION FACTORS AS A FUNCTION OF
FREQUENCY FOR FOUR CANDIDATE FILMS
AT 25° AND 150°C

Film	Dissipation Factor					
	25°C			150°C		
	100 Hz	1000 Hz	100 kHz	100 Hz	1000 Hz	100 kHz
Polyvinylidene fluoride	0.01	0.01	0.1	>0.2*	0.1*	0.03
Polyimide	0.0025	0.003	0.008	0.002	0.0015	0.002
Polysulfone	0.0008	0.001	0.0025	0.002	NA	NA
Polyester	0.003	0.006	0.016	0.0075	0.008	0.016
* - extrapolated values						
NA - data not available						

TABLE 3. DIELECTRIC CONSTANTS AS A FUNCTION OF
FREQUENCY FOR FOUR CANDIDATE FILMS
AT 25° AND 150°C

Film	Dielectric Constant					
	25°C			150°C		
	100 Hz	1000 Hz	100 kHz	100 Hz	1000 Hz	100 kHz
Polyvinylidene fluoride	11	10.5	9.5	12.5	11	10
Polyimide	3.5	3.5	3.5	3.0	3.0	3.0
Polysulfone	3.1	3.1	3.0	2.9	NA	NA
Polyester	3.4	3.4	3.3	NA	3.8	3.7
NA - data not available						

TABLE 4. PHYSICAL PROPERTIES OF CANDIDATE CAPACITOR FILMS

Property	Material					
	Polyvinylidene Fluoride	Kapton H-Film	Polysulfone	Mylar	Polycarbonate	Polytetrafluoroethylene TFE Teflon
T _m Melting °C	158° - 197°C	Degrades/Stable Before Melting >500°C	Degradation Temp 200°C	250° - 265°C Decomp =280°C		327°C
Crystal- linity	Depends on manufacturer	Amorphous	Depends on manufacturer	45 - 65%	Depends on manufacturer	45-
Density g cm ³	1.75 - 1.80	1.42	1.24	1.377	1.21	2.3
Crystal Morphology	2 Phases i. Planar Zig Zag ii. Trans-Gauche - Trans-Conformation	--				2-Phases trichloric hexagonal
T _g °C	-40°C	None Below 300°C	180° - 245°C (190°C)	Amorphous 70°C Cryst 81°C, Cryst & Oriented 125°C	147°C	12°C
Secondary Transitions	Apparently none	Apparently none	-100°C	γ transition =30°C	--	-97°C
Heat Capacity	0.33 cal/g°C at Room Temp	0.261	0.31 cal/g°C	0.315 cal/g°C	0.3 cal/g°C	0.23 cal/g°C
Thermal Conductivity	3.0 x 10 ⁻⁴ cal/(cm ²)(sec) (°C/cm)	3.89 x 10 ⁻⁴ cal/(cm ²)(sec) (°C/cm)	6.2 x 10 ⁻⁴ cal/(cm ²)(sec) (°C/cm)	3.4 x 10 ⁻⁴ cal/(cm ²)(sec) (°C/cm)	4.6 x 10 ⁻⁴ cal/(cm ²) (sec)(°C/cm)	6.0 x 10 ⁻⁴ cal/(cm ²)(sec) (°C/cm)
Thermal Expansion in/in °C	12 x 10 ⁻⁵ /°C	2.0 x 10 ⁻⁵ /°C	5.2-5.6 x 10 ⁻⁵ / °C	1.7 x 10 ⁻⁵ /°C at 20°-50°C	7 x 10 ⁻⁵ /°C	100
Tensile Strength	At Temp Strength 25°C 6100-8500 psi 100°C 6000 psi	Temp Strength -195°C 35,000 psi 25°C 25,000 psi 200°C 17,000 psi 300°C 14,000 psi 450°C	10,200 psi	40,000 psi at 23°C	8500 - 10,500 psi	2000 - 2500 psi

TABLE 5. MAXIMUM ENERGY STORAGE DENSITIES
OF DIELECTRIC FILMS

Film	Energy Storage Density, Maximum (joules/gm)
Polyvinylidene fluoride	0.84
Polyimide	1.08
Polysulfone	0.96

a built-in temperature limiter. The effect would prevent thermal runaway in a component where the majority of the dissipation occurred in the film.

The chemical reactivity with the other likely materials of construction does not pose any problems with the possible exception of the sulfone and the PCB fluid. This combination has not been evaluated however, based on the solubility characteristics of the sulfone in chlorinated hydrocarbons it is probable that this combination would not be compatible. The chemical compatibilities of the three films and the candidate fluids is given in Table 6. These determinations were made at 125°C.

TABLE 6. CHEMICAL COMPATIBILITIES OF CANDIDATE
DIELECTRIC FILMS AND FLUIDS

Fluid	Film		
	Polyimide	Polysulfone	Polyvinylidene Fluoride
DOP	C	C	*
Mineral Oil	C	C	C
PCB	C	*	*
Silicone Oil	C	C	C
* \equiv Not evaluated			

The three films selected exhibit the best overall combination of properties — energy storage density, electrical loss and chemical compatibility — of the seven initial candidates. Each of the others demonstrated at least one major limitation which would limit its use in this application.

2.3 FOILS

The foils in a high energy storage capacitor also play a role in the final energy storage density of the device. Four basic requirements exist for a foil:

- Low resistivity
- Low density
- Low chemical reactivity
- Capability of being electrically joined

The first two requirements, low resistivity and low density, are needed to attain high energy storage density while the latter two are necessary for performance and reliability within the device.

The requirements for a low resistivity and a low density are evident if these terms are combined to define the conductance per unit mass (k), using the following formula:

$$k = \frac{1}{\rho_e \rho_m}$$

where ρ_m is the density and ρ_e the resistivity. For the capacitor foil, the highest possible value of k is desired.

Four foils were considered for use

- Aluminum
- Copper
- Nickel
- Tin

Their properties are summarized in Table 7.

TABLE 7. PROPERTIES OF CANDIDATE CAPACITOR FOILS

Foil Metal	Volume Resistivity (ohm-cm $\times 10^{-6}$)	Density at 20°C (g/cm ³)
Al	2.8 at 20°C 3.9 at 100°C	2.70
Cu	1.8 at 20°C 3.0 at 200°C	8.89
Ni	6.8 at 20°C 10.3 at 100°C	8.90
Sn	11.5 at 20°C 20.3 at 200°C	7.30

After reviewing their properties, aluminum was selected as the preferred foil material. Aluminum has the lowest mass resistance, it is chemically nonreactive with the other candidate materials (PCB being a possible exception), and can be either welded or mechanically joined to provide joints of low electrical resistance.

Copper, while having the lowest resistivity because of its relatively high density, has a high mass. Of the four metals, Cu is probably the easiest to electrically join and yields the lowest joint resistance. Nickel and tin were rejected because of their high resistivities and densities and because of their potential chemical reactivities. In addition, Sn salts, if formed, can induce polymerization of silicone fluids or may aid in saponification of esters such as dioctylphthalate if moisture is present.

2.4 DIELECTRIC PAPERS AND FLUIDS

The discussion of the evaluation of papers and fluids is combined because in fact the two materials function together uniquely within the capacitor. Even though the properties of a fluid-impregnated paper are unique, these properties are dependent on the individual properties of the paper and the fluid. Because of this dependence the properties of the papers

and the fluids were studied separately as well as in combinations. It should be noted that these property studies were limited to investigations of electric loss and capacitance as a function of frequency and temperatures. No critical field strength or electrical breakdown determinations were performed in these evaluations.

The following sections summarize the preliminary selection phases and experimental studies for the papers and fluids as performed separately and for various combinations. Also included are those results of thermal aging tests conducted with selected combinations.

Before discussing the experimental results, a review of the general requirements is in order. Like the films, the papers and fluids serve a major role in the energy storage of the capacitor. The major function of the paper-fluid combination is to eliminate gaseous regions between the films. Furthermore, because of their properties, the combination also plays an active role as a dielectric. The properties of the paper-fluid combinations can affect the voltage distribution within the capacitor and hence the energy density of the device. Because it is a charge-storing media with related electrical losses, it can also contribute to heating within the device. Because the paper-fluid is an active dielectric within the device, the combination has requirements essentially the same as those of the films.

2.4.1 Dielectric Papers

A primary function of the paper in a capacitor is to provide positive separation between the film and foil. It is also used between multiple film layers as a separator. This separation combined with the irregular nature of paper aids in the elimination of trapped gases when the combination is properly impregnated with a dielectric fluid. Since it is to function as an active dielectric, certain properties of the paper become important in defining its behavior. These include:

- True (fiber) density
- Dielectric constant
- Electrical loss characteristics

- Thermal stability
- Fluid compatibility
- Thickness

The general discussions given for similar properties of films can also be applied here to the papers. Thickness is included as a property of the paper because of the thickness limit frequently encountered in papers. The general goal is to have the thinnest paper possible while not sacrificing handling and manufacturing requirements. Thin paper having the appropriate dielectric properties will result in the maximum energy storage density.

In this evaluation of papers, seven materials were initially considered:

- Kraft paper (capacitor grade)
- Pure alpha-cellulose
- Lens tissue
- Ashless filter paper
- Polyester paper
- Aromatic polyamide
- Microporous polypropylene

The first four papers are all cellulose materials. The basic difference lies in the types of fiber binder materials and fillers which can affect the basic properties. The final three are synthetic papers, so-called because the basic films are man-made.

An initial review of the properties of the seven materials suggested four materials for further consideration and experimentation. These were:

- Kraft paper
- Lens tissue
- Aromatic polyamide
- Polyester

Of the three synthetics, the polypropylene was eliminated because of its temperature limitations. This paper has a melting point of 140-145°C which is below the 150°C design requirement. The two synthetics selected have operating temperatures in excess of 175°C. Both appear to be compatible with the candidate fluids.

Selection of two cellulosic papers permitted the investigation of the effects of binder type on the characteristics of this class of papers. The kraft paper was chosen as being representative of a high ash content material. The lens tissue has an especially low ash content. The ash contents were 3.1 and 0.6%, respectively. It should be noted that the lens tissue did not have the lowest ash content, the ashless filter paper, Whatman's No. 44, being the lowest at 0.02 percent. However, the lens tissue was available in a form in which test devices could be made, whereas the filter paper was not. In addition, if the tests with the lens tissue were successful, it would be available in a 1 mil thickness as a standard item, while the ashless papers were available only in 2 mil or greater thicknesses.

Paper Experiments

Two sets of experiments were conducted on the four papers. One set involved a methanol extraction while the other was a characterization of the dielectric constant and dissipation factor as a function of frequency.

The test device used in both evaluations consisted of a cylindrical capacitor wound with the paper being studied. The device was wound on a Teflon core and used aluminum foil electrodes with nickel attachment tabs. The capacitance values for the test devices ranged from 1000 to 6000 picofarads. Figure 2 shows a typical test device.

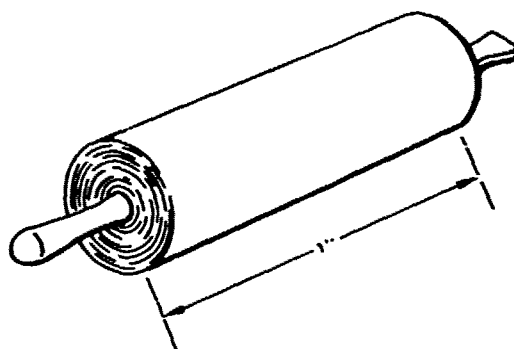


Figure 2. Typical test device used in paper and paper-fluid evaluations.

The methanol extractions were conducted to determine the effects of the removal of polar, soluble materials on the electrical loss properties of the papers. Such loss reductions, if resulting, could be significant in the performance of the capacitor by reducing temperature rises due to such losses.

In these experiments, the test devices were first dried for 72 hours at 105°C. Next, the capacitance and loss were measured at room temperature and 1.0 kHz. It should be noted that the devices were maintained in a desiccator until measured to assure their dryness. After measuring, the devices were placed in a Soxhlet extractor containing spectrochemical grade methanol and extracted. The number of extraction cycles and the cycling rates varied for the different papers because different extractors were used for each paper. The extraction information for each paper appears in Table 8. After the extraction was complete, each device was vacuum dried for 72 hours at 100°C and 0.1 torr. The devices were then retested. All of the devices showed a reduction in loss as a result of extraction. In no case was there a change in capacitance, hence, dielectric constant.

While these results suggest extraction for all papers, it should be emphasized that these results apply only for 1.0 kHz values at room temperature. It has been stated that such extractions can remove all of the lignin from the kraft paper resulting in increased losses at elevated temperatures and higher frequencies. This characteristic was not verified in these experiments. If such were the case, it is also possible that the extractables noted with the polyester and to a lesser degree with the aromatic amide, could behave similarly. Again these possibilities were not studied in this evaluation.

Until such studies are undertaken, it is felt that extraction should not be introduced into the capacitor process.

The final paper experiments dealt with characterizing the dielectric constants and dissipation factors as a function of frequency. The purpose here was to develop data which could be used in designing devices and interpreting their performance.

TABLE 8. EFFECTS OF METHANOL EXTRACTION ON THE CAPACITANCE AND DISSIPATION OF CAPACITOR PAPERS

Capacitor Paper	Device Serial Number	Conditioning	Capacitance at 1 kHz and R. T. (pF)	Dissipation Factor at 1 kHz and R. T., $\times 10^4$	Change in Dissipation Factor Due to Conditioning (1) %
Kraft 1.0 mil	1	Vacuum dried at 105°C for 72 hours	6193	38	
	2		5863	35	
	3		5757	36	
	4		5891	36	
	14		5857	42	
	1	Methanol extraction; (2) vacuum dried (3)	6334	30	-21
	2		6034	31	-11
	3		5910	30	-17
	4		6159	31	-14
	14			31	-26
Kraft 0.5 mil	1	Vacuum dried at 105°C for 72 hours	4997	36	
	2		5105	35	
	3		5023	36	
	14		4917	39	
	1	See notes (2) and (3)	5188	26	-28
	2		5336	28	-20
	3		5140	28	-19
	14		5484	30	-23
	1	Vacuum dried at 105°C for 72 hours	1968	32	
	2		1957	22	
Lense Tissue 1.0 mil	1	Methanol extraction; (4) vacuum dried (3)	2100	17	-23
	2		2014	17	-23
	1	Vacuum dried at 105°C for 72 hours	2214	20	
	2		2151	19	
Polyester 1.0 mil	1	Methanol extracted; (4) vacuum dried (3)	2277	14	-30
	2				
	1	Vacuum dried at 105°C for 72 hours	1069	31	
	2		1083	32	
	3		1081	34	
	4		1070	32	
Nomex	1	See notes (5) and (3)	1127	27	-13
	2		1143	30	-6
	3		1128	30	-13
	4		1126	30	-6

(1) $\Delta = \frac{DF \text{ (after extract)} - DF \text{ (before extract)}}{DF \text{ (before extract)}} \times 100$

(2) 240 extraction cycles of 1/2 hours per cycle.

(3) 72 hours at 100°C and 0.1 Torr.

(4) 48 extraction cycles at 2-1/2 hours per cycle.

(5) 192 extraction cycles at 1/2 hours per cycle.

The test devices used were capacitors like those described in the extraction experiment. In these determinations, the devices were first dried at 105°C for 24 hours. The devices were then returned to room temperature, in a desiccator, and the capacitance and dissipation factors measured. Measurements were made at 100, 1.0 kHz, 10.0 kHz and 100 kHz.

The dielectric constants and dissipation factors observed in these tests are given in Table 9. No significant change in dielectric constant is noted for any of the papers over the frequency range tested, while all showed an increase in the dissipation factor. It should be noted that the lens tissue has a lower dissipation factor over the frequency range than does the kraft paper. Since the kraft was unextracted, hence containing lignin, and the lens tissue is essentially lignin free, these results do not support the postulated advantage previously stated for kraft paper. Further studies, however, are required to definitely establish the lignin effect. It should be noted that none of the papers used in these evaluations were extracted.

TABLE 9. CAPACITANCE AND DISSIPATION FACTOR AS A FUNCTION OF FREQUENCY FOR CANDIDATE PAPERS - MEASURED AT 23°C

Paper	Evaluation Frequency							
	100 Hz		1.0 kHz		10.0 kHz		100 kHz	
	Capacitance (pF)	Dissipation Factor	Capacitance (pF)	Dissipation Factor	Capacitance (pF)	Dissipation Factor	Capacitance (pF)	Dissipation Factor
Kraft (1 mil)	5648	0.0034	5616	0.0042	5580	0.0054	5541	0.0110
Lenze Tissue (1 mil)	1892	0.0016	1887	0.0019	1881	0.0026	1873	0.0052
Nomex (3 mils)	1116	0.0024	1112	0.0032	1106	0.0036	1100	0.0045
Polyester (1 mil)	2223	0.0008	2219	0.0020	2211	0.0040	2194	0.0073

THIS PAGE IS BEST QUALITY PRACTICABLE
FROM COPY FURNISHED TO DDC

Of the four papers, the kraft paper has the highest apparent dielectric constant and the polyester the lowest.

Kraft paper has the highest dissipation factor with the lens tissue and the polyester the lowest. The dissipation factor for the aromatic polyamide is least affected by frequency over the test range.

The results of these frequency studies combined with other property data indicate that each of these papers is potentially suitable for use as a capacitor dielectric. The determination, however, will be based on the properties resulting when fluid impregnated and their compatibility with those fluids.

2.4.2 Dielectric Fluids

The dielectric fluid, like the paper, is an active element in the capacitor. The fluid functions together with the paper to achieve a gas-free condition between films and foil layers. Property considerations for fluids used include:

- Low density
- High dielectric constant
- Low electrical loss
- Thermal stability
- High specific heat
- Low surface tension

Since the fluid will contribute to the energy storage density, it is desirable to optimize those properties contributing to energy storage: i. e., the dielectric constant and the density. In addition, it is necessary to have a high critical field strength, although for most dielectric fluids the values under comparable conditions are nearly equivalent. Of the materials of construction, the electrical losses of the fluids are potentially the highest and certainly the most dependent on processing and conditioning. As with the other materials of construction, the fluids must be chemically compatible with these other materials and must remain thermally stable under the conditions of operation. For the fluids, particular attention must be given to reactions or conditions which could lead to gas formation. Gassing would be

catastrophic to the device. Since the fluid is present as a major mass in the device, a high specific heat could lower the temperature rise associated with intermittent operation. Finally, the lower the surface tension, the better the wetting and degree of impregnation.

With these property considerations as the guide, ten dielectric fluids were selected for initial consideration.

- Polychlorinated biphenyl (Inerteen 100-42)
- Alkylated benzene (Chevron D.O 100)
- Fluorinated polyether (Freon E-5)
- Polyisobutylene (Chevron 32E)
- Mineral oil, capacitor grade
- Polyphenyl ether (OS-124)
- Alkylphenyl siloxane (SF-1050)
- Castor oil
- Dioctylphthalate
- Poly(dimethylsiloxane) [DC200]

The properties of these fluids are given in Table 10. After reviewing the properties of these materials, four were selected for evaluation with the papers. These were:

- Mineral oil (capacitor grade)
- Dioctyl phthalate
- Polychlorinated biphenyl
- Silicone fluid (SF-1050)

Mineral oil was selected because of its long record of successful use in high voltage capacitors. This fluid in the absence of oxygen or oxidizing agents is among the more inert and thermally stable materials. Dioctylphthalate (DOP) was selected for its potentially high energy density storage properties. DOP combines a relatively high (by comparison) dielectric constant and a low density. In the absence of reactive metals and moisture DOP is a high stable compound. One concern with DOP was electrical loss characteristics. Any material synthesized from an organic acid has the possibility of having high electrical loss. The polychlorinated biphenyl

TABLE 10. PROPERTIES OF CANDIDATE FLUIDS

Dielectric Liquid	PHYSICAL			ELECTRICAL						THERMAL				Surface Tension (dynes/cm)
	Density (g/cm ³)	Thermal Expansion Coefficient (cm ³ × 10 ⁻⁶ /cm ³ /C)	Freezing Point (°C)	Boiling Point (°C)	Dielectric Constant		Dissipation Factor		Volume Resistivity (ohm-cm)	Electrical Breakdown Strength (volts/mil)	Arc Effects	Thermal Conductivity (cgs units)	Specific Heat (cal/cm ² /°C)	
					1 KHz	1 MHz	1 KHz	1 MHz						
PCB Arochlor 1242	1.39	700	-19	325-366	5.8		0.001			550		28 × 10 ⁻⁵	0.26 at 25° 0.30 at 50°	
Alkylated Benzene Chevron EO-100	0.87	790	-50		2.1		0.002		1 × 10 ¹⁵			25 × 10 ⁻⁵	0.42 at 20°	
Fluorinated polyether Chevron E-5	1.79	650	<-84	224	2.45		<0.00006		4 × 10 ¹⁴	400		16 × 10 ⁻⁵	0.24 at 25°	16
Fluorinated polyether Chevron 425	1.90	920	-35		2.15		0.003						0.24 at 38°	20
Polyisobutylene	0.90	670	<0		2.20		0.0004		1 × 10 ¹⁶			27 × 10 ⁻⁵ at 25°C 21 × 10 ⁻⁵ at 150°C	0.47 at 25° 0.65 at 150°	
Mineral Oil	0.81	720	-45		2.2		0.0005		1 × 10 ¹⁴	390		30 × 10 ⁻⁵ at 30°	0.41 at 30°	30-40
Polyphenyl ether	1.20				4.5		0.0001		7 × 10 ¹²			32 × 10 ⁻⁵ at 38° 24 × 10 ⁻⁵ at 150°	0.37 at 38° 0.43 at 150°	50
SF-1050	0.92		-100	261	2.48		<0.005		1 × 10 ¹⁵	480		27 × 10 ⁻⁵ at 25° 24 × 10 ⁻⁵ at 150°	0.41 at 20° 0.49 at 100°	22
Castor oil	0.96		-15		4.7		0.001							
DOP	0.99		<-45		5.1									

(PCB), sometimes referred to as an askarel, was chosen because of its high dielectric constant. Unlike DOP, the energy storage density for PCB is not expected to be high because the high dielectric constant is combined with high density. Although the energy density may be low, the high dielectric constant of the fluid could contribute the high capacity sought for the paper-fluid combination. The limitation on the PCB is its regulation as an environmentally controlled material. There was also some concern regarding a possible reaction with aluminum. The latter was studied experimentally and will be described in a following section.

The final fluid chosen was a pure silicone compound. This material was selected for its chemical inertness and high thermal stability. The silicones, having very low surface tensions, should be excellent impregnants, as has been previously demonstrated. It was postulated that if any problems were encountered with mineral oil, the silicone could be an adequate substitute.

Reasons for nonselection of other materials included cost (fluorinated esters and polyphenyl ether), marginal chemical and thermal stability (castor oil), and equivalent properties to a selected material (silicone oil and alkylated benzene).

The four fluids selected for evaluation with the papers were believed to be capable of providing a representative summary of the properties to be expected from such combinations.

Fluid Experiments

Three experiments were conducted with the selected fluids. These included:

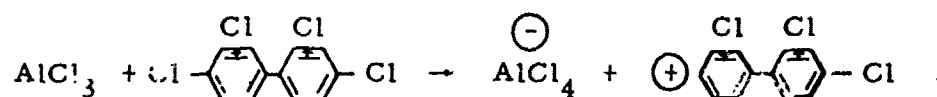
- PCB - aluminum foil compatibility tests
- Studies of purification methods
- Characterization of dielectric constants and dissipation factors as a function of frequency.

Following are summaries of these experiments:

PCB - Aluminum Foil Compatibility. These experiments were undertaken to examine the possibility for this combination of materials to result in a Friedel-Krafts reaction.

This reaction is initiated by the formation of $AlCl_3$ which then could serve as the catalyst for a dehydrohalogenation reaction. Such a series of reactions, if they occurred, would completely degrade the fluid and result in failure of the device. Thus, before further studies were made with the PCB, this potential reactivity had to be characterized.

Friedel-Krafts reactions are reaction-catalyzed by Lewis acids and $AlCl_3$ is one of the most active catalysts of this type. Its effectiveness is attributed to its very strong affinity for a pair of electrons; thus, in a fluid such as PCB, it would complex with halogen atoms of the fluid molecule and thus induce cleavage. This may be illustrated as follows:



The degraded fluid could then interact with other fluid molecules to yield higher molecular weight products, eliminate a proton, or in the presence of moisture couple with the hydroxyl ion and generate a proton which ultimately would end up as corrosive hydrogen chloride.

To determine the reactivity of the PCB and Al the following tests were conducted. In these tests Al foil was exposed to the PCB (Westinghouse Inerteen 100-42) at 23°, 52° and 100°C. In one set of conditions the foil was formed into cylindrical electrodes which were positioned concentrically, immersed in the PCB and electrified with a dc potential at the test temperature. In this test, the electrode spacing was normally 0.2 inches and the applied voltage was 1000 Vdc. The purpose of this experiment was to identify electrical effects as an initiator or accelerator for chemical reactions between the foil and the PCB and if occurring characterize the electrode polarity behavior. In the other condition evaluated, a sample of Al foil was

simply immersed in the PCB and heated. The test samples are shown in Figure 3. In both conditions the foil weights were recorded at the beginning and end of the exposure periods. In addition the appearance was noted for both foils and the fluid. The dc volume resistivity of the fluid was measured at the beginning and end of the test period and the dc leakage currents were monitored throughout the exposure periods for the electrified samples. It should be noted that the PCB was used as received in these tests.

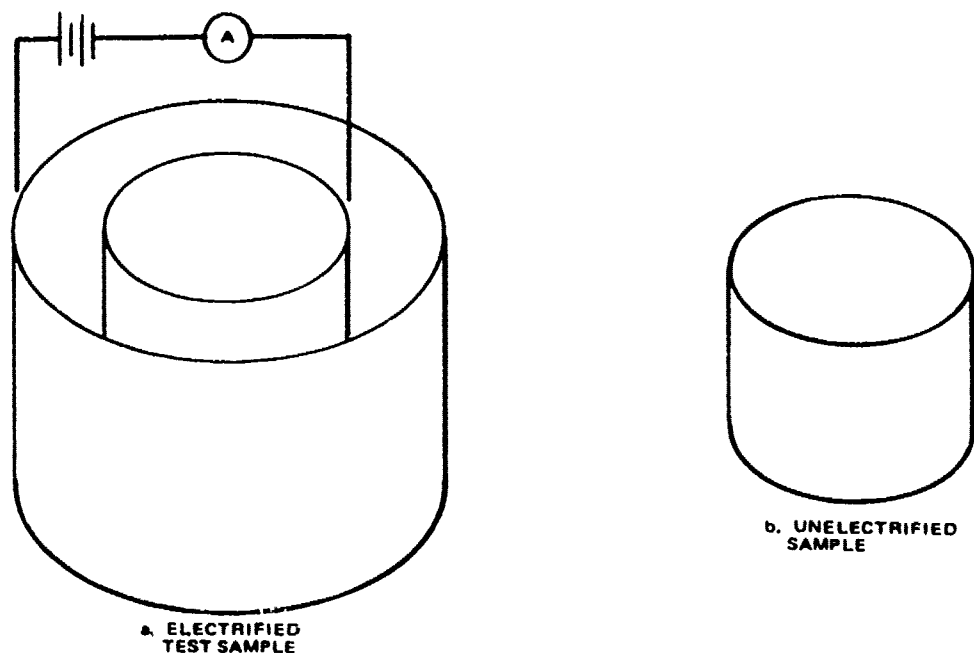


Figure 3. Test samples used in PCB-Al foil reaction tests.

The results of the 192 hour exposure at 23°C, 532 hours exposure at 52°C, and 355 hours at 100°C are given in Table 11. No detectable weight changes were noted in either the electrified or unelectrified foils at the low temperature exposures. After the 100°C exposure all of the foils showed a slight increase in weight (less than 0.1 percent) but with no change in appearance. Throughout the tests the fluid remained unchanged in appearance and viscosity with no evidence of turbidity, precipitation or separation. These experiments were run serially using the same foils and fluids.

TABLE 11. ALUMINUM FOIL - PCB (INERTEEN 100-42) COMPATIBILITY TEST RESULTS

Exposure Time	Temperature °C	Conductance at Test Temp. (at 1 kVdc)		Electrode Weights ^a						Unelectrified Foil Weight (gms)		
				Anode			Cathode					
		Initial	Final	Before	After	% Change	Before	After	% Change	Before	After	% Change
192	23	1.35×10^{-6}	0.34×10^{-6}	0.2349	0.2349	0	0.1402	0.1402	0	—	—	
532	52	0.49×10^{-6}	0.4×10^{-6}	0.2349	0.2349	0	0.1402	0.1402	0	0.187 ^a	0.187 ^a	
Exposure Temp (°C)	Time (Hrs)	Conductance at Test Temp. (at 1 kVdc)		Electrode Weights						Unelectrified Foil Weight		
				Anode			Cathode					
		Initial	Final	Before	After	%Δ	Before	After	%Δ	Before	After	%Δ
100	355	1.04×10^{-6}	0.33×10^{-6}	0.234 ^a	0.2351	+0.08	0.1402	0.1403	+0.07	0.187 ^a	0.1880	+0.05

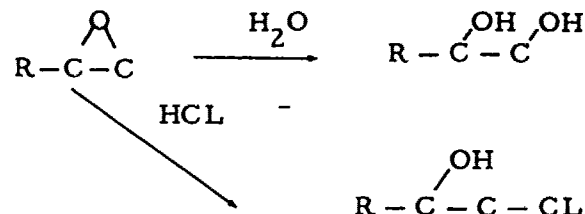
^aVariations in the 5th decimal place were noted, but they were within the error of the balance.

^aVariations in the 5th decimal place were noted, but they were within the error of the balance.

The slight increase in volume resistivity noted for the PCB is probably the result of electrophoretic and electrolytic removal of trace ionic contaminants. Such processes could account for the reduced conductance noted during each exposure.

The results of these tests indicate that the PCB, Westinghouse Inerteen 100-42, would be non-reactive with a pure (99.5%) Al foil for limited exposures at temperatures in excess of 100°C.

However, this non-reactivity may in part be due to the presence of a monofunctional epoxide compound which is present in the fluid and which if destroyed or consumed could greatly alter the observed reactivity. For the Friedel-Krafts reaction to occur AlCl_3 must be present. In the Al-PCB system, AlCl_3 would result from the formation of HCl which could be generated by dehalogenation of the PCB and the subsequent reaction with moisture. With the epoxide present both the moisture content and HCl are greatly reduced or eliminated. Epoxides are "getters" for both H_2O and HCl



Thus, it becomes apparent that conditions which could deplete or eliminate the epoxide compounds could lead to the destructive Friedel-Krafts reaction between the Al foil and the PCB.

Purification. The purity of the dielectric fluids will determine to a significant extent their electrical loss properties. The losses in a dielectric are derived from several sources. Among these are ionizable materials and moisture. Their concentration will in part determine the conductance of the fluid with their elimination resulting in lower electrical losses. Following is a summary of the purification methods employed on three of

the selected fluids. It should be noted that the PCB in all evaluations was used either "as-received" or after filtering it through a 5 micron TFE filter. Purification methods were not used because of concern for removing or altering the epoxide compound.

The three fluids purified were

- Dioctyl phtahlate
- Mineral oil (capacitor grade)
- Alkylaryl silicone fluid (GE SF-1050)

Two grades of DOP were compared in the purification study, a purified material from Eastman Chemical and a plasticizer grade from BASF. It should be noted that the two grades were compared because of cost differences with the purified material costing approximately 20 times more than the plasticizer.

In these evaluations the effects of purification were determined by measuring the dc resistivities and the dissipation factors. Both measurements were made using a Balsbaugh G-350 test cell. The dc measurements were made at 500 Vdc, while the ac measurements were made at 100, 1.0 K, 10.0 K and 100 kHz and a voltage of 10 Vdc. All measurements were made at 23°C.

The DOP purifications were undertaken using anhydrous, neutral alumina (Al_2O_3). The first experiments were performed using the purified compound to establish the effectiveness of Al_2O_3 as a purification media. In these evaluations, two columns were prepared using 140 mesh Al_2O_3 . One column was approximately 100 grams of Al_2O_3 . The other was approximately 4 inches high and 2-1/2 inches in diameter and contained 200 grams of Al_2O_3 .

For the long column approximately 300 milliliters were purified and for the short column, 800 milliliters. The results of these purifications are

given in Table 12. The results show both columns to be of comparable effectiveness as purifiers for the DOP. Both result in approximately 50 times increase in the volume resistivity putting this material in the range

TABLE 12. A COMPARISON OF COLUMN LENGTH ON THE PURIFICATION OF DOP (PURIFIED GRADE) WITH Al_2O_3

Column Length and (Amount of Al_2O_3)	Volume Resistivity (ohm-cm)	Dissipation Factor Frequency	
		1.0 kHz	100 kHz
None (As received)	7.4×10^{10}	0.004	0.0001
18 inches (100 grams)	4.9×10^{12}	0.0005	0.0003
2 inches (100 grams)	5.0×10^{12}	<0.00005	0.0004

where it could function as a reasonable dielectric. With this improvement observed after one pass the question was raised concerning the effects of a multiple pass through the column. This was tried using a new long column and fluid from the initial long column run. The results, given in Table 13, show very little change. A third pass through the long column resulted in no further change in the electrical loss properties when compared with two passes.

TABLE 13. EFFECTS OF MULTIPLE PASSES THROUGH AN Al_2O_3 COLUMN OF THE PURITY OF DOP (EASTMAN)

Number of Passes Through Long Column	Volume Resistivity (ohm-cm)	Dissipation Factor	
		1 kHz	100 kHz
None (As received)	7.4×10^{10}	0.004	0.0001
1	4.9×10^{12}	0.0005	0.0003
2	5.2×10^{12}	0.0005	0.0003
3	5.0×10^{12}	0.0006	0.0004

Although the DOP used in these evaluations was colorless in appearance the columns after the initial pass both contained a light brown color at the top and turned a light yellow throughout the lower lengths. The multiple pass columns were both light yellow after processing. The extracted materials were not analyzed so their contribution to the losses cannot be assessed.

Having demonstrated that the electrical losses of DOP could be lowered by Al_2O_3 purification, the purification of the plasticizer grade material was undertaken. Because of the increased flow rate the short column was used. As with the purified grade, approximately 800 milliliters was purified using 200 grams of Al_2O_3 .

The results of the plasticizer grade DOP purification, given in Table 14, show this material to have electrical loss properties comparable to the purified grade after both have been Al_2O_3 treated.

TABLE 14. PURIFICATION OF PLASTICIZER GRADE DOP
USING Al_2O_3

Conditioning	Volume Resistivity at 500 Vdc (ohm-cm)	Dissipation Factor Frequency	
		1.0 kHz	100 kHz
None	1.7×10^{11}	0.002	0.0006
Single pass through Al_2O_3	5×10^{12}	<0.00002	0.0005

The capacitor grade mineral oil was processed using the standard hot evacuation process. In this method the oil is first evacuated to approximately 0.2 Torr and then heated to 105°C - 110°C . The basic effect of this process is to remove moisture and dissolved air. The moisture is significant with respect to losses while the dissolved air has a significant effect on the critical field strength. The latter was not, however, relevant to these tests.

In this evaluation 500 milliliters of oil was placed in a 1 liter beaker and evacuated to 0.2 Torr. Next, the oil was heated while stirring to 105°C . The oil was maintained under these conditions for 8 hours, then cooled under vacuum. The chamber was filled with dry nitrogen and the oil transferred to a clean, dry, glass bottle. Measurements made on this oil were those previously described for DOP.

The results of this processing are given in Table 15. Note that the volume resistivity increased approximately 20 times. It is important to note that in this case the electrical properties of the "as received" oil were very good. When a low loss fluid is initially available the hot evacuation provides adequate purification. If, however, the starting material

TABLE 15. ELECTRICAL PROPERTIES OF CANDIDATE FLUIDS AT 23°C

Property	Inerteen 100-42 As Rec'd	Diocetyl Phthalate As Rec'd (Reagent Type)	Diocetyl Phthalate Al ₂ O ₃	M.O. As Rec'd	Mineral Oil Proc'd.	SF-1050 As Rec'd	SF-1050 Clay Treat	SF-1050 Al ₂ O ₃	DC-200 (50 cS) As Rec'd
Volume Resistivity (ohm-cm)	9×10^{11}	9×10^9	6×10^{12}	8×10^{14}	4×10^{16}	1×10^{13}	2×10^{15}	9×10^{16}	2×10^{16}
Dielectric Constant									
100 Hz	4.6	4.6	4.6		2.3	2.2	2.2	2.2	2.4
300	4.6	4.6	4.6		2.3	2.2	2.2	2.2	2.4
1000	4.6	4.6	4.6		2.3	2.2	2.2	2.2	2.4
10 K	4.6	4.6	4.6		2.3	2.2	2.2	2.2	2.4
100 K	4.6	4.5	4.5		2.3	2.2	2.2	2.2	2.4
Dissipation Factor									
100 Hz	0.028	0.045	0.0047	0.005	0.005	0.0020	0.0009	0.0006	0.0018
300	0.010	0.014	0.0024	0.005	0.0039	0.002	0.0006	0.0004	0.0011
1000	0.003	0.0045	0.0013	0.003	0.0025	0.001	0.0003	0.0002	0.0004
10 K	0.0003	0.00047	0.00050	0.0015	0.0010	0.0002	0.00009	0.00006	0.00009
100 K	0.00000	0.0001	0.0003	0.0010	0.0006	<0.0001	0.00000	0.00000	0.00000

were of a low or even unacceptable quality, e. g. . a volume resistivity of $10^{12} - 10^{13}$ ohm-centimeters, then, a hot clay treatment followed by hot evacuation would be required.

SF-1050, an alkylaryl silicone fluid, was the final material purified. It should be noted that the material used in this evaluation was of marginal quality. Three purification methods were used with this silicone:

- recirculating through a clay filter
- percolating through a clay column
- percolating through an Al_2O_3 column

In the first method, approximately one gallon of fluid was recirculated through one pound of attapulgus clay for 6 hours at room temperature. This process brought the volume resistivity to the minimum acceptable level, 1×10^{15} ohm-centimeter.

Next, a sample of the clay was baked at approximately $300^{\circ}C$ overnight. The clay was then introduced into a 24-inch column one inch in diameter. A 600 milliliter sample was then passed through the column. The resulting volume resistivity for this treatment was slightly higher (2×10^{15} ohm-centimeters) than that achieved using the recirculating method.

In the final method a 24 inch column was packed with approximately 150 grams of anhydrous, neutral Al_2O_3 and 500 milliliters of fluid were percolated through the column at room temperature. This method resulted in the largest increase in resistivity, producing a volume resistivity of 4×10^{16} ohm-centimeters.

The results of the silicone purifications are given in Table 15. It is of interest to note that while each purification method produced measurable changes in the volume resistivity of the silicone no significant differences were noted in the dissipation factors resulting from the different methods. All resulted in a comparable reduction in the ac loss. In all cases, the dielectric constant remained unchanged by the processing.

From the purification studies of the three fluids evaluated it is seen that in each case an improvement in electrical losses results. These results confirm the earlier statement regarding the sensitive nature of electrical losses within liquids and support the need for special handling and processing.

Characterization. Finally, in this study of the dielectric fluids, their dielectric constants, dissipation factors and volume resistivities were characterized. The ac measurements were made at 10 volts and at frequencies of 100, 1.0k, 10.0k and 100kHz. The volume resistivities were determined at 500 Vdc. The Balsbaugh cell was used.

The samples were purified as follows:

- DOP (plasticizer grade): percolated 800 milliliters through 200 gms of Al_2O_3 on a 4 inch X 2 1/2 inch diameter column at room temperature.
- mineral oil (capacitor grade): evacuated to 0.2 Torr and heated with stirring to 105°C for 8 hours cooled to room temperature under vacuum.
- PCB: filtered through 5 micron TFE filter
- silicone fluid: percolated 600 milliliters through attapulgas clay previously baked overnight at 300°C on 24 inches x 1 inch diameter column at room temperature.

The electrical properties for the four fluids processed as stated are given in Table 15.

2.4.3 Paper-Fluid Combinations

As previously indicated, four papers and four fluids have been selected for evaluation. In previous sections the electrical properties of these eight materials have been presented. In this section the electrical properties of these materials when in combination will be summarized.

Each of the four papers was impregnated with each of the four fluids, yielding a total of 16 paper-fluid combinations. The test samples used in these evaluations, like the original paper studies, consisted of a cylindrical capacitor wound on a Teflon core and utilizing Al foil electrodes.

The capacitor samples were contained in glass tubes such as shown in Figure 4. To prepare the test samples, the paper capacitors were first baked at 105°C for 24 hours. Next, the fluids which had been processed were introduced into the tubes and the combination heated to 100°C . While hot, the samples were then evacuated at 0.3 Torr or less for 3 hours. The chamber was then back filled with nitrogen, the sample tubes removed and sealed with TFE tape.

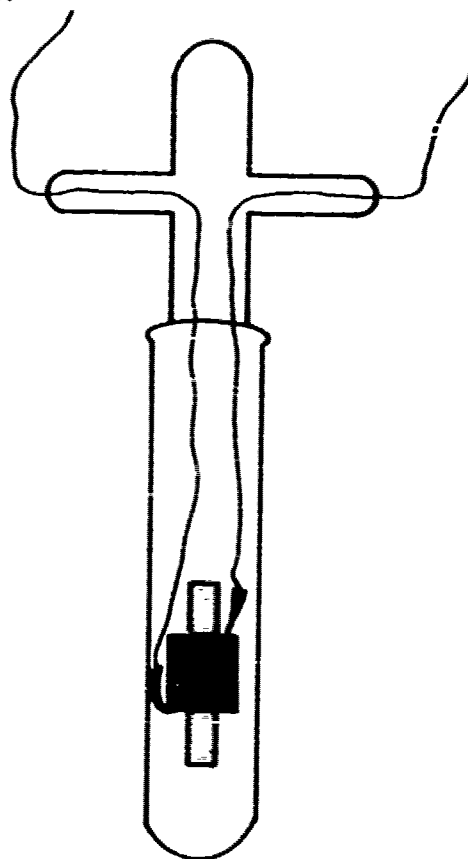


Figure 4. Test sample used in paper-fluid electrical properties determinations.

After cooling to room temperature the electrical properties were measured. First, the dielectric constants and dissipation factors were determined at 100, 1.0kHz, 10kHz, 10.0kHz and 100 kHz. Next, the dc resistance was measured using a 90 volt potential. After the determinations were completed the sample was heated to 150°C and maintained at this temperature for one hour. After this time the ac and dc measurements performed

at room temperature were repeated. At the completion of these tests the samples were returned to room temperature and inspected for evidence of degradation.

The results of the paper-oil evaluations are presented in Tables 16 through 23. Of significance for these evaluations are dielectric constants resulting for the various combinations and the effects of frequency and temperature on the electrical losses. It should be noted that the dielectric constants for any of the combinations show negligible frequency dependence over the frequency range studied. The maximum frequency dependence was demonstrated by the PCB impregnated combinations. Of the combinations studied, the kraft paper - DOP and the kraft paper - PCB produced the highest dielectric constants while polyester-mineral oil and polyester-silicone yielded the lowest. At 150°C certain of the combinations exhibit some variation in dielectric constants while others remained unchanged. An attempt to correlate these increases with either paper or oil type shows a general dependency on one or the other for predicting changes. For example, kraft paper shows a reduction with PCB, an increase with mineral oil, and is essentially unchanged with the silicone. All mineral oil combinations showed a slight lowering of the dielectric constant, while the kraft paper silicone combination showed a negligible increase in dielectric constant, and the lens tissue and Nomex-silicone combinations yielded a decrease. Also of significance, is the increased capacitance, i. e., dielectric constant, at elevated temperature noted for certain papers and the high loss fluid PCB. At the low frequencies, a large increase in capacitance exists for these combinations. With the exception of these large variations for the PCB combinations, none of the variations exceeded 10 percent over the temperature range studied.

The lowest average electrical loss at room temperature exists with the lens tissue and polyester paper in combination with the mineral and silicone oils. These four combinations are essentially equivalent. At room temperature each of the combinations shows an increase in loss for increasing frequencies. The approximate equivalent circuit for these combinations would be a series R-C element, although none of the combinations specifically conform to this equivalent. At room temperature the

TABLE 16. ELECTRICAL MEASUREMENTS OF DOP
IMPREGNATED PAPERS AT 23°C

Paper	Frequency (Hz)	Capacitance Before Impreg. (pf)	Capacitance After Impreg. (pf)	Dissipation Factor Impregnated Paper
Kraft	100.0	5848	14870	0.010
	1.0K	5813	14700	0.010
	10.0K	5774	14460	0.014
	100.0K	5734	14250	0.027
Lense	100.0			
Tissue	1.0K	1959		
	10.0K			
	100.0K	1944		
Nomex	100.0		-	-
	1.0K	1031	3148	0.029
	10.0K		3112	0.010
	100.0K	1020	3077	0.009
Polyester	100.0		-	-
	1.0K		6490	0.017
	10.0K		6447	0.008
	100.0K		6392	0.020

TABLE 17. ELECTRICAL MEASUREMENTS OF DOP IMPREGNATED PAPERS MEASURED AT 150°C

Paper	Frequency (Hz)	Capacitance Before Impreg. (pf)	Capacitance After Impreg. (pf)	Dissipation Factor Impregnated Paper
Kraft	100.0		10440	0.041
	1.0K			
	10.0K			
	100.0K			
Lense Tissue	100.0		8690	0.98
	1.0K			
	10.0K			
	100.0K			
Nomex	100.0			
	1.0K			
	10.0K			
	100.0K			
Polyester	100.0			
	1.0K			
	10.0K			
	100.0K			

**TABLE 18. ELECTRICAL MEASUREMENTS OF MINERAL OIL
IMPREGNATED PAPERS MEASURED AT 23°C**

Paper	Frequency (Hz)	Capacitance Before Impreg. (pf)	Capacitance After Impreg. (pf)	Dissipation Factor Impregnated Paper
Kraft	100.0	5648	9180	0.0056
	1.0K	5618	9104	0.0059
	10.0K	5580	9024	0.0077
	100.0K	5543	8958	0.0178
Lense	100.0	1892	3698	0.0017
Tissue	1.0K	1887	3688	0.0021
	10.0K	1881	3676	0.0031
	100.0K	1873	3660	0.0092
Nomex	100.0	1097	1930	0.0030
	1.0K	1093	1920	0.0043
	10.0K	1088	1909	0.0079
	100.0K	1082	1894	0.0041
Polyester	100.0	2223	3729	0.0011
	1.0K	2219	3721	0.0025
	10.0K	2211	3702	0.0049
	100.0K	2194	3669	0.0074

TABLE 19. ELECTRICAL MEASUREMENTS OF MINERAL OIL
IMPREGNATED PAPERS MEASURED AT 150°C

Paper	Frequency (Hz)	Capacitance at 150°C (pf)	Dissipation Factor Impregnated Paper
Kraft	100.0	9663	0.0108
	1.0K	9608	0.0041
	10.0K	9563	0.0027
	100.0K	9601	0.0058
Lense	100.0	3670	0.0180
Tissue	1.0K	3635	0.0052
	10.0K	3623	0.0021
	100.0K	3619	0.0029
Nomex	100.0	1955	0.0160
	1.0K	1944	0.0052
	10.0K	1933	0.0039
	100.0K	1923	0.0054
Polyester	100.0	3867	0.0331
	1.0K	3824	0.0079
	10.0K	3796	0.0053
	100.0K	3771	0.0069

TABLE 20. ELECTRICAL MEASUREMENTS OF PCB IMPREG-
NATED PAPERS MEASURED AT 23°C

Paper	Frequency (Hz)	Capacitance Before Impreg. (pf)	Capacitance After Impreg. (pf)	Dissipation Factor Impregnated Paper
Kraft	100.0		13940	0.02
	1.0K		14050	0.011
	10.0K		13840	0.013
	100.0K		13640	0.021
Lense	100.0		7800	0.080
Tissue	1.0K		7676	0.011
	10.0K		7627	0.006
	100.0K		7589	0.013
Nomex	100.0		-	-
	1.0K		3482	0.17
	10.0K		3318	0.02
	100.0K		3282	0.01
Polyester	100.0		6294	0.04
	1.0K		6234	0.008
	10.0K		6180	0.007
	100.0K		6129	0.018

TABLE 21. ELECTRICAL MEASUREMENTS OF PCB IMPREG-
NATED PAPERS MEASURED AT 150°C

Paper	Frequency (Hz)	Capacitance at 150°C (pf)	Dissipation Factor Impregnated Paper
Kraft	100.0	-	-
	1.0K	12160	0.047
	10.0K	11830	0.011
	100.0K	11860	0.008
Lense	100.0	-	-
Tissue	1.0K	10270	0.6
	10.0K	6360	0.10
	100.0K	6220	0.02
Nomex	100.0	-	-
	1.0K	7807	0.8
	10.0K	3191	0.2
	100.0K	2981	0.03
Polyester	100.0	-	-
	1.0K	13850	0.8
	10.0K	6080	0.2
	100.0K	5725	0.02

TABLE 22. ELECTRICAL MEASUREMENT OF SILICONE OIL
IMPREGNATED PAPERS MEASURED AT 23°C

Paper	Frequency (Hz)	Capacitance Before Impreg. (pf)	Capacitance After Impreg. (pf)	Dissipation Factor Impregnated Paper
Kraft	100.0		9721	0.0051
	1.0K		9638	0.0067
	10.0K		9540	0.0088
	100.0K		9459	0.0186
Lense	100.0		4062	0.0024
Tissue	1.0K		4050	0.0024
	10.0K		4037	0.0031
	100.0K		4020	0.0068
Nomex	100.0		2119	0.0040
	1.0K		2108	0.0047
	10.0K		2093	0.0058
	100.0K		2077	0.0124
Polyester	100.0		4196	0.016
	1.0K		4186	0.0028
	10.0K		4162	0.0055
	100.0K		4124	0.0091

TABLE 23. ELECTRICAL MEASUREMENTS OF SILICONE OIL
IMPREGNATED PAPERS MEASURED AT 150°C

Paper	Frequency (Hz)	Capacitance at 150°C (pf)	Dissipation Factor Impregnated Paper
Kraft	100.0	9843	0.0130
	1.0K	9766	0.0043
	10.0K	9726	0.0028
	100.0K	9760	0.0060
Lense	100.0	3869	0.0650
Tissue	1.0K	3738	0.0134
	10.0K	3711	0.0040
	100.0K	3704	0.0037
Nomex	100.0	2049	0.0380
	1.0K	2036	0.0081
	10.0K	2024	0.0045
	100.0K	2010	0.0050
Polyester	100.0	4302	0.0800
	1.0K	4182	0.0157
	10.0K	4141	0.0070
	100.0K	4111	0.0080

highest losses were observed with PCB combinations, with only slightly lower losses noted with DOP. At room temperature the losses are primarily determined by the fluid with the papers acting in some secondary manner to produce the minor differences noted for the different papers.

At elevated temperatures the losses experience a change in character. In general the low frequency losses are greater than the corresponding room temperature value, while the high frequency values are lower than their high temperature low frequency counterparts and lower temperature values at the same frequency. At 150°C the combinations now more closely approximate a parallel R-C element. For the combinations evaluated the lowest average loss at elevated temperature exists with the mineral oil and silicone combinations. At 150°C all of the papers are nearly equivalent with these oils. As was noted at room temperature, the fluid is the loss determinant at elevated temperatures.

For maximum energy storage density the preferred paper-oil combination would be kraft paper and DOP. The limitation for this combination is the electrical loss at elevated temperature which could exceed 10 percent at low frequency operation. As an alternative to have minimum losses over the frequency and temperature ranges of interest, kraft paper and either mineral oil or the silicone should be selected. These combinations provide slightly higher energy storage than would result with the other papers.

Paper-Oil Compatibility

The compatibility of the paper-oil combinations was determined by elevated temperature exposure. The purpose in these tests was to determine changes in the electrical properties for those combinations which could result from either elevated temperatures or from prolonged exposure at lower temperatures. In these evaluations the potential interactions were determined by monitoring changes in the dielectric constants, dissipation factors and dc resistances occurring after an extended exposure at 150°C. It should be noted that changes observed in these tests are indicative only of interactions occurring at these exposure conditions and are not necessarily indicative of an incompatibility at lower temperature. Lower temperature compatibilities could only be established by temperature tests and in

a conservative approach to material selection, deleterious changes noted in these elevated temperature experiments will be concluded to represent also longer term lower temperature reactions which could restrict the use of the combination in question.

Experimental Procedure and Results - In these evaluations the paper-oil combinations previously characterized were exposed at 150°C for 240 hours. These samples, contained in Pyrex test tubes having ground glass joints sealed with Teflon tape, were maintained in a circulating air oven for the exposure. After the exposure period, the samples were returned to room temperature and the dielectric constants, dissipation factors and dc resistance were again determined. In addition to the electrical determination, general observations were made for changes in color and physical characteristics such as apparent viscosity, size, etc., which could also indicate chemical interaction.

The results of the compatibility tests are summarized in Table 24. In the table the dielectric constants and dissipation factors before and after exposure are given along with the dc resistances. None of the combinations experienced a significant change in dielectric constant. The absence of change in this property is not surprising when the loss properties are compared. For an appreciable change in dielectric constant to have occurred, a substantial chemical or physical change would be required. Such changes are not in evidence based on a comparison of dissipation factors or physical appearance. The dissipation factors show only minor changes for any of the combinations. These changes could be accounted for by further moisture elimination or experimental error. Only the mineral oil showed a change in appearance with the exposed sample having a slightly darker color from a light straw color to a golden yellow. Such color changes are suggestive of fluid oxidation. However, the level of oxidation resulting did not significantly alter the electrical losses for any of the paper combinations. It should be noted that all of the samples initially as well as terminally contained whitish flocculent suspended material which was soluble at 150°C

TABLE 24. EFFECTS OF 168 HOUR, 150°C EXPOSURE ON THE ELECTRICAL PROPERTIES OF PAPER-OIL COMBINATIONS

Paper-Oil Combination	Electrical Properties			
	Before Exposure		After Exposure	
	Capacitance	Dissipation Factor	Capacitance	Dissipation Factor
DOP - Kraft	14700		14650	
- Lens tissue		0.010		0.008
- Nomex	3148	0.029	3120	0.021
- Polyester	6490	0.017	6470	0.014
Mineral Oil - Kraft	9180	0.0059	9160	0.0068
- Lens tissue	3688	0.0021	3640	0.0041
- Nomex	1920	0.0043	1910	0.0050
- Polyester	3721	0.0025	3692	0.0032
PCB - Kraft	14050	0.011	13900	0.014
- Lens tissue	7676	0.011	7640	0.014
- Nomex	3482	0.17	3470	0.095
- Polyester	6234	0.008	6190	0.010
Silicone Oil - Kraft	9638	0.0067	9630	0.0078
- Lens tissue	4050	0.0024	4005	0.0042
- Nomex	2108	0.0047	2100	0.0040
- Polyester	4186	0.0028	4150	0.0037

with all of the fluids. The source of this material was assumed to be the heat shrinkage sleeving used to bind the windings. This material was first noted after the 150°C high temperature measurements. Subsequent loss measurements at room temperature showed no change and the material - probably of parafinic nature - was assumed to be benign.

Based on the changes observed, all of the combinations are considered to be suitable for use at 150°C. From these results it is also concluded that extended exposures at lower temperatures should not result in degrading changes. As part of any longer term or elevated temperature use, all of the combinations must, however, be maintained in nonoxidizing, moisture-free conditions.

2.5 CONCLUSION

Based on these evaluations, the following materials are recommended for constructing high energy density capacitors.

2.5.1 Films

Three films are potentially suitable. These are

- polyvinylidene fluoride
- polyimide
- polysulfone

The possible limitations for the vinylidene fluoride are the electrical loss and an upper temperature limit of approximately 150°C. Both the imide and the sulfone have considerably lower losses and higher operating temperatures. The energy storage densities for these three materials are comparable and all are chemically compatible with the selected fluids.

2.5.2 Paper-Oil Combinations

Two paper-oil combinations are recommended. These are

- kraft paper - mineral oil
- kraft paper - DOP

The highest energy storage density is achieved with the kraft-DOP. However, the losses associated with this combination could limit its use. For minimum loss while maintaining a high energy density the kraft-mineral oil would be preferred.

It should be noted that if very high temperatures are found to exist in these devices the silicone aromatic amide paper should be considered. The limitation here is the paper thickness which is currently available only a 3.9 mils or thicker.

2.5.3 Foil

Only one foil was selected - aluminum. Aluminum has the highest conductance per unit mass and is chemically compatible with the other construction materials.

3.0 PAD DESIGN

The design of the individual pads or sections which make up a large capacitor normally separates into two distinct tasks: the design of the dielectric sandwich, and the choice of section shape. In the first task, the designer must choose the number, type, and thickness of the dielectric layers and determine effective dielectric constant and required area. In the second task, the designer chooses the width of the foil, and from that determines winding length and section conformation.

To achieve the energy density required in this program, the single most important goal is the development of a large enough electric field across the dielectric sandwich. The increase in energy density which might be achieved by the adjustment of film and foil widths is a second order effect compared to having enough field. Therefore, in this task a single choice of film and foil width was made, and the majority of the effort was directed at design of the dielectric sandwich.

3.1 ENERGY DENSITY

From time to time confusion arises as to the exact meaning of a particular "energy density" quoted as a component specification. This discussion is presented to aid in understanding what is meant.

As used in the passive component field, energy density is taken to mean stored energy per unit weight, normally expressed in joules per pound. There is no particular problem in computing the stored energy:

$$\text{Stored Energy} = \frac{1}{2} CV^2 \quad (1)$$

where C is the capacitance and V the applied voltage. The problem arises because different weights are used to arrive at energy density.

The best possible energy density is obtained when the only weight considered is that of the dielectric actually storing energy. This is the value usually presented in reports (as in AFAPL-TR-74-79, "218 joules per pound of active storage volume"). The formula for this value is:

$$ED = 4.425 \times 10^{-14} K E^2 / d \text{ (cgs units)} \quad (2)$$

where K is the effective dielectric constant of the insulation stack, E is the applied electric field (V/cm), d is the effective density of the stack (g/cm^3), and ED is the energy density (J/g).

A more realistic number for development purposes is the energy density in the active portion of the section. By this, it is meant that the weight of the foils is added to the weight of the active dielectric. The expression is then:

$$ED = 4.425 \times 10^{-14} K E^2 / (d_d + t_f d_f / t_d) \quad (3)$$

where d_d and t_d are density and thickness of the dielectric stack, d_f and t_f are density and thickness of the foil, and other terms and units are as above.

The only number of concern to systems designers is the mission energy density, which includes case, termination, margins, and connections. This value is obtained by dividing the stored energy by the finished capacitor weight, and is normally much smaller than the value found by equation 2.

As an example, a capacitor was designed and weights determined. This capacitor is not a type used in the tests described below. Nevertheless, the results displayed in Table 25 are interesting.

TABLE 25. TYPICAL ENERGY DENSITY

1. In active dielectric:	80J/lb
2. In active section:	67J/lb
3. System density:	50J/lb

This shows that the final mission weight is larger than that of a section, as one would expect. Since the system energy density is dependent on light-weight case design, the energy densities defined in equations 2 and 3 were employed in the initial phase of this program.

3.2 LAYER DESIGN CONCEPTS

Capacitors are normally designed with several thin layers of insulation between foils rather than one thicker layer. This improves the capacitor reliability by precluding shorting because of a pin-hole or conducting particle in a single layer. Also, since the dielectric strength of a thin layer is larger than that of a thicker layer, capacitors made from many thin layers may be operated at higher stresses than those of equivalent thickness made from a few thicker layers.

The earliest capacitors were made from paper sheet, and kraft capacitor paper is today an important dielectric. The least expensive components have all kraft paper layers, but the field and energy density at which they may be operated are limited by the low dielectric strength of the paper. Modern pulse capacitors use polymeric film dielectric with the kraft, to take advantage of the higher dielectric strength of the polymeric film. The kraft paper, interleaved between the plastic and foil, has been retained despite its low dielectric strength because its irregular surface traps impregnation fluid and thus prevents fluid squeeze-out, bubble formation, and subsequent corona damage. Numerous schemes have been proposed for the elimination of kraft paper in pulse service components, but none has been successful in practice.

The thickness of the individual layers and the number of layers are normally governed by the available thicknesses of the dielectric materials,

the capacitor operating voltage, and the designer's preference. Very little has been written about any other selection criteria.

3.3 FIELD BALANCE

The experience on this program has been that the most successful capacitors have the best field balance in the dielectric. This means that each element in the dielectric stack is operated at the same percentage of its dielectric strength. Capacitors are not normally designed this way.

Experiments on conventionally-wound components show that the average fluid layer thickness is 15% of the interfoil separation. This means that any design based on field balance must treat three layer types (paper, plastic, fluid) rather than just the two solid layers. Since many of the conventionally-wound section failure mechanisms involve the fluid, this is especially true.

The electric fields in each layer are calculated from the equation:

$$E_a = \frac{\kappa_b \kappa_c V}{t_a \kappa_b \kappa_c + t_b \kappa_a \kappa_c + t_c \kappa_a \kappa_b}$$

At the moment the electric field calculations are done after-the-fact, and the designs are adjusted iteratively to achieve the best possible field balance. A computer program to accomplish the same task (as well as the thermal analysis) is conceptually simple, although substantial programming effort would be required.

As part of the field balance design problem, it was thought to write a minimization routine to design a dielectric sandwich based on the following data:

- layer dielectric constants
- layer densities
- required energy density

The routine was to adjust layer thicknesses so as to minimize the electric field in each layer. The results were instructive but somewhat unexpected. It turned out that in any two layer system, the ideal layer thickness (given different layer dielectric constants) of one layer to minimize the fields is

zero. That is, a capacitor made of just one material always has lower fields in the dielectric than any two-material structure. The lesson is obvious: each layer type must give enough advantage to offset the increased layer fields.

3.4 MATERIALS

In the Dielectric Systems Selection section many materials were discussed. Designs were made during this task for capacitor systems composed of the following plastics:

- Polysulfone (P. J. Schweitzer)
- Kapton (DuPont)
- Mylar (DuPont)
- Polyvinylidene Fluoride (Kureha Chemical KF Film)

and the following papers:

- Regular kraft (Weyerhaeuser)
- Regular kraft (P. J. Schweitzer)
- Extra-strength kraft ("EIB Paper", P. J. Schweitzer)

Because of the very high price, large minimum purchase, and poor quality of thin films (as reported in TR-75-69), Kapton was not actually tested experimentally. The Weyerhaeuser paper had been in stock for some time, and was found to have worse electrical properties than the Schweitzer paper. This may have been due to storage conditions. Therefore, the Weyerhaeuser paper was used only with the Mylar to test tab insertion processes. Capacitors of every other combination (plastic-paper) were designed, built, and tested.

3.5 LAYER DESIGNS

The designs presented below in Table 26 are layer designs only. Details of other construction are to be found in the section on "Wrinkle Free Pads".

Design 1 was built out of non-optimized materials solely to test winding tab insertion, and extended foil termination techniques. It

was wound round and flattened after winding, or wound on small solid mandrels. All other designs were wound flat.

It is important to realize that each of these designs was conceived after the previous design had been built, tested, failed, and analyzed. There was no intention to produce any statistical data, as the data in Table 27 demonstrates.

TABLE 26. LAYER DESIGNS

Design	Film	Paper
I	2 - 100 ga Mylar	3 - 0.3 mil kraft
A	2 - 24 ga PS	3 - 0.4 mil EIB kraft
B	2 - 24 ga PS	3 - 0.4 mil EIB kraft
C	2 - 48 ga PS	3 - 0.4 mil EIB kraft
D	2 - 32 ga PS	3 - 0.3 mil kraft
E	2 - 50 ga PVF2	3 - 0.4 mil EIB kraft
F	2 - 50 ga PVF2	3 - 0.4 mil EIB kraft
G	2 - 100 ga PVF2	3 - 0.3 mil kraft
H	2 - 100 ga PVF2	3 - 0.3 mil kraft
I	2 - 32 ga PS	3 - 0.3 mil kraft
J	None	5 - 0.3 mil kraft
K	None	5 - 0.4 mil EIB kraft
L	2 - 48 ga PS	None
M	2 - metallized 24 ga PVF2	1 - 0.3 mil kraft

TABLE 27. PULSE TEST SUMMARY

39	Capacitors for Test
4	Basic Dielectric Combinations
16	Different Designs
30	Tested to Failure
37	Failure Analyzed
2	In Test

4.0 WRINKLE-FREE PADS

The work conducted under this task, to develop uniform wrinkle-free capacitor sections (or pads), is the heart of this entire program, because the individual pads are the building-blocks from which larger capacitors are constructed. The effort was approximately equally divided between development of fabrication processes and development of test methods.

4.1 WINDING WRINKLE-FREE PADS

Conceptually, the winding of wrinkle-free capacitors is not very difficult, because it would seem to consist largely of using greatly increased care and meticulousness. These factors are usually lacking in a production environment.

Wrinkles basically have two causes. The first is uneven tension control during the winding, which may be the result of dielectric web wander, uneven unreeling, or changes in winding speed. Actually, it is very nearly impossible to fabricate a completely wrinkle-free pad on a conventional winder. Second, after a pad is removed from the spindle it is flattened in a press, which causes wrinkles and other effects. To eliminate wrinkles the winding process must be redesigned and the flattening step eliminated.

This section outlines the basic methods for achieving wrinkle-free fabrication of two pad shapes. It is possible either to use a very small core and wind a cylindrical capacitor that does not need to be flattened to obtain the maximum packing factor, or to wind flat pads directly, eliminating all wrinkles.

The classic method of winding capacitors is basically very simple. A round split mandrel driven by a variable-speed motor is used to wind up

multiple layers of insulation and conducting foil. The insulation and foil are supplied from rolls mounted on friction-braked shafts. The purpose of the friction brake is to supply tension and reduce the bulk of the finished capacitor.

Figure 5 is a photograph of a typical split winding mandrel on a commercial winding machine. The foil and insulation are pinched in the split mandrel to facilitate startup. The mandrel is withdrawn from opposite ends of the capacitor pad when the winding is complete.

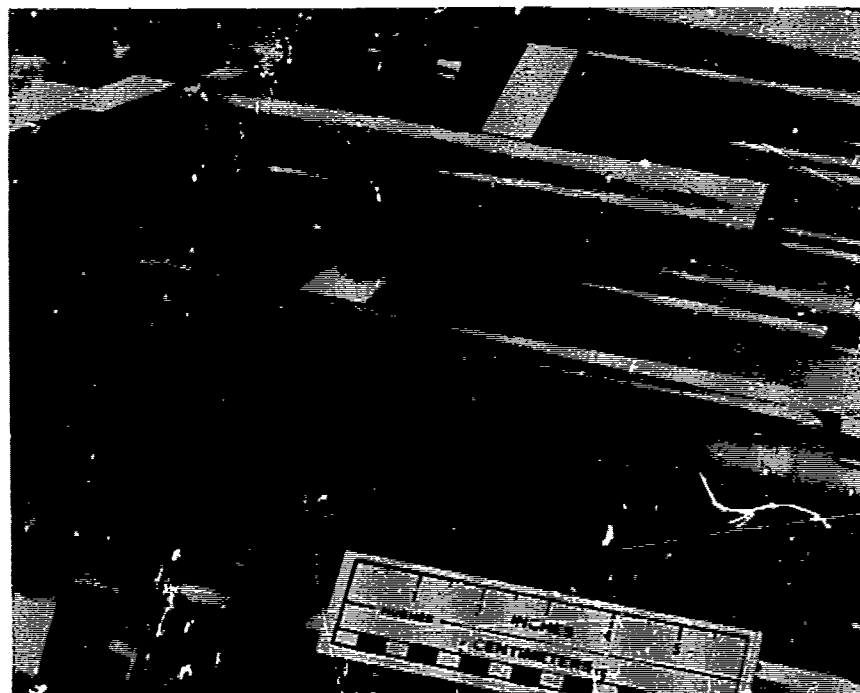


Figure 5. Split Mandrel

Figure 6 is a photograph of a typical friction brake (properly called a prony brake) on a commercial winding machine. The original tension controls consist of "V" groove pulleys which rotate with the supply roll of material. A round fabric belt is wrapped around the pulley and its tension is controlled by a swing arm over which the winding material passes.

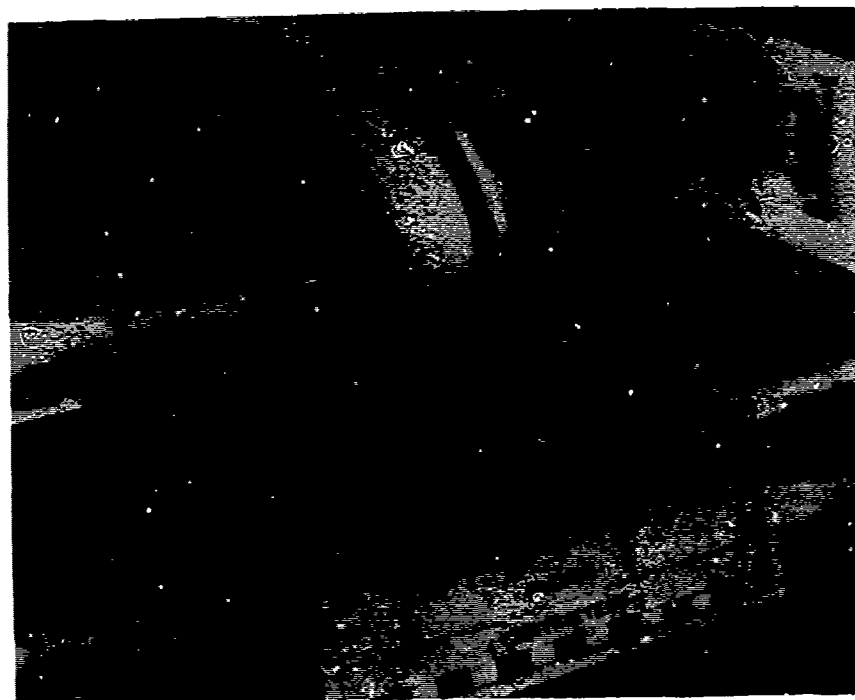


Figure 6. Typical Friction Brake

There are several basic problems with the drag friction approach to holding film and foil tension. There is a 3.6 to 1 ratio between starting friction and running friction. In addition there is almost a 2 to 1 variation of friction depending on the pulley speed. A plot for the machine illustrated in Figure 6 is given in Figure 7. If it becomes necessary to stop the winding operation to insert a tab, or make adjustments, the tension falls to zero.

The winding of large capacitor pads results in a roll that has large variations in tension throughout its cross section which promotes wrinkles.

The solution to the tension problem was found in the magnetic tape recording industry technology, where constant tape tensions are maintained over wide ranges of speed and of forward and reverse direction of transport through use of torque motors on the tape reels. For this purpose the conventional friction-brake supply spindles were replaced with supply spindles controlled by DC torque motors which cause the output-shaft torques to be proportional to the motor current and independent of speed and direction over a rather wide range.

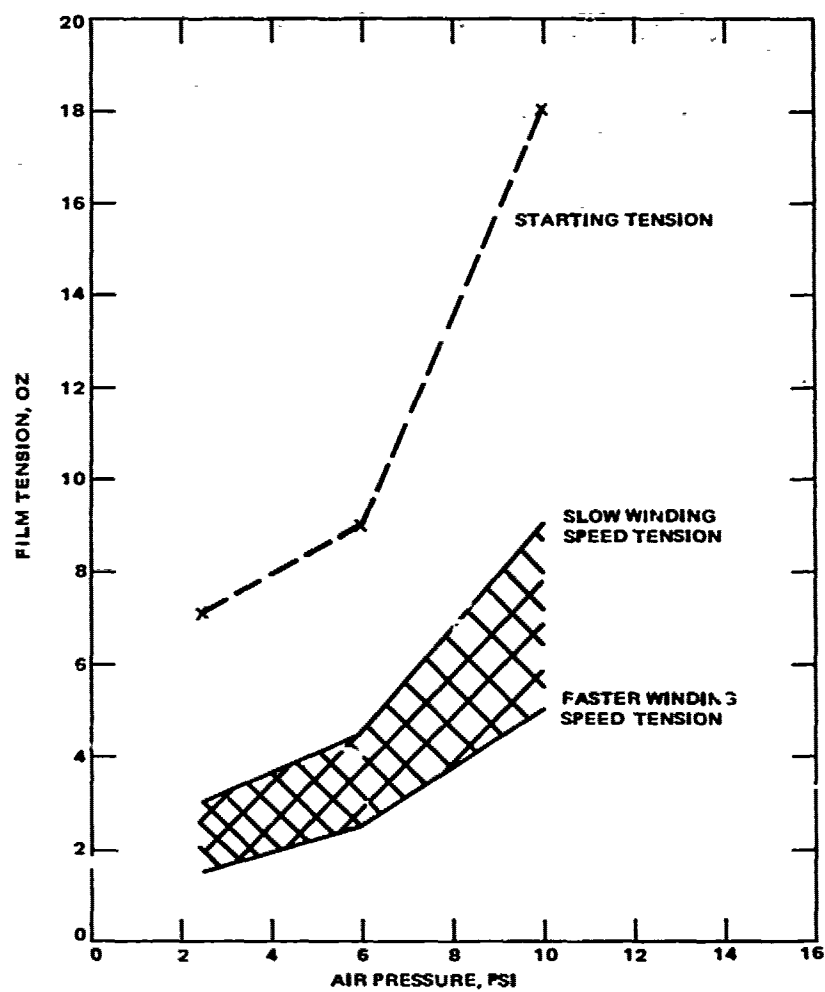


Figure 7. Capacitor winder friction brake tension characteristics.

The motor current is controlled with a solid state controller, and can be monitored on an ammeter. Thus the operator can exercise complete control of each spindle torque and may adjust the torque during the winding process.

Although the torque motor produces constant torque for a given input current, the diameter of the supply roll of foil or film changes. The net result is a change in foil or film tension. In order to compensate, the actual film tension is compared to a calibrated torsion spring and the error fed back to the torque motor. The system is a closed loop servo with a torsion spring as a reference. See Figure 8 for a simplified diagram.

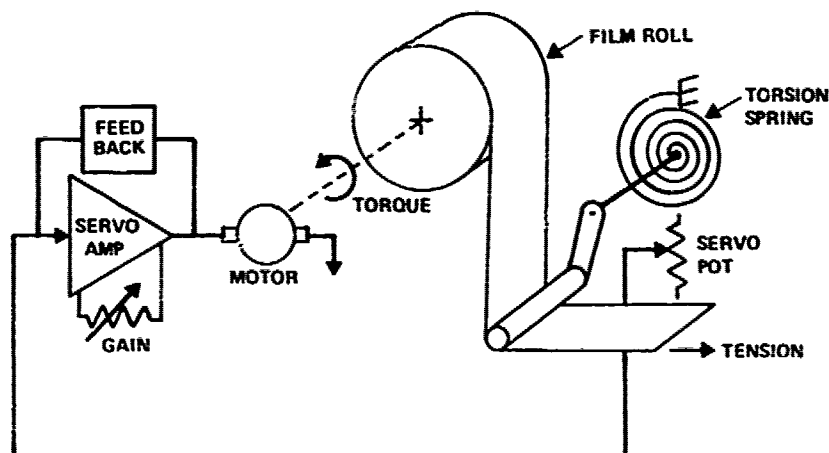


Figure 8. Single web servo control.

The original machine design did not provide for separating the foils and film after they were unreeled and before they were combined in the capacitor roll. Static charges were built upon the surface of the plastic films which attracted adjacent foils and films resulting in complete loss of tension control. The fastest moving film would drag all the adjacent films along and result in tucks or folds in the material that is feeding too fast, ergo wrinkles in the capacitor.

A series of fingers or posts had to be placed at strategic points to keep the films and foils from contacting until they are combined into the

capacitor. The location of the fingers can be seen in the photograph of Figure 9(a) and the drawing of Figure 9(b). Two combs are placed just before the windup mandrel to provide final control for the films and foils.

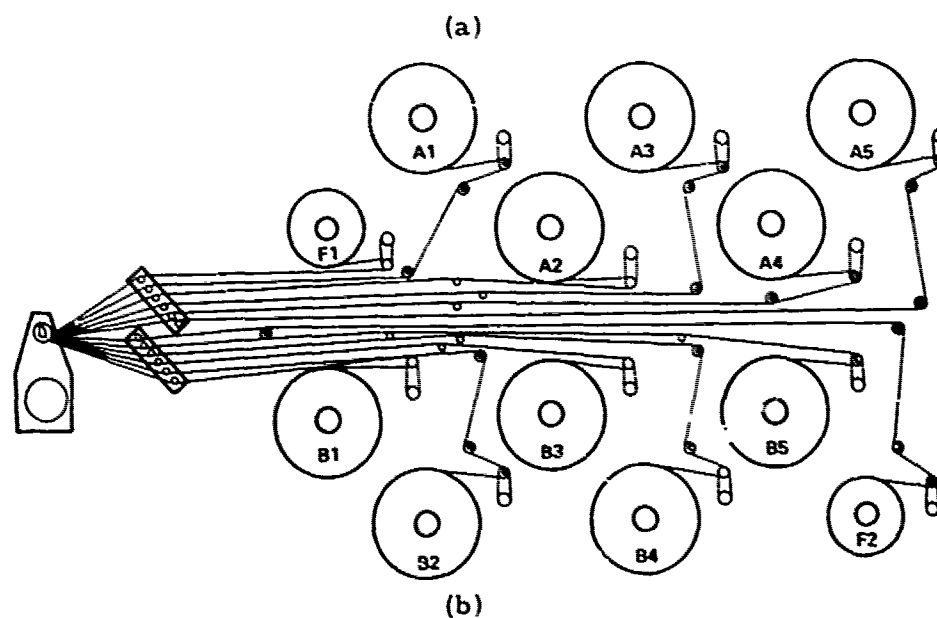


Figure 9. Revised winder web paths.

Figure 10 is a photograph of the back of the capacitor winder showing the torque motors, servo pots and electronics cabinet. Figure 11 is a photograph of the operator end of the machine showing the control panel for each individual spindle.



Figure 10. Rear of modified winder.

The following drawings are provided to show the details of the individual piece parts that were fabricated to complete the conversion of the capacitor winder. Each drawing is to be found in Appendix B.

Drawing H-7607 is a cutaway assembly of the spindle and torque motor drive.

Drawing H-7608 is a cutaway assembly of the tension arm control.

- H7579 Torque spring
- H7580 Dial clamp
- H7581 Adapter
- H7582 Shaft
- H7583 Bearing shaft
- H7584 Bolt
- H7595 Spacer



Figure 11. Operator position-modified winder.

H7586	Mounting plate (servo pot)
H7592	Drive bushing
H7593	Spindle drive assembly
H7594	Adjusting wheel
H7595	Spacer (torque motor)
H7596	Mounting plate (torque motor)
H7578	Roller assembly (tension arm)
H7587	Plate (drilling)
H7588	Spring drum
H7589	Spindle
H7590	Support shaft
H7591	Drive shaft

H7597 Plate (drill jig)
H7598 Electrical drawing
3393068 Mounting bracket torquer brake capacitor winder
3393069 Controller capacitor winder
3393072 Cabinet assembly capacitor winder

The problem of damaging the films and papers and causing wrinkles during the flattening procedure normally employed was solved by using a flat winding mandrel and winding the capacitor sections directly in a flattened configuration. The result is a section which is flat, but not stretched or wrinkled. This technique is only possible with a constant tension machine, because the velocity of the film and foil varies from zero to maximum and back to zero twice each revolution. Drawings H7603, 7604, and 7605 contain the details of the flat mandrel used for this work. The flat mandrel can be seen in the center right side of Figure 11, and at the left under the operator's left hand in Figure 9(a).

4.2 DRYING CAPACITOR PADS

Capacitor sections are normally dried at as high a temperature as is possible, so that the processing time is short. Some manufacturers pre-dry in air, but most dry in rough vacuum. Unfortunately, the quick drying cycle in itself causes the dielectric sandwich to wrinkle. The drying process was therefore examined to insure as dry a section as possible, but without wrinkles.

The principal problem is the kraft paper in the sandwich. Kraft normally contains 7% water, which is the equilibrium value for 50% relative humidity. Sadly, completely dry kraft is brittle, so the damp material must be wound into a pad and then dried. Upon drying, the kraft shrinks a few tenths of a percent in length and width, and several percent in thickness. Wrinkles are caused by uneven drying.

When a paper-plastic capacitor section is heated in vacuum, the moisture must escape out the ends of the pad at the tabs or other termination, because the plastic film barrier prevents any other moisture flow. If high temperatures are used to accelerate drying, a large moisture

gradient develops between the pad center and the ends. This gradient causes the paper to shrink unevenly, resulting in the wrinkles shown in Figure 12(a). For reference, a winding made on an unmodified winder and dried at high temperature is shown in Figure 12(b).

The gradient is reduced by drying for a longer time at a lower temperature. The result of such an experiment is shown in Figure 12(c). This pad was dried at 50°C compared with 125°C for Figure 12(a). Pads were also dried at room temperature in vacuum, and in nitrogen in dessicators. Both these methods produce wrinkle-free pads, but longer times are required.

That the pads were completely dry was confirmed by monitoring the dissipation factor during drying. An additional quality control step consisted of analysis of the impregnation fluid for water. Samples taken during filling were compared with samples taken after test, and no change was found.

4.3 CAPACITOR IMPREGNATION

Having gotten the capacitor sections dry without wrinkling them, one must fill them with dry, degassed, high resistivity fluid. The impregnation must be clean, total, and must not wrinkle the sections. Necessarily the drying and impregnation are carried out as a single step, so the process design must take this into account.

The equipment which was ultimately heavily modified to achieve these results was a standard type fluid impregnator manufactured by Red Point. It consisted of a capacitor chamber, a side loader for the fluid, and a very high capacity pump. Unmodified, it delivers fluid to the capacitor which is dirtier and of lower resistivity than that with which it is loaded.

It was decided on the basis of initial experiments that the only practical way to use this equipment for high-resistivity impregnation was to continuously filter and purify the oil under vacuum in the machine. When the capacitors were ready for impregnation, the fluid would be diverted

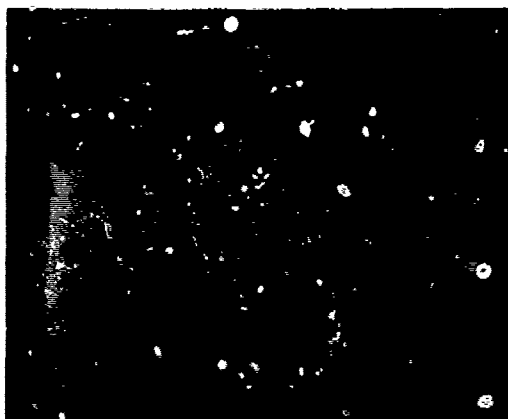


Figure 12(a). Wound-flat stack.

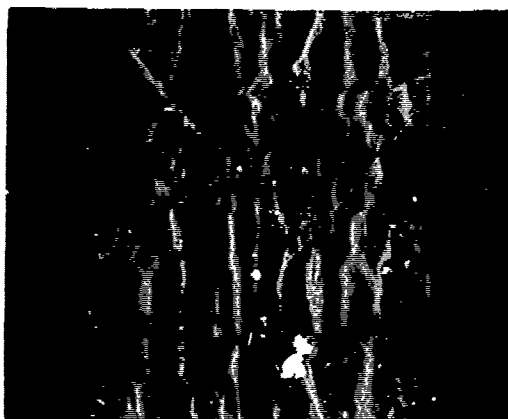


Figure 12(b). Wrinkled dielectric stack.

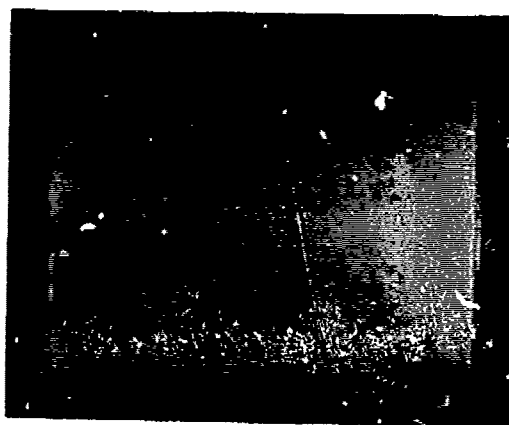


Figure 12(c). Special drying.

from its cycle loop and poured into the capacitors. In this way, the purest possible fluid would be obtained for the capacitors.

The modified filter loop is schematically depicted in Figure 13. The entire circuit, as well as the chamber (not shown) in which the capacitors are dried, is maintained under vacuum by the large process pump attached to the machine. The added lines and recirculating pump have no exposed metal parts, so as to minimize the chance of introducing metal particles into the fluid.

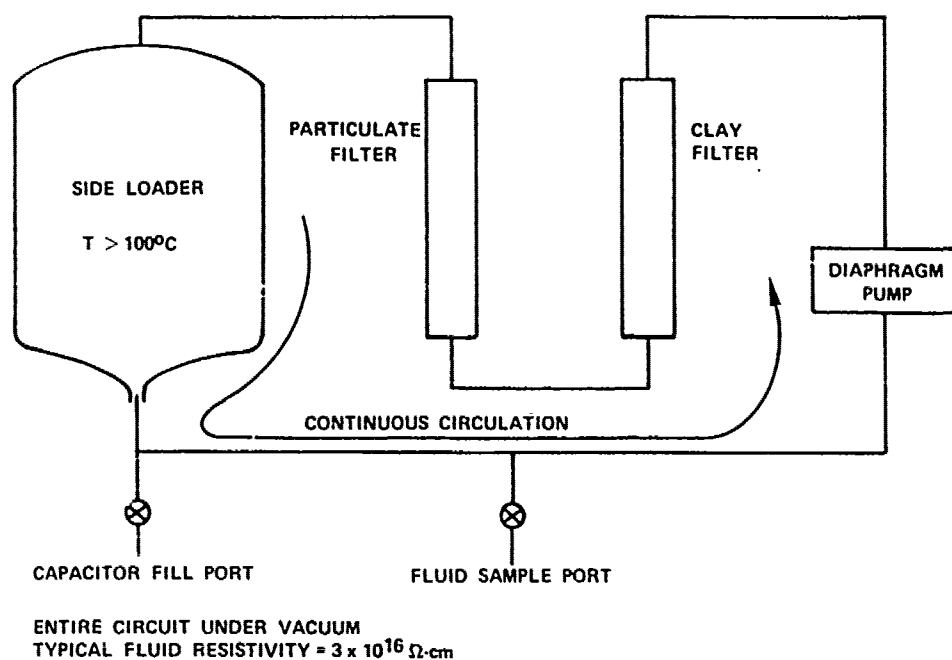


Figure 13. Fluid process cycle.

The impregnation procedure is straightforward. The side-loader is filled with fluid, and the capacitors to be filled are placed in the main chamber. Vacuum is obtained in both areas, and the fluid is heated, filtered, and degassed. The fluid is sampled at the end of this cycle to be sure it is sufficiently pure, and the capacitors are monitored for dissipation factor to make sure they are dry. When all conditions are right, the capacitors are filled with the clean fluid. A detailed procedure for this entire operation is found in Appendix C.

4.4 PAD TEST CONFIGURATION

The physical configuration in which the individual pads were tested was designed to duplicate conditions in a full-sized capacitor. Because general purpose reusable cans were used, it was necessary to make a capacitor pad support fixture which did not rely on can wall contact, as a conventional capacitor would.

A complete assembly of a $1.1\mu\text{F}$ pad is shown in Figure 14. At the upper left is a complete unit ready for test. The component parts of the can are in plastic bags, as delivered from the cleaning laboratory. A typical pad is shown in the center, and a pad completely mounted is shown at lower right. A detail of the mounted pad is shown in Figure 15. The epoxy-glass boards and compression screws simulate the packing into a stiff flat-sided can. The copper strap provides a low-inductance structure to allow pad testing using an exact PFN waveform. The two holes in the strap attach to two bolts in the lid of the reusable can.

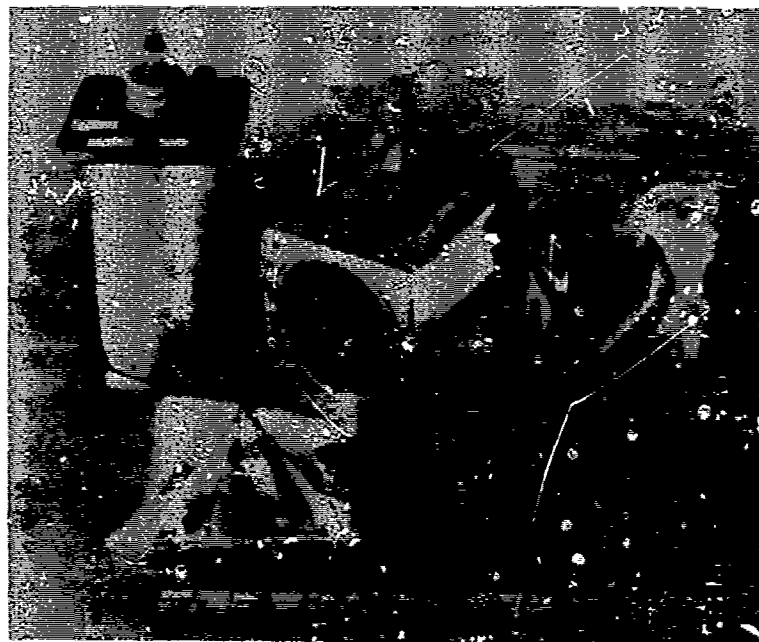


Figure 14. Test pad assembly and can.

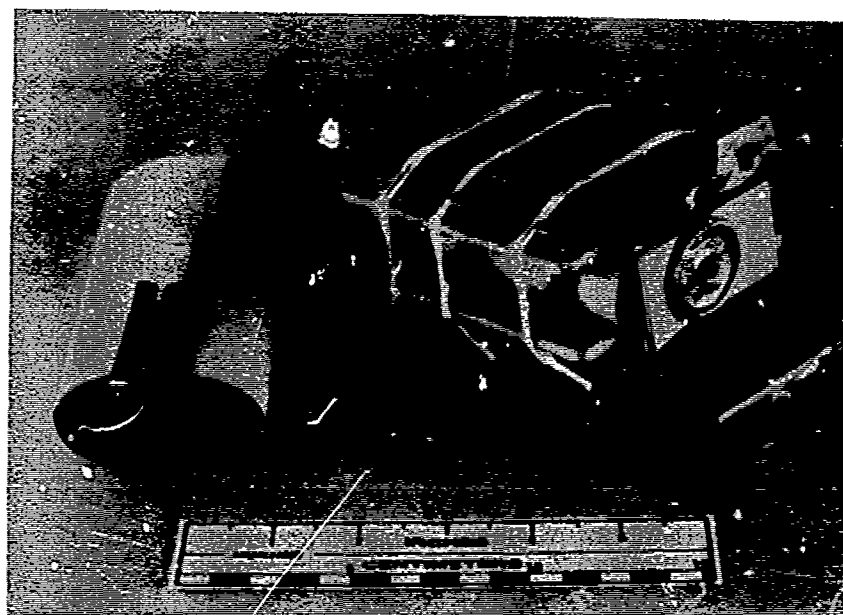


Figure 15. Test pad detail.

4.5 FAD TEST CIRCUITS

To perform valid tests on these specialized PFN components, it was necessary to use a current discharge waveshape representative of actual PFN service. Thus, the work specified as Task 7 - PFN Operating Environment was performed in support of this design. The equipment actually used to test pads, and that which will be used to test full-sized capacitors, meets the requirements of Task 7 as well as those of Task 3.

4.5.1 Analysis

A computer program for transient analysis was used to generate a plot of actual discharge current in a capacitor used in a 6-section PFN. Such a plot is shown in Figure 16 for a 20 μ s output pulse. Analyses were conducted for both the 20 μ s output pulse and the specified 20 μ s current discharge pulse (see Appendix A).

After the actual waveshapes had been obtained, they were decomposed into their Fourier components. Table 28 shows the values for a 1.1 μ F pad operated at 300 pps with a 20 μ s discharge pulse. Using these values, a simple test waveform containing the correct components was constructed. This waveform is shown in Figure 17, for a typical test specimen.

TABLE 28. CAPACITOR CURRENT SPECTRUM

	Charge	Discharge					All
		f_1	f_2	f_3	f_4	f_5	
Frequency KHz	0.15	12.5	25.0	37.5	50.0	62.5	-
Current Amps RMS	2.9	26.4	28.2	16.3	8.6	5.3	46.5

4.5.2 Pulse Test Apparatus

To obtain the waveform shown in the previous section, a resonantly charged modulator-type circuit with a series-resonant load was employed. A simplified circuit is shown in Figure 18. The capacitor under test is resonantly charged by the DC supply through the charging choke while the HY-5 hydrogen thyratron is open. The thyratron is then triggered, and the test capacitor discharges through the load and inductor, the RLC product controlling the waveshape. Various clipper and blocking diodes control reversal and ringing, and prevent damage to the HY-5 tube.

In order to achieve the correct waveform, it was necessary to design an extremely low inductance load. The use of this component allows the waveshape to be tailored to a variety of widths by the adjustment of the external series inductor. An exploded view of the load is shown in Figure 19. There are 16 rod resistors inserted into the hollow tubes. The current travels down the resistor and back through the tube, thus providing a low inductance path. Cooling is provided by air forced down the center of the resistor, back over the outside, and thence to exhaust. This load handles 70 kW continuous, 220 kW burst, and has an inductance of less than 20 nH. The resistance is varied to fit the test situation by changing elements.

An overall view of the high voltage parts of the pulse test apparatus is shown in Figure 20. The load is on the right, the inductor and test

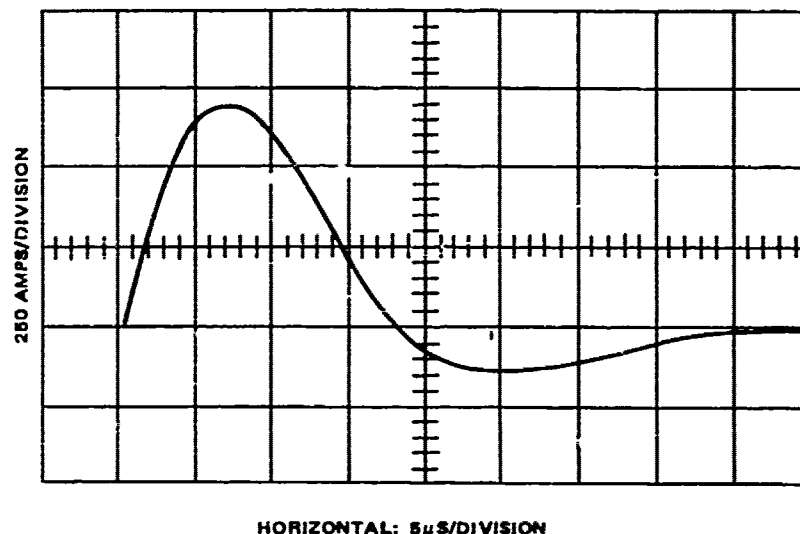


Figure 17. Discharge current waveform.

capacitors in the center, and the switch on the left. Because the tests were run in the burst mode, four vacuum contactors were used to switch 4 capacitors sequentially. This speeded up the pulse testing. Figure 21 shows a better view of the load and contactors.

The controls, interlocks, and monitors were housed in another high voltage cage area, and are shown in Figure 22. The DC supply is on the right, the control units in the center, and the waveshape monitor on the left. The upper part of the control box panel (with the 4 meters) housed the HY-5 controls and interlocks, as well as the capacitor voltage monitor. The lower part housed the driver, clock circuitry, and rate controls. The following capacitor parameters were monitored:

- Internal temperature
- Charging current ($\pm 0.1\%$)
- Capacitor voltage ($\pm 0.1\%$)
- Number of pulses

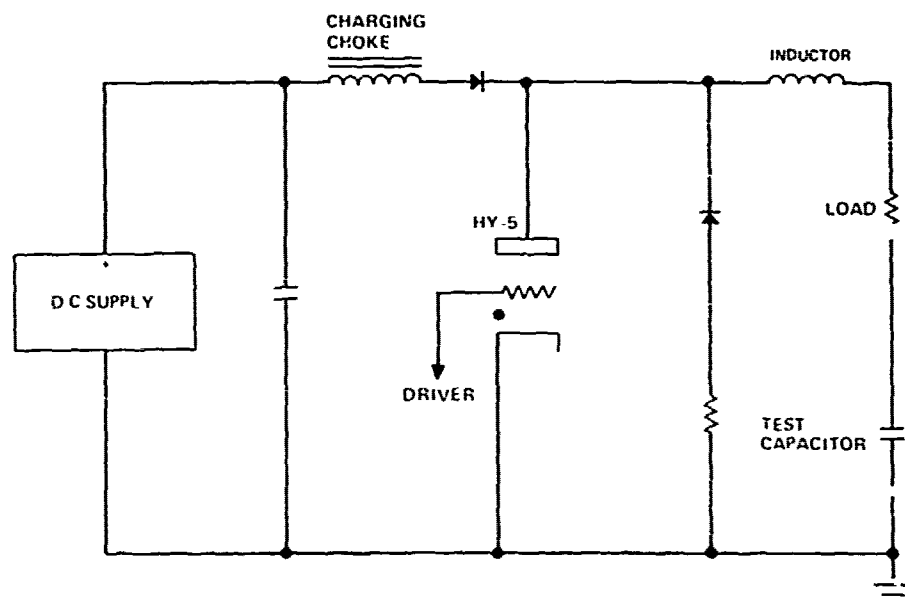


Figure 18. Pulse tester simplified circuit.



Figure 19. High power load components.



Figure 20. High voltage section of pulse test.

The capacitor voltage was obtained by a sample and hold circuit triggered just before each discharge.

4.6 CORONA TEST ACTIVITY

Because of Hughes extensive favorable experience with corona tests as a life-predictive technique, it was decided to test the 1.1 μF pads to see what could be learned. To do this, it was necessary to heavily modify a standard Biddle corona test set.

Two modifications were performed. It was necessary to develop a resonator to allow the Biddle power supply to generate a high AC voltage across the large specimen. It was also found necessary to do much work to increase instrument sensitivity and lower power supply noise. This was important because the sensitivity varies as the inverse of the sample capacitance.



Figure 21. Pulse test load and contactors.

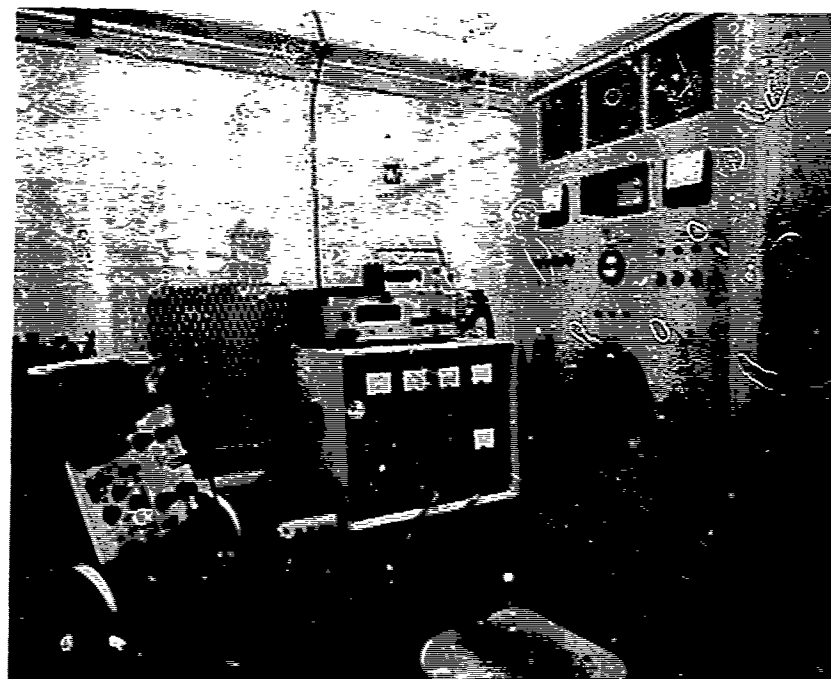


Figure 22. Pulse test controls.

The test circuit for the resonator is shown in Figure 23. This unit is tunable over the range 0.9 to 1.2 μF . The large tapped inductor and the isolation capacitor operate at high voltage, and are therefore housed in an oil tank. They are shown before immersion in Figure 24. This circuit produces a 60 Hz sine wave, which never crosses zero, as in Figure 25, to simulate actual PFN voltage operation. It may also be operated in an unbiased mode, to simulate standard AC operation.

An overview of the equipment is shown in Figure 26. The rack at the left contains the corona pulse counter, the low-voltage parts of the resonator and its controls, and power conditioning apparatus. The center section is the modified Biddle unit. The resonator tank is out of sight to the right, the connection entering thru the large port at the top right.

This modified unit can test capacitors in the range 0.9 to 1.2 μF up to 15 kV (peak) in the non-zero-crossing mode. Its sensitivity at 2:1 signal to noise is 40 pC for that capacitance range. The unmodified unit had a 1000 pC sensitivity for the same samples.

The data taken using this apparatus have been consistent and puzzling. A new capacitor shows an acceptably high corona reading, but after pulsing the corona inception voltage falls to below 1 kV and remains there indefinitely. This is attributed either to bubble formation or to impregnant degradation,

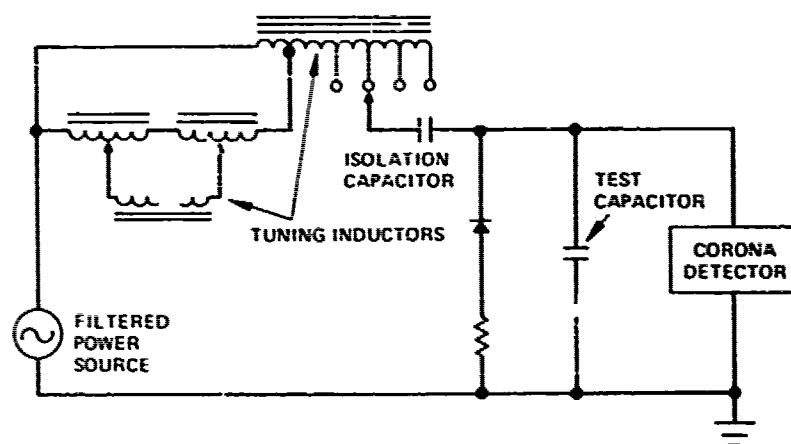


Figure 23. Corona test circuit.

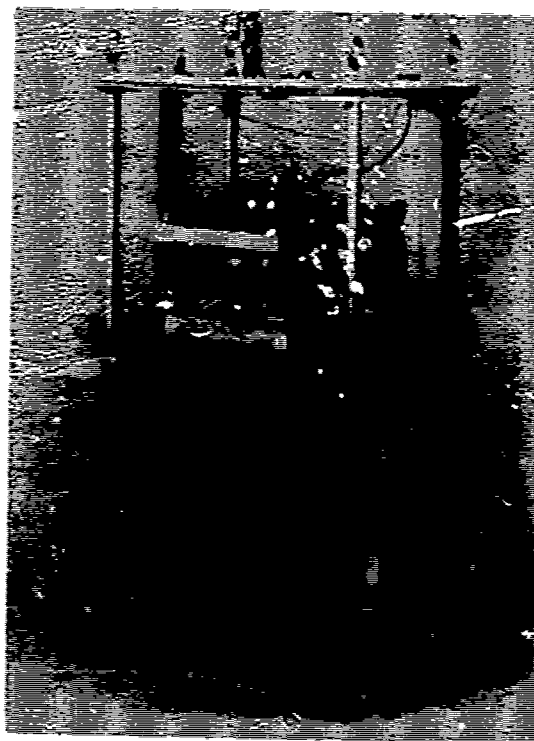


Figure 24. Corona test resonator.

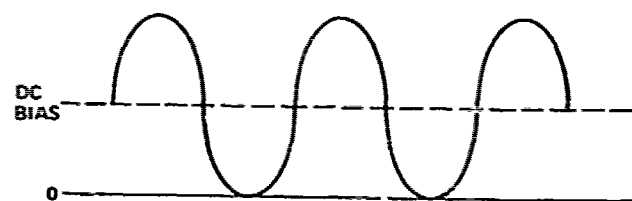


Figure 25. Biased corona test waveform.

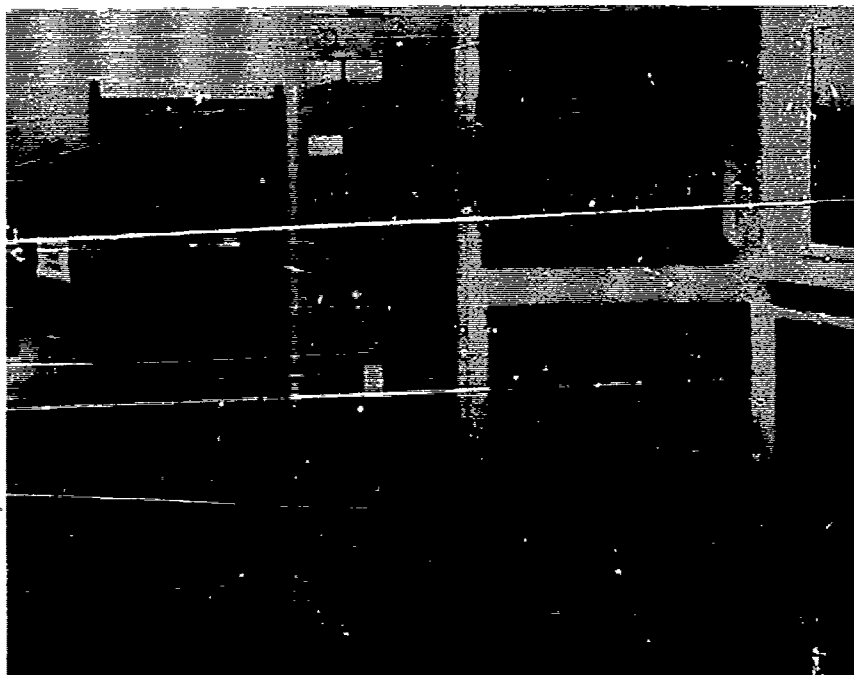


Figure 26. Corona test system.

and has been previously reported in the literature. Nevertheless, the project team is not comfortable about either the data or the explanation.

4.7 PULSE TEST RESULTS

4.7.1 Summary

This section contains data and analyses obtained during the pad pulse life tests conducted in 1976.

All tests were run with the equipment described in Section 4.5.2, using a 20 μ s wide current discharge pulse for the capacitor, per the requirement of Appendix A. The pulse reversal and harmonic content simulated a PFN where this pulse width might be obtained.

The following summarizes the test effort:

Number of capacitors:	39
Number tested (pulse):	37
Number of designs:	16
Total shots run:	10,034,000

4.7.2 Introduction

As discussed previously, an interactive design-test-design program was employed, so that each design was the result of the previous work and problems. A very large amount of data was taken during the test effort, and unfortunately it will only be possible to present summaries of portions of it here. Much of the data was taken to help in the design process. Examples are:

- Internal operating temperature
- Leakage vs T
- C and DF vs T and f
- Corona measurements

Some of this data was extremely helpful, other portions less so.

Two unique efforts bear mention. The first was a glass-encased capacitor (serial No. 17) for use in checking mechanical motion. This test, shown in Figure 27, was conducted by pulsing the capacitor while observing the end with a long-focus microscope. It was found that the improved winding process produced a section with no motion larger than 1 mil, a data point corroborated by the lack of noise during operation. The second unique experiment was the analysis of the gas produced by one of the PVF2 components (serial No. 26). The gas was collected and analyzed with a mass spectrometer. It was found to be primarily H_2 , with almost no combustion products. It was apparently produced by the high-field gassing of mineral oil because of the large field imbalance in the PVF2 component. This effect has been previously reported.

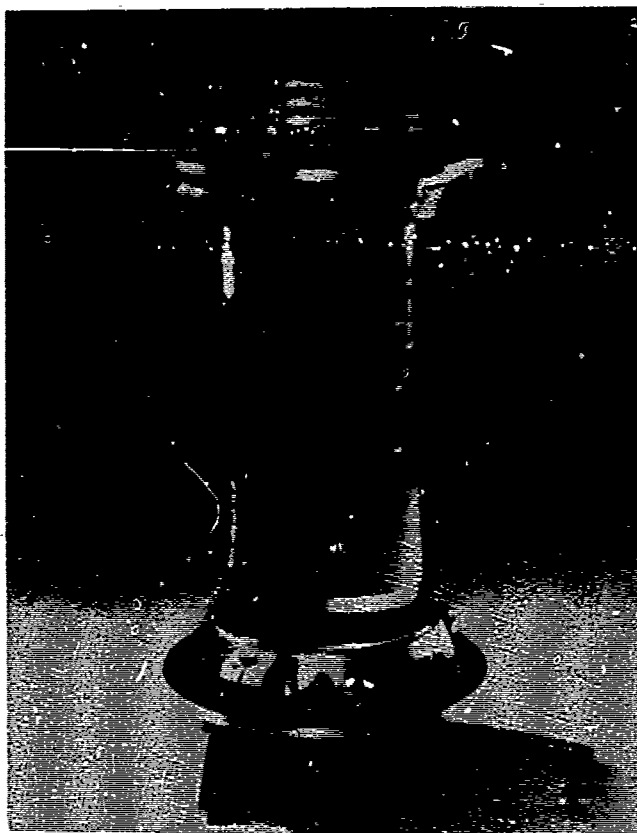


Figure 27. Glass-encased capacitor for observing section motion.

4.7.3 Test Data

The following are summaries of the pulse test data collected during this program. In each section, the designs are first described, and then the life-test data presented. Energy density is discussed in the final section and related to the individual tests.

4.7.3.1 Initial Tests

These tests were run using Mylar/kraft designs to test the winding process and termination techniques. A number of changes and adjustments were made as a result, the most important being the use of a larger than normal flag on the tab to eliminate the oil pocket above the flag in conventional construction. This pocket breaks down at high stress and the damage appears to have been caused by a faulty flag.

All designs were interleaved layers 4.5 inches wide with 3.675 inch foils, wound flat. Five layer construction of 2 sheets 1 mil Mylar and 3 sheets 0.3 mil kraft was used. The kraft was not very high quality, but these tests were not for energy density. The data is shown in Table 29.

TABLE 29. INITIAL TESTS

Serial	Rate	Voltage (kV)	Life (10^3 shots)	Failure	Duty
1	300	4	100	None- disassembled	C
2	300	4	216	None- disassembled	C
3	300	7	20	top tab	1/15
4	300	5	209	top tab	1/15
5	300	5	525	top tab	1/15
6	300	7	20	top tab	1/15
7	300	5	1,964	none	1/15
8	300	5	3,000	none	1/15
9		Step to 11	300	edge	1/15

C \equiv continuous duty

1/15 \equiv 1 minute on, 15 off

The dramatic improvement in 7, 8, and 9 was obtained by using larger flags on the tabs and by arranging tab placement so that none overlapped.

4.7.3.2 High Density Tests

These tests were conducted using the materials selected in Task 1. All capacitor sections used 4.5 inch wide insulations and 3.675 inch wide foils, except designs D1, D2, and M. The impregnant was mineral oil (Golden Bear GB-100M). The layer designs are shown in Table 30.

Sections from serial 15 onward featured internal thermocouple temperature sensors mounted at the section center. This data was used to adjust duty cycles to avoid overheating. The thermocouple leads can be seen just to the lower right of the high voltage insulator of test section 28, shown in Figure 28. In most cases a shorter rest period than that specified in Appendix A is possible.

The test data is presented in Table 31, for all high energy density sections. The notation "step" means a higher voltage at each burst or group of bursts. The voltage given next to "step" is the last voltage at which a burst group was successfully completed.

Serial 17, the glass unit, has not been extensively tested because the container is slightly leaky. Designs J and K were assembled to examine all-kraft units of dimension similar to the PS/kraft units. Serial 25 gassed excessively, and had the gas bled off and analyzed. It is still operational. Designs D₁ and D₂ were devised to eliminate corona damage at the winding start and finish. Design L was to see how good the mineral oil impregnation process was in an all-film capacitor, while design M examined a method of eliminating foil edge corona damage by using metallized films next to the foil. L was successful. M was not, but the technique shows promise.

TABLE 30. HIGH DENSITY LAYER DESIGNS

Design	Film	Paper
A	2-24 ga PS	3-0.3 mil kraft
B	2-24 ga PS	3-0.4 mil ElB kraft
C	2-48 ga PS	3-0.4 mil ElB kraft
D	2-32 ga PS	3-0.4 mil ElE kraft
E	2-50 ga PVF2	3-0.3 mil kraft,
F	2-50 ga PVF2	3-0.4 mil ElB kraft
G	2-100 ga PVF2	3-0.4 mil ElB kraft
H	2-100 ga PVF2	3-0.3 mil kraft
I	2-32 ga PS	3-0.3 mil kraft
J	None	5-0.3 mil kraft
K	None	5-0.4 mil ElB kraft
L	2-48 ga PS	None
M	2-metallized 24 ga PVF2	1-0.3 mil kraft

D1 - design D with folded ends
 D2 - design D with sandwiched ends.

Notes:

- 1) Kraft, ElE kraft, and Polysulfone from Peter J. Schweitzer Div, Kimberly-Clark.
- 2) PVF2 from Kreha Corporation of America.
- 3) All foil 0.25 mil Republic Electro-Dry.



Figure 28. Top of reusable can showing thermocouple lead wires for external temperature measurement.

TABLE 31. HIGH ENERGY DENSITY TESTS

Serial	Design	V(kV)	Rate	Burst	Life ($\times 10^3$)	TC	Corona	Comments
10	A	5	300	1/10	305	No	No	
11	A	5	300	1/10	209	No	No	
12	A	5.5	300	1/60	95	No	No	
13	C	8	200	1/30	60	Yes	No	TC trouble
14	C	8	200	1/60	90	Yes	No	Oil leak
15	D	Step 7	300	1/30	737	Yes	Yes	
16	D	4	300	1/30	310	Yes	Yes	Did not fail
17	E	V	V	V		No	Yes	Glass unit
18	B	Step 6	300	1/30	159	Yes	Yes	
19	B	6	300	1/30	54	Yes	Yes	Did not fail
20	B	6	300	1/30	100	Yes	Yes	Did not fail
21	E	6	50	1/60		Yes	Yes	
22	E	5.5	50	1/60	50	Yes	Yes	
23	F	6	50	-	14	Yes	Yes	
24	F	Step 5	50	1/60	122	Yes	Yes	Did not fail
25	G	Step 9	50	1/60	81	Yes	Yes	Did not fail*
26	G	Step 9	50	1/60	100	Yes	Yes	Did not fail**
27	H	Step 7	50	1/60	54	Yes	Yes	
28	H	7	50	1/60	240	Yes	Yes	Did not fail
29	I	7	300	1/60	25	Yes	Yes	
30	I	6	300	1/30	100	Yes	Yes	
31	J	6	300	-	16	Yes	Yes	
32	J	6	150	1/60	12	Yes	Yes	
33	K	6	100	1/60	60	Yes	Yes	
34	K							Not tested
35	D1	6	300	1/30	170	Yes	Yes	
36	D2	Step 7	300	1/30	180	Yes	Yes	
37	L							Not tested
38	J	Step 5	300	1/30	486	Yes	Yes	
39	M							Destroyed in corona test

Notes: *Subsequently destroyed when run at 300 pps by mistake
 **Gassy

4. 7. 3. 3 Energy Density

As these units were tested in large cans designed to be durable and reusable, it was not considered a good measure of energy density to use finished component weight in the calculations. Therefore, for each design both the "Active Energy Density" as defined in equation (2) on page 51 and the "Pad Energy Density" as defined in equation (3) on the same page are reported. The "Active Energy Density" takes into account only the weight of the dielectric actually storing energy, while the "Pad Energy Density" takes into account the foil weight. The "Pad Energy Density" is lower, more realistic, and sensitive to changes in the layer designs.

The values reported for Arochlor or DOP impregnant were obtained by measurements of capacitance change on pads of the appropriate design. No pulse testing was conducted using these pads. These values are reported, nevertheless, to give an idea of the difference between the results obtained using different impregnants.

For each design, the voltage listed in Table 31 is used. For step stress tests, the highest voltage is used.

4. 7. 4 Failure Mechanisms

The most-commonly-reported capacitor failure mechanism, corona failure at winding wrinkles, was completely eliminated by the new winding methods. The majority of the capacitor failures from serial 10 onward were at the foil edge, halfway along the winding length (from start to finish), in the center of one of the flat sides. During the development process three mechanisms other than failure at wrinkles were encountered, and these are discussed in this section.

The first failures of the Mylar/kraft capacitors appeared to be caused by foil irregularities or material defects in the vicinity of a tab connection. Components 1 and 2 were therefore tested until a 1% rise in charging current was noticed, at which time they were disassembled and examined. The mechanism found by this technique is illustrated in Figure 29. The figure shows a section through a tab termination made in the conventional way. The oil in the pocket formed by the short flag was breaking down opposite the other foil edge. This problem was cured in units from serial 7 onward by using a flag the same width as the foil to eliminate the oil pocket.

TABLE 32. ENERGY DENSITY

Design	Energy Density J/lb				Energy Density J/kg			
	Active		Pad		Active		Pad	
	M	A	M	A	M	A	M	A
A	160	187	116	135	353	412	255	297
B	131	151	100	119	290	344	220	262
C	133	150	107	121	293	331	236	266
D	146	170	113	132	321	375	249	291
E	135	163	110	133	297	359	243	294
F	95	117	80	98	209	257	176	216
G	110	129	98	115	242	284	215	253
H	86	99	75	87	189	217	166	191
I	203	232	151	173	446	511	332	380
J	204	272	147	196	449	598	323	432
K	115	153	89	118	253	336	196	261
L	211	211	137	137	464	464	302	302

M = Mineral Oil Impregnant
A = Arochlor (PCB) or Dioctyl Phthalate (DOP) Impregnant

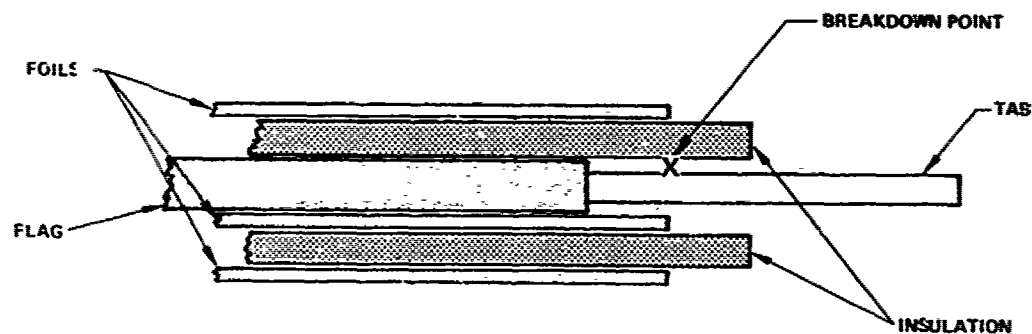
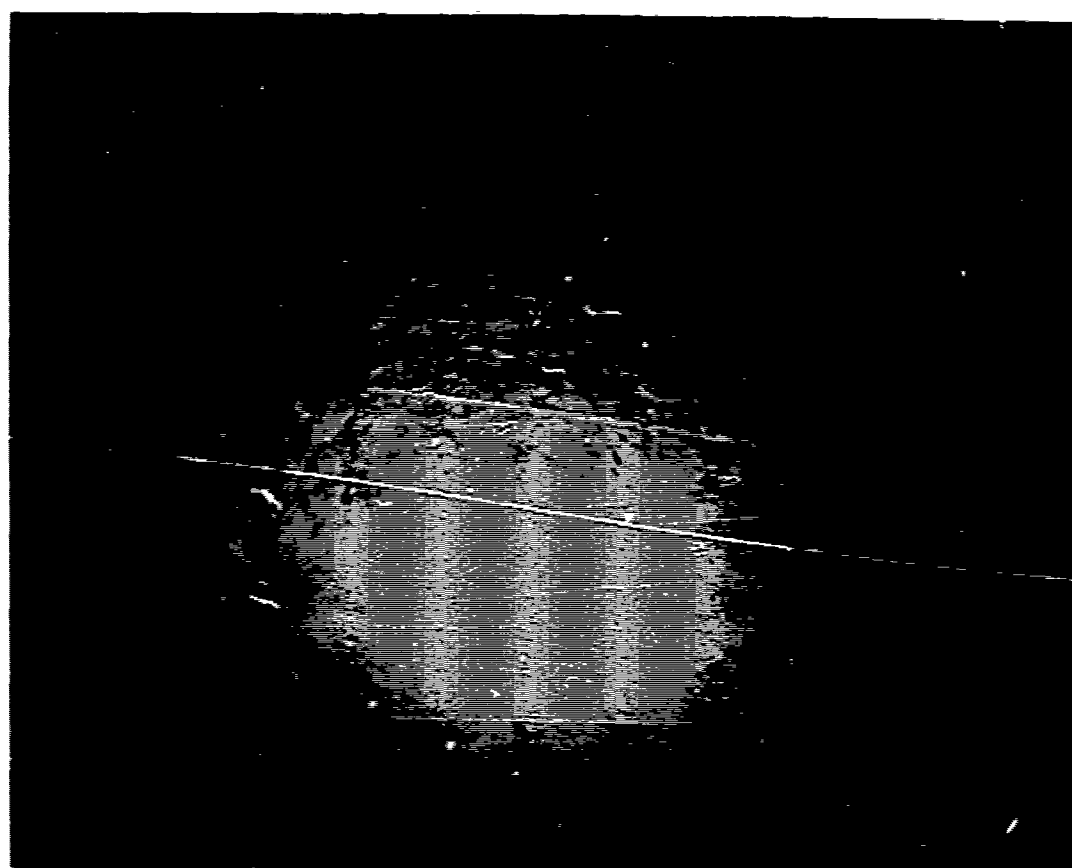


Figure 29. Tab breakdown mechanism.

In the first PS/kraft units, a cloudiness of the PS film at the foil edges was observed upon disassembly. This cloudiness was most pronounced in areas corresponding to the center of the flat sides of the section. Figure 30 shows this effect. The polysulfone was overheated, shrank, and stress-relieved itself through the formation of the tiny diamond-shaped holes. The overheating was judged to be caused by conduction or corona in the excessive amount of oil present at the centers of the flat sides near the foil edge. An improved clamping fixture was devised to more perfectly duplicate conditions in a real capacitor, and this effect disappeared.

Capacitors from serial 10 onward failed principally from uniform corona along the edges of the foil. This effect is shown in Figure 31. The burns occur only in the paper, not in the film. Eventual failure occurs at the weakest point. A complete analysis has been completed on this problem. More work was done on this program in this area.

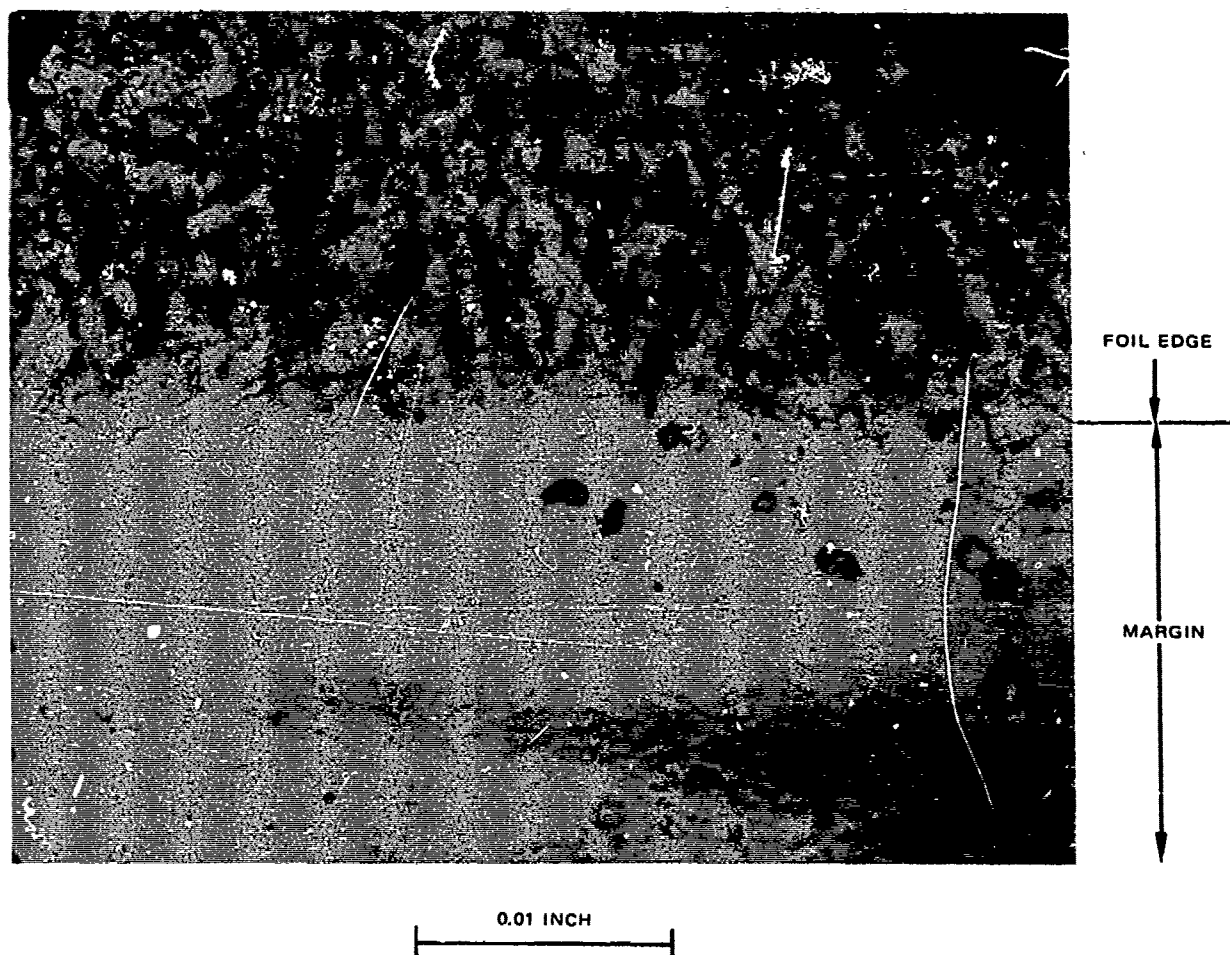


0.01 INCH



(a)

Figure 30(a). Polysulfone edge damage.



(b)

Figure 30(b). Polysulfone edge damage.

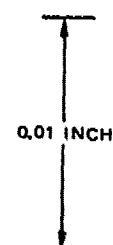
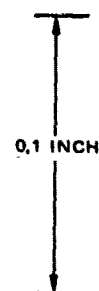
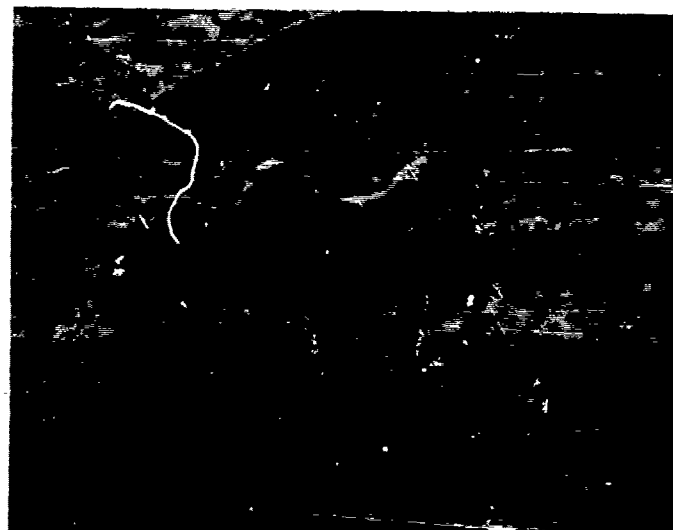


Figure 31. Corona damage edge of foil.

5.0 CAPACITOR DESIGNS

This section presents the design details for the two different 15 kV components which were built and tested. These components were designed for high repetition rate operation, and differ in the impregnant, the electrical stress, and the energy density.

The heavier of the two components, P/N 014, was designed directly from the results of the pad tests, and was placed in a conservative, well-constructed metal box such as is normally used on military-type components of that size. The lighter component, P/N 026, utilized a different impregnant and field balance, and was encased in a very lightweight stainless steel case, which was designed as part of the case weight minimization study.

5.1 PART NUMBER 014

The initial capacitor was designed using directly the results of the layer designs and pad testing described above, with a substantial case and ample safety factor.

5.1.1 Layer Design and Number of Pads

The layer design was chosen on the basis that as large an energy density as possible must be achieved, but that some safety factor must be used because the use of a multiple pad design was anticipated. Referring to Table 30, it can be seen that the designs suitable for high repetition rate use are A, B, C, D, I, and L. Referring to Table 31, it can be seen that the highest successful operating voltage for any of these designs was 8 kV for design C, and those tests were not particularly successful. Therefore, a 3-series-pad arrangement was chosen.

The 3-series-pad arrangement means that each pad operates at 5 kV. The energy densities at 5 kV for the candidate designs are shown in Table 33. These data are extracted from Table 32. Designs A and L were not chosen because not enough safety margin existed and, particularly for design A, they are more difficult than average to wind. Of the remainder, design B was selected over design I because of better life test data. The layer configuration chosen was, then, 3 layers of 0.4 mil EIB kraft interleaved with 2 layers of 24 gauge (6 μ m) polysulfone, impregnated with mineral oil.

To achieve the required capacitance in a 3 series section arrangement, it is necessary to use 3 series pads with value 6.6 μ F each. A quick calculation showed that these would be physically very large pads, and so two parallel strings of 3 3.3 μ F pads were used, as shown in Figure 32. (It had been proved in previous experience that it was unwise to attempt a pad that was thicker than half the width. This configuration presumably allows more non-uniform oil pockets and therefore a greater risk of failure. For this particular combination of winding mandrel and insulation thickness, the 3.3 μ F is the largest safe value.)

The field balance for this design was calculated, using techniques previously displayed in Section 3.3. A series of experiments designed to determine the thickness of the individual fluid layers between layers of solid dielectric had arrived at the value 0.3 mil (7.6 μ m) for the total average thickness of the six fluid layers present between foils in a five layer design. This value was used in the field balance calculations, the results of which are

TABLE 33. HIGH RATE LAYER DESIGN ENERGY DENSITIES AT 5 kV

Design	Highest Test Voltage (kV)	Energy Density at 5 kV
A	5.5	211 J/kg
B	6	152 J/kg
C	8	92 J/kg
D	7	127 J/kg
I	7	169 J/kg
L	5	302 J/kg

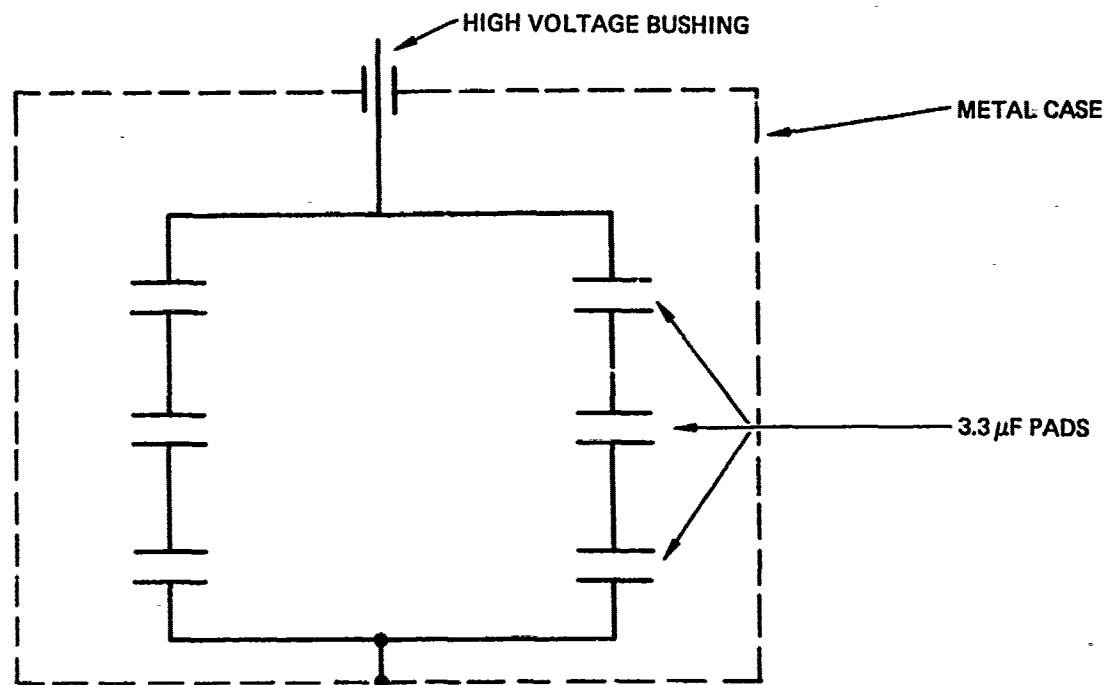


Figure 32. Internal schematic, P/N 014.

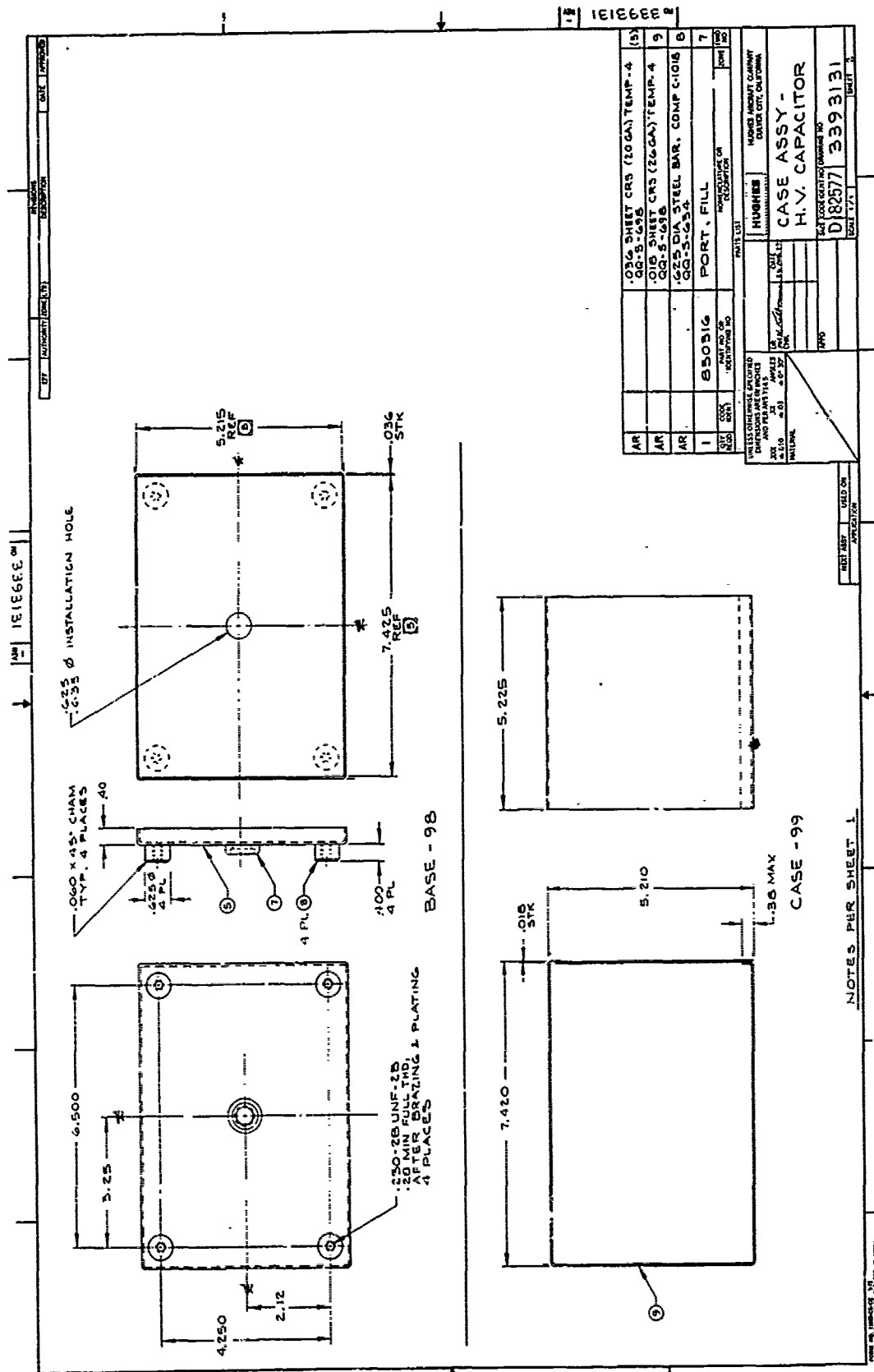
shown in Table 34. The values indicate that neither the paper nor the plastic are unreasonably stressed. The field in the fluid is high, but because of the extraordinary thinness of the fluid layer (0.05 mil or 1.2 μm) produced by the carefully controlled winding the fluid will stand the stress.

5.1.2 Packaging Design

For simplicity, these components were wound with the same material widths used in the pad tests. The can to be used was designed around the finished capacitor pads, and is shown in Figure 33. The case insulation and interior packaging was conservatively designed, and is shown in Figure 34.

TABLE 34. CALCULATED FIELDS FOR P/N 014

Material	Thickness (mil)	Field (V/mil)
Oil	0.3	4113
Polysulfone	0.48	2918
Kraft paper	1.2	1904



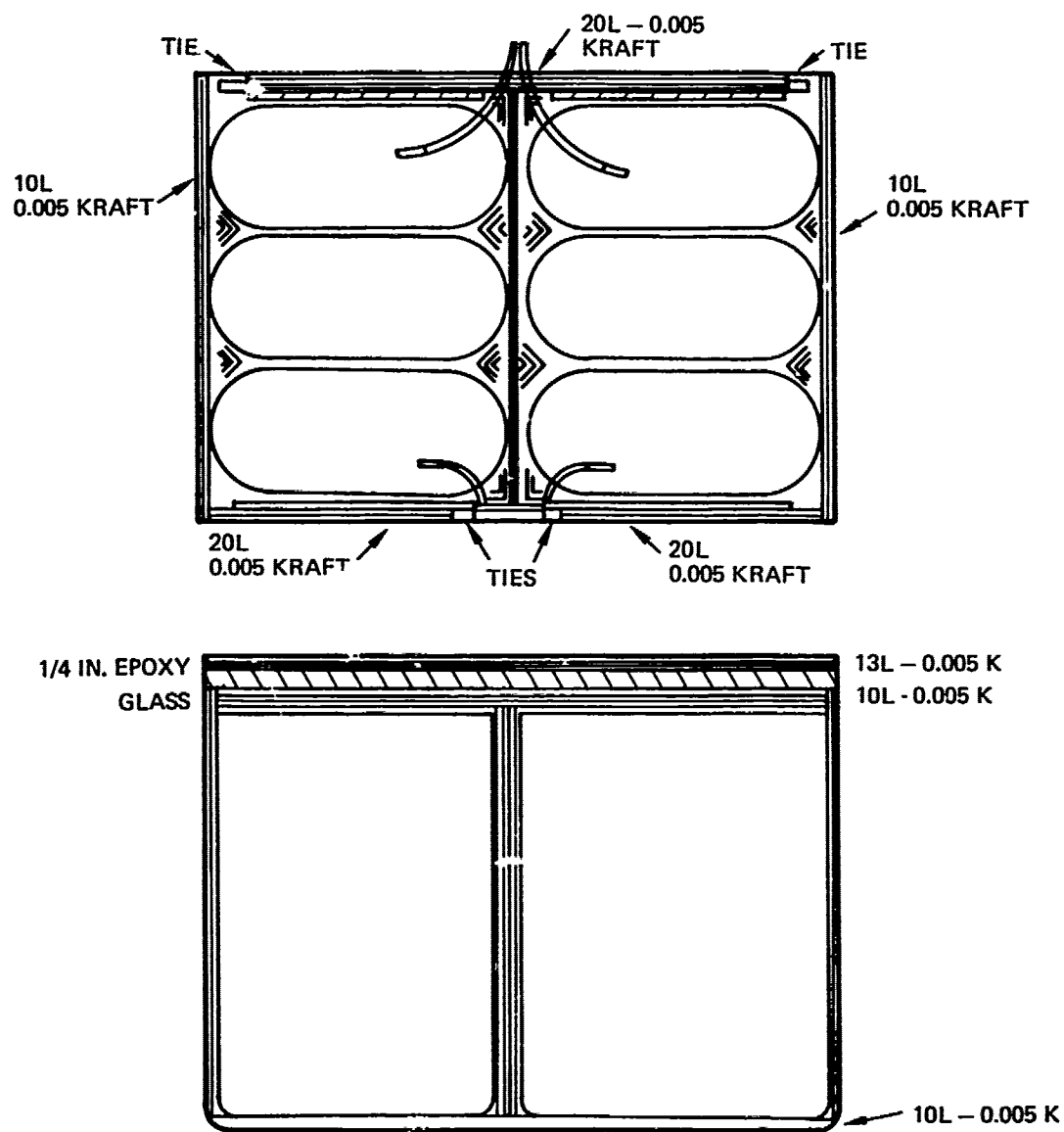


Figure 34. Packaging Design, P/N 014

5.1.3 Design Weight Summary

The design weights of the various parts of this capacitor are shown in Table 35. The actual capacitors came to this weight within a few percent. The average packaged energy density was 48 J/kg (21.7 J/lb).

5.2 PART NUMBER 026

This component was designed to be as light as possible, consistent with meeting the electrical specifications. A super light case, designed as part of the case weight minimization study, was used. The impregnant was changed to improve the field balance, and the stresses were increased.

5.2.1 Layer Design and Number of Pads

It was thought the dielectric element most likely to break down in service if highly stressed was the oil. In the pad testing it had been found that the maximum average oil field was about 5200 V/mil for useful life. Therefore, ways of increasing the pad energy density while keeping the oil field below this value were investigated. The result was the use of the same layer design as the 014 part, but with dioctylphthalate instead of mineral oil to improve the field balance.

Two strings of two 2.2 μ F pads in series were used, with the section voltage then being 7500V. The field balance for this design is given in Table 36, where it is compared to the values found for the 014 component (operated at 5 kV/section). The field values for the paper and polysulfone are about at the largest reported operating fields for those materials,

TABLE 35. WEIGHT OF CAPACITOR PARTS, P/N 014

Item	Weight (kg/lb)
2-3 pad bundles	2.63/5.79
Case and terminal	9.5/2.1
Epoxy board	0.29/0.64
Case insulation	0.25/0.56
Oil	1.09/2.4
Total	5.22/11.5

TABLE 36. FIELD BALANCE FOR P/N 014 AND 026

Material	Field (V/mil)	
	014 (5 kV/section)	026 (7500V/section)
Oil	4113	2961
Polysulfone	2918	5266
Kraft paper	1904	3430

while the field in the oil is substantially reduced. This is electrically a much better design than P/N 014.

5.2.2 Packaging Design

These pads were wound with margins reduced to the minimum. This was accomplished by increasing the foil width to 4.0 inches, leaving 0.25 inch margins. The can was made from 5 mil stainless steel, and is shown in Figure 35. There is very little interior insulation.

5.2.3 Design Weight Summary

The design weights of the various parts of this very lightweight capacitor are shown in Table 37. The average energy density was 169 J/kg (77 J/lb), and the true energy density was 0.21 J/cm³.

TABLE 37. WEIGHT OF CAPACITOR PARTS, P/N 026

Item	Weight (g)
2-2 pad bundles (wet)	1126
Case	120
Bushing	50
Case insulation	70
Extra oil	100
Total	1466g/3.2 lb.

6.0 CAPACITOR FABRICATION AND TEST

While the statement of work called for the fabrication of twenty capacitors to a single specification, it was felt that more information would be gained if a quantity of each of two designs to the same electrical specification were fabricated and tested. Therefore, fifteen of the 014 part and twelve of the 026 part, for a total of 27 components, were fabricated. It was desired to be able to use either component in the PFN described in Section 10.0, so six capacitors of each type were held out of testing in this task. Nine 014 units and six 026 units were tested. In addition, two special components were made using 014 pieces: one to test high voltage airborne connectors, and one to check out the pulse test bay.

6.1 CAPACITOR FABRICATION

The two types of capacitor were fabricated using all the procedures, processes, and equipment developed earlier in the program. In addition, special drying schedules and impregnant purification techniques had to be worked out for the dioctylphthalate used in the 026 component.

6.1.1 Winding and Termination

The capacitors were wound on the constant tension machine using a 1.5 inch wide flat mandrel, as shown in Figure 36. Winding information is given in Table 38. The very last component built of the 014 was wound using 5 tabs per foil, to test both the regularity of the insulation structure with 10 total tabs and the differences in tab heating when carrying large currents.

The packaging design for the 014 component was previously shown in Figure 34. The packaging used for the 026 is shown in Figure 37. Each



Figure 36. Constant tension winder.

TABLE 38. WINDING DATA, 014 AND 026

Item	014	026
Insulation length	1108	642
Foil length	1068	542
Margins	0.437	0.250
Tabs per foil	2*	2
Tab separation	360	180
Insulation width	4.5	4.5
Foil width	3.625	4.0
Finished dimension L	4.6	4.6
W	3.5	2.53
D	1.55	1.075
Capacitance (μF)	3.3	2.2
All dimensions in inches.		
*014 S/N 15 had 5 tabs per foil.		

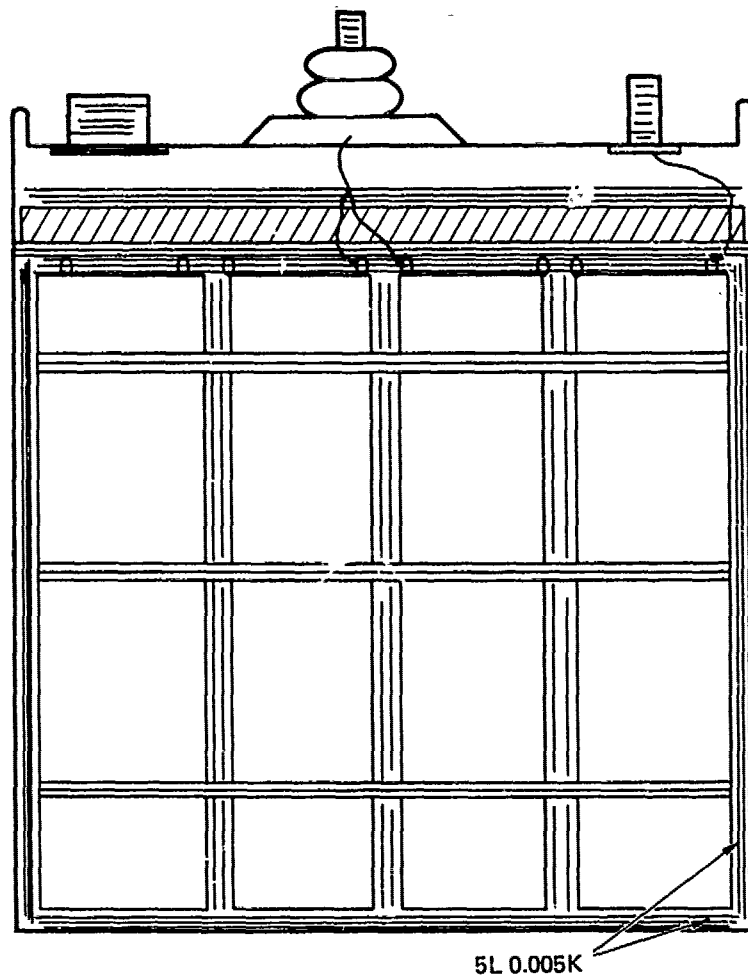


Figure 37. Packaging of 026 unit.

section had two tabs per foil, all tabs emerging from the same end of the section. The capacitors were assembled into cases, described in the previous section, and made ready for impregnation.

6.1.2 Drying and Impregnation

Two problems were encountered which caused deviations from the previously established procedures. It was found that it was very difficult to fully dry an assembled 014, because of the large volume and small case fill hole. Also, additional purification steps had to be taken with the dioctylphthalate.

6.1.2.1 Drying

The large 014 units contain a substantial volume of very tightly wound kraft paper, which is approximately 7 percent water by weight. The fill orifice in the can is only 1/8 pipe. When the components were vacuum-dried and the dissipation factor monitored, it was found that insufficient drying was taking place, presumably because of the low pumping speed of the pads and orifice. Simultaneously, it was found that the time it took for water to reabsorb into a once-dried wound stack was of the order of 10s of hours. Therefore, the components were dried with the bottom lids removed from the can. They were then quickly removed, had the lids attached, and replaced in the vacuum chamber, at which time they were further dried. Monitoring of the dissipation factor during the drying cycle assured dry components.

6.1.2.2 Fluid Purification - DOP

The dioctylphthalate (DOP), as received, had a volume resistivity of about $5 \times 10^{10} \Omega\text{-cm}$. It was found that circulation in the system shown in Figure 13, but bypassing the clay filters (as is normally used for mineral oil) was insufficient to raise the resistivity. The clay filters were therefore used.

Two facts about DOP emerged during a series of tests. First, it was found that the water content did not contribute materially to the low resistivity (although there is an adverse long-term effect when the fluid contains water). Second, it was found much harder to purify DOP, a high dielectric constant liquid, than mineral oil, a low dielectric constant liquid. This is attributed to the relative ease with which a high dielectric constant liquid dissociates molecules into ionic charge carriers. The final resistivity achieved for DOP was $2 \times 10^{12} \Omega\text{-cm}$, compared to $1 \times 10^{16} \Omega\text{-cm}$ for mineral oil.

6.1.2.3 Impregnation

Excepting the changes discussed in the subsections above, the components were dried, impregnated, and sealed according to previously developed procedures.

6.1.3 Acceptance Data

The two finished component types are shown in Figure 38. The final static measurements are shown in Table 39 for the 014, and Table 40 for the 026. It is worthwhile to note the very small differences in capacitance, dissipation factor, and leakage in these components, particularly since every component built is reported. A statistical analysis is shown in Table 41.

A capacitance standard deviation of only 8 percent amongst all 014 parts manufactured is remarkable, and is primarily due to the good control of the winding, and to the binding before encasement (if the 5-tab experiment is eliminated this value is only 6 percent). Note that the 5-tab per foil capacitor has a much lower dissipation factor than the other units. The 026 parts had even better uniformity.

6.2 CAPACITOR TEST

Before testing could begin, a number of modifications were necessary to change from the 1.1 μF 7.5 kV max pad testing to 2.2 μF 15 kV max capacitor testing. After these modifications were made to the pulse test unit, the capacitor testing was carried out.



Figure 38. Pulse capacitors 014 (left) and 026 (right), 2.2 μF 15 kV.

TABLE 39. FINAL MEASUREMENTS, PART NUMBER 014

Ser No.	Date Impreg'd	Cap (μ F)	D. F.	DC Leakage 10 K \bar{V} DC (μ A) (3 mins)	Weight (lbs.)
1	10/27/77	2.42	0.43%	1.35	-
2	10/27/77	2.35	0.45%	1.35	11.6
3	10/27/77	2.36	0.43%	1.35	-
4	5/30/78	2.36	0.49%	1.60	11.6
5	5/30/78	2.38	0.50%	2.25	11.6
6	5/30/78	2.36	0.51%	1.5	11.6
7	5/30/78	2.34	0.50%	1.3	11.6
8	6/9/78	2.90	0.65%	2.0	11.5
9	6/9/78	2.39	0.48%	1.6	11.5
10	6/9/78	2.34	0.47%	1.5	11.5
11	6/9/78	2.36	0.47%	1.55	11.5
12	6/16/78	2.31	0.47%	1.5	11.5
13	6/16/78	2.34	0.47%	1.65	11.5
14	6/16/78	2.32	0.47%	1.55	11.5
15	6/16/78	2.96	0.36%	5.9	11.4

TABLE 40. ACCEPTANCE DATA, PART NUMBER 026

Serial	Capacitance (μ F)	Dissipation Factor, %	Leakage Current (μ A) 10 kV - 3 Minutes	Weight (kg)
1	2.302	0.40	3.9	1.704
2	2.315	0.40	4.1	1.696
3	2.327	0.40	4.5	1.697
4	2.328	0.39	4.2	1.700
5	2.317	0.39	4.4	1.697
6	2.305	0.39	4.0	1.705
7	2.322	0.39	4.5	1.702
8	2.316	0.40	5.2	1.704
9	2.315	0.40	4.3	1.706
10	2.322	0.39	4.4	1.703
11	2.332	0.39	4.5	1.689
12	2.319	0.39	4.7	1.700

TABLE 41. ANALYSIS OF ACCEPTANCE TEST DATA

	Capacitance	DF	Leakage
Mean Value	2.43/2.318	0.473/0.394	1.575*/4.392
Standard Deviation	0.20/0.008	0.061/0.005	0.26* /0.34
Values displayed for P/N: 014/026. *Excluding S/N 15.			

6.2.1 Test Stand Modifications

Four basic changes were necessary to test the larger valued components. A more powerful power supply was needed, capable of 8 kV at 10A or more. The load resistors had to be changed, so that the test waveform, obtained from an LRC resonant circuit, remained the same. A higher-capacity switch tube was required. Finally, all the overload cut-outs, clipping circuits, and current metering circuits had to be adjusted for the higher current. Because the original design of the test bay anticipated the need to make these changes, the modifications proceeded easily.

The new larger power supply was designed and built in-house, and was not charged against the contract. It provides 0 to 8.5 kV at up to 11A to the resonant charging circuit. It was designed to operate from 3 phase 400 Hz power, to avoid harmonic resonances of 60 Hz at higher repetition rates. The load change merely involved the replacement of the rod resistors in the air-cooled load with a new value. A block diagram of the system is shown in Figure 39. For these tests, the HY-5 tube was replaced with an HY-5001.

During the course of the modifications it was desired to test the packaging of the 014 part, before the changeover of the test bay to the new capacitance value. Therefore, a twin 1.1 μ F capacitor, identical to the 014 except for the extra terminal, was made. This is shown in Figure 40.

6.2.2 Test Results

The plan of test as prescribed by the statement of work was more of a proof-of-design (POD) test than a developmental test. Inasmuch as it was felt that this work had not progressed to the point of blithely attempting a POD test, as exemplified by the two different component types, a developmental

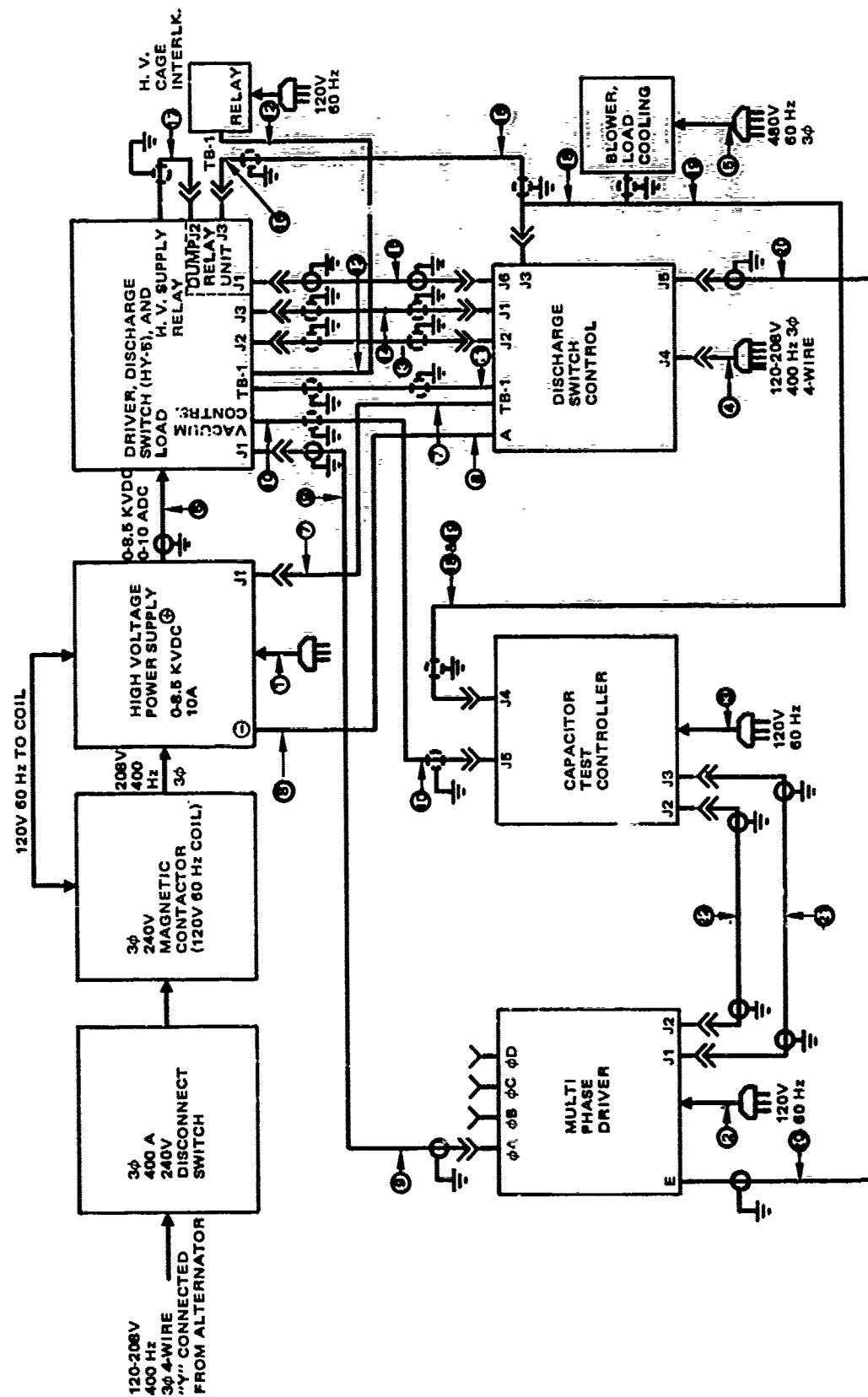


Figure 39. Capacitor pulser block diagram.

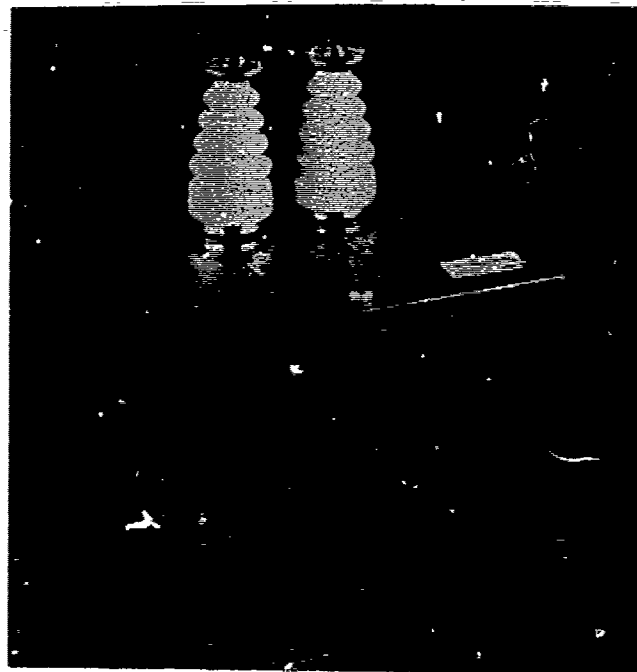


Figure 40. Twin 1.1 μ F capacitor
for pulser check-out.

type test was used. The 014 components were quite rugged, the 026 less so but better than one might expect given the fearful electric fields.

6.2.2.1 Test Summary, P/N 014

The summary of pulse testing for this part type is given in Table 42. Number 2 was the painted demonstration unit, and number 15 was the experimental 5-tab unit.

Temperature rise data was taken on one capacitor during a test of four, by attaching a thermocouple to the center of the capacitor end. The outside case temperature rise was 3 to 5 degrees C at the end of the burst, and 25 degrees after a 30 minute wait. This was the peak case temperature rise observed.

TABLE 42. PULSE TEST SUMMARY, PART NUMBER 014

Serial Number	Total Shots (1000s)	Voltage (kV)	Notes
1	233	15.0	OK
2	Not tested		
3	220	15.0	OK
4	223	15.0	OK
5	11	6.5	Failed
6	113	12.5	Shorted
7	107	15.1	OK
8	32	4.0	Failed
9	56	7.5	OK*
10	51	7.5	OK*
11	52	7.5	OK*
12	51	7.5	OK*
13	50	7.5	OK*
14	51	7.5	OK*
15	-	7.5	Failed

*Capacitors screened for use in PFN.
Duty was 330 pps for 1 minute, 2 hours between bursts, or equivalent.

6.2.2.2 Test Summary, P/N 026

The summary of pulse testing for this part type is given in Table 43. An extra unit was held out for the PFN testing, giving 7 capacitors for that use. It was found that running 3 bursts at half voltage was an excellent screen. If the component survived these, it would also perform at full voltage.

Temperature measurements here revealed a 26 to 30 degree rise, as might be expected from the higher energy density.

6.2.3 Failures and Failure Analysis

Of the twenty-six components tested, there were six failures, four 014 and two 026.

The 014 failures normally occurred at the end of a burst, and in two cases resulted in severely distended cans. No fluid leakage occurred,

TABLE 43. PULSE TEST SUMMARY, PART NUMBER 026

Serial Number	Total Shots (1000s)	Voltage kV	Notes
1	32	15.0	Failed
2	146	13.5	Failed
3	187	14.0	OK
4	49	7.5	OK*
5	156	14.0	OK
6	176	14.0	OK
7	51	7.5	OK*
8	51	7.5	OK*
9	67	7.5	OK*
10	51	7.5	OK*
11	50	7.5	OK*
12	51	7.5	OK*

*Capacitor screened for pulse forming network.

however. Serials 5 and 8 were found to have been bulk failures, while serial 6 was an edge failure. Serials 5 and 8 could have been screened with the half-voltage test. Serial 15, the experimental 5-tab unit, failed at a tab because of poor insertion. The individual pads in unit 6, which had handled the highest power, showed slight discoloration of the insulation at the places where the tab passed through the margin.

The 026 failures both occurred at the foil edge, and neither resulted in appreciable distension of the can. The characteristic puncture is shown in Figure 41. Pronounced discoloration and stiffening of the dielectric material around the tab was found in S/N 2, the longest-lived component, as shown in Figure 42. A curious effect, apparently related to either the high field or the use of the impregnant, was also found.

A cross-section of the construction of a tab termination is shown in Figure 43. It was found that many small holes appeared in the capacitor foil wherever it contacted the flag. This was true for both tabs on both foils, but the effect was most pronounced under the ground tab. An overview scanning electron micrograph (SEM) is shown in Figure 44(a). A close-up of one of the hole structures is shown in Figure 44(b). One thought to occur was that

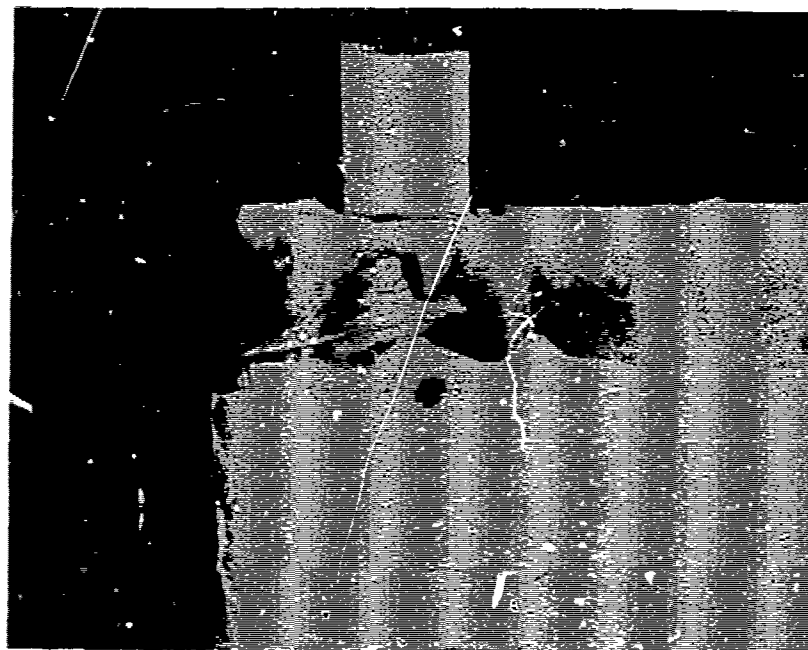


Figure 41. Edge failure in 026 unit, S/N 2.



Figure 42. Discoloration of dielectric near tab,
026 unit S/N 2.

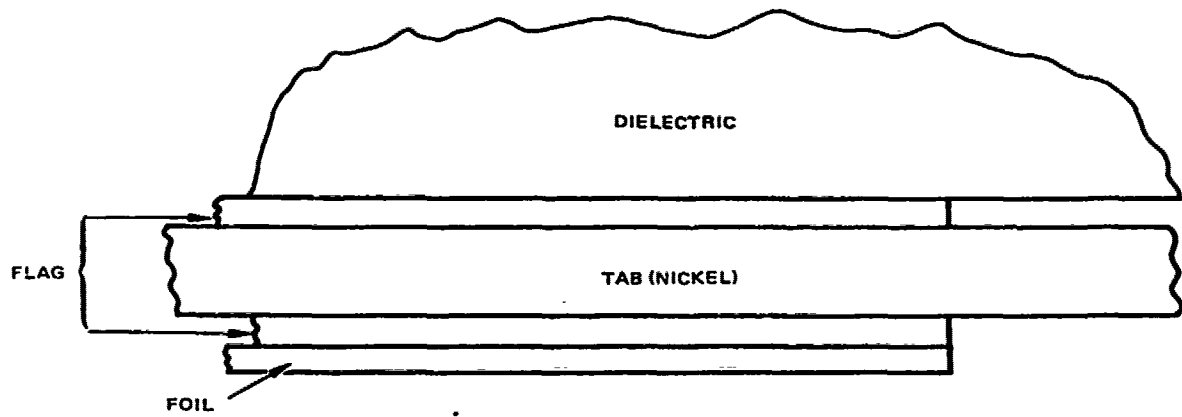
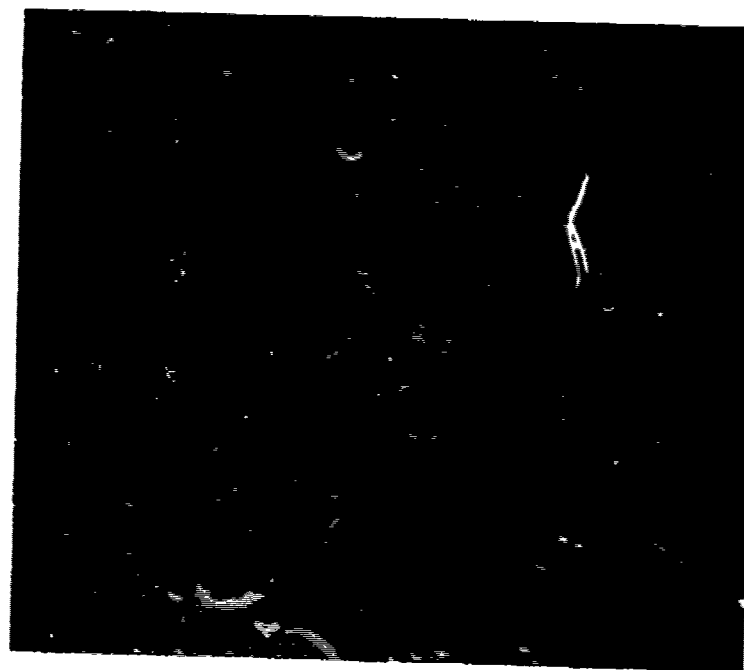


Figure 43. Cross section of tab-termination.



(a) SEM. 43X



(b) SEM, 86X

Figure 44. Holes in aluminum foil,
026 unit S/N 2.

corona degradation had caused some changes in the DOP impregnant. Acid value tests were run. It was found that the acid value had approximately doubled, from 3.9×10^{-2} mg/g (KOH) to 8.2×10^{-2} mg/g (KOH), but the value was still very small. Perhaps some sort of electroplating process was involved.

6.2.4 Connector Tests

A connector test fixture was made up to examine several different airborne DC-rated high-voltage connectors for their usefulness in pulse situations. This unit, assembled from 014 pieces, is shown in Figure 45. This unit utilized 5 Amp connectors in addition to the ceramic bushing. It was found that all connectors performed well so long as their rated RMS current was not exceeded during the burst. These connectors were found to have AC CIV greater than their DC rating.



Figure 45. Connector pulse test capacitor.

7.0 HEAT SINK/COOLING TRADE-OFF INVESTIGATION

Presented in this section is the summary report of the thermal analyses on single sections. The specialized computer program employed has been retained for any future use.

7.1 SUMMARY

The thermal analysis of the Capacitors for Aircraft High Power initially involved a parametric study of sixteen potential capacitors. The dielectrics (polysulfone and kapton) each were considered with two cross sections, two cores, and two types of electrical contacts. The capacitors were assumed to be installed in pairs in an oil-filled case with a beryllium oxide plate across the top and bottom of the two capacitors. One additional configuration (without the top and bottom plate) was evaluated. The original sixteen capacitors were evaluated for one minute operating time and two hours cooldown.

Results indicated the variations in temperature rises for the eight configurations of each dielectric type capacitor was sufficiently small to recommend selection of any one of the eight for production. Since these first sixteen runs maintained a fixed capacitor case temperature, it was decided to reevaluate with the capacitor case free to seek its own temperature rise with the surrounding ambient at a fixed temperature. The reevaluation involved only four configurations of polysulfone capacitors and one kapton. Results of these runs also indicated any configuration of each dielectric was as good as the rest. Results also showed that the kapton capacitors would be considerably hotter than the polysulfone capacitors. The hot spot rises after one minute with power on would be about 135 and 68°F, respectively.

Results are included in this report for twelve hours of operation of polysulfone, circular, hollow core (oil-filled), with end tabs for electrical contact type capacitors. This was evaluated for one minute on and both one- and two-hour cooldown. The two-hour cooldown produced about a 30°F cooler capacitor.

The polysulfone capacitor that was analyzed without the top and bottom beryllium oxide plates was hotter than its counterpart. The difference was only about 7 to 8°F and it will have to be considered feasible with that in mind.

7.2 INTRODUCTION

This thermal analysis involved a parametric study of potential Capacitors for Aircraft High Power. The parameters investigated included the following:

- Dielectrics - Polysulfone vs kapton
- Cross Sections - Circular vs rectangular
- Cores - Hollow vs beryllium oxide
- Contacts - Extended foil vs end tabs.

The above combinations produced 16 distinct capacitors, each of which was represented by a nodal model. Table 44 presents the number of nodes and connectors for all 16 nodal models as well as the Run Number related to the computer solution. Figures 46 and 47 show schematics of all polysulfone and kapton dielectrics, respectively. These figures depict how the nodes were generated as well as the basic capacitor dimensions.

Table 45 is a list of the physical constants used for each material involved in the thermal analysis.

Subsequent to performing the first 16 runs, some of the models were modified. The modifications included adding an ambient air node (in lieu of holding the case at a constant temperature) and adding a separate node for the oil inside the core of the hollow core capacitors. This was done only for five models, which were then designated 1B, 2B, 3A, 4A, and 9B.

TABLE 44. CAPACITOR CONFIGURATION, NODES,
AND CONNECTORS

Run No.	Dielectric		Cross Section.		Core		Contacts		Nodes	Comments
	P	K	C	R	H	S	T	E		
1	x		x		x		x		220	467
2	x		x		x			x	220	467
3	x		x			x	x		221	469
4	x		x			x		x	221	469
5	x			x	x		x		130	282
6	x			x	x			x	130	282
7	x			x		x	x		131	284
8	x			x		x		x	131	284
9		x	x		x		x		202	430
10		x	x		x			x	202	430
11		x	x			x	x		203	432
12		x	x			x		x	203	432
13		x		x	x		x		112	245
14		x		x	x			x	112	245
15		x		x		x	x		113	247
16		x		x		x		x	113	247
									<u>Tot. Length</u>	<u>Watts</u>
Dielectric		{ P = Polysulfone K = Kapton							538"	201.9
									324"	314.7
Cross Section		{ C = Circular R = Rectangular								
Core		{ H = Hollow (just oil) S = Solid ($B_e O$)								
Contacts		{ T = Tabs (at ends) E = Extended foil (top and bottom)								

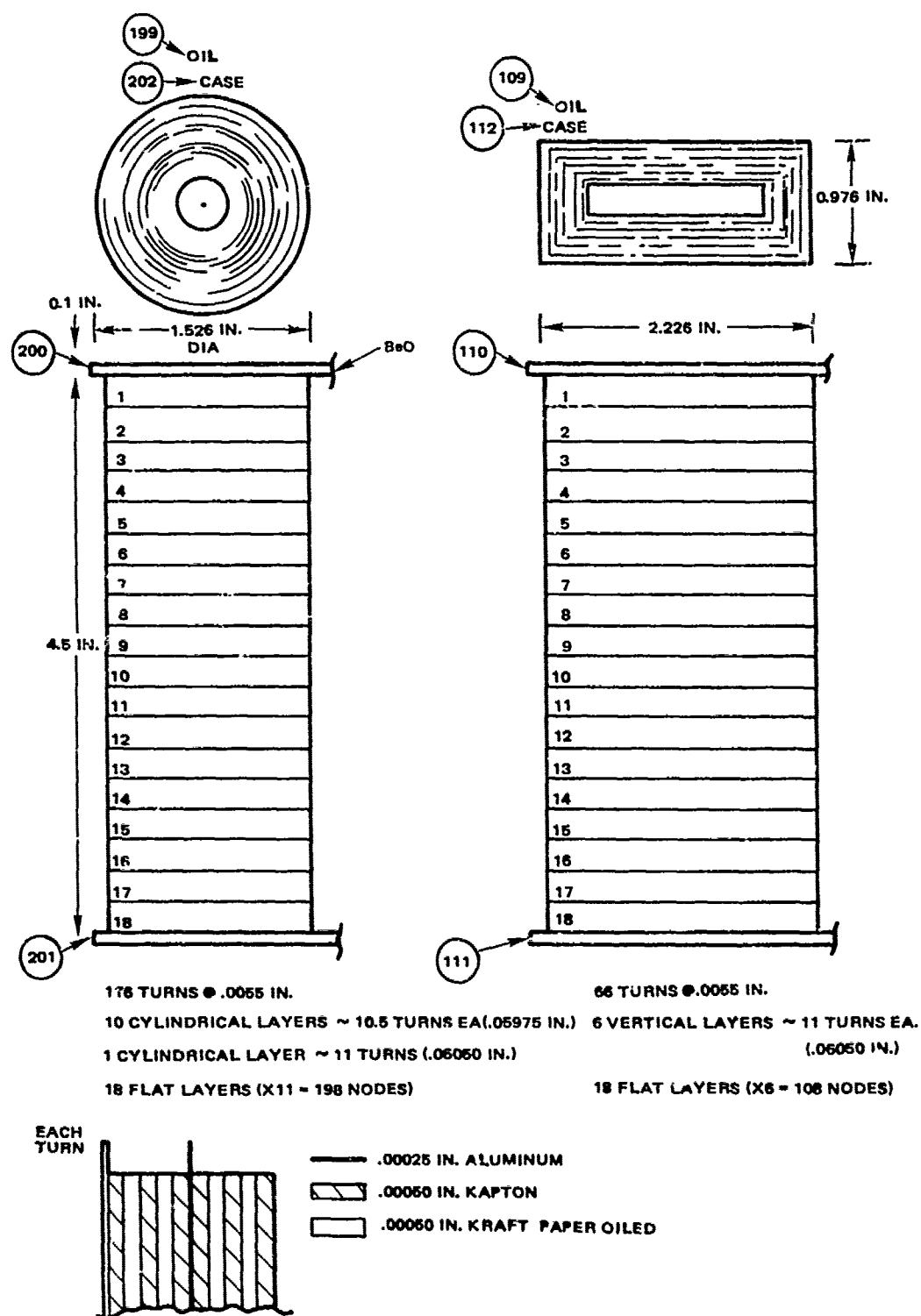


Figure 47. Kapton capacitor - schematic and model.

TABLE 45. PHYSICAL CONSTANTS

Material	Density	Thermal Conductivity	Heat Capacity
	lbs/ft ³	BTU/Hr ft ² F	BTU/lb ² F
Aluminum	170	100	0.23
Polysulfone	77.4	0.155	0.31
Kraft Paper/Oil	84.7	0.073	0.35
Kapton	88.7	0.094	0.26
Oil (Mineral)	55.5	0.073	0.41
Beryllium Oxide	96.5	115	0.30
Combinations:			
Type I			
Polysulfone - 6 at 0.00038"	Thru*	0.128	
Kraft Paper/Oil - 4 at 0.00030" 89.8	Type I		0.32
Aluminum Foil - 2 at 0.00025"	Along*	12.67	
Type II	Type I		
Kapton - 6 at 0.00050"	Thru*	0.093	
Kraft Paper/Oil - 4 at 0.00050" 94.0	Type II		0.29
Aluminum Foil - 2 at 0.00025"	Along*	9.12	
*Since each layer of the capacitors is made up of 6 layers of film dielectric, 4 Kraft paper with oil, and 2 aluminum foil, the thermal conductivity is different when heat is going from inside to outside (or vice versa) than when going along the length or height of the capacitor (see Figure 1 for order of individual layers).			

Following this change, the investigation was extended to evaluate two additional operational cycles of model 1B:

- 1 minute on - 2 hours off - 12 hours total (Run 1C)
- 1 minute on - 1 hour off - 12 hours total (Run 1D)

The last run (1E) was to evaluate removal of the beryllium oxide top and bottom plates. Model 1C was modified accordingly and the operational cycle evaluated was 1 minute on, 2 hours off, and 4 hours total.

7.3 RESULTS

The first series of sixteen runs were based on the models shown in Figures 46 and 47 and Table 44. The operation consisted of one minute on and two hours cooldown. In addition, these models were based on maintaining the capacitor case at a constant temperature and combined all the oil in the capacitor as one node. Results are shown in Table 46. It is readily seen that there was relatively little differences between the hot spot temperature rises in the various configurations (cross sections, cores, and contacts) other than between the two dielectrics. The eight polysulfone capacitors only varied $\pm 1.9^{\circ}\text{F}$ from the average hot spot temperature rise. Similarly, the eight kapton capacitors varied $\pm 2.7^{\circ}\text{F}$ at the end of the one minute power on operation.

Based on these results, it was felt there was a need to permit the capacitor case to seek its own temperature level. This was accomplished by adding a node to represent a fixed ambient temperature to surround the case. For the capacitors without a solid beryllium oxide core, another node was established for the core oil to keep it separate from the case oil. Models 1B, 2B, and 9B had both modifications while 3A and 4A (with solid cores) only had the modification to the case. Results of these five runs are shown in Table 47. Again, the variations due to cross section, core, and contacts were so slight that all further investigations was made on Model 1 - polysulfone, circular, hollow core (just oil), and tabs at the ends of the aluminum foil for electrical contact.

TABLE 46. CAPACITOR HOTSPOT TEMPERATURES —
FIRST 16 CASES

Run*	Time, Min →	Temperature, °F				
		1.0	1.25	10	60	120
1		69.4	69.4	2.3	3E-5	5E-11
2		69.3	69.3	2.3	2E-5	5E-11
3		69.3	69.3	2.1	3E-5	7E-11
4		69.3	69.3	2.0	3E-5	7E-11
5		67.8	67.8	2.9	9E-5	4E-10
6		67.7	67.7	2.8	9E-5	4E-10
7		66.2	66.2	2.2	1E-4	1E-9
8		66.6	66.6	2.1	1E-4	9E-10
9		138.4	138.6	14.0	0.14	1E-3
10		138.3	137.3	13.5	0.14	1E-3
11		138.2	137.8	12.6	0.14	2E-3
12		138.1	136.9	12.6	0.14	2E-5
13		133.3	129.0	8.0	0.02	3E-5
14		133.2	129.0	8.0	0.02	3E-5
15		133.2	128.9	8.0	0.02	3E-5
16		133.2	128.8	8.1	0.02	3E-5

*See Table 44 for configuration

Notes:

1. These runs based on case = 0°F
2. Power on 1 minute only
3. Cooldown - 2 hours

TABLE 47. TEMPERATURE RISES FOR MODIFIED NODAL MODELS

A - 1 Hour Operation						
Time, Minutes	Run	1B	2B	3A	4A	9B
1.0		70.3	70.2	70.2	70.1	138.6
1.2		69.8	69.6	69.2	69.4	140.1
10		30.0	29.9	29.7	29.6	63.5
60		18.5	18.4	18.3	18.3	44.0
B - Multiple Hour Operation						
Time, Minutes	Hours	Run	1C	1D	1E	
1.0			70.3	70.3	72.4	
60	1		18.5	18.5	23.0	
61			--	88.6	--	
120	2		11.1	29.6	14.4	
121			81.3	99.6	86.8	
180	3		25.2	36.4	32.1	
181			--	106.4	--	
240	4		15.2	40.4	20.1	
241			85.4	110.4		
300	5		27.6	42.9		
301			--	112.8		
360	6		16.7	44.3		
361			86.8	114.3		
420	7		28.5	45.2		
421			--	115.0		
480	8		17.2	45.6		
481			87.4	115.5		
540	9		28.8	46.0		
541			--	115.9		
600	10		17.3	46.2		
601			87.9	116.1		
660	11		28.9	46.3		
661			--	116.3		
720	12		17.4	46.3		
Notes:						
1. Temperatures = °F						
2. 1-hour operation has 1 min power						
3. Runs 1C and 1E have 1 min on/2 hours off						
4. Run 1D has 1 min on/1 hour off						
5. Letter after run number, ambient = 0°C. Case seeks its own temp.						
6. Letter B, C, D indicates oil in core separate from oil in case						
7. Run 1E assumes no beryllium oxide top and bottom plates						

For comparison of the original and final temperatures, Figure 48 presents graphic results of runs 1 and 1B hot spot temperature rises. Also shown is the temperature rise/time profile of the capacitor case for run 1B. The capacitor case in run 1B reaches its peak temperature rise considerably below the polysulfone hot spot (36.5 vs 70.3°F) and both temperatures begin to converge (within 1°F) in less than 20 minutes of cooldown.

Figure 49 depicts the same comparisons for the kapton, circular, hollow, tabbed capacitor. Run 9B hot spot peaked at 140.1°F (0.2 minutes

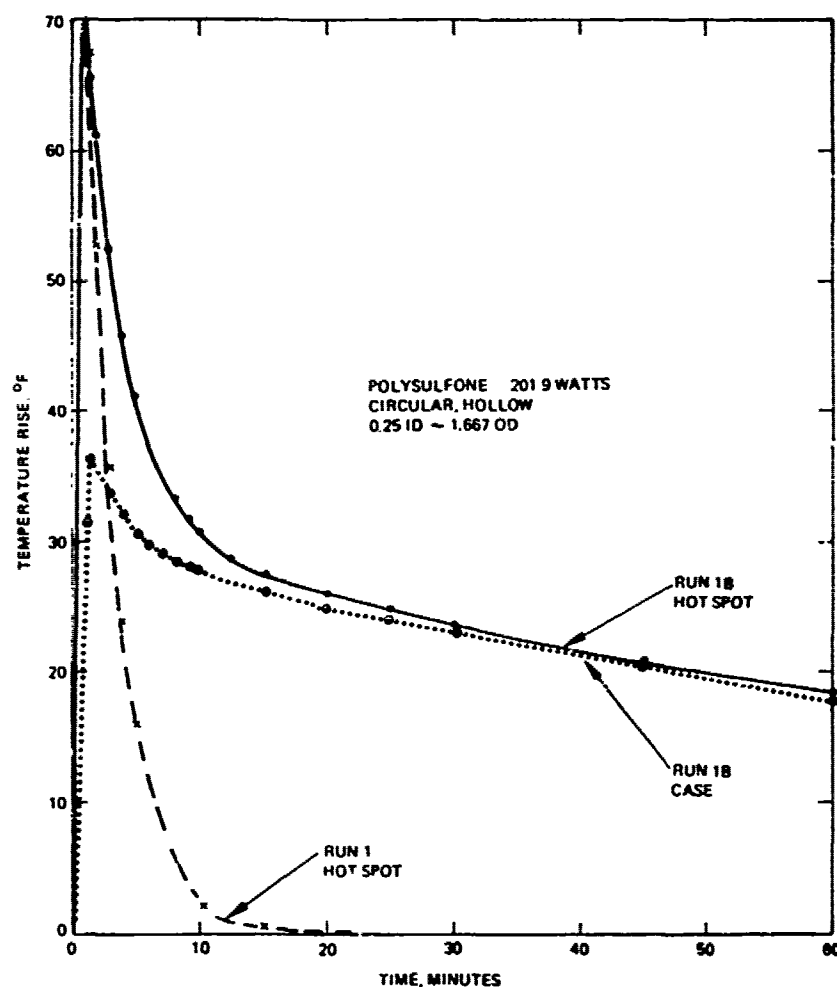


Figure 48. Capacitor study (Both Runs, 1 minute on 1 hour off).

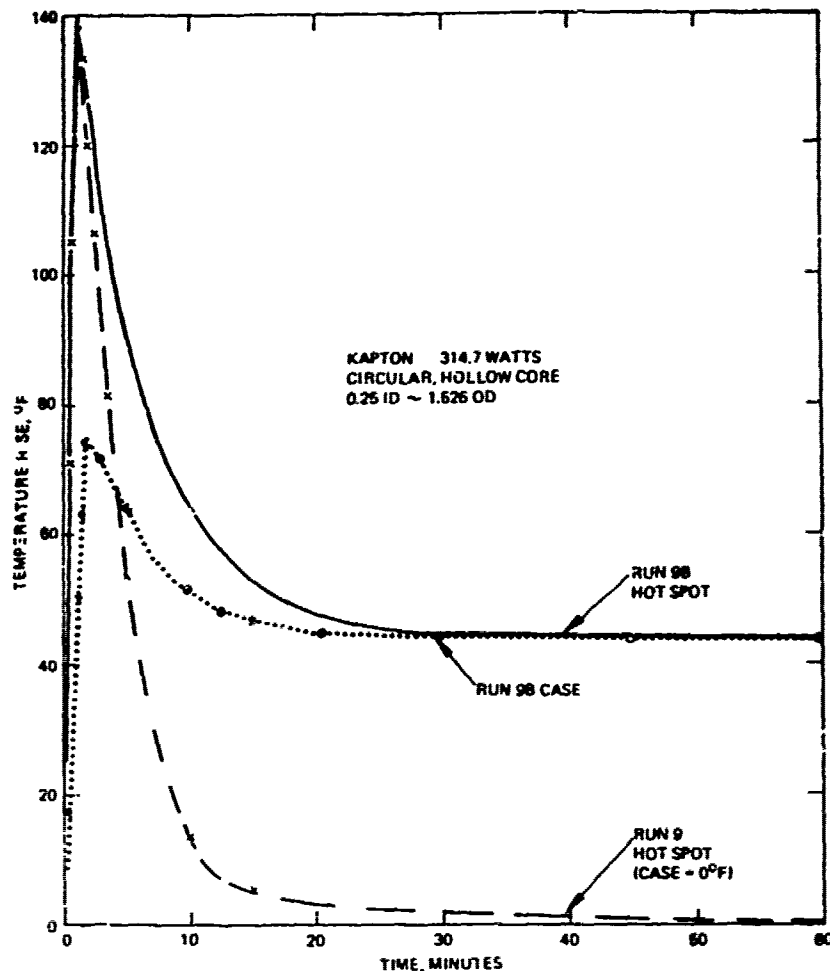


Figure 49. Capacitor study (1 minute on - 1 hour off).

after power operation) while the case peaked at 73.6°F (2.0 minutes after power). Convergence (within 1°F) occurred in about 25 minutes of cooldown.

Runs 1C and 1D used the same model as run 1B with the operation cycles changed. Run 1C ran 12 hours with 1 minute on, 2 hours cooldown. Run 1D was run for 12 hours with 1 minute on but only 1 hour cooldown. The hot spot temperature rises are plotted in Figures 50 and 51, respectively. In addition, the last four hours were plotted together in Figure 52. These results show a cooler peak hot spot temperature rise for run 1C by nearly 30°F (87.8°F vs 116.2°F) and a similarly cooler final cooldown temperature (17.8°F vs 46.6°F).

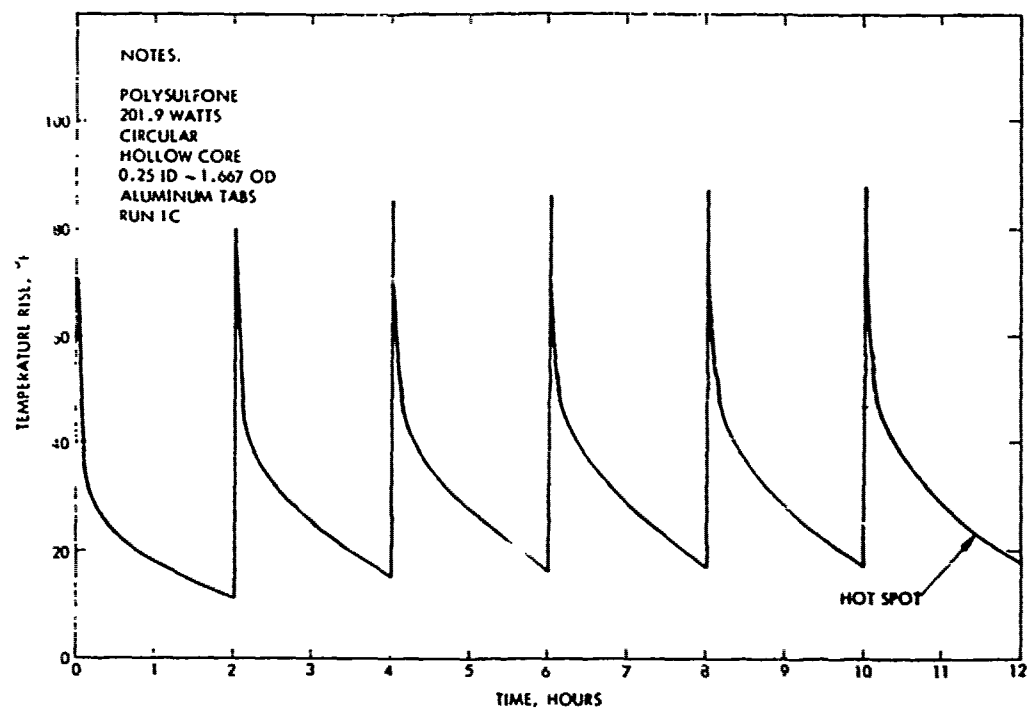


Figure 50. Capacitor study (1 minute on - 2 hours off).

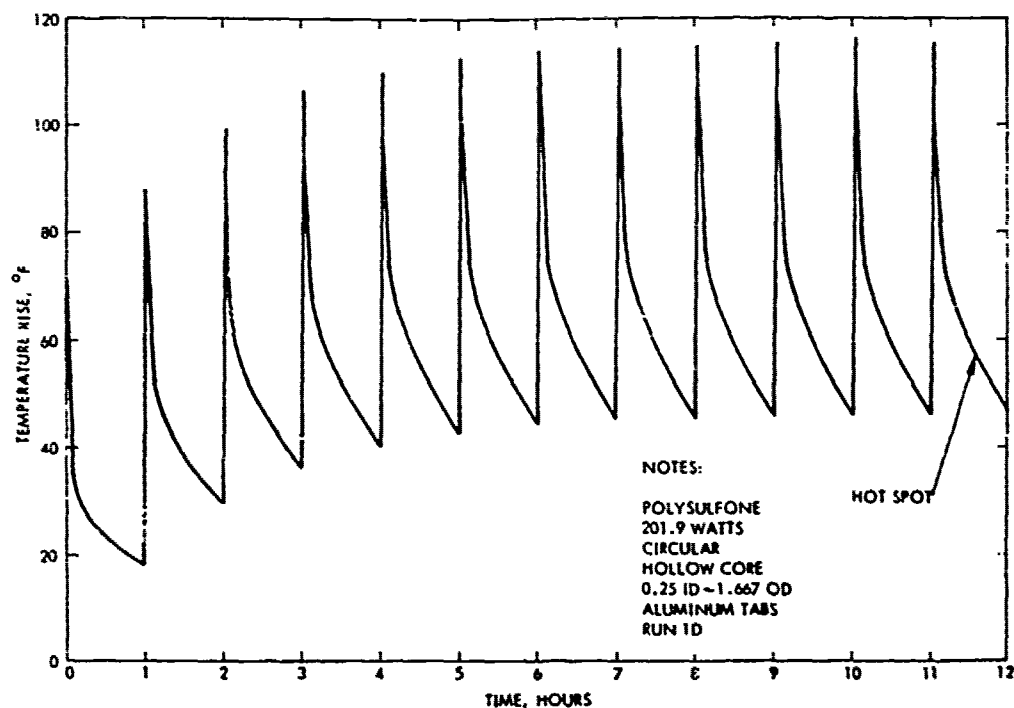


Figure 51. Capacitor study (1 minute on - 1 hour off).

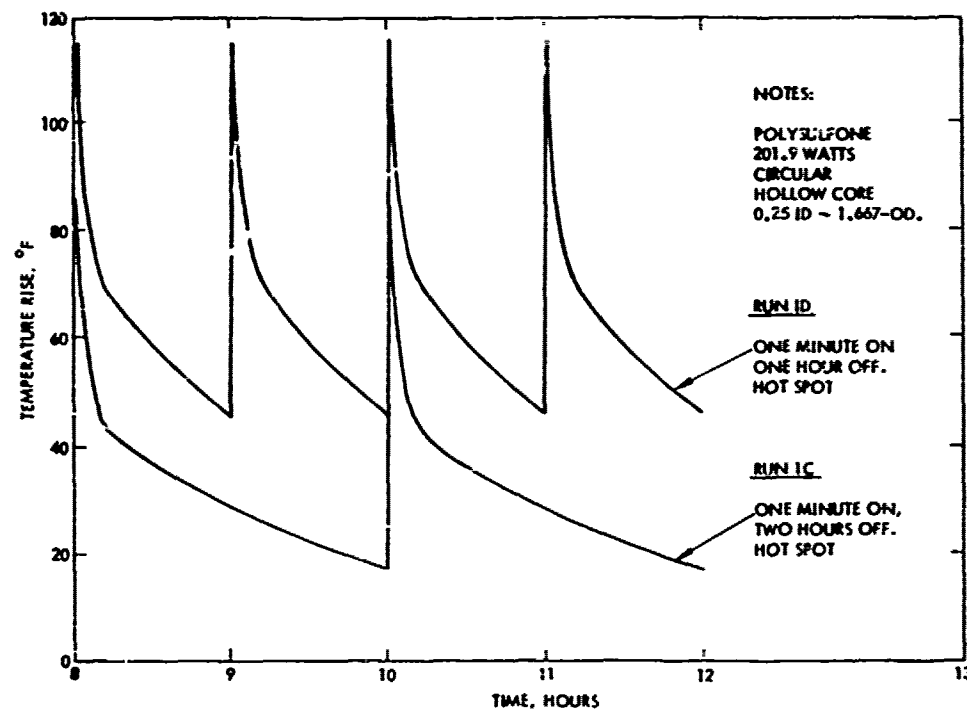


Figure 52. Capacitor study (last four hours).

The final configuration tested (run 1E) was the same as run 1C except it was modified to eliminate the top and bottom beryllium oxide plates and only two 2-hour cycles were run. The hot spot temperature rise after the second on cycle was 86.8°F and 20.1°F after the second cooldown. This is shown in Figure 53. Figure 54 presents the comparative plots of runs 1C and 1E. Also shown in Figure 54 are the loci of minimum and maximum temperature rises for run 1C. By extrapolating parallel loci for run 1E, the final temperature rises appear to be 96°F and 24°F, respectively. Thus, run 1E is about 7 to 8°F hotter than run 1C.

7.4 CONCLUSIONS

Based on the results of this thermal analysis the following conclusions appear valid:

1. Any configuration evaluated is thermally as good as the others of the same dielectric.

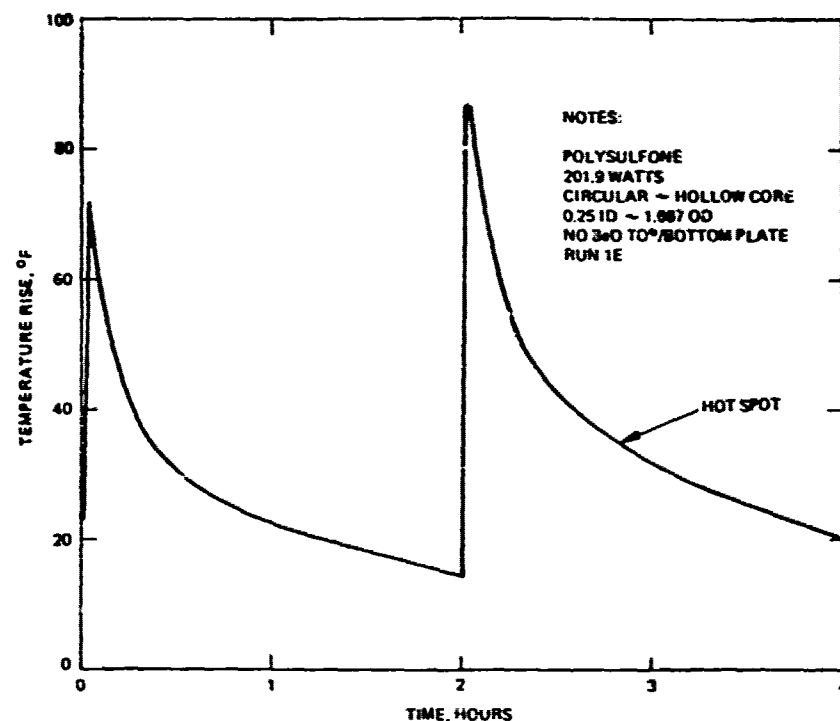


Figure 53. Capacitor study (1 minute on - 2 hours off).

2. Kapton capacitors will operate about 70°F hotter than polysulfone.
3. Two-hour vs one-hour cooldown will result in about 25°F cooler operation after four hours.
4. Omitting the beryllium oxide top and bottom plates increases the capacitor temperature rise by about 80°F.

7.5 EXPERIMENTAL

The thermocouples inserted within the sections of units 13 forward produced results which agreed well with this calculated data. The one experimental fact which the calculations did not reveal is that the temperature rise during a burst will grow quickly in the last few bursts before failure. This indicates a dissipative mechanism, possibly corona degradation at foil edges.

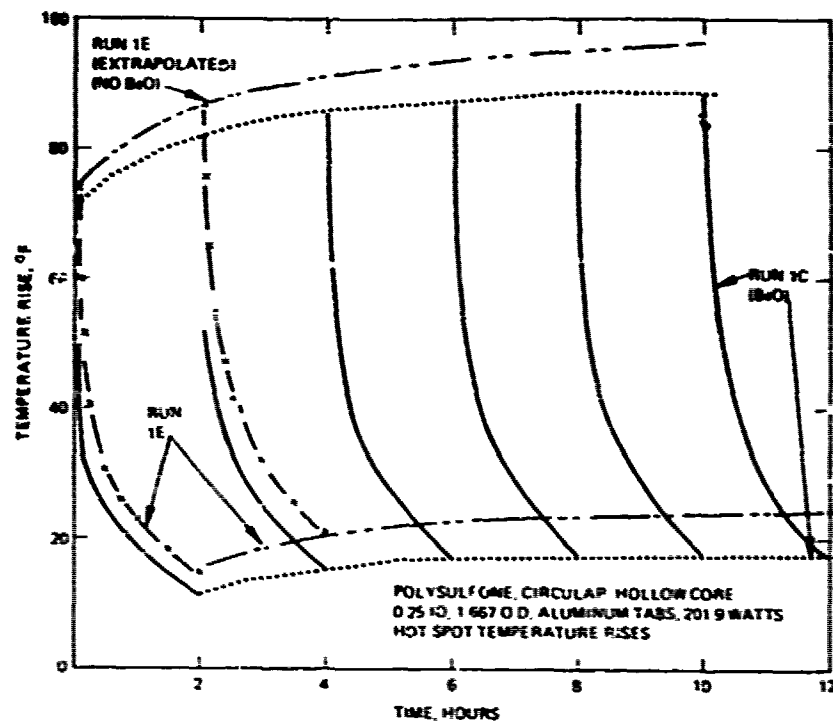


Figure 5-4. Capacitor study (1 minute on, 2 hours off with and without beryllium oxide top and bottom plates).

8.0 PFN OPERATING ENVIRONMENT

This task requires the analysis of the conditions under which a PFN capacitor operates, so that effective tests may be designed. Obviously, the work required on this task needed to be performed in support of the fabrication of the pulse test facility. Summaries of the effort appear both in Sections 4.4 and 4.5, and below.

8.1 PFN DESIGN

The specifications given for this development assume a standard type E network for use in a line-type pulser. This network employs a continuous solenoid of total inductance $L_N = \tau Z_N/2$, with the individual capacitances tapped onto the inductor for equal inductance for all sections except the ends, which are 20 to 30 percent larger. For a 6-section PFN, this is illustrated in Figure 55. The PFN is commonly used in a circuit such as that shown in Figure 56. It is well known that in such a circuit each capacitor except the last (C_6) produces two equal current pulses on discharges, while the last capacitor produces one large pulse. A schematic of voltage and current for one capacitor is shown in Figure 57.

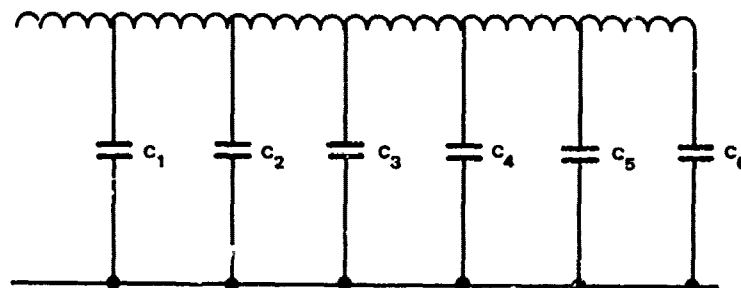


Figure 55. Type E PFN schematic.

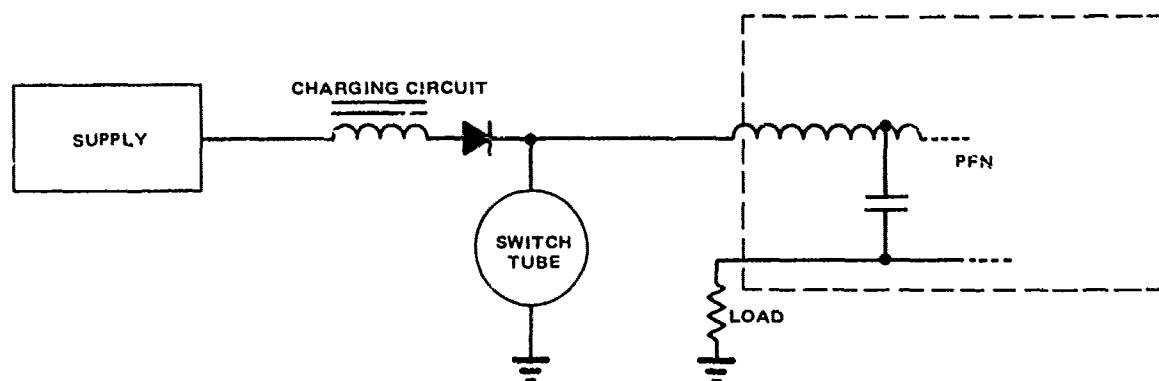


Figure 56. Typical type E PFN application.

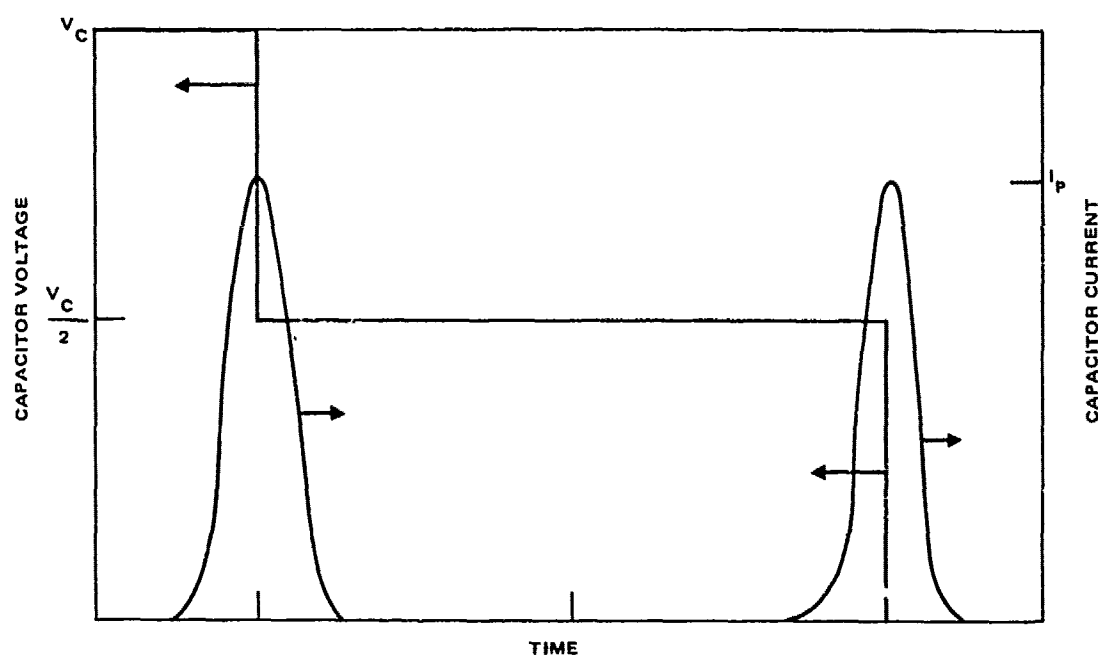


Figure 57. Schematic of current and voltage, PFN capacitor.

8.2 COMPUTER MODELLING

The capacitor current waveform for both charge and discharge was modelled on a computer, so that the various frequency components and currents could be found. These are useful to calculate total power loss in the capacitors, since the dissipation factor and equivalent series resistance (ESR) versus frequency can also be measured. The values found are given in Table 48 for a PFN with a 20 μ S wide current pulse per capacitor (the specification of Task 4, paragraph 4.4 of the SOW), and in Table 49 for a PFN with a 20 μ S rectangular output pulse (the specification of Task 9, paragraph 4.10 of the SOW). The fact that the power loss for the short pulse is several times larger than the transfer of an equivalent amount of energy in a longer pulse is not suprising. Power loss depends on the square of the RMS current, and the current clearly gets larger for a shorter pulse.

The ESR of capacitor sections of various types was laboriously measured using several different apparatuses at different points in the frequency spectrum. This data is displayed in Figure 58, together with the squares of the current data from Tables 48 and 49. Thus, an idea of the power dissipation can be gotten, as the power dissipation is simply $I^2 \times \text{ESR}$.

TABLE 48. CAPACITOR CURRENT SPECTRUM

	Charge	Discharge					Sum
		Frequency Components					
		f ₁	f ₂	f ₃	f ₄	f ₅	
Frequency, kHz	0.15	12.5	25	37.5	50	62.5	46.5
Current, A Rms	2.9	26.4	28.2	16.3	8.6	5.3	
Typical Loss, Watts	10	45	41	12	3.2	1.1	
Notes: a) 300 pps rate assumed, operating into matched resistive load							
b) Current values for 1.0 μF capacitor							
c) Power loss for polysulfone /kraft construction							

TABLE 49. CAPACITOR CURRENT SPECTRUM, 20 μ S PFN OUTPUT

	Charge	Dishcharge					Sum
		Frequency Components					
		f ₁	f ₂	f ₃	f ₄	f ₅	
Frequency, kHz	0.15	75.5	151	226	302	337	
Current, A Rms	2.9	66.7	71.3	41.1	21.8	13.3	117
Typical Loss, Watts	10	173	178	57	16	5.7	506

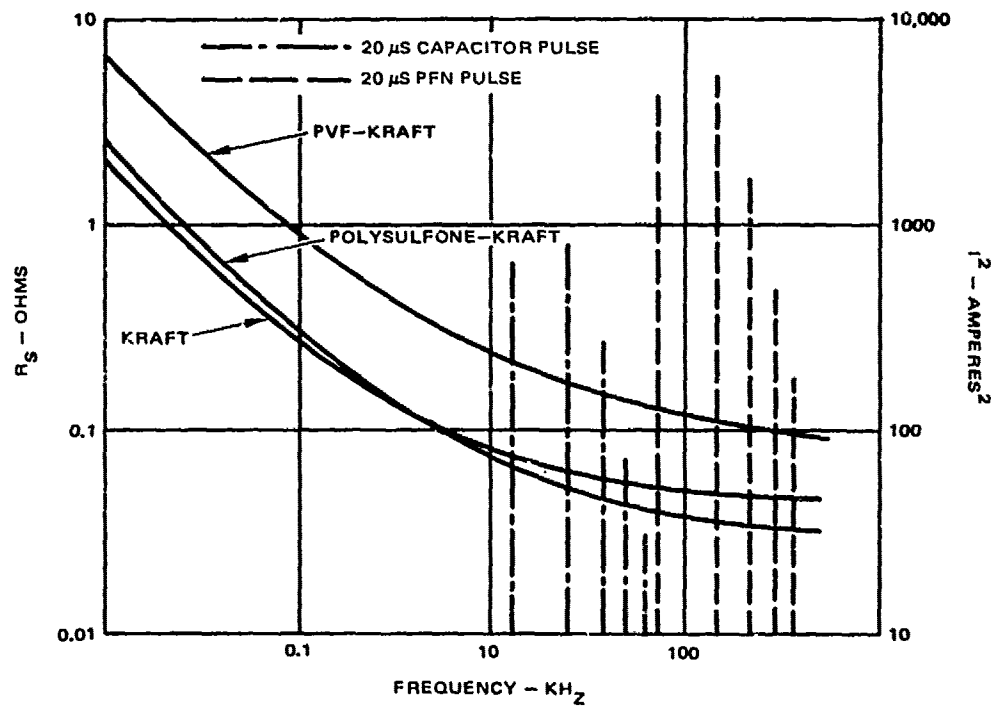


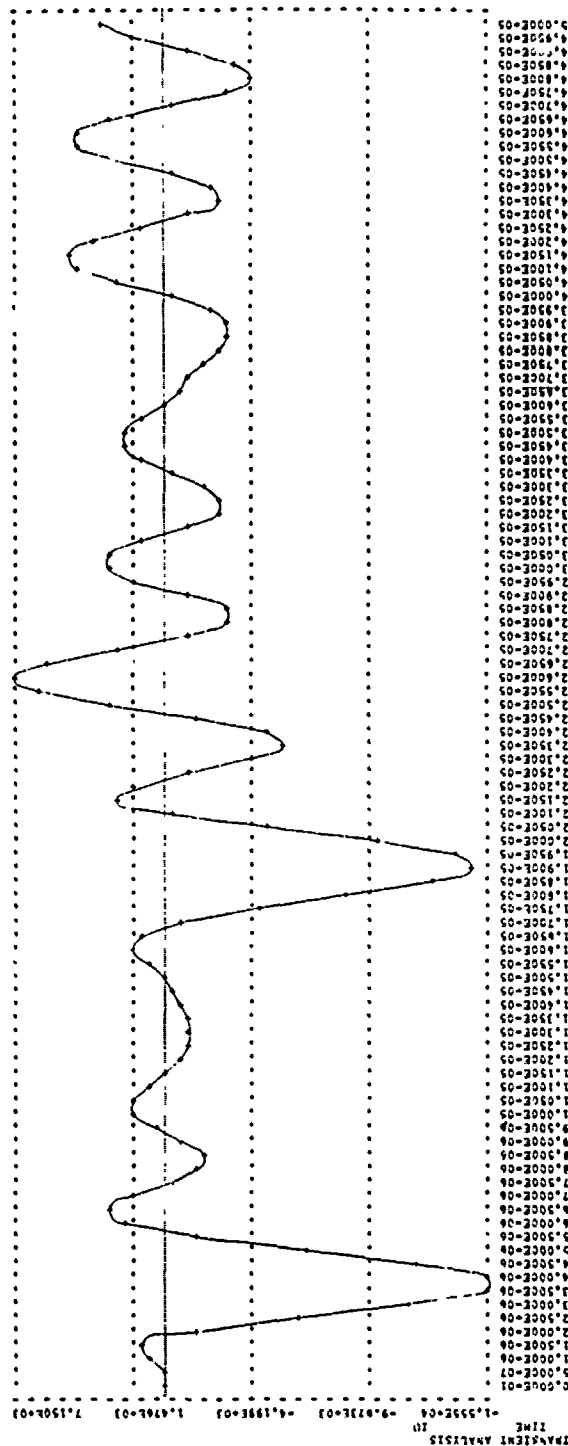
Figure 58. ESR and harmonic discharge current.

Computer plots of the capacitor current waveforms were made for each capacitor. One such waveform is shown in Figure 59, for a capacitor in the 20 μ S output PFN. These waveforms were verified by building low-voltage scaled-down PFNs and actually measuring the currents with an oscilloscope.

8.3 DESIGN OF TEST APPARATUS

The apparatus to test these PFN capacitors must clearly be of one of two forms. Obviously, a full PFN with appropriate switch, load, and power supply could be used. This is very expensive and unwieldy for the present situation, unless other uses could be found for the equipment, since about 500 kW of power is involved.

The approach adopted for this program was to test single capacitors, using an RLC resonant circuit of which the capacitor is the specimen to achieve the same distribution of frequency harmonics as actually occurs. This equipment is discussed in detail in Section 4, and an additional block diagram is to be found in Section 6.



TIME - SECONDS

Figure 59. 20 μ S capacitor current waveform.

CURRENT - AMPERES

THIS PAGE IS BEST QUALITY PRACTICABLE
FROM COPY FURNISHED TO DDC

9.0 RELIABILITY AND MAINTAINABILITY ANALYSIS

The capacitors and pulse-forming networks (PFNs) developed under this program typically fail through failure of a single capacitor element, or pad. This failure may then also destroy other parts of the capacitor or PFN. Because of the small number of components fabricated and tested, it is difficult to perform a full statistical analysis. However, some conclusions can be reached.

The term "screening" is taken to mean the half-voltage 3 burst test designed to weed out infant mortalities. The data for both part types is given, on a per-pad basis, in Table 50.

Maintenance must be performed whenever there is a failure. If the PFN is a single sealed unit, the entire unit must be discarded and replaced. The capacitors, once impregnated, are not repairable.

TABLE 50. FAILURE RATE DATA

	Unscreened		Screened	
	014	026	014	026
Total Section Failures	4	2	2	1
Section Failure Rate, per 1000 shots	0.003%	0.004%	0.003%	0.002%
Capacitor Failure Rate, Per 1000 shots	0.018%	0.016%	0.008%	0.009%
PFN Failure Rate, per 1000 shots	0.11%	0.094%	0.045%	0.052%

10.0 PULSE FORMING NETWORK

One type E PFN was fabricated, checked out, and tested. The PFN coil was supported by the capacitors such that either 014 or 026 components could be used in the line. After static tests at Hughes, the PFN coil and 13 capacitors were shipped to the Air Force High Power Laboratory, Griffiss AFB, New York, for testing. During the testing no failures were encountered. After testing, the PFN coil and 12 capacitors were shipped to the Aero Propulsion Laboratory at Wright-Patterson AFB, Ohio.

10.1 PFN CONSTRUCTION

The only design necessary was that of the PFN coil, since the SOW specified that the previously fabricated capacitors were to be used.

10.1.1 Capacitor Inductance

Within certain limits, the actual inductance of the capacitor is not a limiting factor, since a careful PFN design takes the inductance into account. It was necessary to measure capacitor inductance to do this, using a self-resonant frequency technique. Simultaneously, the ESR was obtained. The test set-up is shown in Figure 60. The capacitors' inductance as measured turned out to be somewhat larger than the 20 nH specification goal, but this was probably due to the common use of the single type of ceramic bushing that was not designed for low inductance. The PFN design was not adversely affected. Capacitor data is shown in Table 51, where component 036 is the large 1.1 μ F 30 kV capacitor described in Sections 14-16.

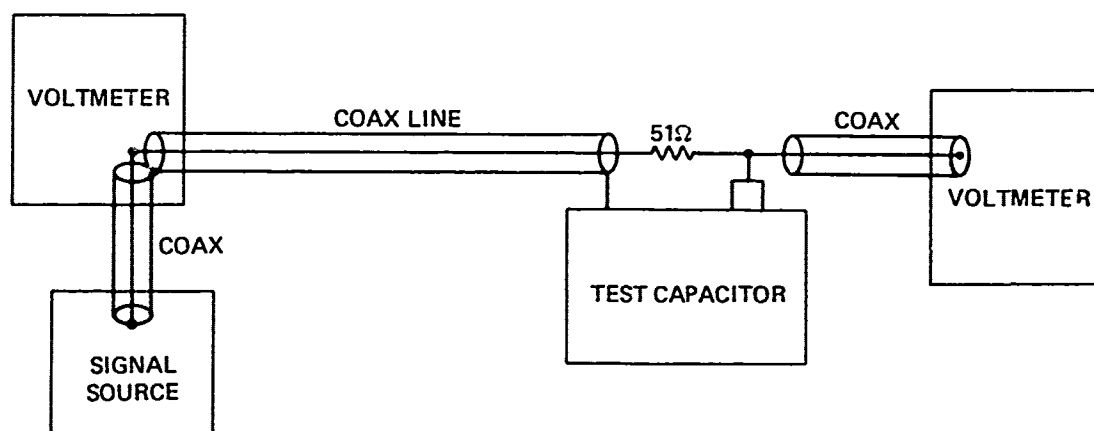


Figure 60. Capacitor inductance measuring arrangement.

TABLE 51. CAPACITOR INDUCTANCE DATA

Capacitor p/n	C (μ F)	SRF	L (nH)	ESR ($m\Omega$)
014	2.39	347 kHz	90.	132
026	2.33	355 kHz	90.	54
036	1.1	550 kHz	115.	30

10.1.2 Design Considerations

It is important to realize that the design of a PFN coil is a non-trivial problem. Without going into the details of such a design, which are well documented in the literature, the following different considerations entered into the final design:

- Power dissipation, heat capacity, and temperature rise of the coil
- Inductance of capacitor and interconnection
- Location of taps

- Correction for non-zero wire diameter
- Correct inductance and mutual inductance

The final design was modelled on a computer with all the measured parameters to ensure a good pulse shape.

10.1.3 Coil Construction

The coil was made from thick wall copper tubing. The specifications were:

Material : 0.625 OD, 0.032 wall copper tube
 Coil Diameter : 6.095 inch ID
 Coil Length : 32.7 inches
 Conductor Length : 295 inches

The schematic and a detailed view of a tap are shown in Figure 61.

10.2 PFN CHECKOUT

The capacitors had previously been individually tested, as described above. Therefore, checkout was limited to a partially charged test of the proper wave shape.

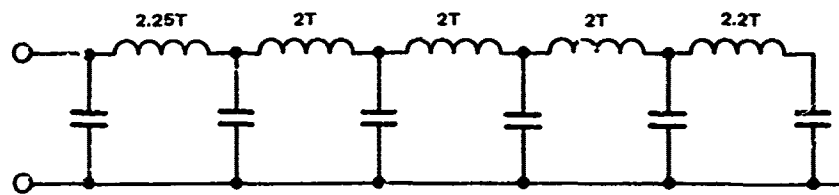
10.3 PFN TEST

The PFN testing was accomplished 9-11 October 1979 at the High Power Laboratory, with the helpful and valued assistance of Bobby Gray. Mr. Dougherty, the Project Monitor, witnessed the testing.

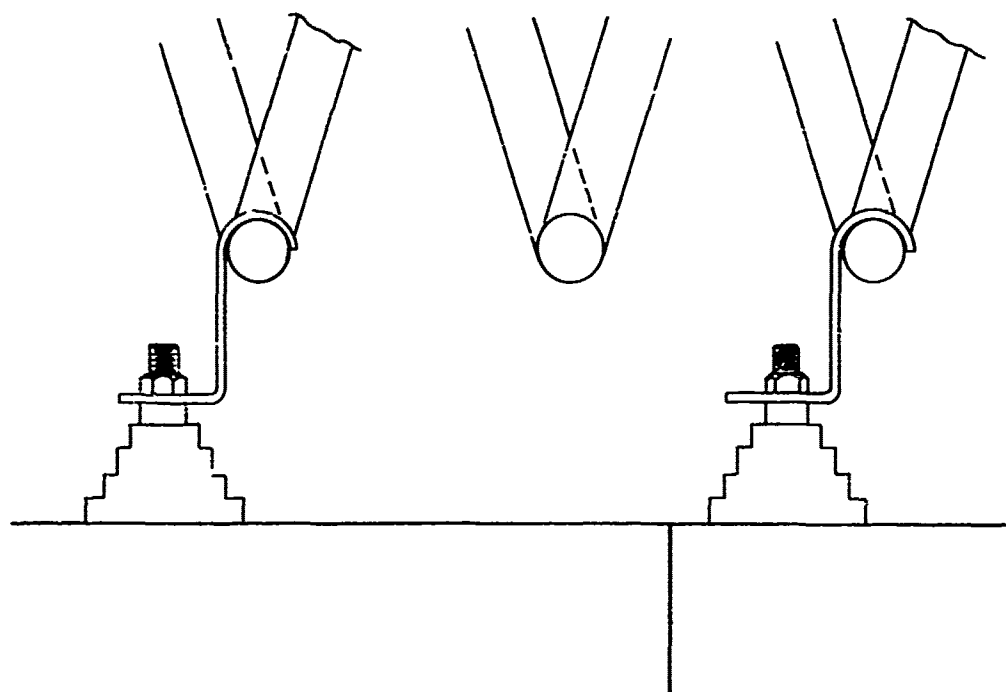
10.3.1 Set-up

A standard test circuit was used. The switch tubes were two Tung-Sol X1222 operating in parallel. The load was a low inductance coaxial copper sulfate load, working into an Energy Systems heat exchanger, which fed into a liquid-to-air heat exchanger. Waveforms and voltages were monitored with a Tektronics 555 oscilloscope and high voltage probes.

The PFN itself was placed on a copper sheet ground plane. Ground connections were made with pieces of the copper sheet. The arrangement is shown in Figure 62. The power supply used was the large 3.9 megawatt unit in the main test bay.



(a) COIL SHOWING NUMBER OF TURNS (T)



(b) TAP DETAIL

Figure 61. PFN coil construction.

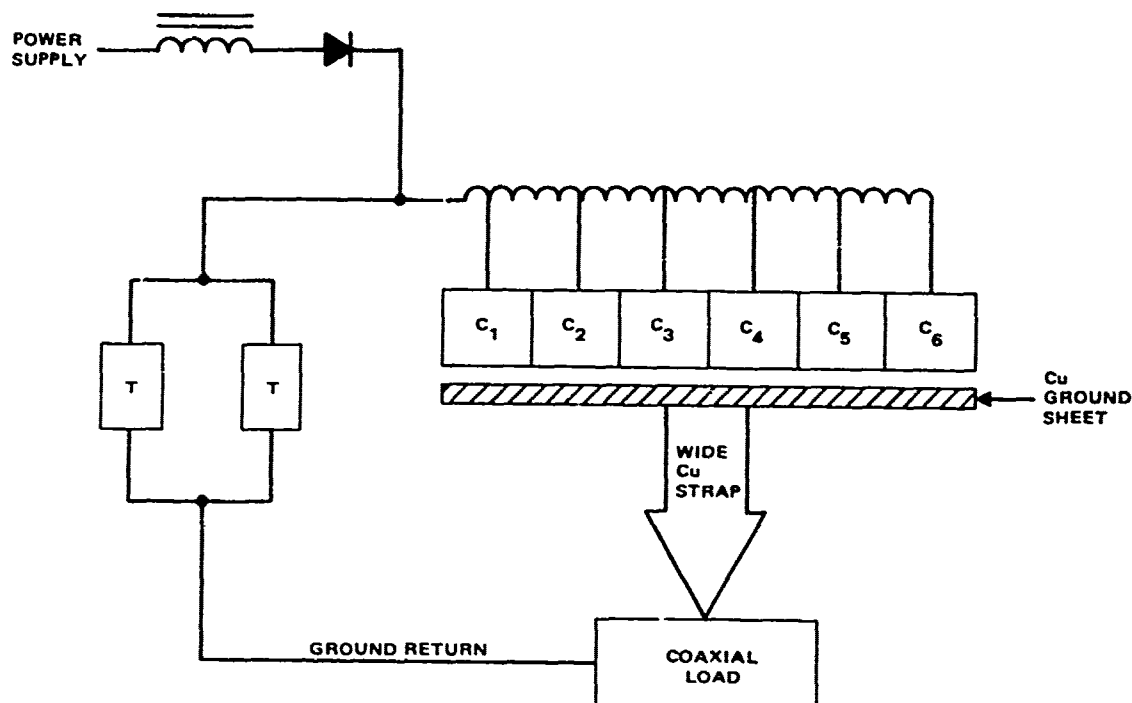


Figure 62. Diagram of test setup.

10.3.2 Tests and Results

Throughout the testing, triggering problems were encountered with the switch tubes, so that occasionally the exact test profile desired could not be run.

The initial tests were run on 014 components for the purpose of checking the waveshape. The observed pulse was rectangular, with the following constants measured approximately from the oscilloscope screen:

Pulse width, zero-to-zero:	24 μ S
Rise :	2 to 3 μ S
Fall :	6 μ S
Charge Time :	8mS

The charge time was determined by the power supply and charging reactor, and limited the maximum PRF selected to 125 pps.

A summary of the test data using the 014 capacitors is given in Table 52. The capacitors performed well in this service. During the testing, the case temperature of C_6 , the most highly stressed unit, was monitored. It was noted that C_6 was noticeably warmer than the other five capacitors. Referring to Table 52, runs 10-13 were accomplished in a period of about 8 minutes. The maximum case temperature of C_6 occurred 47 minutes after the test, and was 12°C larger than the starting temperature. The peak current at 15 kV was 9600A.

Because of the time pressure, and because the Project Monitor expressed the desire to have at least 6 good 026 units, it was decided to replace C_6 in the 014 line with an 026 capacitor, S/N 12, rather than use all 6 026 units. This component was instrumented for case temperature measurement, and four additional runs were made. This data is shown in Table 53. The component got quite warm, but performed well. Temperature data is shown in Table 54.

TABLE 52. 014 PFN TESTING SUMMARY

Run Number	Rate	Voltage (kV)	Total Shots
1	100	6	60,000
2	125	7	75,000
3	125	3	15,000
4	125	7	5,625
5	125	10	7,500
6	125	13	7,500
7	5	15	1,200
8	30	15	5,400
9	>200	15	4,500
10	>200	15	15,000
11	3	15	360
12	33	15	1,650
13	125	15	15,000

TABLE 53. PFN DATA WITH 1 026 CAPACITOR

Run	Rate	Voltage (kV)	Total Shots
14	50	10	9,000
15	50	13	4,500
16	50	15.0	9,900
17	>200	15.0	16,500
18	50	15.0	18,000

TABLE 54. C₆ CASE TEMPERATURE DATA

Run	T _{initial} (°C)	T _{final} (°C)	T _{max} /Time
14	26	32	41/13 min
15	41	43	49/10 min
16/17	36	51	66/10 min
Note: T _{max} /time means the maximum case temperature (°C) at how long after the run.			

11.0 FOIL EDGE INVESTIGATION

One of the energy density limiting factors previously identified was capacitor failure through corona at the edges of the capacitor foil (see Figure 31). It was therefore decided to investigate methods of smoothing the foil edge, and to perform weight minimizations based on the smooth edge.

11.1 FOIL EDGE TREATMENT

A study was undertaken to evaluate techniques of capacitor foil edge treatments. A rounded foil edge would be expected to provide a higher corona inception voltage for capacitors than the normal rough sheared edge. An obvious constraint on any practical process is that the edge treatment must be usable on rolls of capacitor foil.

A sheared edge is shown in Figure 63. These are SEM microphotographs of 0.00025 inch thick aluminum foil. Figure 64 is a treated edge. This particular edge is propane torch conditioned, but the shape is typical of all treated edges. All testing was performed on this type foil. Testing consisted of edge treatment, SEM examination, and corona inception measurement in an oil encapsulated two plate capacitor. The capacitor, shown in Figure 65, is a special configuration which provides for maximum electrical stress at the treated foil edge. It is assumed that the corona breakdown mechanism will occur at the test edge of Figure 65.



(a) 1/4 mil rough side.



(b) 1/4 mil edge view.

Figure 63. Untreated 1/4 mil foil.

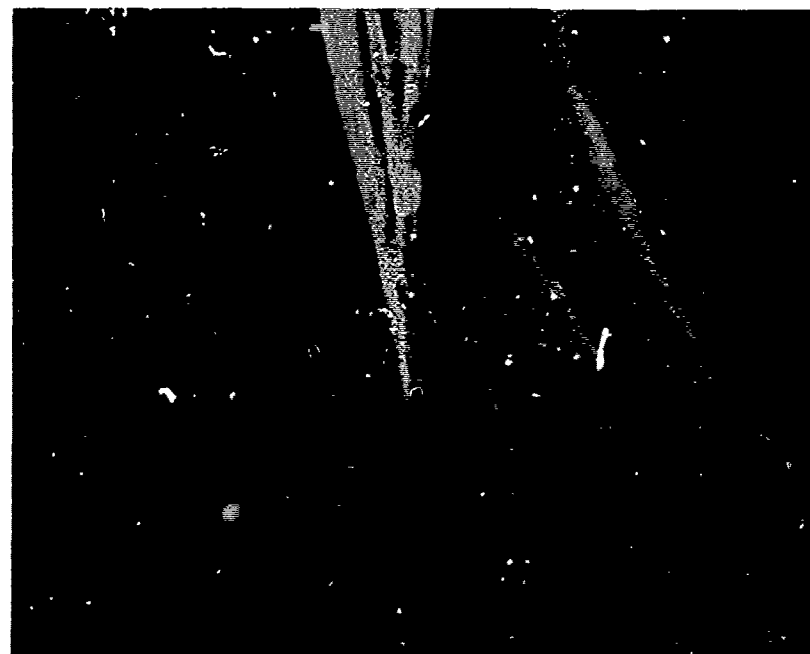


Figure 64. Treated foil edge.

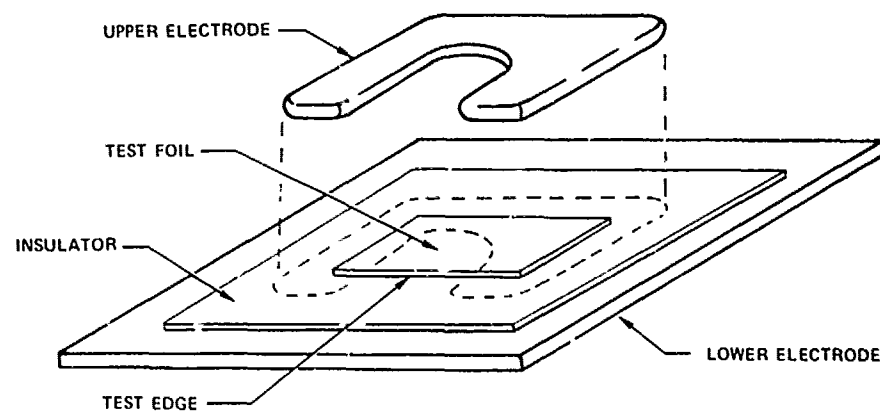


Figure 65. Foil edge corona test fixture.

11.1.1 Processing Limitation

Processes which can change foil edge geometry are:

- Folding to create a new edge
- Spark erosion treatment
- Laser cutting
- Flame treatment
- Gaseous discharge plasma etching
- Chemical etching
- Fine grit blasting
- Electropolishing

Examination of a roll of capacitor foil leads to the conclusion that any process dependent upon rerolling prior to capacitor winding will be extremely difficult, and probably would require a machine like a capacitor winder to implement. The edge distortion and unevenness of the edge, coupled with the extreme distortion in handling operations led to this conclusion.

Because the edges on different wraps within a roll were not well aligned, bulk treatment of the edge would not be expected to be uniform. For these two reasons, gaseous plasma etching and wet chemical processing were discarded as potential treatments.

Spark erosion techniques could be used to cut a new edge on a bulk roll. Spark erosion, folding, laser cutting, fine grit blasting and flame treatment could all be done on a capacitor winding machine as the foil is being unrolled.

11.1.2 Process Evaluation

Four different processes were evaluated. Electropolishing had been previously tested, and was found to produce a poor edge. Folding is possible, and the improvement has been well established.

11.1.2.1 Laser Cutting

Laser cutting was performed on a "Q" switched Korad machine usually used for resistance trimming of hybrid substrates. Lasers cut material by

localized heating due to absorption of light energy. This melting is analogous to a cutting torch action.

The cut edge resembles a miniaturization of a steel plate cut with a torch as shown in Figure 66. Rounding is pronounced at the edge and confirmed by corona measurements but scattered material from the cutting action is also present in the region around the edge. The particle contamination is inherent in the cutting mechanism. This technique has the capability of being controlled adequately, but is not recommended for capacitor foil treatment because of high levels of particulate contamination which would be generated by such edge treatment.

11.1.2.2 Spark Erosion Treatment

Spark erosion cutting was done on a Charmille machine. This machine is used for removal of broken taps and machining of precision parts such as apertures and blind grooves. A matrix of cutting parameters was established. The control parameters which influence edge shape were cutting tool feed rate and spark energy. A typical edge is shown in Figure 67.

Additional tests were performed on multiple pieces of foil stacked up. Particulate contamination was excessive near the cut edge. This contamination naturally was minimized on the stacked material. Cutting of this type would not be recommended on the winding machine because of the creation of particulate contamination by the process. Rolls of material could be pretreated by spark erosion machining of the entire roll of foil. To efficiently do this, the foil should be supplied on an aluminum core rather than the usual cardboard core.

11.1.2.3 Fine Grit Blasting

Hybrid substrates sometimes have silk screened resistance elements. These resistors are fired and trimmed to final value using a grit blaster with a very narrow beam. Some foil was cut using the same technique. The edge had poor shape and was heavily contaminated. No further testing was done.

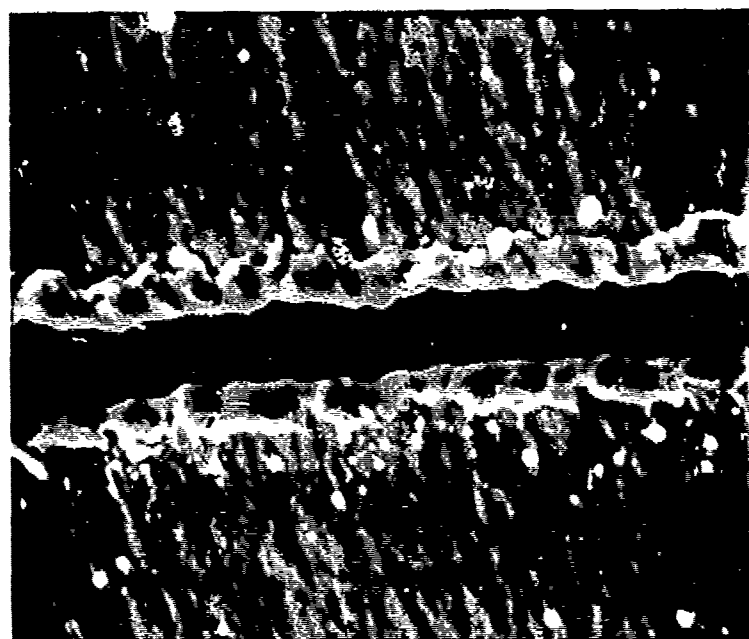
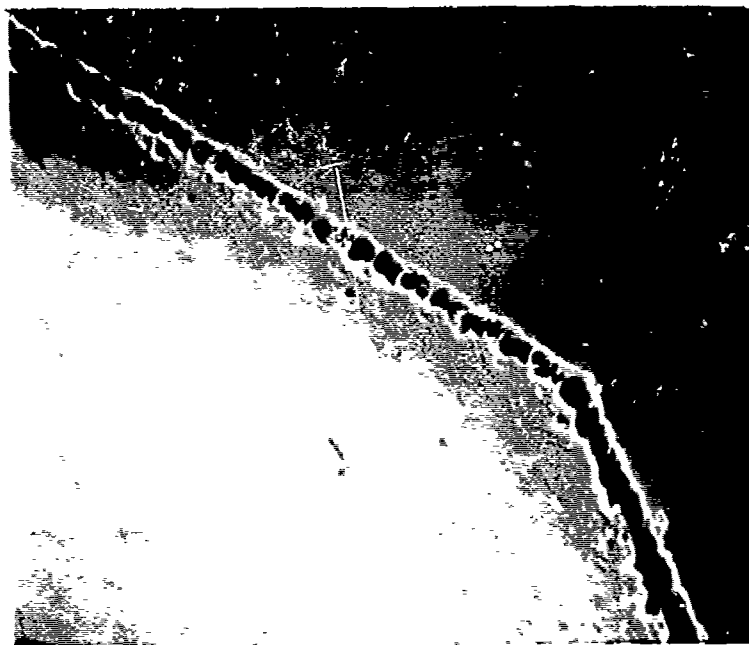


Figure 66. Laser cut foil edge.

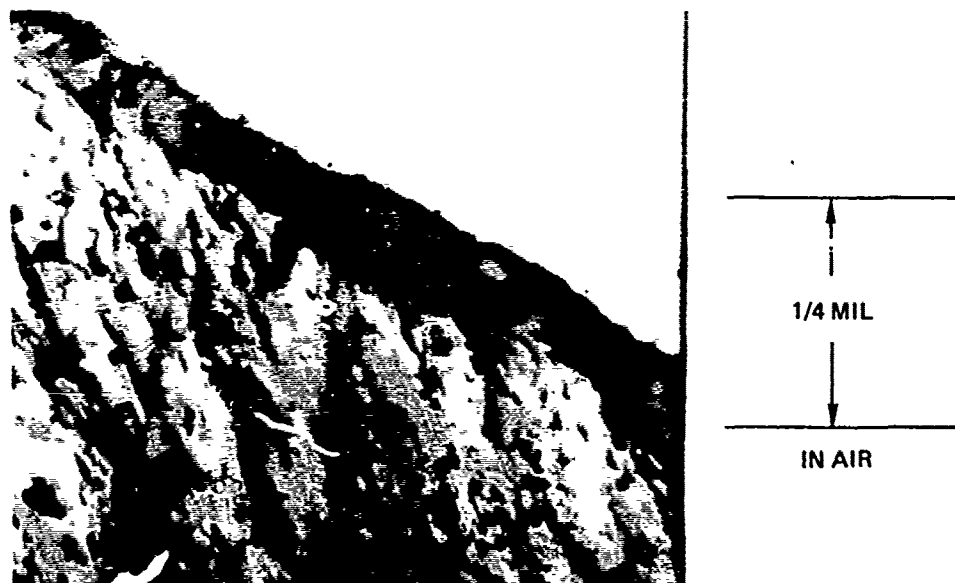


Figure 67. Spark erosion treated foil edge.

11.1.2.4 Flame Treatment

It was speculated that a torch flame could be used to remelt the foil edge to eliminate the sharp points. Initial tests produced non-local heating and distortion because aluminum is such a good heat conductor. Laying the foil on cooled surface solved that problem. A propane torch which had a poor flame control was used. It was expected that the rounding could be observed using this torch and if the technique had any validity, finer methods of control of the torch would be evaluated. The concepts of a large heat sink in contact with the foil worked so well that further work on better torches wasn't necessary. The basic conclusion is that large variations in flame distance and size will burn off or remelt the edge of the foil away from the heat sink and stop its action where the aluminum foil is well heat sinked. It is expected that a heated air jet would behave equally well, although this was not checked.

A torch treatment method would be very easy to build into a conventional capacitor winder. A water cooled metal roller would be necessary in the treatment area.

11.1.3 Corona Testing

The fixture shown in Figure 65 was used for foil edge evaluation.

The insulation was:

- 0.003 inch kraft paper
- 32 gauge polysulfone film
- 0.0003 inch kraft paper
- 32 gauge polysulfone film
- 0.0003 inch kraft paper

The fixture was placed in a pyrex dish and vacuum baked at 105°C for one hour at 30-50 microns pressure. It was then filled with processed mineral oil while in the vacuum chamber. The filling was done over a 1/2 hour period. Each fixture filling had a number of preprepared sample stacks consisting of insulation and aluminum foil under the oil surface. These were positioned as shown using tweezers. The samples were not moved above the oil surface during positioning so no air bubbles were trapped.

Each sample was measured for its corona inception voltage, defined by a 300 picocoulomb in 30 seconds discharge rate. Table 55 shows the data taken.

As expected, the four edge treatments all give a higher corona inception voltage than the original edge configuration. The data shows large scatter. However, it is comparable to previously published data.

11.1.4 Conclusions:

Spark erosion, laser cutting and flame torch treatment will all increase the corona inception voltage of foil edges.

TABLE 55. CORONA INCEPTION VOLTAGE, FOIL EDGES

Fixture Only	Normal Edge	Folded Edge	Spark Erosion	Laser	Torch
4490	4000	4210	4050	4160	4340
	4000	4250	4110	3850	4100

- The flame treatment is the easiest to implement.
- Spark erosion cutting of bulk foil rolls is worth testing.
- Corona inception voltage measurements only show trends and aren't repeatable enough to be considered definitive.
- A large sample of capacitors must be built before one can evaluate how energy storage or reliability is improved by capacitor edge foil treatment.

11.2 CAPACITOR WEIGHT MINIMIZATION

Capacitors constructed on this program which survive the first few tests normally fail because of corona at the foil edges. If a foil with a rounded edge, produced by any of the mechanisms described in 11.1, were used, the limit on the achievable energy density would be the peak field at the edge of the foil, not the average field. This minimization is based on that assumption.

The energy stored in the capacitor is

$$U = \frac{C \epsilon A V^2}{t_d}$$

where C is a constant, ϵ the average dielectric constant A the area, V the applied voltage, and t_d the dielectric thickness. The average field is V/t_d , so

$$U = C \epsilon A t_d E_{AV}^2$$

The weights of the dielectric and foil are:

$$W_d = A t_d d_d$$

$$W_f = A t_f d_f$$

where d is the material density. The energy density is then:

$$\begin{aligned} ED &= U / (W_d + W_f) \\ &= E_{AV}^2 / \left[d_d + \frac{t_f}{t_d} d_f \right] \end{aligned}$$

Using f = Edge Enhancement Factor = $E_{\text{edge}}/E_{\text{av}}$, $R = d_f/d_d$, and $D = t_d/t_f$, this becomes:

$$ED = \frac{D \epsilon E_{\text{edge}}^2}{d_f f^2 (D/R + 1)}$$

A plot of the Field Enhancement factor vs D is shown in Figure 68.

Rather than using this rather complex expression to test various designs, one may define a quality parameter. This parameter contains only design variables, and has the property that the maximum value of the quality parameter contains the optimum design values. Such a quality parameter is

$$Q = \frac{D}{f^2 (D/R + 1)}$$

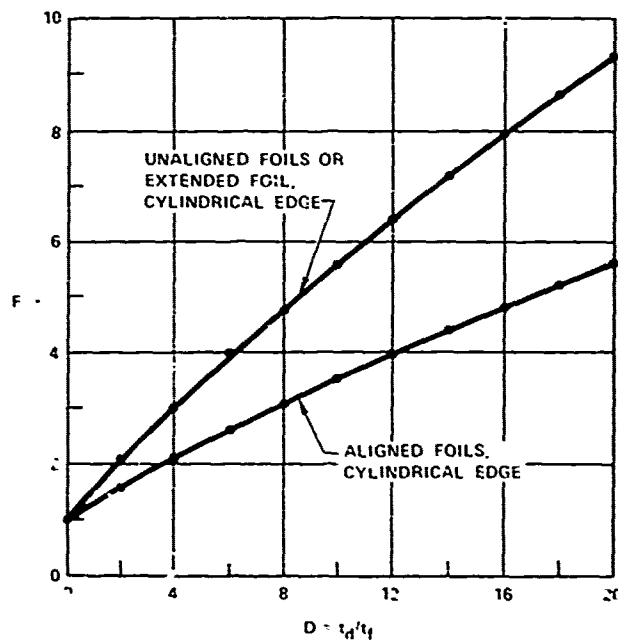


Figure 68. Field enhancement factor f vs thickness ratio, for cylindrical foil edges.

A plot of Q versus D for selected R values is shown in Figure 69, and shows that the maximum of Q occurs in the range $1 < D < 2$. Most common capacitor construction has D in the range 5 to 15. For example, design B on page 86 has D approximately 8. Therefore, according to this model, best results obtain when the foil and dielectric are of about the same thickness.

It must be added that there are refinements which could be incorporated into this model. The dielectric constant of the bulk insulation is rarely the same as that of the fluid, and it is the fluid which is up against the foil edge. It is possible to have a variety of different quality parameters. For example, suppose one maximizes ED at the same time holding E_{edge} at or below a particular value.

Capacitors with thick foil have been built, most notably the Westinghouse Mark VII and VIII power capacitors. These also incorporate folded foil, and the manufacturer claims greatly increased life.

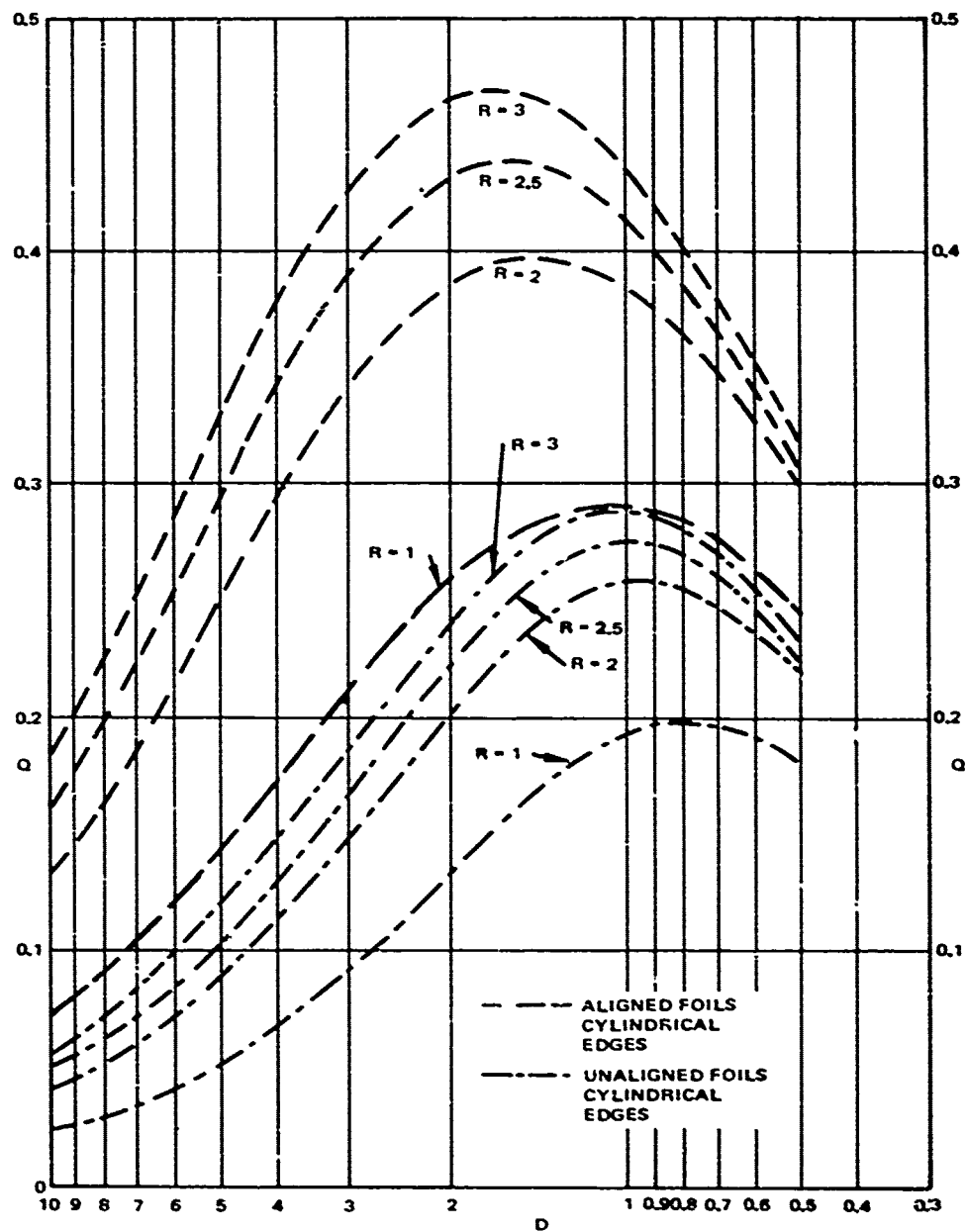


Figure 69. Quality parameter for foil edge effect.

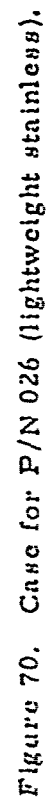
12.0 CASE WEIGHT MINIMIZATION

In a conventional capacitor of the size considered on this program, the case, case insulation, and terminal are an appreciable fraction of the total capacitor weight. This is illustrated vividly in Table 35, for P/N 014. Therefore, the development of two different types of lightweight case, metal and plastic, was undertaken. Because of the exploratory nature of this program, and because the exact intended conditions of use are not known and are presumed to be changing, little consideration of the operating environment was given. For example, the stainless steel encased units are very light and hermetically sealed, but they break if dropped and probably would not function well in a variable pressure environment unless the sides were stiffened.

12.1 METAL CASES

It was decided to design and fabricate as light a metal case as was possible to assemble. The capacitor chosen for assembly into the case was P/N 026. The result of the design is shown in Figure 70. The case itself is made of 5 mil stainless steel sheet. It is carefully folded into the shape shown in Detail 99, and spot welded to hold it together. The seams are then soldered; the soldering is facilitated by a 0.3 mil tin plating. Soldering was chosen over brazing because of the ease of assembly. The fill-port and ground posts are also made lighter than those usually used. The entire case without bushing weighs 75g. A completed capacitor using this case is shown in Figure 71.

A much larger design was then attempted, to house the 500 joule (1.1 μ F 30 kV) capacitor (P/N 036) described in Sections 14, 15, and 16. A scaled up version of the previous design, this case also had a larger fill port and only one ground post. It is shown in Figure 72.



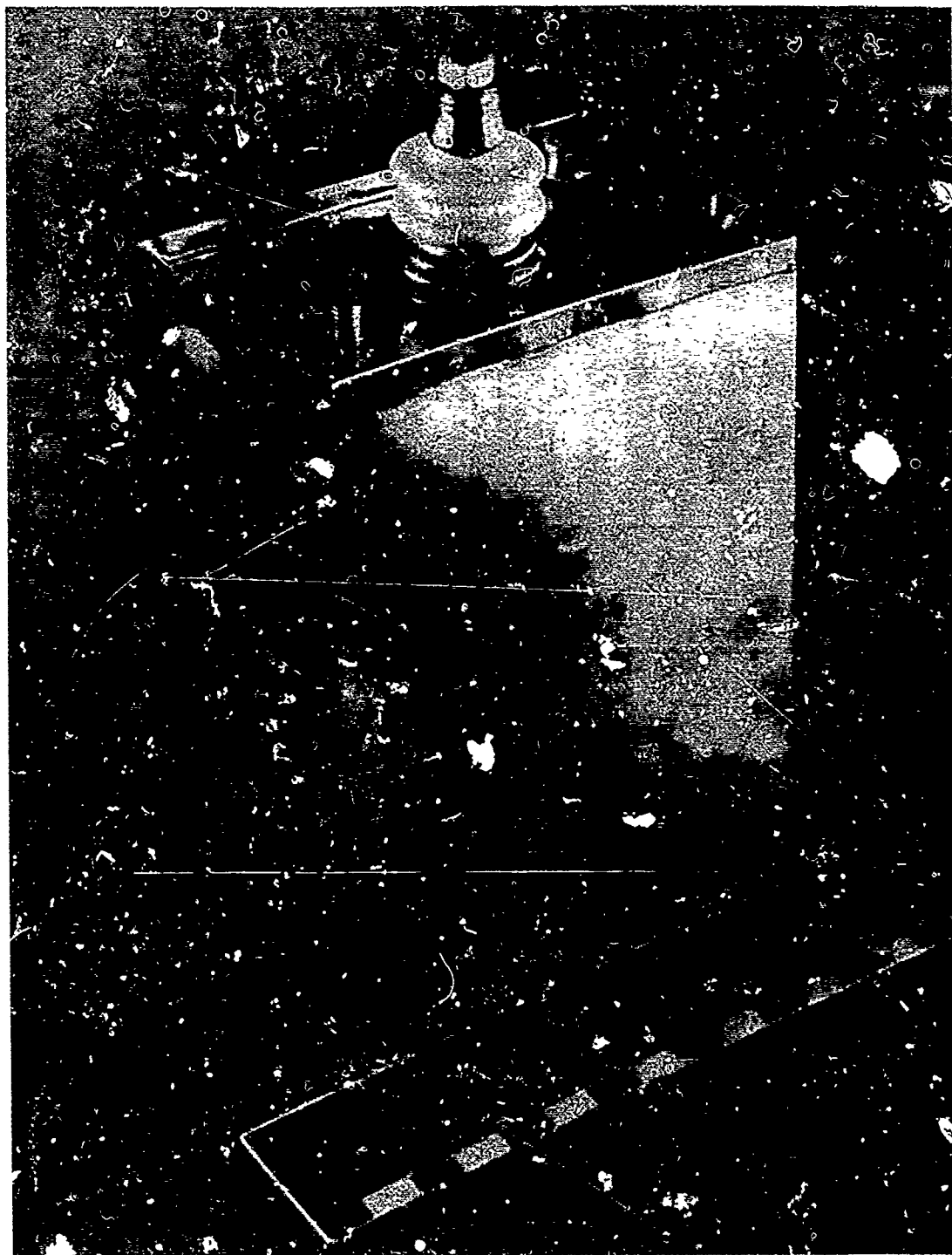


Figure 71. Capacitor P/N 026 utilizing very lightweight stainless steel case.

Both cases were moderately difficult to assemble, because of the care required in soldering the seams and handling the flimsy cans before the capacitors were assembled into them. The 026 case contained the capacitors well during testing, but the 036 case failed catastrophically in two instances, as described in Section 16. Standard ceramic bushings were used for both cases. However, for airborne operation high voltage connectors could be used, saving approximately 30 percent of the bushing weight.

12.2 PLASTIC CASES

Three fiber glass containers were designed and fabricated, to test their use as capacitor cases. Cases of this type have three main advantages: light weight, high strength, and built-in high voltage terminals.

12.2.1 Summary

Pressurization test of 5 psig showed that the cases have a volume increase of approximately 8 cubic inches, which is enough for a typical capacitor of this size over a temperature range of -58°F to $+194^{\circ}\text{F}$.

The containers showed evidence of oil seepage at 150°F . However, they did not have a seal coat, and vacuum impregnation or a Gel-coat would prevent this.

Limited testing shows excellent feasibility.

12.2.2 Fabrication Procedure

Case size was 5.48" x 7.13" x 5.0" with a corner radius of 0.875". Wall thickness was 0.050". The top was flared to accept a flat lid. Lid thickness was 0.120".

Three capacitor containers were formed as a laminated structure using 6 plies of preimpregnated glass cloth. After cleaning the aluminum layup tool, plies of the epoxy pre-preg were formed on the tool surface, with the cloth wrap fibers direction rotated 90° for alternate layers. The (6) ply layup was then covered with a nylon film, sealed off and evacuated to 28 inches of mercury. The vacuum bagged assembly was then placed in a hot air-circulating oven and cured under vacuum pressure for 3 hours at 350°F .

The cured part was allowed to cool to room temperature, and then stripped from the mold.

The rough molded containers were machined on an open set-up to finish dimensions. The lid or cover was formed from the same prepreg material, cured in a heated platen press at the same cure temperature and time as the container. After cure the cover was trimmed to fit the container.

On one container the cover was fitted with an air inlet tube for pressurization. This was then bonded to the case using a gap filling epoxy paste adhesive (Epibond 934).

The second container was assembled into a working capacitor. The unit contained 10 capacitor pads (pad size 0.845" x 2.7" x 4.656") and was filled with mineral oil. The combined pad size with fiberglass ends was 4.375" x 5.5" x 4.656". (Volume 101.36 in³.) Volume of the container was 192.08 in³. The terminals were 10-32 bolts, held in place by epoxy. Two 1/8" pipe plugs were used to seal the fill hoses. This unit is shown in Figure 73.

12.2.3 Testing

Testing of one unit consisted of pressurization to 5 psig and measuring the deflection on the length and width.

Testing of the completed capacitor (3.02 MFD, 0.30 percent DF, 10 KVDC) was conducted at 150°F where the unit was checked for leakage.

Weight of the unit was 9.38 lbs, compared to 11.7 lbs for a P/N014. The plastic case weighs about 30 percent as much as the metal case.

12.2.4 Results and Discussion

The Table 56 shows the difference in measurements when the case was subjected to 5 psig. Measurements were taken at the center part of the ends and sides.

When the pressure was shut off a build up of approximately 12 psig occurred. This blew the cover off with failure occurring at the bond line of the lid and case. A proper design of case and lid would prevent this. With the flat lid, failure was caused by peeling of the adhesive.

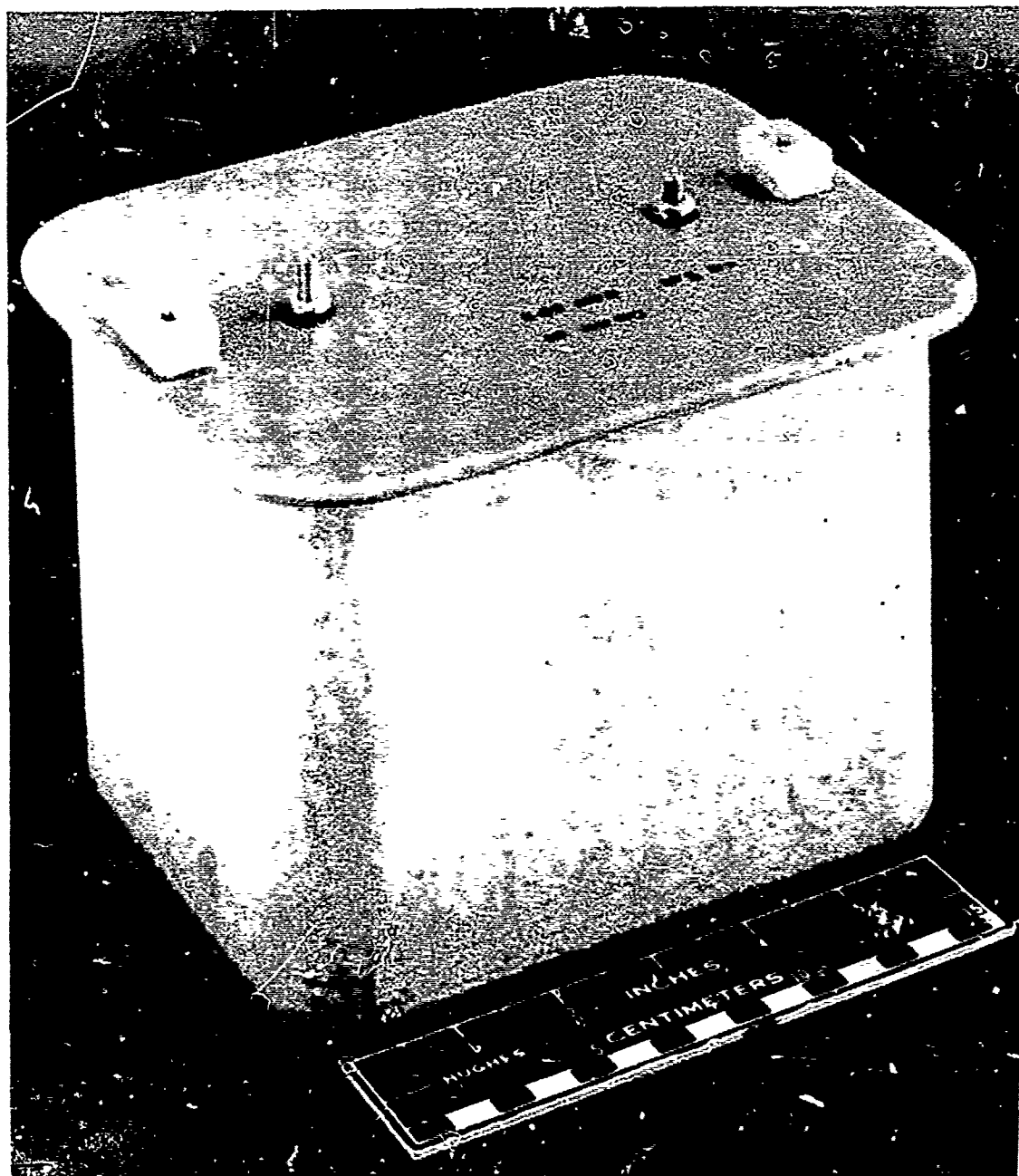


Figure 73. Lightweight plastic case with 014-type capacitor inside.

TABLE 56. PLASTIC CASE DISTENSION MEASUREMENT

	Measurement Initial	Measurement with 5 psig pressure	Increase
End Measurement	7.130	7.222	0.192
Side Measurement	5.485	5.712	0.227

The deflection on the sides and ends, and assuming the same on the bottom as the sides provides a volume increase of approximately 8 in³. Oil displacement in this capacitor over the temperature range of -58°F to +194°F would be 6 in³.

When the completed capacitor was heated to 150°F evidence of oil was noted. This was not a major leak but more of a "seeping" action through the walls of the container. The unit did not have a seal coat, and vacuum impregnation or a Gel-coat would possibly prevent this.

13.0 EXTENDED FOIL TERMINATION

This was the first of four tasks added late in the program, with the objective of applying the developed technology to a different set of service requirements. It was desired to achieve light weight in a 4 section $10\mu\text{S}$ output pulse width PFN. A brief analysis of the currents involved, shown in Section 13, combined with the measurements of ESR versus frequency, shown in Section 5.0, ruled out the tab-type terminations employed on all the other capacitors developed for this program. Therefore, a development of reliable extended-foil type terminations for this service was undertaken.

13.1 SELECTION OF TECHNIQUES

As customarily practiced in the capacitor manufacturing industry, an extended foil termination is made basically by smearing solder on the foil protruding from the end of the section. This technique is at best uncontrolled and subject to wide variation in contact resistance and therefore failure rate. Therefore, other methods not usually applied to extended-foil terminations where foil is used were investigated as well.

Four techniques were examined:

- Commercial soldering.
- Oxy-acetylene welding in nitrogen.
- Flame-spray of metal.
- Electron beam welded strips.

The commercial technique was investigated to determine if the process could be made well controlled and repeatable. The oxy-acetylene welding was tried to see if a carefully controlled bead could be obtained. The flame spray

technique is customarily used on commercial metallized film capacitors, and Hughes had recently developed techniques to produce uniform repeatable low resistance terminations. The electron beam welding was the technique thought to have the most promise, inasmuch as it can be very precisely controlled.

13.2 CONTACT RESISTANCE TESTS

In order to test the efficacy of various techniques, test specimens for the measurement of contact resistance were made. These specimens were similar in size and shape to standard capacitor sections made for extended foil termination. However, the foils used protruded from both sides of the specimen, so that the capacitor was shorted, as shown in Figure 74. When the termination technique was applied to both sides of the specimen, the contact resistance was easily measured using a Kelvin bridge. The foils protruded 0.25 inch (0.63 cm) on each side except where noted.

Both the commercial solder technique and the gas welding produced sloppy, poorly controlled joints which were obviously high in conductive particle residue. Some problems with the solder wetting the foil were encountered. However, an aluminum solder, as reported by TRW (AFAPL-TR-75-69) was not tried, because of an esthetic reluctance to use the necessary extremely corrosive flux.

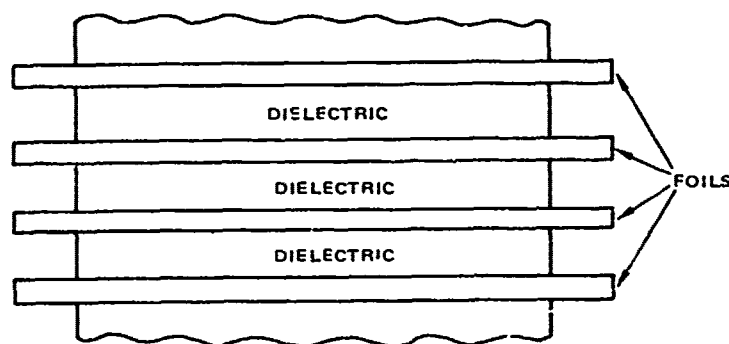


Figure 74. Termination test device, cross section.

For the flame spray tests, two different materials were used in the spray:

- Babbitt only
- Aluminum with babbitt on the top.

For the electron beam work, straps 0.016 inch (0.04 cm) of alloy 2024 were welded to the sample ends. A typical flame spray unit is shown in Figure 75(a), and an electron beam welded unit in Figure 75(b).

Samples of both flame spray types and the electron beam weld were temperature cycled. The DC contact resistance of all specimens was acceptably low, and no changes were observed after temperature cycling. These data are shown in Table.57.

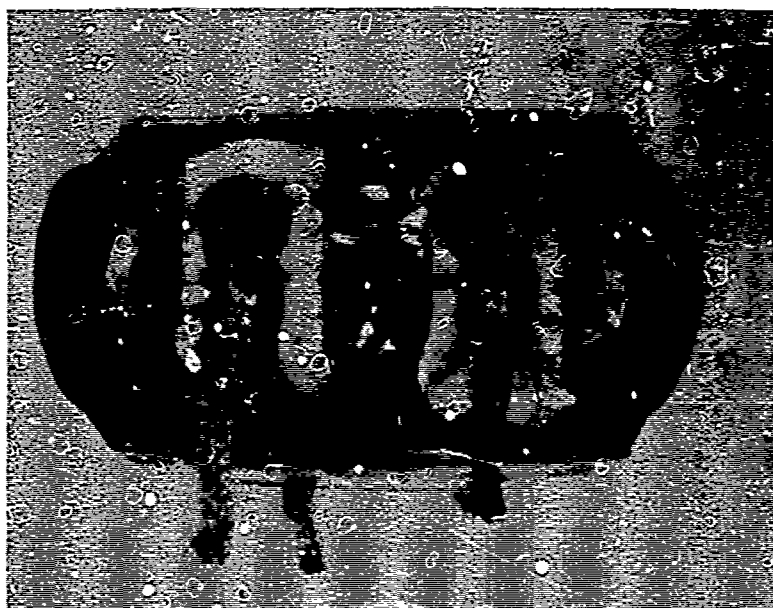
Following the temperature cycling, each specimen was microsectioned to examine the termination. There was some tearing of the thin (0.25 mil or 6 μ m) foil during the polishing process. The babbitt termination is shown in Figure 76(a). There is some evidence of penetration of particulate matter into the dielectric stack. The electron beam termination is shown in Figure 76(b), and as expected the termination is very clean and localized.

The electron beam terminations were not mechanically sturdy, and it was found possible to pull them off by careless handling, as Figure 77 shows. The flame sprayed terminations were quite rugged.

13.3 CAPACITOR PULSE TESTS

Capacitor sections were fabricated for functional evaluation. These sections had layer designs similar to the successful units described in Sections 4 and 5. The samples were wound so that 0.080 inch of foil extended beyond the insulation on each end, which was very satisfactory for the flame-spray termination. The electron beam exhibited a tendency to cut into the capacitor stack, so the units were rewound with 0.25 inch foil projection.

Leads were soldered directly to the babbitt as shown in Figure 78. In a production situation it would be desirable to use ultrasonic soldering techniques to eliminate the flux, which would surely cause ionic degradation of the impregnant. The electron beam welded units had nickel and copper electro plating applied to the strap ends, so that connections could be soldered.



(a) Flame spray babbitt.

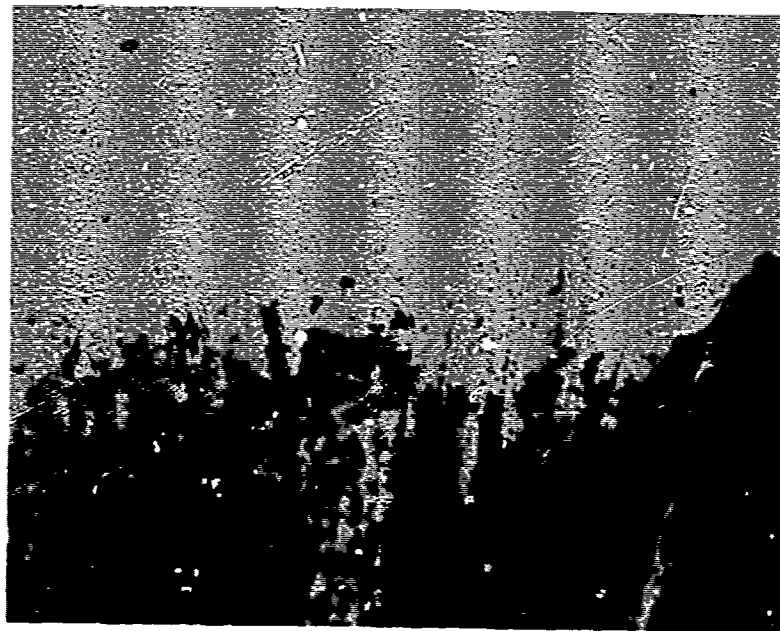


(b) Electron beam weld.

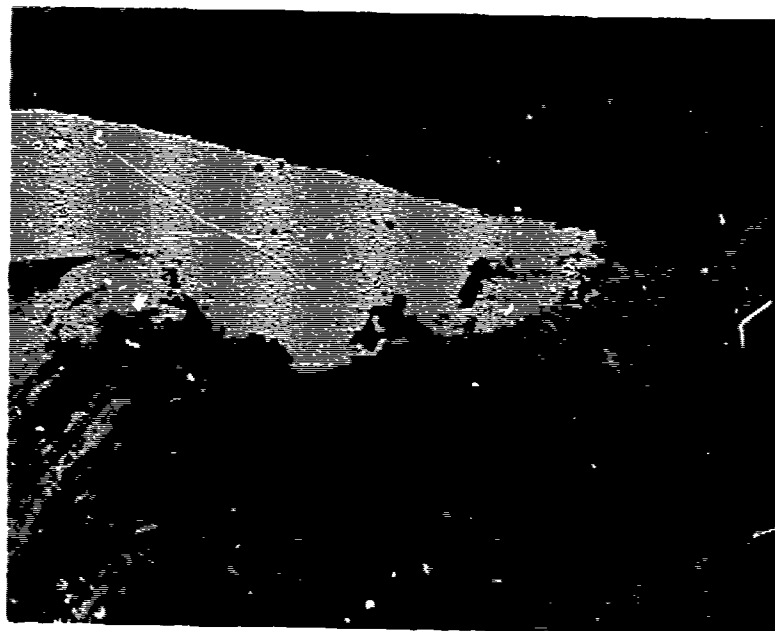
Figure 75. Typical terminations.

TABLE 57. EXTENDED FOIL CONTACT RESISTANCE TESTS

Condition		Resistances in Ohms			
		#1 Babbitt	#2 Bab & Al.	#3 Electron Beam Weld	#4 Electron Beam Weld
Initial Reading	A	0.0005	0.0007	0.0003	0.0003
	B	0.0006	0.0007	0.0003	0.0003
3 Cycles 0° to +100°C	A	0.0005	0.0007	0.0003	0.0003
	B	0.0006	0.0007	0.0003	0.0003
3 Cycles -40° to +125°C	A	0.0004	0.0005	0.0003	0.0003
	B	0.0004	0.0005	0.0003	0.0003
1 Cycle LN ₂ to +150°C	A	0.0007	0.0011	0.00036	0.00072
	B	0.00087	0.00093	0.00048	0.00059
1 Cycle LN ₂ to +150°C	A	0.00052	0.00098	0.00035	0.00073
	B	0.00054	0.00088	0.00048	0.00058
1 Cycle LN ₂ to +150°C	A	0.0005	0.00076	0.00035	0.0007
	B	0.00059	0.00070	0.00042	0.00059



(a) Microsection 60X Babbitt.



(b) Microsection 60X electron beam weld.

Figure 76. Termination microsections.

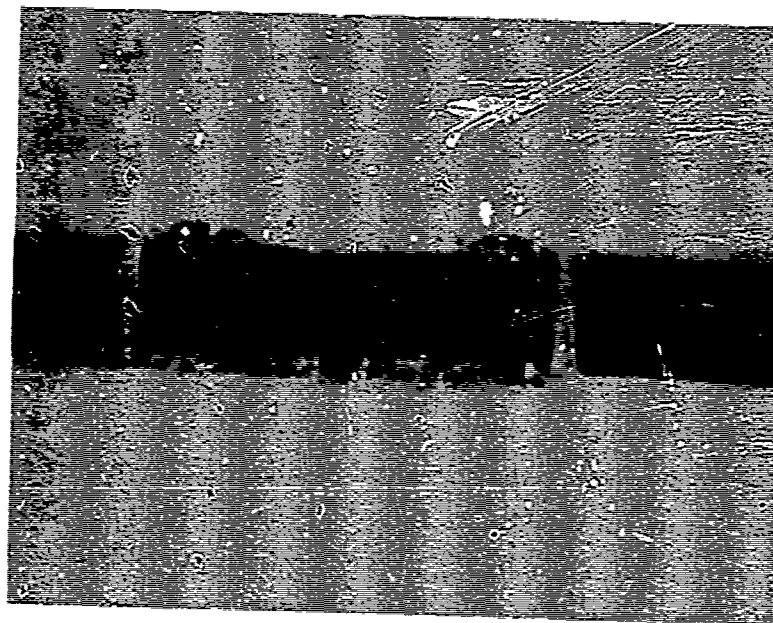


Figure 77. EB weld, torn loose.

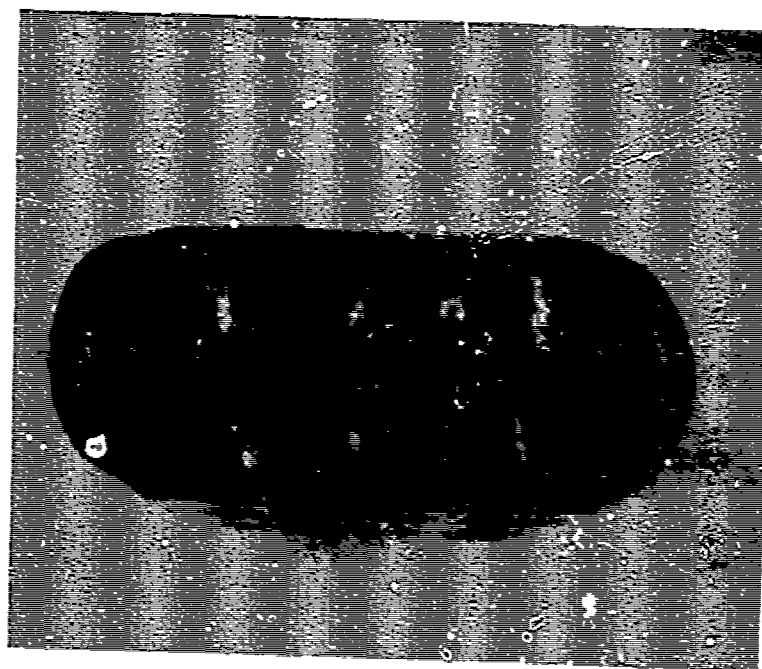


Figure 78. Rabbitt termination.

Two capacitors bearing each type of termination were assembled for pulse testing, using the techniques and fixtures shown in Sections 4.2 through 4.5. The capacitors were 2.2 μ F 7.5 kV units, and were impregnated with mineral oil. A summary of the test results is given in Table 58. The electron beam welded units failed at lower voltages than expected, while the flame sprayed units performed well.

All capacitors were disassembled to determine the cause of failure. The electron beam welded terminations failed because of the inadvertant cutting of the dielectric during welding, as shown in Figure 79(a). It is suprising, in retrospect, that they worked at all. No current crowding was observed. Both flame sprayed units failed at the outer edge of the , about 1/2 inch from the termination, as shown in Figure 79(b). No degradation of the termination was found when the section was unrolled. The failures were not completely understood, but might have been assisted by the inevitable free metal particles produced by the process.

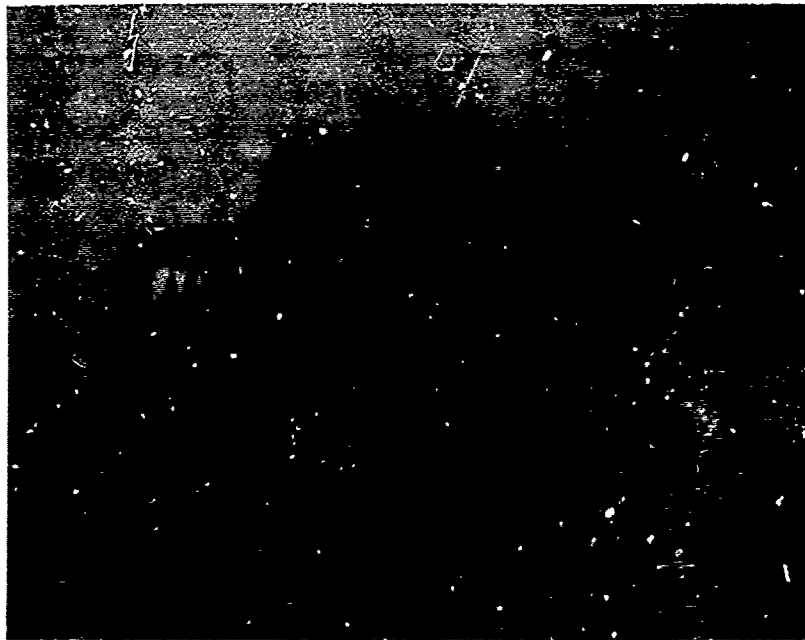
13.4 CONCLUSIONS

The really intriguing development uncovered in this work is the use of electron beam welding to terminate extended foil capacitors. The connections were very good, but further process development would be necessary to eliminate the dielectric cutting observed in these specimens. The termination is mechanically fragile, but very clean.

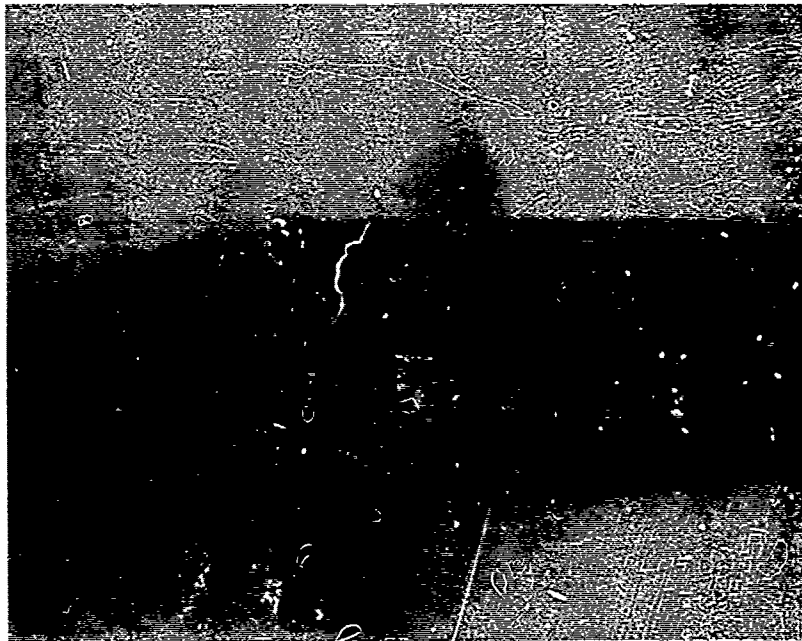
The flame-sprayed babbitt terminations are acceptable and uniform, but have an inherent problem with particulate contamination.

TABLE 58. PULSE TEST OF TERMINATIONS

S/N	Voltage kV	Shots, 1000s	Comments
1	3.0	35	Failed at end of burst.
2	3.0	105	Ok
3	3.0	105	Ok
4	3.0	105	Ok
2	4.0	35	Failed at end of burst
3	4.0	70	Ok
4	4.0	70	Ok
3	5.0	35	Ok
4	5.0	35	Ok
3	6.0	35	Ok
4	6.0	35	Ok
3	7.0	18	Ok
4	7.0	18	Ok
3	7.5	8	Failed during burst
4	7.5	8	Failed during burst
Notes: Shots are cumulative for the voltage given only. S/N 1 and 2 are electron beam. S/N 3 and 4 are flame spray.			



(a) EB cut at arrow.



(b) Failure at arrow-babbitt termination.

Figure 79. Electron beam cut in dielectric

14.0 CAPACITOR DESIGN

This section reports the design of a $1.1\mu\text{F}$ 30 kV capacitor which will operate satisfactorily in a PFN of the following specification:

Type	: E
Number of Sectors	: 4
Output pulse	: Rectangular
Pulse width	: $10\mu\text{s}$
Impedance	: 1.125 ohm
Pulse Rate	: 50 to 100 pps
Duty	: 90s burst every 2hr.

These capacitors use the extended-foil termination reported in the previous section.

14.1 LAYER DESIGN AND NUMBER OF PADS

A number of different trade-offs were considered in the design of this capacitor. Several different layer designs and several different pad arrangements were experimented with to obtain a lightweight but reliable capacitor. It became clear that an arrangement which used the fewest pads was lightest, so therefore four series pads valued at $4.4\mu\text{F}$ were used. In order to make physically realizable sections which would package into a reasonable shape, wider insulation and foil than was used previously was specified.

Because of the results of the 026 testing described in Section 6, various layer designs were examined to see if an increase in operating voltage might be obtained (this design was made before the PFN test

described in Section 9). A variety of configurations was compared for field balance, as shown in Table 59. Weight penalties are displayed in Table 60.

The testing performed in Section 6 showed acceptable performance at 12.5 kV. Because a multiple-section design was to be used, it was decided to add a margin of safety by using 0.32 mil polysulfone, instead of 0.24 mil. This resulted in a field balance only 8 percent larger at 7.5 kV than the 026 layer arrangement at 6.25 kV, with a 13 percent weight penalty. Winding data is shown in Table 61.

TABLE 59. FIELD BALANCE COMPARISONS

No.	Configuration	Field (V/mil)		
		Oil	Paper	Plastic
1	P/N 026 at 15 kV	2761	3430	5622
2	P/N 026 at 12.5 kV	2320	2881	4415
3	Design D, DOP, 7.5 kV/pad	2505	3080	4726
4	5 Sections, P/N 026 pads	2286	2810	4351
5	P/N 026 pads with 36ga P. S.	2384	2930	4538
6	P/N 026 pads with 40ga P. S.	2274	2765	4328

TABLE 60. TRADE-OFF WEIGHT PENALTIES

Trade-off No.	% Thicker	% Lower ϵ	% Heavier
1	0	0	0
3	10	3.1	13
5	12	4	16
6	16	5	21

TABLE 61. WINDING DATA, P/N 036

Item	Value
Insulation Length	1118 in.
Insulation Width	6.0 in.
Foil Length	1078 in.
Foil Width	5.75 in.
Foil Projection	0.25 in.
Active Width	5.25 in.

15.0 PFN DESIGN AND FABRICATION

Two identical $10\mu\text{S}$ 30 kV PFNs were designed and fabricated to the specifications given in Section 10. The design of the PFN coil was accomplished according to the procedures set forth in Section 10, while the capacitors were fabricated according to the procedures in Section 6. Because an assembled PFN would contain 16 sections, the failure of any one of which would abort testing, it was decided to make the physical design of the PFN like that of Section 10, with individually interchangeable capacitors.

15.1 CAPACITOR FABRICATION

Capacitors P/N 036 were fabricated according to the designs and specifications of the previous section, using lightweight cans as described in Section 12. The internal packaging scheme is shown in Figure 80, and a finished capacitor is displayed in Figure 81. Static acceptance data is given in Table 62. Ten capacitors were fabricated, allowing 2 spares. The average capacitor weight was 9.6 lbs complete.

15.2 PFN COIL DESIGN

The PFN coil schematic is shown in Figure 82. The parameters of the design are given in Table 63. The coil was supported on the tops of the capacitors by the capacitor termination only.

15. ENCLOSURE

An enclosure for the PFN was designed. It is shown in Figure 83.

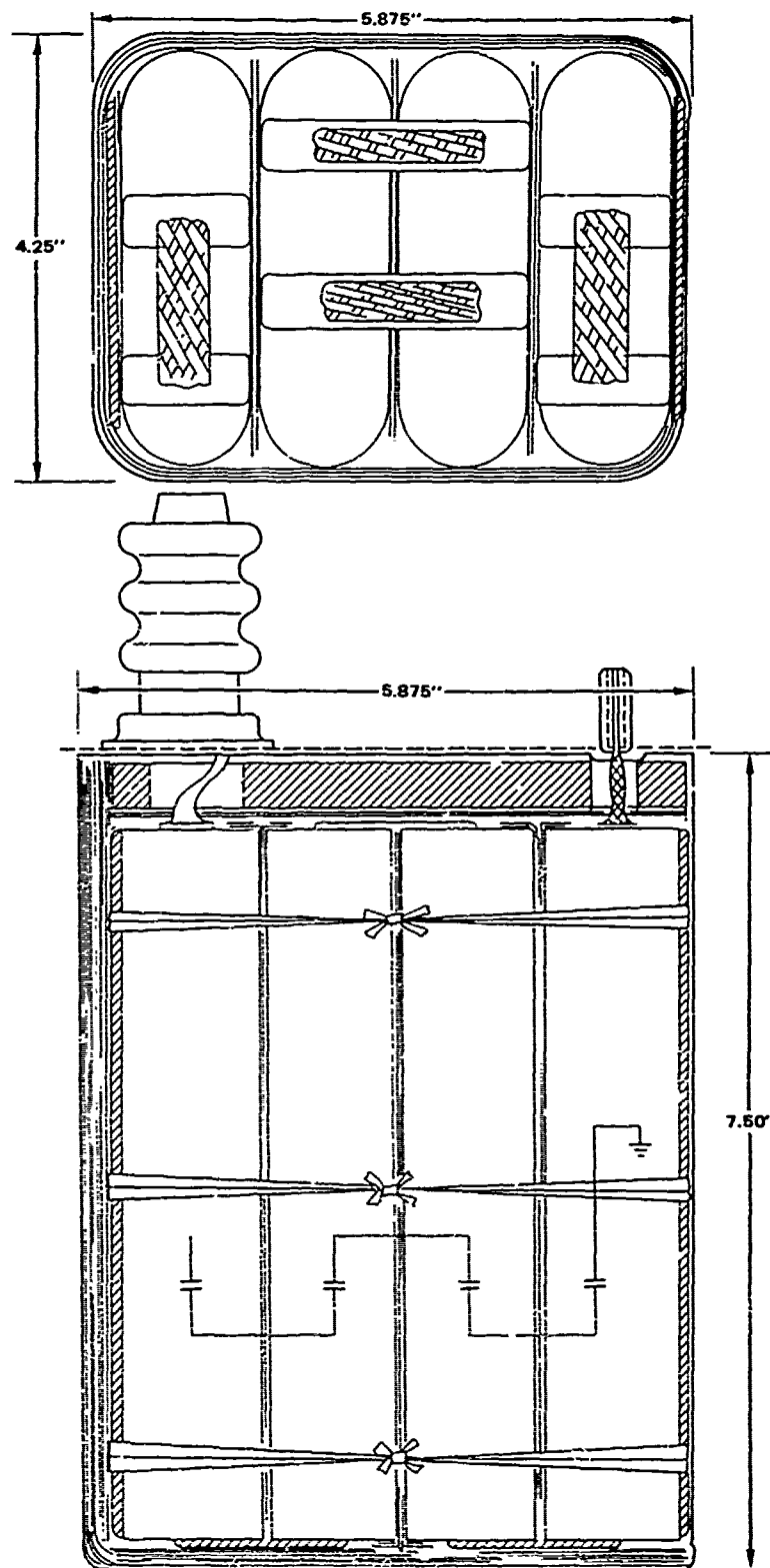


Figure 80. Internal packaging, P/N 036.

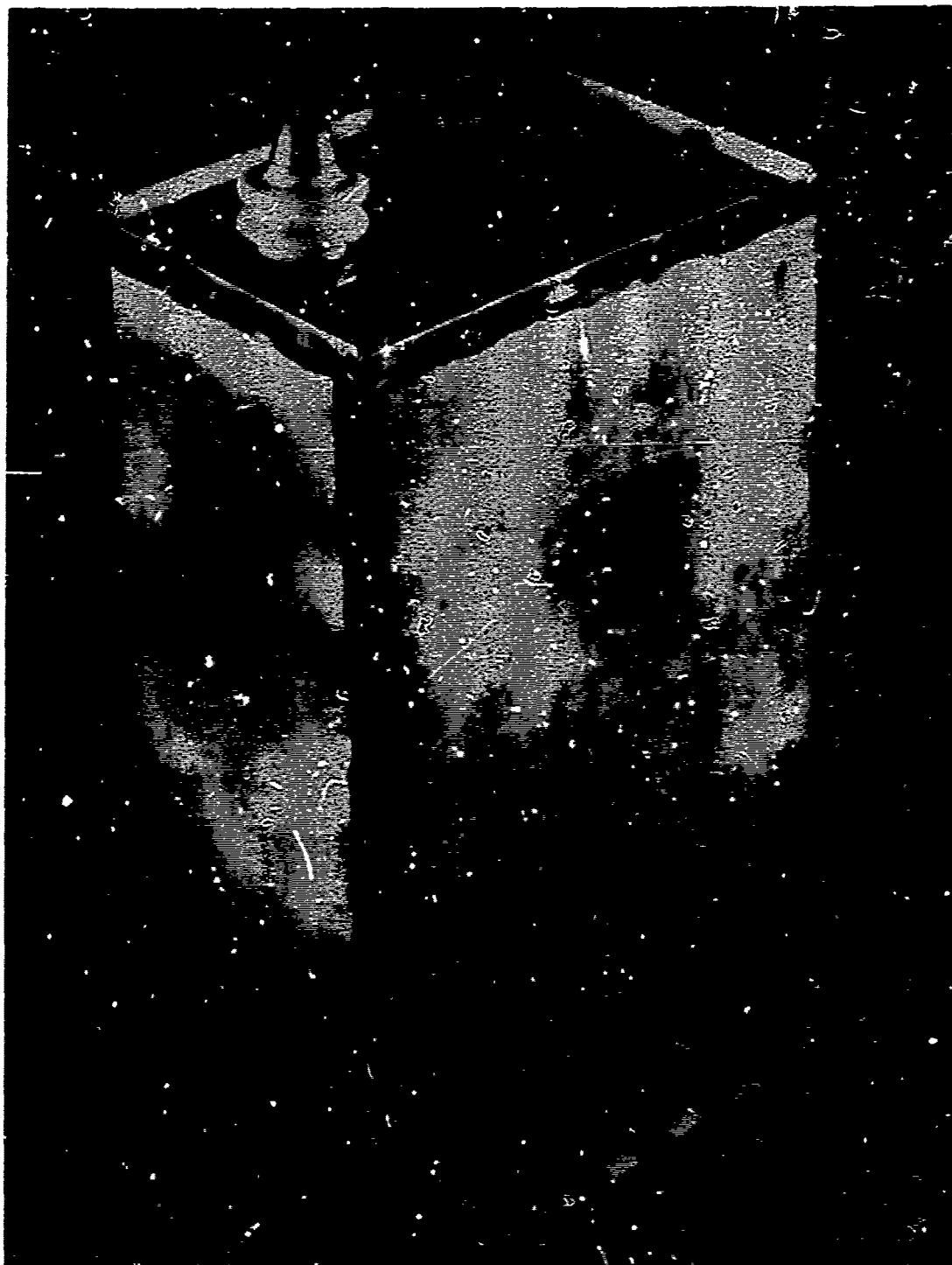


Figure 81. Capacitor P/N 036. 1.1 μ F 30 kV.

TABLE 62. P/N 036 ACCEPTANCE DATA

S/N	Capacitance (μF)	D. F. (%)	D. C. Leakage (6 kV) (μA)
1	1.133	0.38	1.6
2	1.145	0.38	1.8
3	1.159	0.32	1.7
4	1.134	0.32	1.55
5	1.140	0.29	1.45
6	1.137	0.29	1.35
7	1.146	0.28	1.85
8	1.149	0.32	1.25
9	1.142	0.32	1.35
10	1.146	0.30	0.89

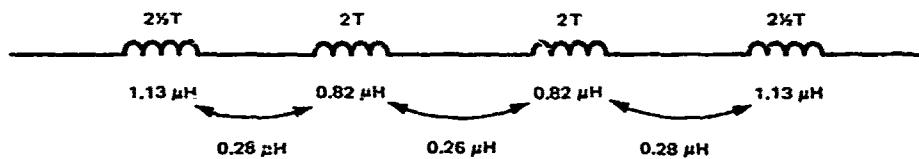


Figure 82. PFN coil schematic.

TABLE 63. PFN COIL PARAMETERS

Item	Value
Coil Material	0.625 dia copper tube, 0.062 wall
Inside Diameter	7.875 inch
Length	18 inches
Total Inductance	5.83 μH

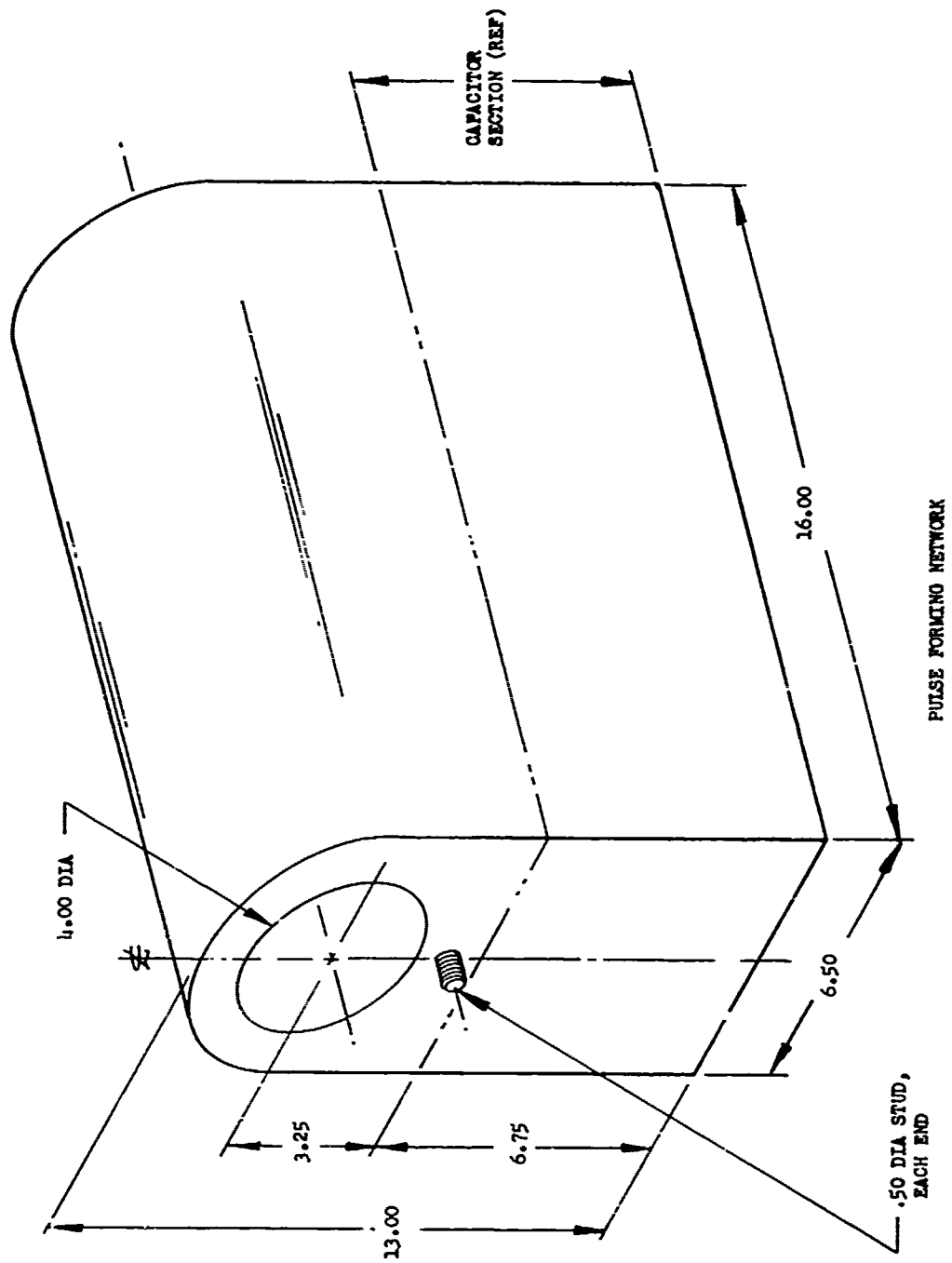


Figure 83. PFN enclosure.

16.0 PFN TEST

Because of the very high voltage involved, very high voltage hi-pot tests were performed on all capacitors. This revealed a problem with the flame spray termination, an electrical cure for which was subsequently devised and implemented.

16.1 CAPACITOR HI-POTS AND CONDITIONING

It was decided to perform a 3 minute 20 kV hi-pot (the limit of the apparatus) on each capacitor. The results were somewhat startling, as much to engineering as to the personnel performing the test. The first unit to be tested, SN 2, burst open with a loud report at 17.5 kV, as shown in Figure 84. Three additional units, S/N 1, 3, and 4, were tested behind a hastily constructed shrapnel barrier, and all failed.

Failure analysis revealed a flashover failure at the termination, similar to Figure 79(b). Dissection of the capacitor section revealed that, because of sloppy application of flame spray and inadequate masking, metal particles had penetrated the margin both at the center and at the outside edge. Additionally, these units had substantially more loose debris than were observed during the tests reported in Section 13. Apparently the components failed by flashing over a bridge of metal particles.

It was therefore felt that it would be possible to electrically condition the capacitors to burn out the bridges while controlling the energy so as not to damage the insulation. A pulsing fixture, to deposit known amounts of



Figure 84. Capacitor with case rupture.

energy, was built up, and all the remaining intact capacitors were pulsed according to the following schedule:

- 4 pulses at 4kV
- 10 pulses at 8kV
- 10 pulses at 12kV
- 10 pulses at 16kV
- 10 pulses at 20kV
- 10 pulses at 24kV
- 3 pulses at 25kV

All units except S/N 6 successfully underwent this treatment, and subsequently survived hipot. However, both leakage current and DF changed. Final and comparison data is shown in Table 64.

16.2 PFN TEST

A single PFN coil and 5 capacitors were shipped to the High Power Laboratory along with the units described in Section 9. Unfortunately, because of delays by the air freight carrier, the capacitors did not arrive until part way through the final day of testing. Because of this, and because the high dissipation factor of the conditioned components would preclude high rate operation, the unit was not tested.

TABLE 64. FINAL DATA, P/N 036

S/N	DF (%)	D. C. Leakage (μ A)	Pulsed?	Notes
1	0.38	1.6	No	Case rupture
5	0.38	1.8	No	Case rupture
3	0.32	1.7	No	Failed 6 kV
4	0.32	1.55	Yes	Failed 5 kV; pulsed; later failed 17 kV
5	0.29 (0.78)	1.45 (17.0)	Yes	Failed hi pot
6	0.28 (1.15)	1.35 (1.3)	Yes	
7	0.28	1.85	Yes	
8	0.32 (1.14)	1.25 (1.20)	Yes	
9	0.32 (0.57)	1.35 (1.40)	Yes	
10	0.30 (0.53)	0.89 (3.8)	Yes	
Values in parentheses after pulsing.				

17.0 CONCLUSIONS

For a long time it had been suspected that the presence of dirt, foreign particles, manufacturing defects, and poor materials has an impact on the life, reliability, and size of energy storage capacitors. However, most such components were made with old machinery and processes relatively unchanged for over 40 years, and as a consequence many different failure mechanisms were observed in each lot of capacitors:

- Winding machine set up
- Paper and foil wander
- Fold-overs
- Wrinkles
- Winding starts
- Foil and paper breakage
- Foreign material
- Solder connections
- Low resistivity oil
- Water in oil
- Gas in oil
- Incomplete impregnation
- Poor drying
- Tab failure
- Bulk insulation failure
- Corona at foil edges

The hypothesis adopted at the beginning of this program was that great increases in life, reliability, and energy density could be made by making the capacitors more mechanically perfect and from controlled materials. An early result of the pursuit of this hypothesis was the tension controlled capacitor winder. This single improvement allowed the electric field to very nearly double while maintaining the required life, and it made the component much more reliable, as well. One by one, the failure mechanisms have been eliminated with process controls until only two types of failures are observed: bulk dielectric failure (or random dielectric failure), usually occurring early in the component life; and corona at foil edges, the principal wear-out mechanism.

In terms of actual components, the results of this program are very good. Capacitors for pulse service have been designed, fabricated, and tested at 15 kV in the range 21J/lb to 77J/lb. Perhaps as impressive, the components are extremely reliable; capacitors from a single lot wear out within a few percent of total life of each other.

Finally, each technique used to develop these components is written down in detail in the sections above. Techniques that were unsuccessful are reported along with techniques that were successful. This has rarely been done in the development of capacitors, and it is hoped that these data will help anyone who is making capacitors to improve their product, and bring the capacitor business closer to engineering and further away from "black art".

APPENDIX A
STATEMENT OF WORK
CAPACITORS FOR AIRCRAFT HIGH POWER

APPENDIX A
STATEMENT OF WORK
CAPACITORS FOR AIRCRAFT HIGH POWER

1.0 INTRODUCTION

The objective of this program is to develop capacitor technology in two performance regimes. One regime is characterized by small capacitors operating at several hundred pulses per second (Hi Rep) and 15 kilovolts. The other regime is characterized by much larger capacitors operating at several tens of pulses per second (Lo Rep) and 40 kilovolts. The performance regimes are sufficiently different that it is unlikely the same dielectric system will satisfy both regimes. Although the dielectric systems may be different, design philosophy and techniques, and manufacturing methods are expected to be common to the capacitors of both regimes. Eventual use of both capacitors is likely to be in pulse forming networks (PFN) so that the capacitors may have to operate in a square pulse mode.

2.0 SCOPE

The contractor shall provide all materials, services, and equipment for the completion of this program. During the first portion of the program, the contractor will select the dielectric systems and conduct pad tests to establish a firm base for achieving the required capacitor performance. As part of the pad development effort, the contractor will determine the feasibility, desirability, and advantages of winding capacitor pads which contain no kinks or wrinkles. An outline of the program tasks is given below:

- Dielectric Systems Selection
- Pad Design
- Wrinkle Free Capacitor Pads

Capacitor Designs
Capacitor Fabrication and Test
Heat Sink/Cooling Tradeoff Investigation
PFN Operating Environment
Reliability and Maintainability Analysis
Pulse Forming Networks
Foil Edge Investigation
Case Weight Minimization
Extended Foil Termination
Capacitor Design
PFN Design and Fabrication
PFN Test

3.0 GENERAL BACKGROUND

During the past several years, pulsed high power requirements have grown to the point where electrical component and systems manufacturers believe the market potential is sufficiently large for them to enter the field. In the case of repetitively pulsed energy storage capacitors, programs funded by the Government have provided the impetus for much needed developments. The result is that the technology is available for energy storage capacitors with energy densities of 50-70 joules/lb at several hundred pulses per second or 200-250 joules/lb at a few pulses per second. Developments in the areas of dielectric films and impregnants, design and fabrication techniques and methods, and understanding of failure mechanisms indicate that increases of three or four in energy density may be attainable. This program is to develop capacitors which operate at several hundred pulses per second with an energy density of 200 joules/lb and capacitors which operate at several tens of pulses per second with an energy density of 500 joules/lb.

4.0 TECHNICAL REQUIREMENTS/TASKS

The contractor shall develop capacitor technology for capacitors operating in two different performance regimes. One regime is characterized by a relatively small capacitor operating at 15 kilovolts and several hundreds of pulses per second. The other regime is characterized by a

much larger capacitor operating at 40 kilovolts and several tens of pulses per second. Throughout this program, the contractor must be aware that this effort is to advance capacitive energy storage for eventual use on aircraft. The success of this program must not be achieved with concepts which are infeasible for airborne use. This is an exploratory development program of which a large portion is experimental in nature. Consequently, accurate and reliable measurements are necessary to the program success. To ensure that measurements made during the program are accurate and reliable, calibrations of all measuring equipment shall be traceable to standards set by the National Bureau of Standards, and a certificate to this effect shall accompany test data. The certificate shall also include the manufacturer, model number, and serial number of the equipment used.

4.1 Dielectric System Selection

The contractor shall conduct analyses and experiments to select the dielectric films and impregnant materials which offer the highest probability of achieving the performance given for the two capacitors in paragraph 4.4. The dielectric system for the two capacitors specified in paragraph 4.4 may not be the same. The contractor shall not construe that the Government is desirous of using the same dielectric system for both capacitors. Material costs shall not be a primary factor in the dielectric system selection. The ease or difficulty of winding wrinkle free pads shall not be a factor in the dielectric film selections. Performance as given in paragraph 4.4 is by far the most important consideration. The contractor shall not reject or eliminate an attractive dielectric film or impregnant for cost reasons without written approval from the AFAPL project engineer through the Procuring Contracting Officer.

4.2 Pad Design

The contractor shall design a pad for each capacitor specified in paragraph 4.4 using the dielectric systems selected in paragraph 4.1. Maximizing performance is the most important factor in the pad designs. For design purposes, the contractor shall assume he can make wrinkle

free pads. Problems associated with acquiring wrinkle free pads shall not be dominant factors in the design. Wrinkle free construction is a means to help achieve the required performance and is not to be considered an end in itself. Normal economies such as using available or standard material, available winding mandrels, winding machines already set up in a specific way, standard or previously designed containers or bushings, etc. shall be included in the design only if performance is in no way reduced.

4.3 Wrinkle Free Capacitor Pads

Capacitor pads are usually wound on a motor driven winding machine which runs at a rather rapid rate. The rapid winding rate is necessary for high production and low unit cost. Materials which must be wound for energy storage capacitor pads are very thin plastic films, paper, and aluminum foil. Rapidly winding such thin materials results in unavoidable kinks and wrinkles in the wound pads. When the pads are incorporated into capacitors and charged to the operating voltage, the kinks and wrinkles become the sites of very high electric fields and can lead to failure. The result is that when a number of such capacitors are tested to establish the performance rating, failures induced by kinks and wrinkles can significantly reduce the performance rating which might have been established had there been no kinks or wrinkles. Typically, capacitor pads are wound round then flattened to increase the packing factor. The flattening process can also produce kinks and wrinkles. A completed capacitor consists of one or more pads in a container. To maintain a high packing factor, the pads are often subjected to considerable pressure as they are encased. Hydraulic and pneumatic presses are frequently used to put pads in the case. This pressing operation is another possible source of kinks and wrinkles in the capacitor pads.

4.3.1 The fabrication of capacitor pads containing no kinks or wrinkles is the major manufacturing thrust of the program to achieve the required performance. Wrinkle free characteristics in themselves are of little interest but significant performance gains are expected in the absence of

kinks and wrinkles. The contractor shall establish the techniques, procedures, processes, etc. necessary to fabricate capacitor pads containing no kinks or wrinkles. Unit fabrication costs shall not be a primary factor in establishing the fabrication techniques, procedures, processes, etc.

4.3.2 The contractor shall fabricate a sufficient number of wrinkle free pads to demonstrate a capacitor mean life of a least 10^6 shots at the performance specified for the two capacitors in paragraph 4.4. The pads shall be fabricated in accordance with the designs generated under paragraph 4.2 and with the fabrication techniques, procedures, processes, etc. established under paragraph 4.3.1. These pads shall not be flattened and shall not be pressed into the case. The contractor shall do everything possible to ensure that these capacitor pads contain no kinks or wrinkles.

4.3.3 The contractor shall test the capacitor pads fabricated under paragraph 4.3.2 and demonstrate a capacitor mean life of 10^6 shots at the performance specified for the two capacitors in paragraph 4.4. Each pad which fails shall be subjected to a failure analysis. The failure analysis shall include complete disassembly of the pad and determination and documentation of the location, nature, probable cause, and suggested remedy of the failure. Any pads which are tested but do not fail shall be disassembled and inspected to determine if, in fact, they contained no kinks or wrinkles.

4.4 Capacitor Designs

Based upon the dielectric systems selected under paragraph 4.1 and the results of the work under paragraph 4.2 and 4.3, the contractor shall design a capacitor for the Hi Rep regime given below:

	<u>Hi Rep</u>	<u>Lo Rep</u>
Energy Density		
Joules/lb	200	500
Joules/in ³	3	10
Voltage	15 kilovolts	40 kilovolts
Pulse Width	20 μ sec	20 μ sec
Pulse Energy	500 joules	2.5 kilojoules
Pulse Rate	300 pulses/sec	50 pulses/sec
Pulse Train Length	2×10^4 pulses	3×10^3 pulses
Time Between Pulse Trains	2 hours	2 hours
Life (number of pulses)	10^6	10^6
% Voltage Reversal	20%	20%
Inductance	20 nh	20 nh
Shelf Life	1 Yr	1 Yr
Ambient Temperature	160°F	160°F

4.4.1 The contractor shall provide an estimate of both the Hi Rep capacitors under the assumption that wrinkle free pads are not available. This is to allow a comparison to be made of capacitors containing wrinkle free pads with capacitors containing standard production pads. The estimates shall include energy density, volume, and life with the other performance parameters given in paragraph 4.4. The estimates shall be based on the contractor's previous experience. Detailed designs, hardware fabrication, or experiments shall not be done to make the estimates. Upon completion of this task, the Contractor shall give an oral presentation covering all effort to date. (See paragraph 5.1.2.)

4.5 Capacitor Fabrication and Test

The contractor shall fabricate wrinkle free capacitors in accordance with the two designs completed under paragraph 4.4. The capacitors shall be fabricated to maximize performance. These wrinkle free capacitors shall be fabricated with the fabrication techniques, procedures, processes, etc. established under paragraph 4.3.2. Fabrication economies may be pursued only if performance is in no way compromised or reduced.

Twenty capacitors shall be fabricated. These capacitors shall be housed in cases specifically designed for this application. The intent is to provide lightweight, though not necessarily weight-optimized, cases. Each capacitor which fails shall be subjected to a failure analysis. The failure analysis shall include complete disassembly of the capacitor and determination of the location, probable cause, and suggested remedy of the failure.

4.6 Special Measurements

4.6.1 Temperature and Voltage Measurements - Throughout the testing portions of this program the contractor shall make accurate temperature and voltage measurements. Temperature measurements of interest are bulk temperatures for the purpose of accurately establishing the temperature rate of rise for capacitors during operation. Whenever feasible the contractor shall measure bulk temperature when both pads and capacitors are tested. Voltage measurements made on pads and capacitors shall be within an accuracy of 0.50%. This requirement is necessary since a number of performance parameters are strong functions of voltage and relatively small error in voltage can produce a relatively large error in the parameter.

4.6.2 Pulse Shape Analysis - During tests of both pads and complete capacitors, the contractor shall include the instrumentation necessary to record and analyze the output pulse shapes. The contractor shall use the resulting information to establish the electrical parameters of the pads and capacitors, evaluate the fabrication techniques and materials, and determine if this information can be used to predict incipient failures.

4.7 Heat Sink/Cooling Tradeoff Investigation

The contractor shall conduct an investigation to determine from weight, volume, and performance considerations when it is advantageous to actively cool capacitors and when it is advantageous to let the capacitor absorb the heat generated, i.e., heat sink. The tradeoff between cooling and heat sinking shall be made as a function of materials, dissipation factor,

repetition rate, average power, running time, ambient temperature, energy stored, geometry, etc. Active cooling investigations shall include such approaches as forced air cooling, forced liquid cooling both internal and external to the capacitor case, conductive heat paths, heat pipes, etc. The results of this investigation shall establish when it is advantageous to use active cooling as compared to heat sinking.

4.8 PFN Operating Environment

The contractor shall establish the conditions to which a capacitor is subjected when it is used as a component in a pulse forming network (PFN). Although this program is to develop capacitors, the eventual applications are expected to be in PFN's. Consequently, it is necessary to establish the PFN environment and ensure that the capacitors will survive in the environment. The contractor shall analytically and/or experimentally establish the conditions under which each capacitor of a six section PFN must function. Based on these findings, the contractor shall generate a test plan for capacitor tests which will demonstrate that the capacitors will survive operation as PFN components. The test plan shall include a description of the equipment necessary to complete the test plan. Ten (10) days approval time required by AFAPL.

4.9 Reliability and Maintainability Analysis

The contractor shall perform a reliability and maintainability analysis on the capacitors and shall include in the final report a qualitative analysis and numerical prediction of the potential reliability and maintainability. Data to be analyzed shall be limited to that developed as a result of the development and testing otherwise required and data otherwise available. Additional or duplicative research or testing for the sake of making the predictions will not be undertaken. The level of effort contemplated for R&M analysis is not to exceed 40 manhours.

4.10 Pulse Forming Networks (PFN)

The contractor shall fabricate, checkout, and deliver one type E PFN. This PFN shall utilize the capacitors fabricated according to 4.5. Since the PFN is based on the successful development of the Hi Rep capacitors, the Government must be sure that the required capacitors have been developed. Therefore, the contractor shall not initiate any effort or expend any funds on this task until he receives written authority from the Procuring Contracting Officer (PCO). Upon receipt of written authority, the contractor shall fabricate one PFN with the following characteristics:

	<u>Hi Rep PFN</u>
Energy Storage/PFN, Kilojoules	3
Number of L-C sections	6
PFN voltage, kilovolts	15
PFN total capacitance, microfarads	26.667
PFN total inductance, microhenries	3.750
Current discharge/PFN, kiloamps	20.0
Current fault/PFN, kiloamps	40.0
Pulse shape	rectangular
Pulse width (90% to 90% amplitude)	20 μ sec
Rise time (10% to 90% amplitude)	2 μ sec
Fall time (90% to 10% amplitude)	4 μ sec
Pulse repetition rate, pulses/sec	300

4.10.1 The contractor shall checkout the PFN to ensure proper operation. To prevent requirements for large power supplies, the contractor shall limit the PFN checkouts to single shot operation.

4.11 The contractor shall investigate methods for treating foil edges to eliminate the irregularities that result from the standard foil manufacturing process and which lead to field enhancement and eventual capacitor failure. Also, the contractor shall perform a capacitor weight minimization study based on the peak field at the foil edges and the ratio of dielectric film to foil thickness.

At the end of this task, the contractor shall give an oral presentation identifying the most promising foil edge treatment technique(s). The contractor shall also describe the edge treatment process in sufficient detail such that this information may be used to define a process and design equipment to produce large quantities of this foil. The results of the capacitor weight minimization study shall also be presented at this time.

4.12 The contractor shall perform a case weight minimization study and build several prototype cases to demonstrate fabrication techniques and verify weight projections. As a minimum, the study shall consider weight, material strength, terminations, and techniques to provide leak-proof seals. The cases shall be of sufficient size to house capacitors of the type described in paragraphs 4.4 and 4.5 and shall include terminals.

4.13 The contractor shall develop appropriate end terminations for extended foil capacitors to be used in pulsed, high voltage, high current applications. Specifically, capacitors with these terminations should operate satisfactorily in the PFN specified in paragraph 4.15.

4.14 Using the termination techniques developed in paragraph 4.13, the contractor shall design capacitors to operate in the pulse forming network (PFN) specified in paragraph 4.15.

4.15 Based upon the capacitor designs of paragraph 4.14, the contractor shall design and fabricate two PFNs to the following specification goal:

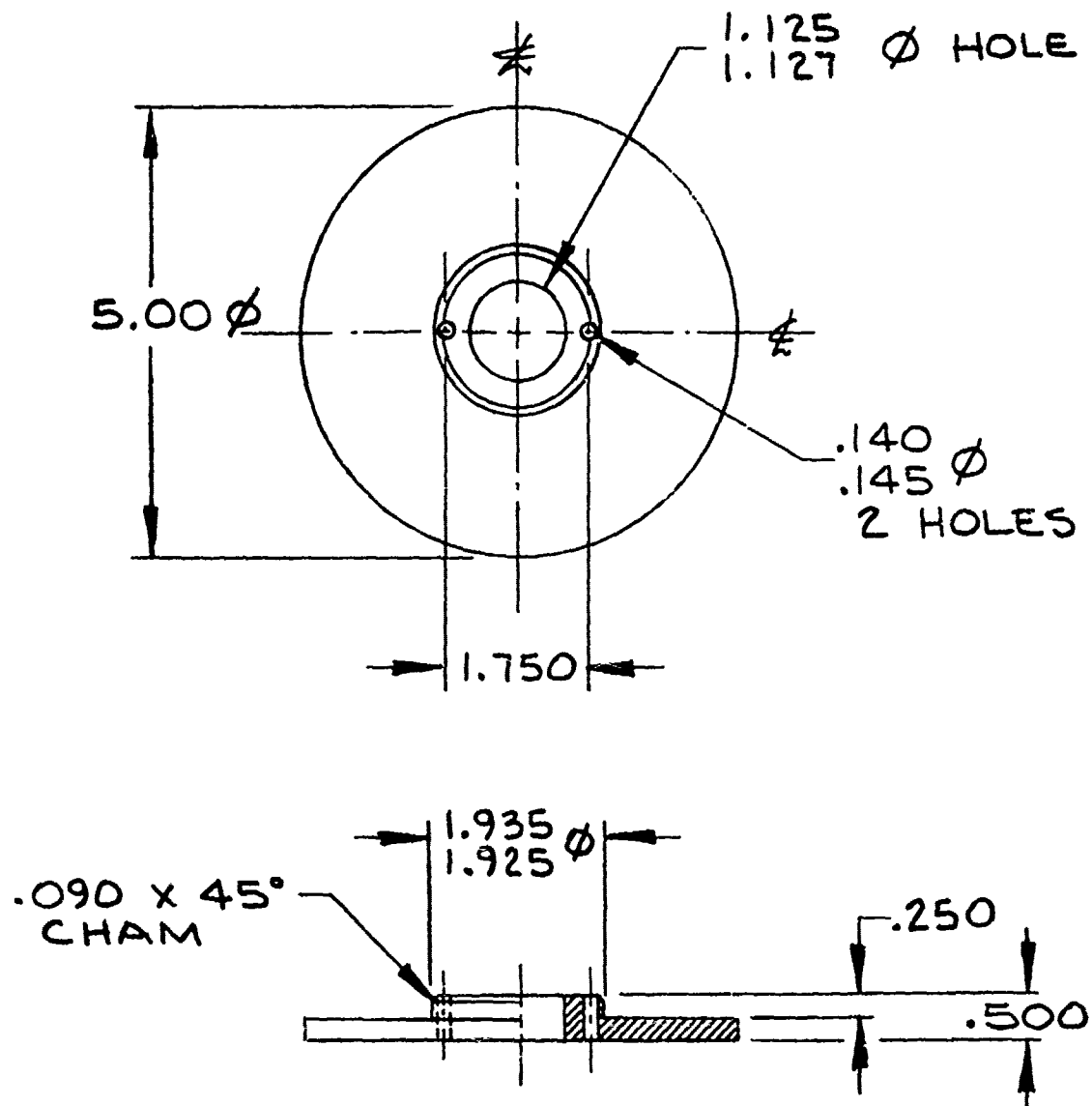
Number of Sections	4
Pulse Width	10 μ sec \pm 5% (50% amplitude)
Characteristic Impedance	1.125 ohms
Total Capacitance	4.44 μ f nominal
Peak Charging Voltage	30 kV
Pulse Rate	50-100 pps
Duty Cycle	90 sec on time burst with 2 hours between bursts

Life Design Goal	10^5 pulses
PFN Total Weight Goal	12 kg
Resonant Charging Time	1.67 msec nominal
Maximum Voltage Reversal	10%

4.16 The contractor shall test the two PFNs fabricated according to paragraph 4.15 to insure proper operation. The testing shall be done at a government installation such as ECOM (Ft. Monmouth) or RADC (Griffis AFB).

APPENDIX B
WINDER DRAWINGS

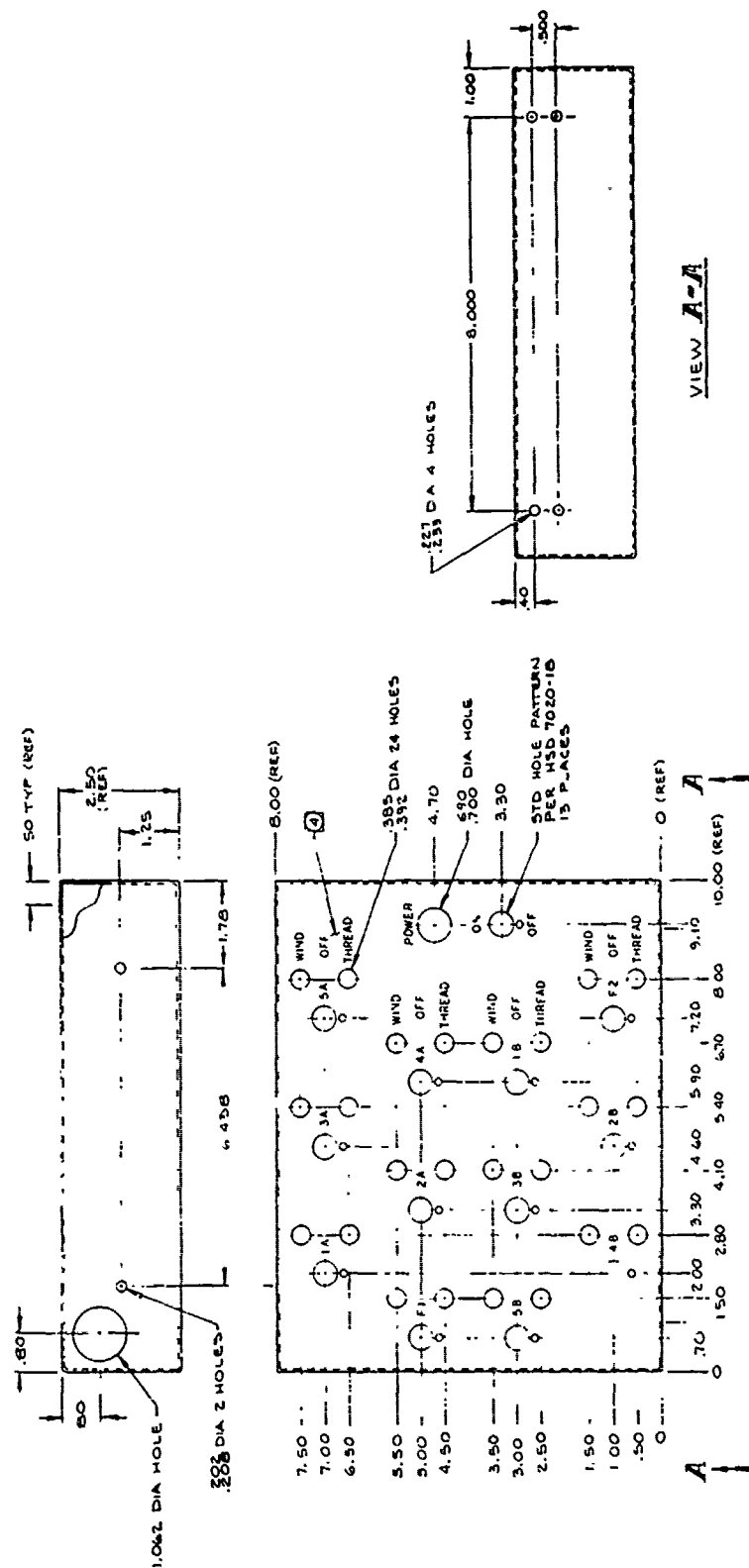
210a



2. REMOVE ALL BURRS & SHARP EDGES
1. MATL: .500 PLATE, AL ALLOY 2024-T4
QQ-A-250/4

NOTES:

Figure 85. Drive disc-capacitor winder.



1. STENCIL WITH HP 9, TYPE 1, CL 3
2. GRADE A FORMS, BLACK, USING 1/4
3. HIGH CHARACTERS
4. PAINT ALL EXTERIOR SURFACES PER MIL SPECIFICATION 131.10-1.2
5. REMOVE ALL BURRS & SHARP EDGES
6. REMOVE ALL BURRS & SHARP EDGES
7. REMOVE ALL BURRS & SHARP EDGES
8. REMOVE ALL BURRS & SHARP EDGES
9. REMOVE ALL BURRS & SHARP EDGES
10. REMOVE ALL BURRS & SHARP EDGES
11. REMOVE ALL BURRS & SHARP EDGES
12. REMOVE ALL BURRS & SHARP EDGES
13. REMOVE ALL BURRS & SHARP EDGES
14. REMOVE ALL BURRS & SHARP EDGES
15. REMOVE ALL BURRS & SHARP EDGES
16. REMOVE ALL BURRS & SHARP EDGES
17. REMOVE ALL BURRS & SHARP EDGES
18. REMOVE ALL BURRS & SHARP EDGES
19. REMOVE ALL BURRS & SHARP EDGES
20. REMOVE ALL BURRS & SHARP EDGES
21. REMOVE ALL BURRS & SHARP EDGES
22. REMOVE ALL BURRS & SHARP EDGES
23. REMOVE ALL BURRS & SHARP EDGES
24. REMOVE ALL BURRS & SHARP EDGES
25. REMOVE ALL BURRS & SHARP EDGES
26. REMOVE ALL BURRS & SHARP EDGES
27. REMOVE ALL BURRS & SHARP EDGES
28. REMOVE ALL BURRS & SHARP EDGES
29. REMOVE ALL BURRS & SHARP EDGES
30. REMOVE ALL BURRS & SHARP EDGES
31. REMOVE ALL BURRS & SHARP EDGES
32. REMOVE ALL BURRS & SHARP EDGES
33. REMOVE ALL BURRS & SHARP EDGES
34. REMOVE ALL BURRS & SHARP EDGES
35. REMOVE ALL BURRS & SHARP EDGES
36. REMOVE ALL BURRS & SHARP EDGES
37. REMOVE ALL BURRS & SHARP EDGES
38. REMOVE ALL BURRS & SHARP EDGES
39. REMOVE ALL BURRS & SHARP EDGES
40. REMOVE ALL BURRS & SHARP EDGES
41. REMOVE ALL BURRS & SHARP EDGES
42. REMOVE ALL BURRS & SHARP EDGES
43. REMOVE ALL BURRS & SHARP EDGES
44. REMOVE ALL BURRS & SHARP EDGES
45. REMOVE ALL BURRS & SHARP EDGES
46. REMOVE ALL BURRS & SHARP EDGES
47. REMOVE ALL BURRS & SHARP EDGES
48. REMOVE ALL BURRS & SHARP EDGES
49. REMOVE ALL BURRS & SHARP EDGES
50. REMOVE ALL BURRS & SHARP EDGES
51. REMOVE ALL BURRS & SHARP EDGES
52. REMOVE ALL BURRS & SHARP EDGES
53. REMOVE ALL BURRS & SHARP EDGES
54. REMOVE ALL BURRS & SHARP EDGES
55. REMOVE ALL BURRS & SHARP EDGES
56. REMOVE ALL BURRS & SHARP EDGES
57. REMOVE ALL BURRS & SHARP EDGES
58. REMOVE ALL BURRS & SHARP EDGES
59. REMOVE ALL BURRS & SHARP EDGES
60. REMOVE ALL BURRS & SHARP EDGES
61. REMOVE ALL BURRS & SHARP EDGES
62. REMOVE ALL BURRS & SHARP EDGES
63. REMOVE ALL BURRS & SHARP EDGES
64. REMOVE ALL BURRS & SHARP EDGES
65. REMOVE ALL BURRS & SHARP EDGES
66. REMOVE ALL BURRS & SHARP EDGES
67. REMOVE ALL BURRS & SHARP EDGES
68. REMOVE ALL BURRS & SHARP EDGES
69. REMOVE ALL BURRS & SHARP EDGES
70. REMOVE ALL BURRS & SHARP EDGES
71. REMOVE ALL BURRS & SHARP EDGES
72. REMOVE ALL BURRS & SHARP EDGES
73. REMOVE ALL BURRS & SHARP EDGES
74. REMOVE ALL BURRS & SHARP EDGES
75. REMOVE ALL BURRS & SHARP EDGES
76. REMOVE ALL BURRS & SHARP EDGES
77. REMOVE ALL BURRS & SHARP EDGES
78. REMOVE ALL BURRS & SHARP EDGES
79. REMOVE ALL BURRS & SHARP EDGES
80. REMOVE ALL BURRS & SHARP EDGES
81. REMOVE ALL BURRS & SHARP EDGES
82. REMOVE ALL BURRS & SHARP EDGES
83. REMOVE ALL BURRS & SHARP EDGES
84. REMOVE ALL BURRS & SHARP EDGES
85. REMOVE ALL BURRS & SHARP EDGES
86. REMOVE ALL BURRS & SHARP EDGES
87. REMOVE ALL BURRS & SHARP EDGES
88. REMOVE ALL BURRS & SHARP EDGES
89. REMOVE ALL BURRS & SHARP EDGES
90. REMOVE ALL BURRS & SHARP EDGES
91. REMOVE ALL BURRS & SHARP EDGES
92. REMOVE ALL BURRS & SHARP EDGES
93. REMOVE ALL BURRS & SHARP EDGES
94. REMOVE ALL BURRS & SHARP EDGES
95. REMOVE ALL BURRS & SHARP EDGES
96. REMOVE ALL BURRS & SHARP EDGES
97. REMOVE ALL BURRS & SHARP EDGES
98. REMOVE ALL BURRS & SHARP EDGES
99. REMOVE ALL BURRS & SHARP EDGES
100. REMOVE ALL BURRS & SHARP EDGES

Figure 86. Controller - capacitor winder (sheet 1 of 2).

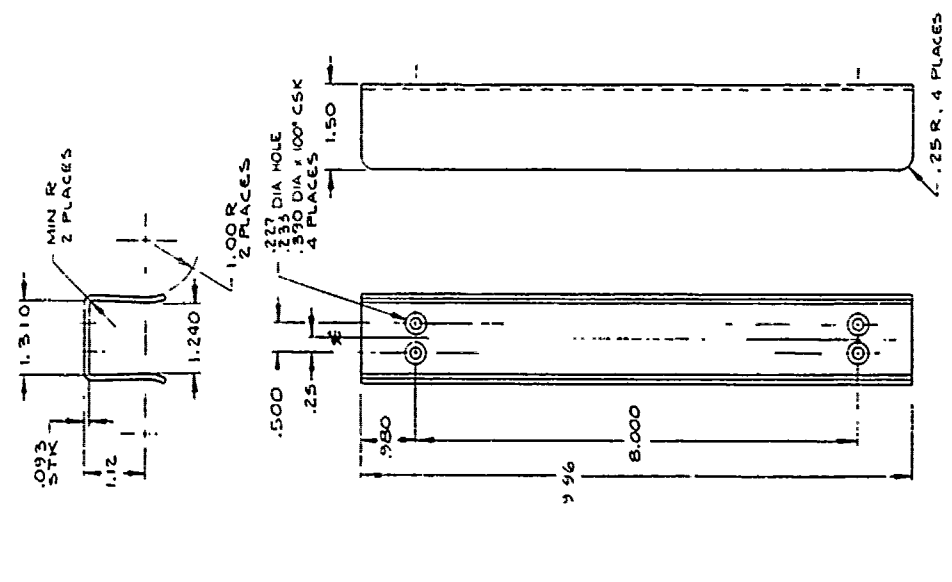
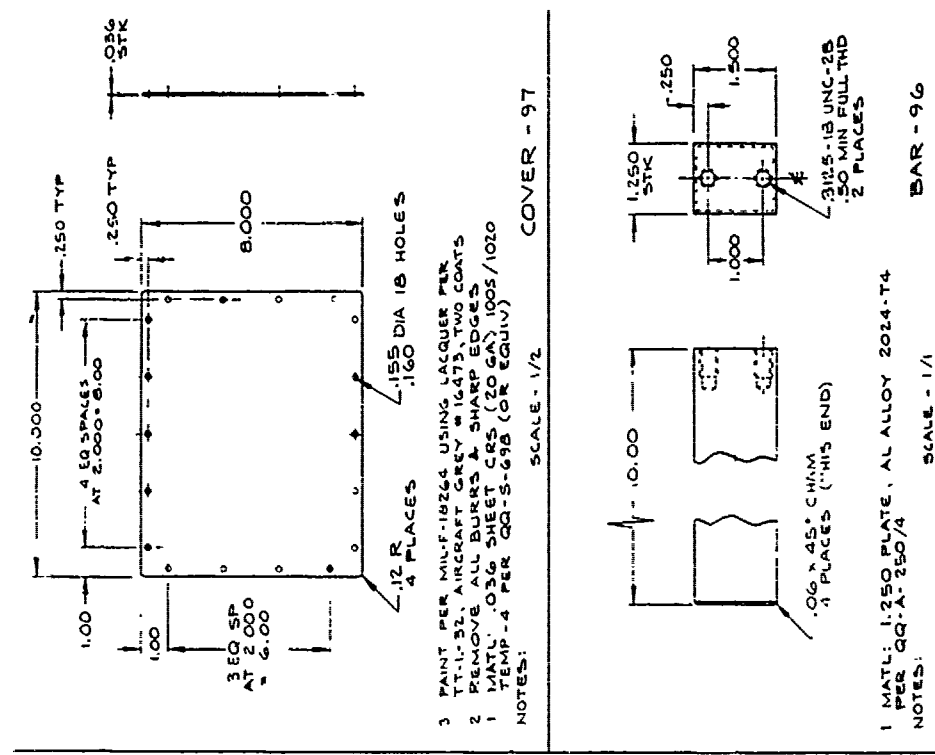
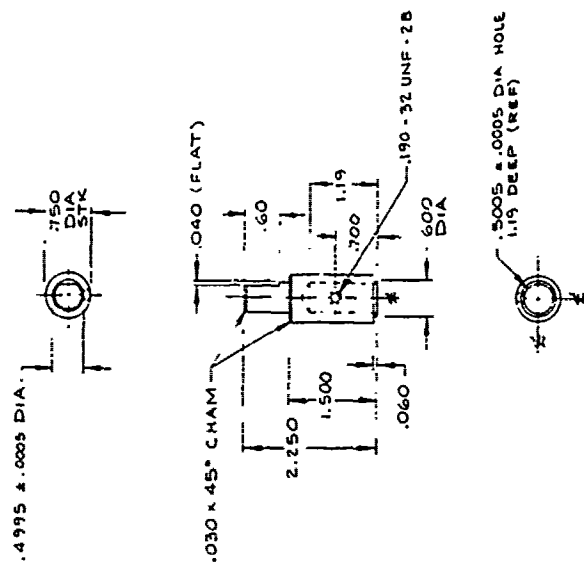


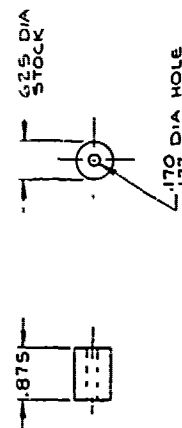
Figure 86. Controller - capacitor winder (sheet 2 of 2).



MOUNTING PLATE - 99

2. REMOVE ALL BURRS & SHARP EDGES
1. MATL: .250 x 1.500 RECT BAR, AL ALLOY
- 2024-T4 PER QQ-A-225/6 OR QQ-A-200-3

NOTES:



SPACER - 97

3. 2 EACH REQD PER UNIT (REF)
2. REMOVE ALL BURRS & SHARP EDGES
1. MATL: .625 DIA ROD, AL ALLOY
- 2024-T4 PER QQ-A-225/6

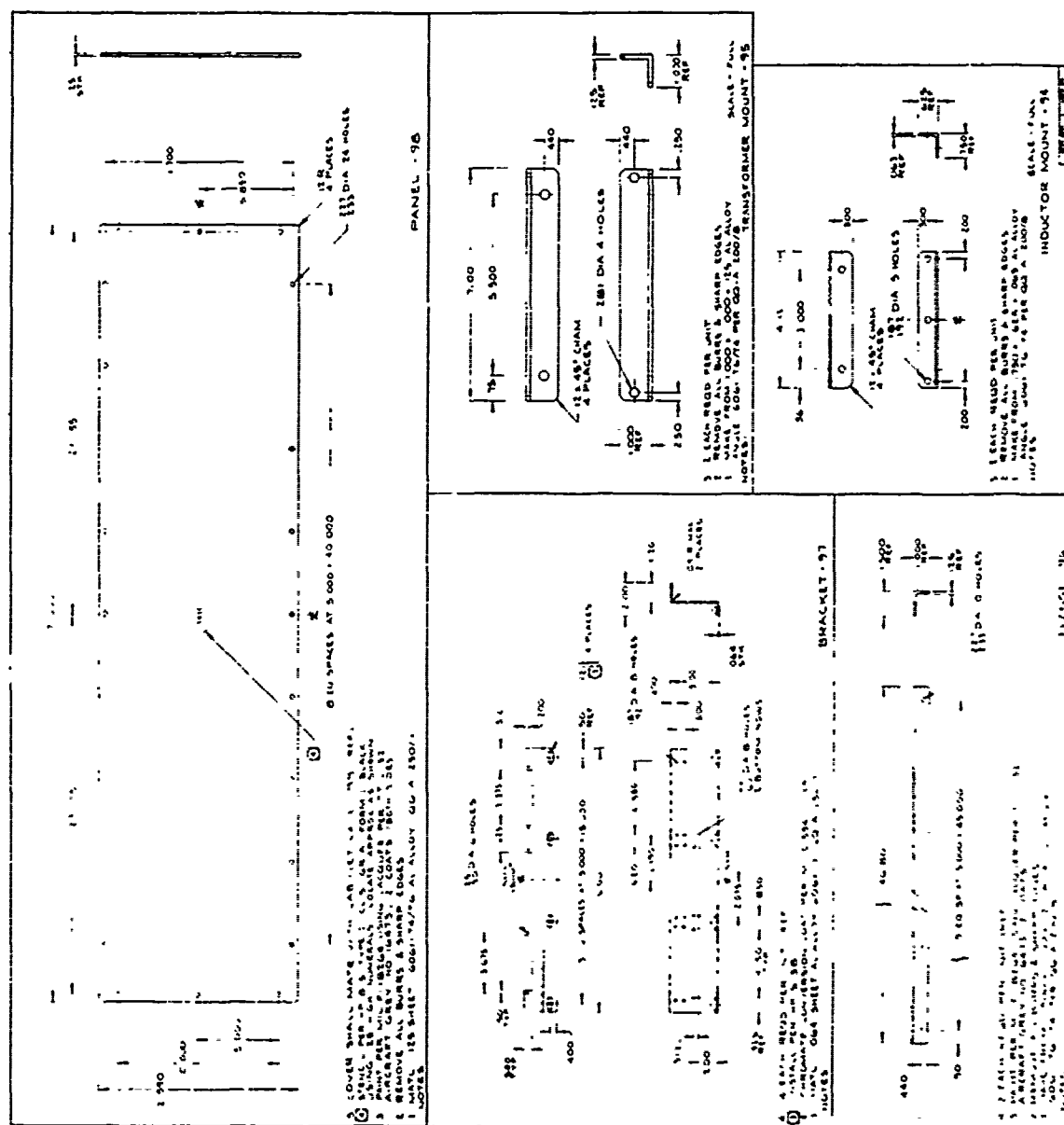
NOTES:

2. REMOVE ALL BURRS & SHARP EDGES
1. MATL: .750 DIA CHRS ROD COMP 504.
- COND AF, QQ-S-763

NOTES

SHAFT EXTENSION - 98

Figure 87. Mounting bracket-torquer brake, capacitor winder.



~~THIS PAGE IS BEST QUALITY PRACTICABLE~~
FROM COPY FURNISHED TO DDC

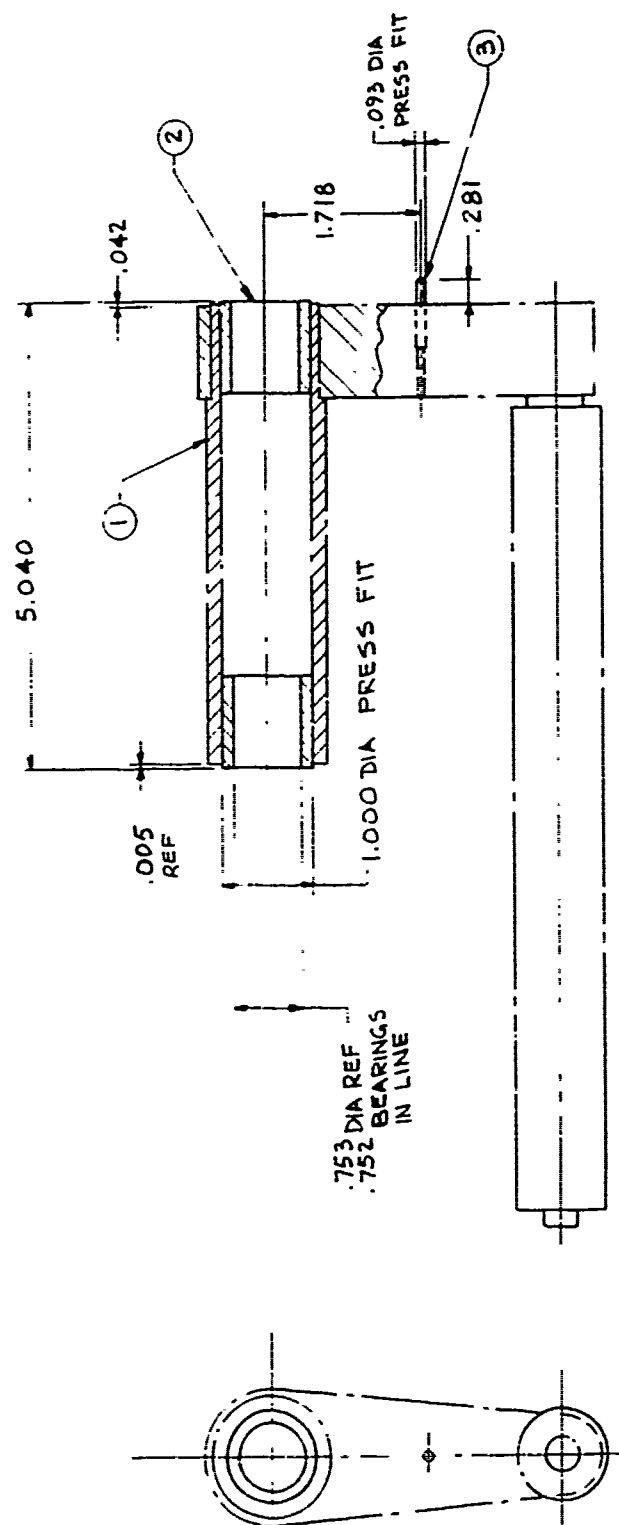
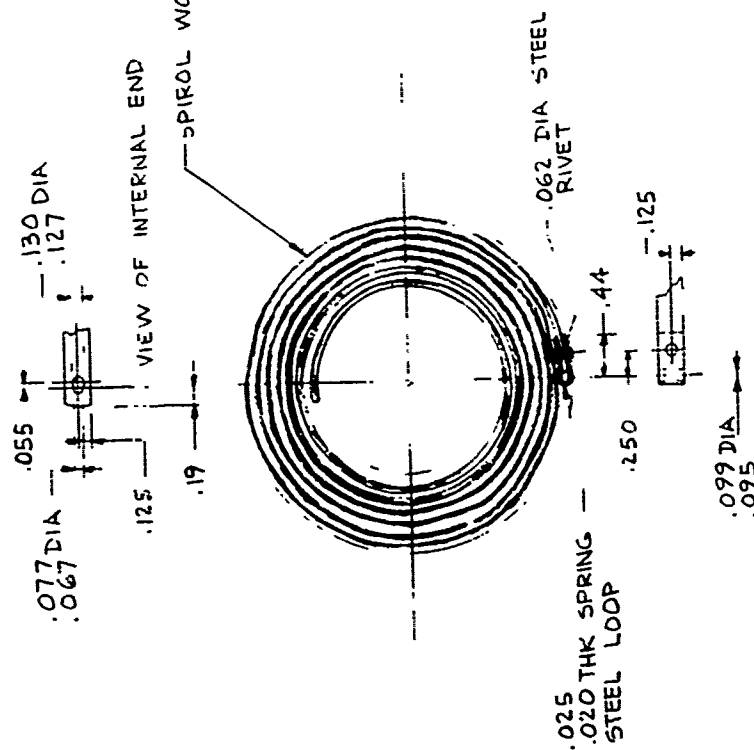


Figure 89. Roller assembly.



TORQUE SPRING REQUIREMENTS

MATERIAL: SAE 1095 ROCKWELL C48
(LOCK SPRING STEEL (FUND EDGE))

ARBOR DIAMETER: 1.875

DRUM DIAMETER: 3.50

SPRING THICKNESS: .062

SPRING WIDTH: .250

SPRING LENGTH: 56.00 APPROX

TORQUE WHEN WOUND 1.5 TURNS: 18 IN-LBS

Figure 90. Torque spring.

NOTES

1. REMOVE BURRS & BREAK EDGES .015 MAX.

2. FILLET RADIUS .010 MAX.

3. CLEAR ANODIZE

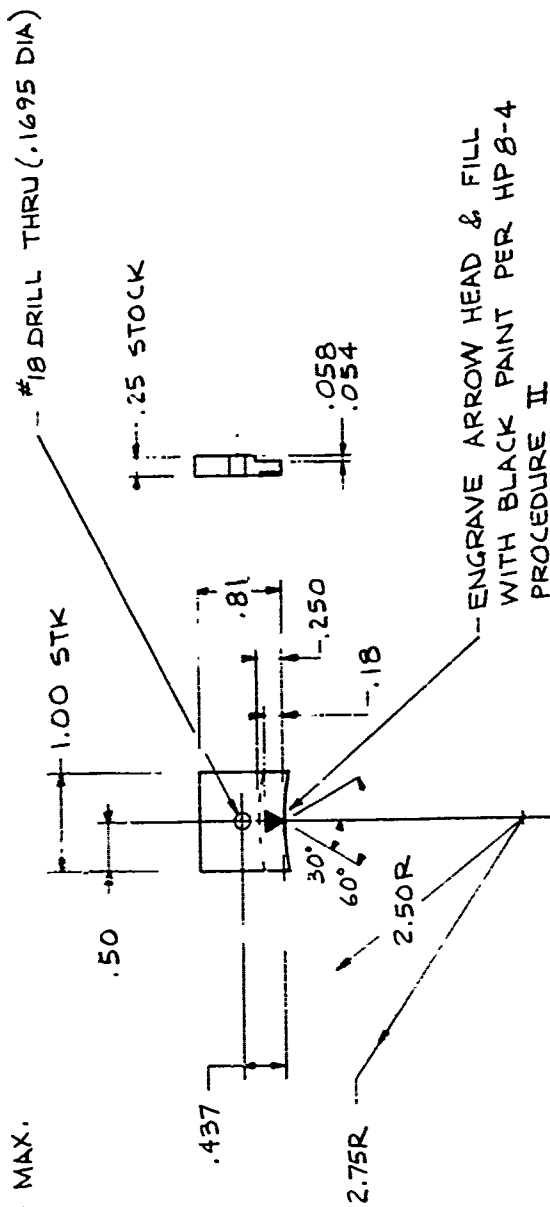


Figure 91. Dial clamp.

NOTES

1. REMOVE BURRS & BREAK EDGES .015 MAX.
2. FILLET RADIUS .010 MAX.

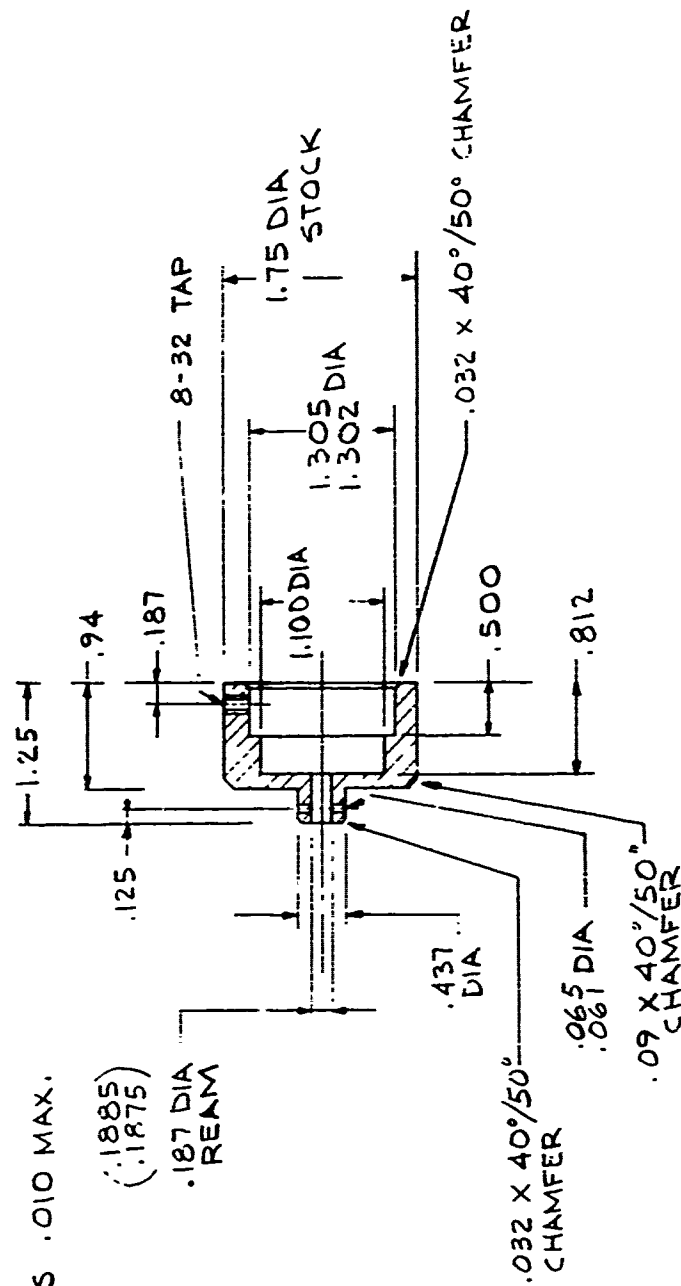


Figure 92. Adapter.

NOTE:
1. REMOVE BURRS

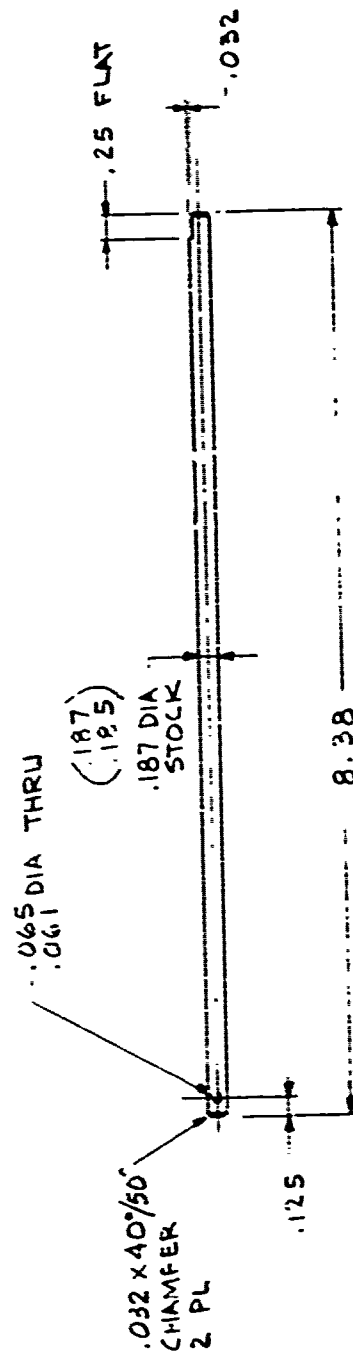


Figure 93. Shaft.

NOTES

1. REMOVE BURRS & BREAK EDGES .015 MAX.
2. FILLET RADIUS .010 MAX.

1. REMOVE BURRS & BREAK EDGES .015 MAX.
2. FILLET RADIUS .010 MAX.

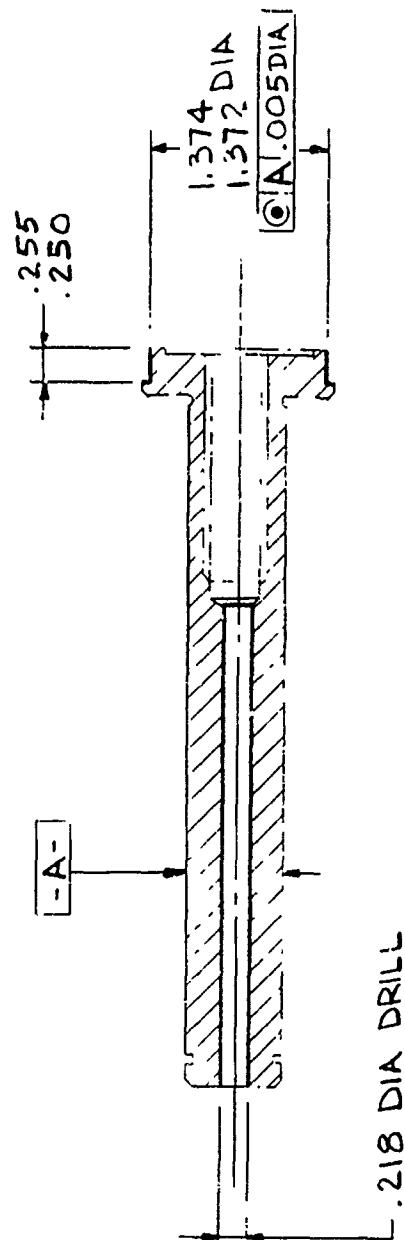


Figure 94. Bearing shaft.

NOTES

1. REMOVE BURRS & BREAK EDGES

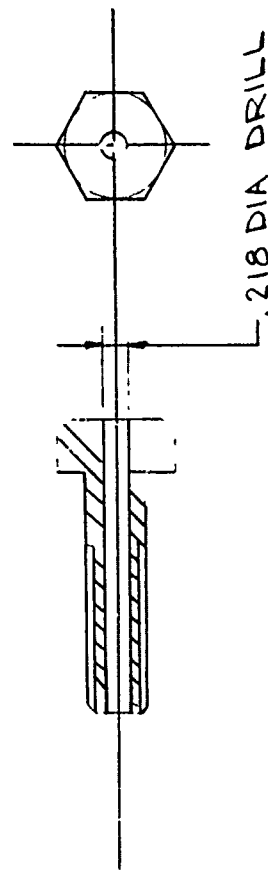


Figure 95. Bolt.

NOTES

1. REMOVE BURRS & BREAK EDGES .015 MAX.

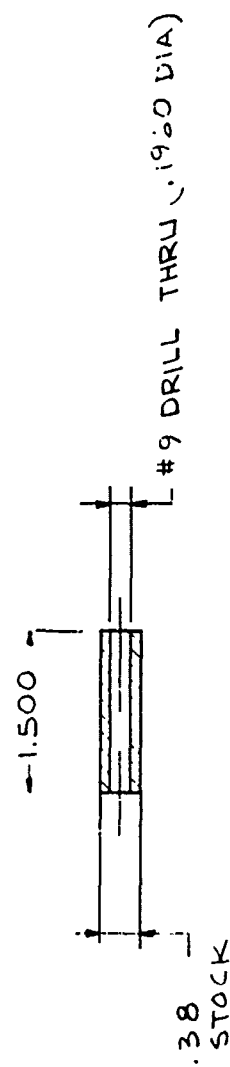


Figure 96. Spacer.

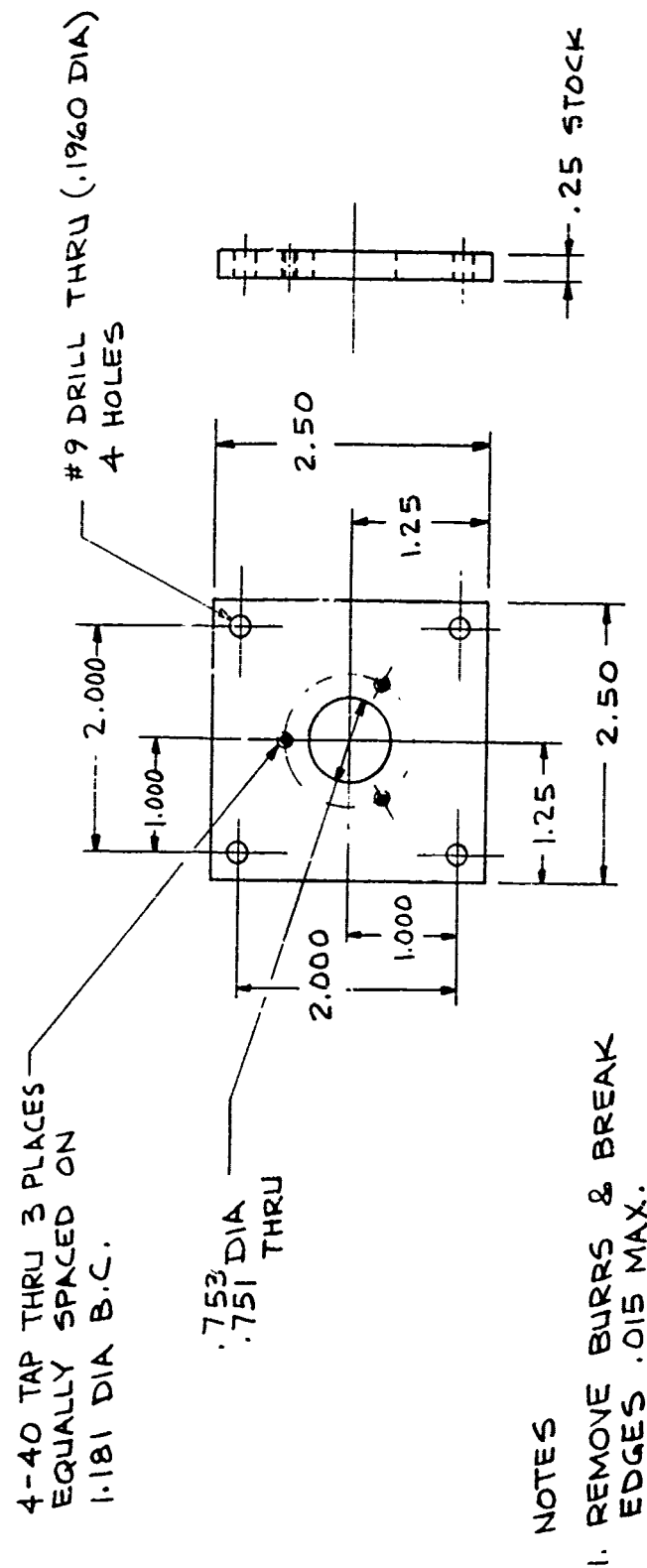


Figure 97. Mounting plate.

NOTE:
1. REMOVE BURRS & BREAK EDGES .015 MAX

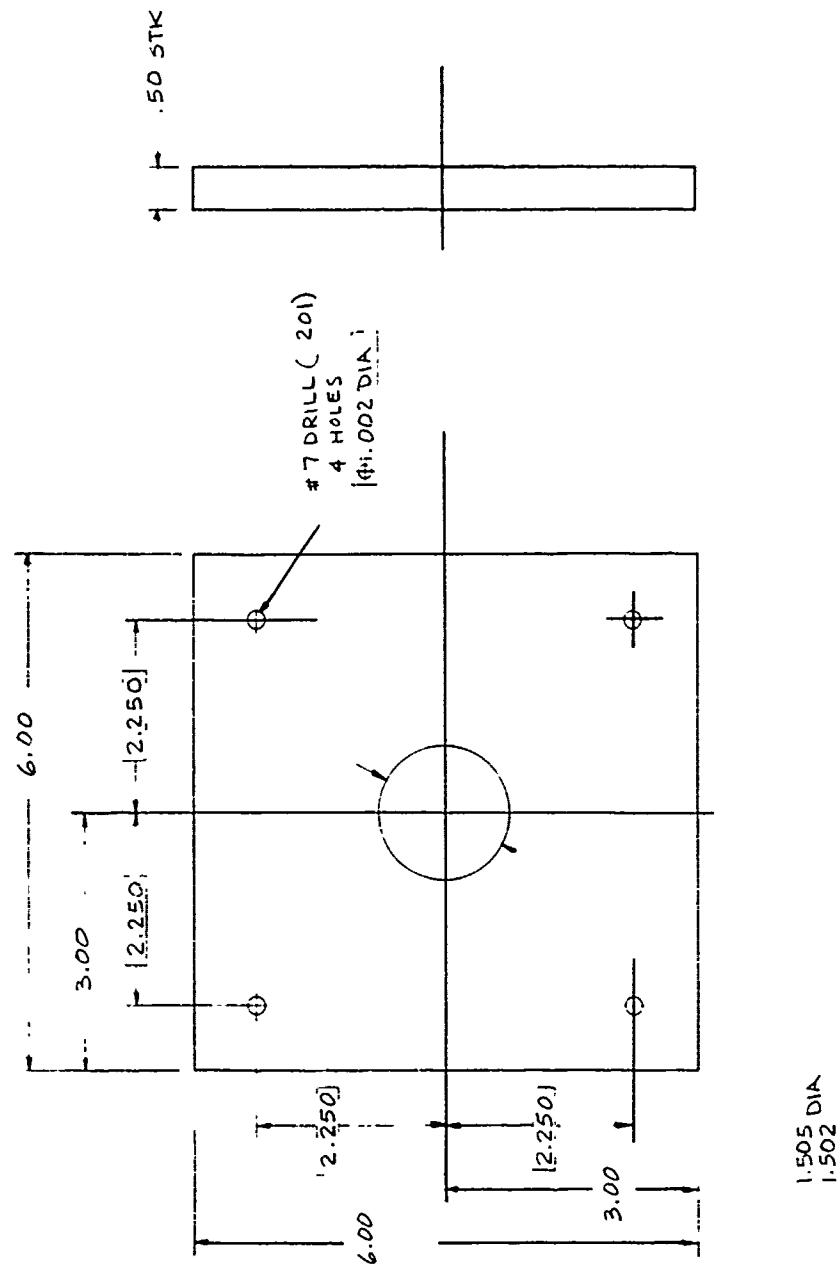


Figure 98. Plate.

NOTES

1. REMOVE BURRS & BREAK EDGES .015 MAX.
2. FILLET RADIUS .010 MAX.

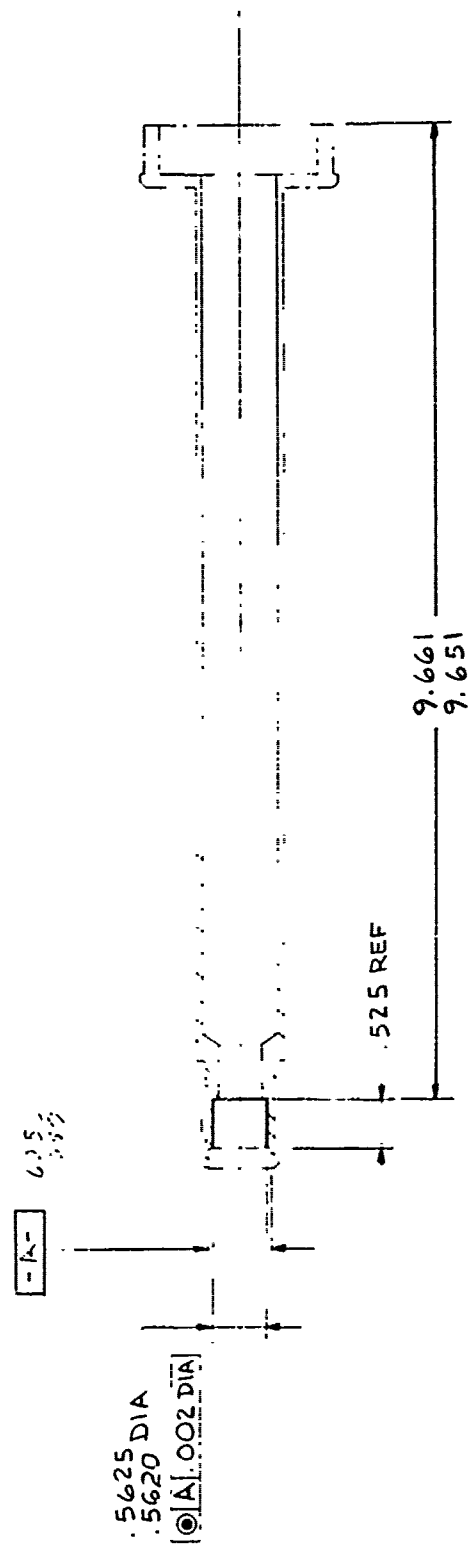


Figure 100. Spindle.

NOTES

1. REMOVE BURRS & BREAK EDGES .015 MAX.
2. FILLET RADIUS .010 MAX.
3. DO NOT HARDEN ENTIRE LENGTH

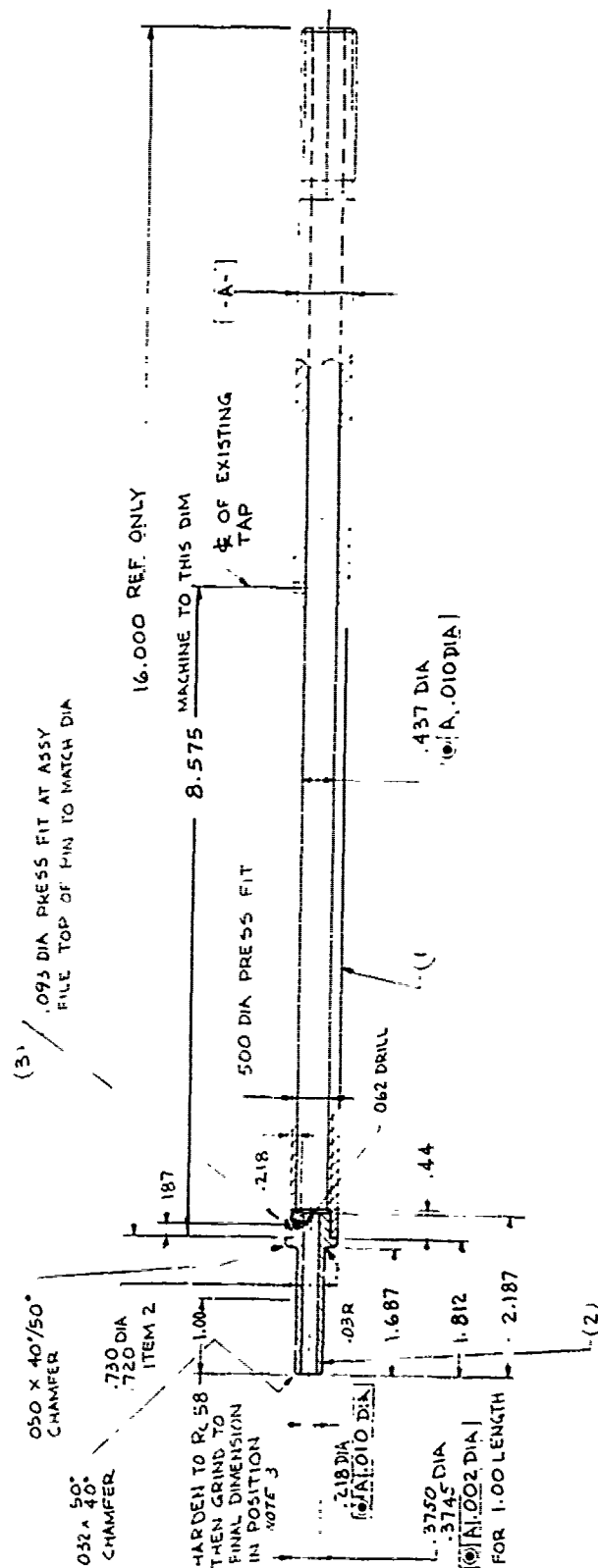


Figure 101. Support shaft.

NOTES

1. REMOVE BURRS & BREAK EDGES .015 MAX.
2. FILLET RADIUS .010 MAX.

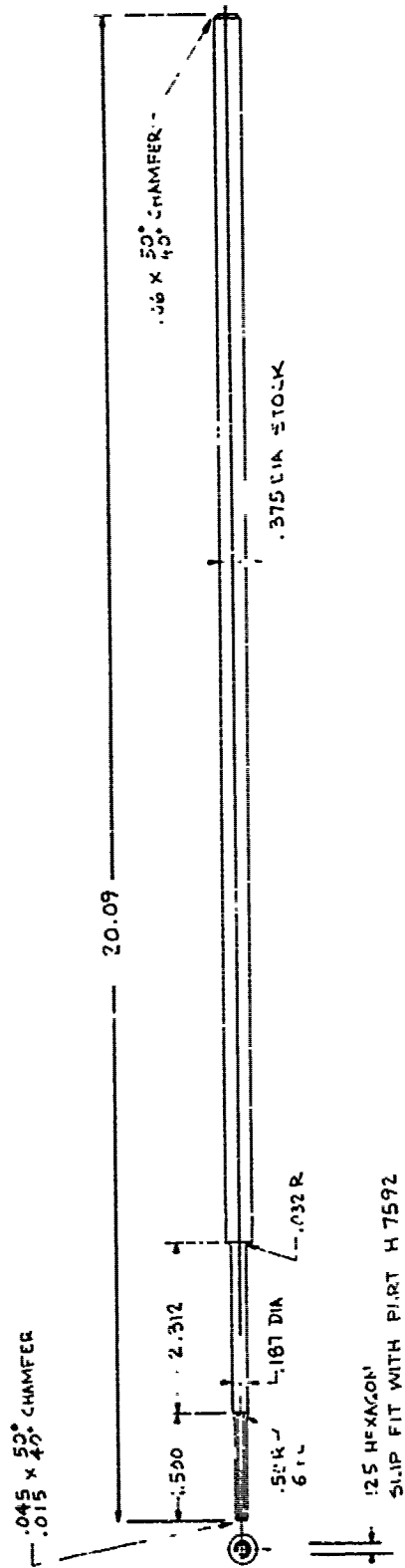


Figure 102. Drive shaft.

NOTES

1. REMOVE BURRS & BREAK EDGES .015 MAX
2. FILLET RADIUS .010 MAX

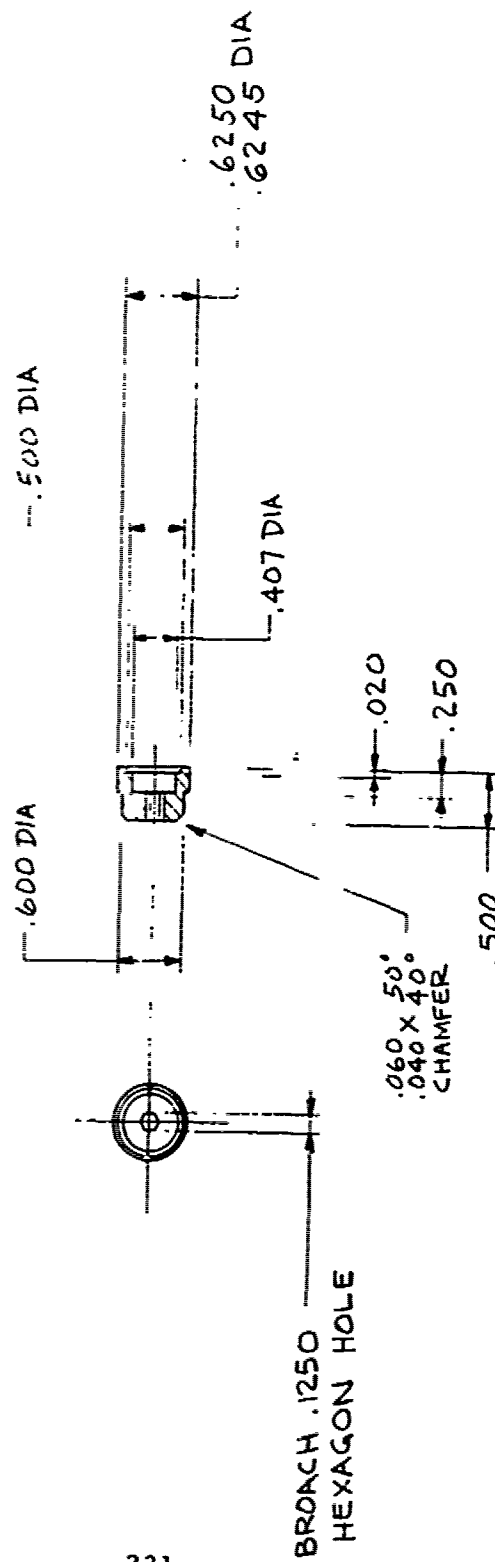


Figure 103. Drive bushing.

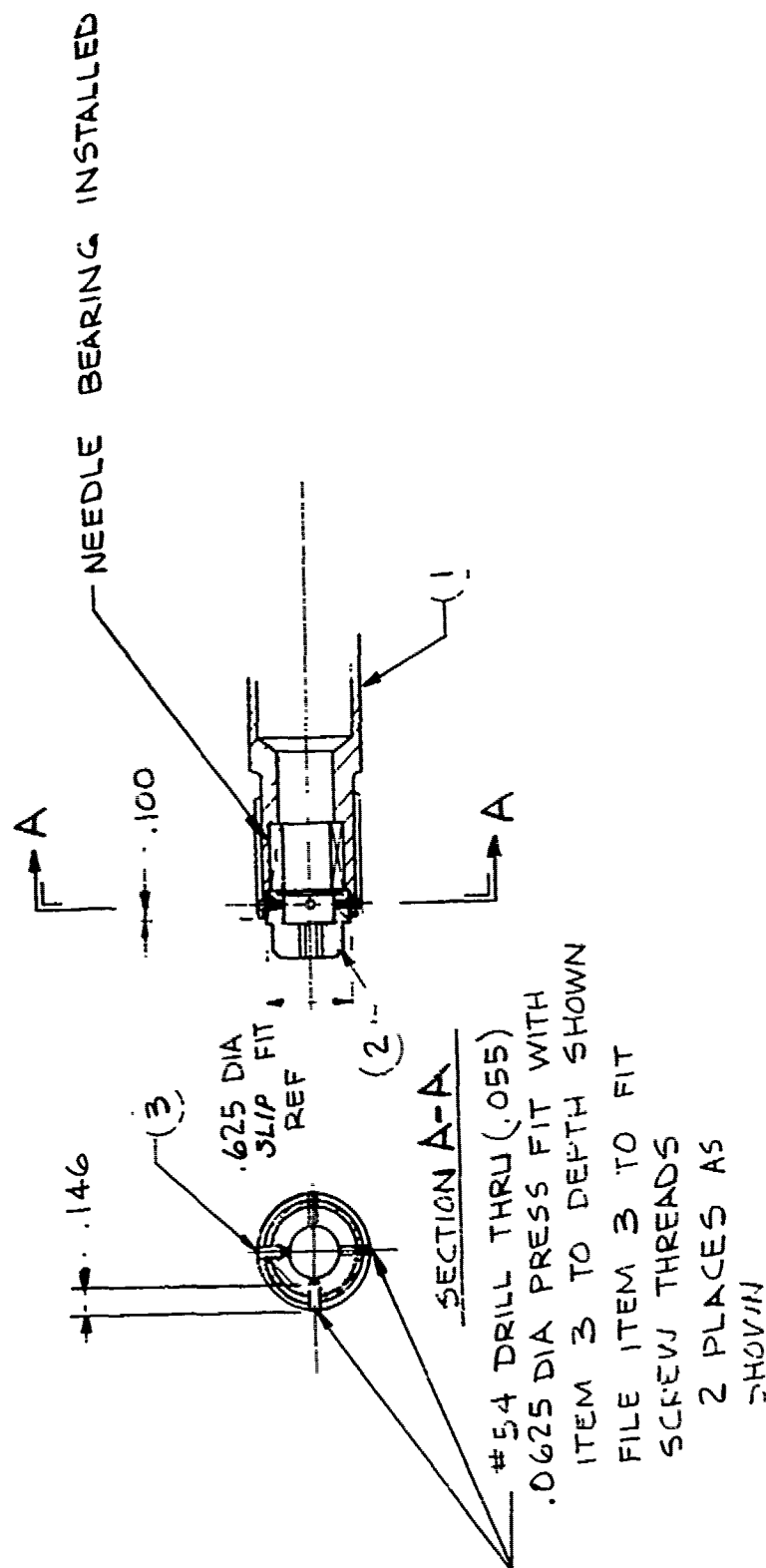


Figure 104. Spindle drive assembly.

NOTES

1. REMOVE BURRS & BREAK EDGES .015 MAX.
2. FILLET RADIUS .010 MAX.

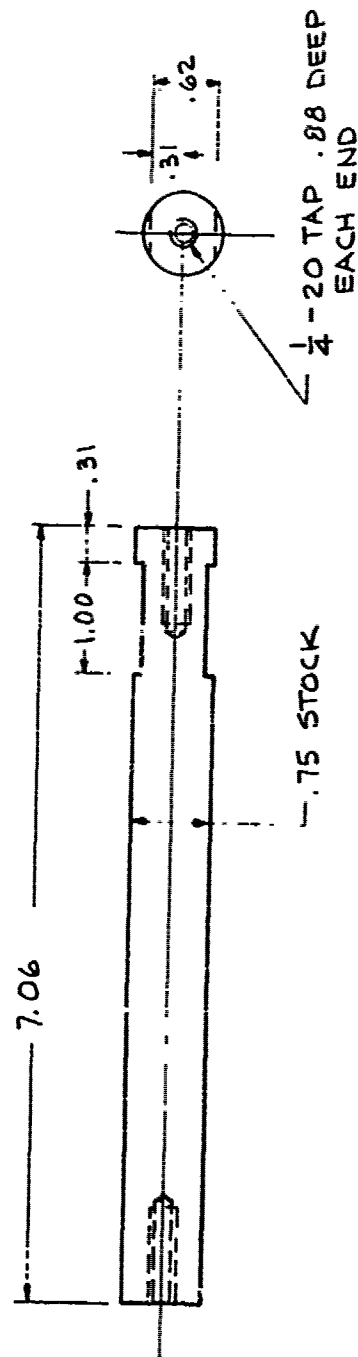


Figure 106. Spacer.

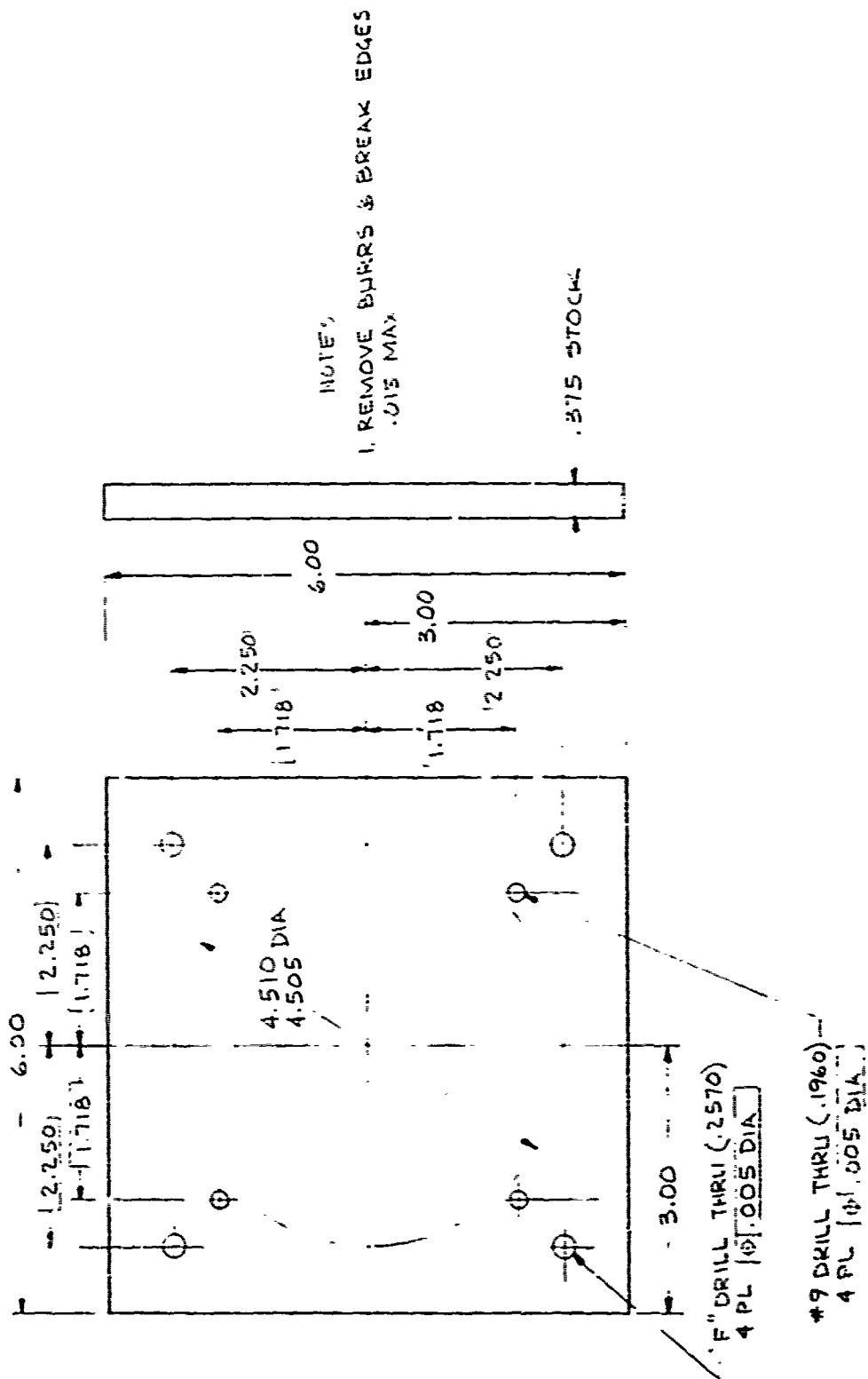


Figure 107. Mounting plate.

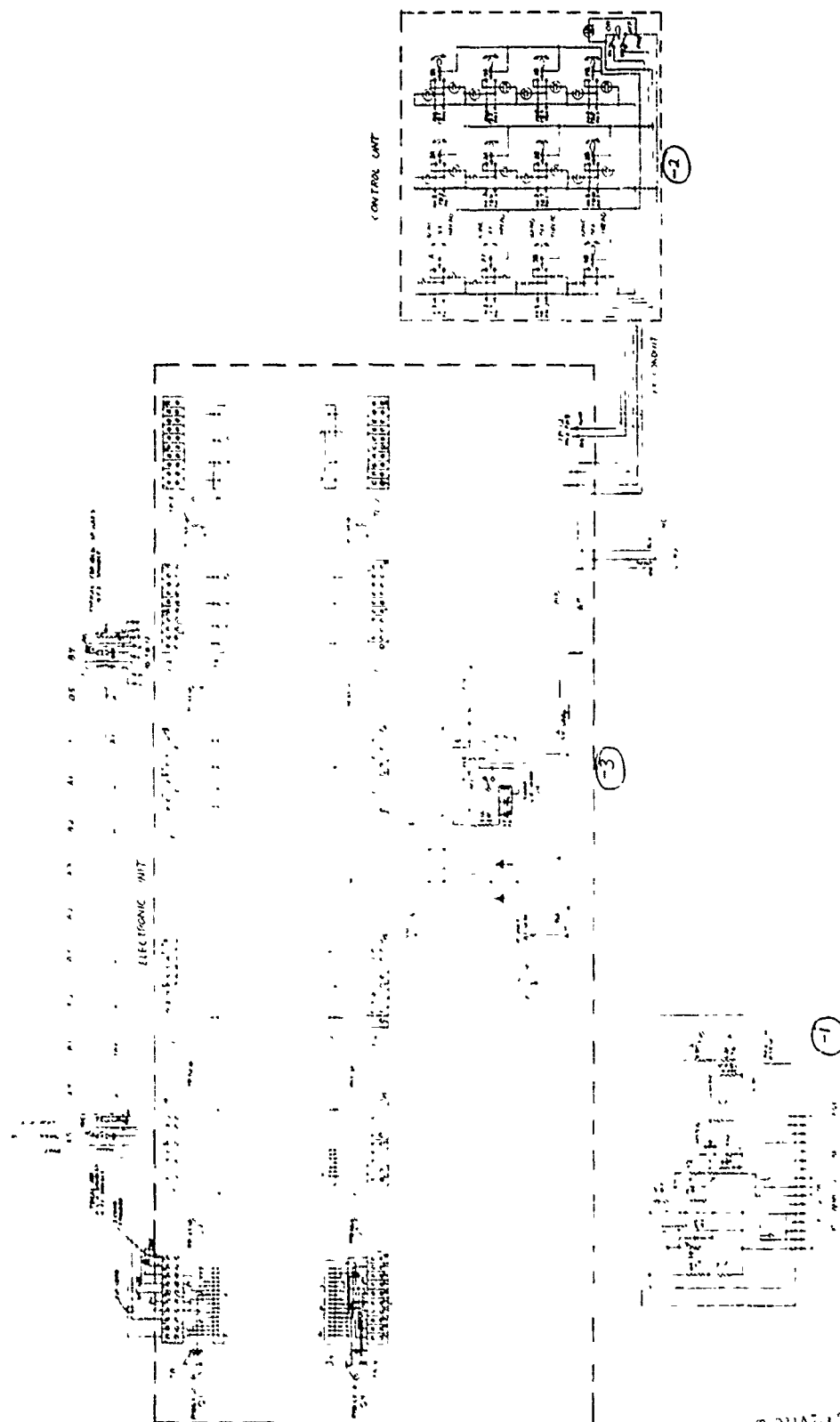
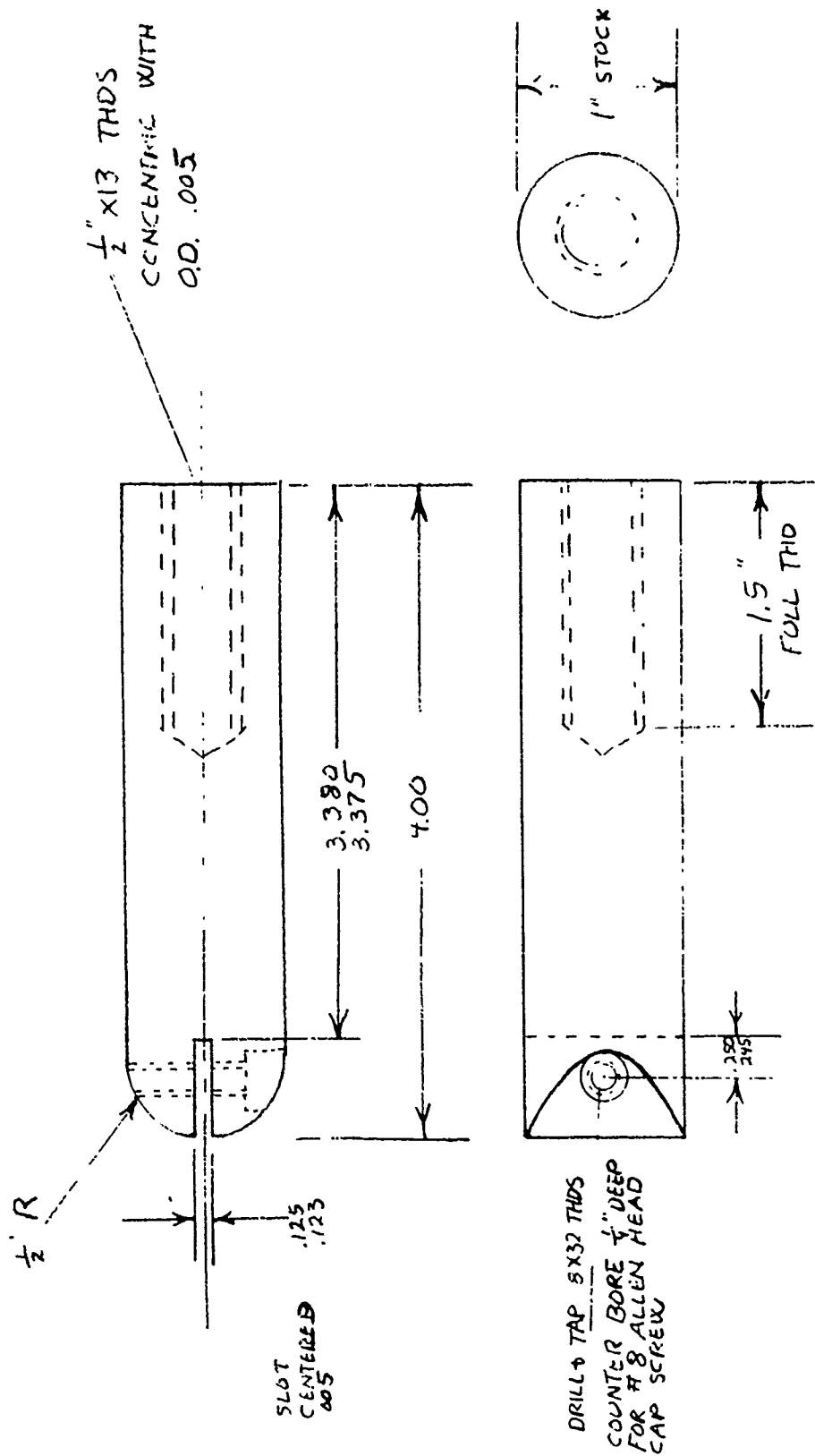


Figure 109. Tensioning device, capacitor winder electronic CKT.



MTL DILL ROD

Figure 110. Flat mandrel drive.

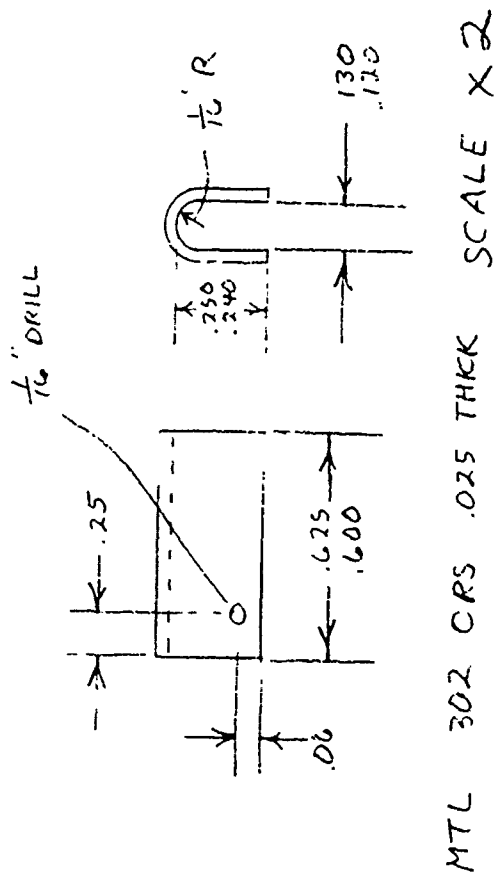


Figure 111. Stirrup.

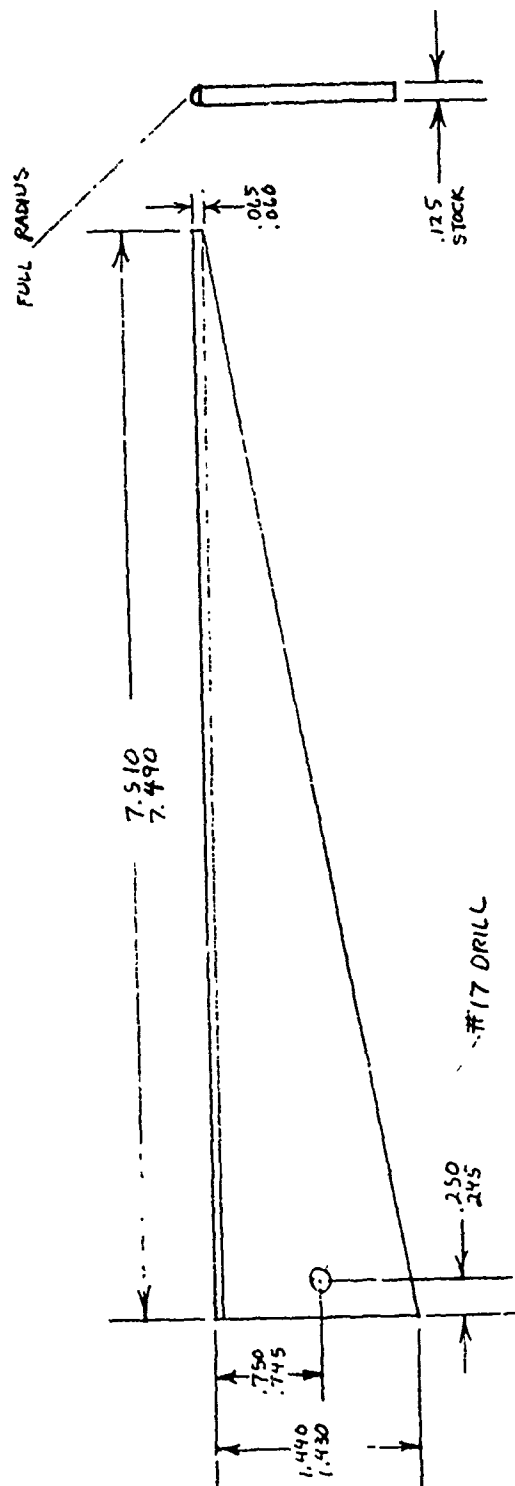


Figure 112. Wedge.

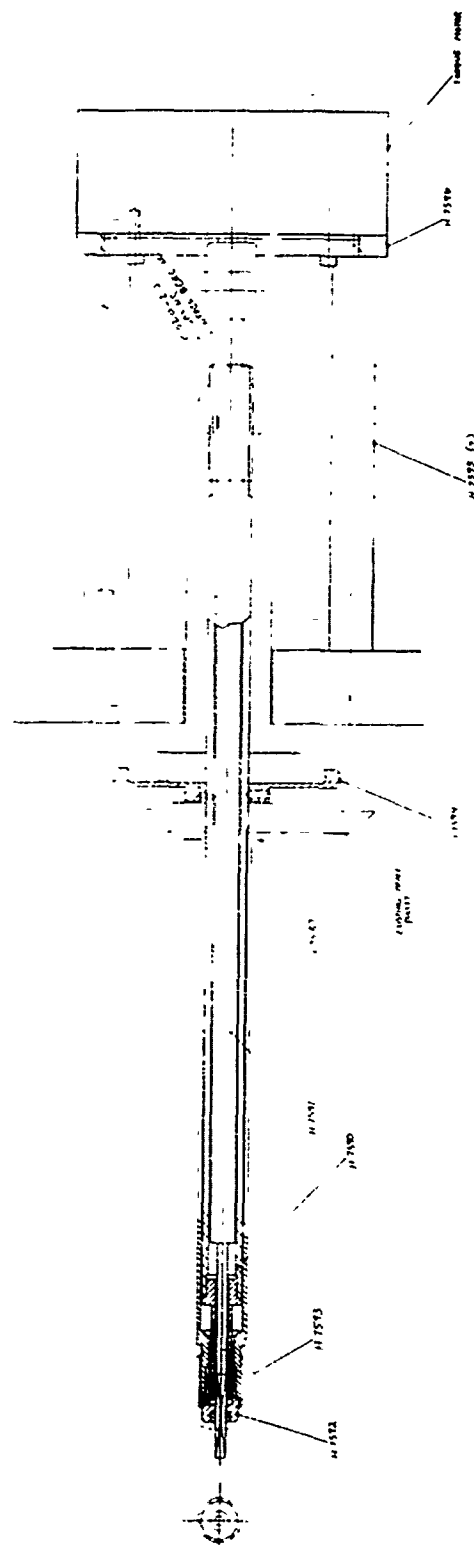
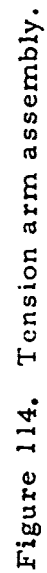


Figure 113. Torque motor drive spindle assembly.



242

APPENDIX C

OPERATING INSTRUCTIONS
OIL IMPREGNATION SYSTEM

APPENDIX C
OPERATING INSTRUCTIONS
OIL IMPREGNATION SYSTEM

1. Dielectric fluids use to fill capacitors and other oil impregnated units shall be delivered to the site in the original shipping containers or in five gallon stainless steel safety cans.
2. Transfer fluid to the side loader of the Red Point as follows.
(See drawing)
 - 2.1 Obtain a pre-cleaned, 5 gallon, stainless steel pressure vessel (Millipore XX67-000-55 or equivalent) from the Cleaning Lab.
 - 2.2 Pour fluid from original container or safety can into the pressure vessel. Use a large stainless steel funnel to minimize spillage. Secure the cover on the vessel and open the vent valve.
 - 2.3 Disconnect flex line (A) at T-fitting (B), and connect flex line to the outlet fitting or the pressure vessel.
 - 2.4 Close the vacuum valve on the main chamber.
 - 2.5 Close fluid valves 1, 2, 3, and 4, and the bleed and backfill valves.
 - 2.6 Open the vacuum valve on the side loader.
 - 2.7 Turn on the vacuum pump switch on the console.
 - 2.8 Turn on the lamp switch. Adjust lamp (C) over the rear viewing port to illuminate the interior of the side loader when viewed through the front viewing port.
 - 2.9 Crack valve (1) slowly to let fluid flow into the side loader. Adjust the flow rate to minimize splashing and foaming. Fill the inner can to approximately four (4) inches from the top.
 - 2.10 Close valve (1).
 - 2.11 Turn off the vacuum pump.

- 2.12 Open the bleed valve to vent the side loader.
- 2.13 Disconnect flex line (A) from the pressure vessel and reconnect the flex line to T-fitting (B).
3. Filter the fluid to remove particle contamination as follows.
 - 3.1 Read the Operating Instructions for the Model SAI-A Sandpiper Pump.
 - 3.2 Open valves (1) and (2).
 - 3.3 Open the air supply valve on the wall.
 - 3.4 Adjust the air pressure regulator on the pump to 40 PSIG.
 - 3.5 Adjust the air inlet metering valve to give a pump cycling rate of approximately 60 cycles per minute.
 - 3.6 Pump fluid through the filter for five (5) hours.
 - 3.7 Obtain pre-cleaned 500 ml bottles from the Bldg. 20 Cleaning Lab.
 - 3.8 Open sampling valve (4) slowly and drain off approximately 500 ml of fluid into a waste can.
 - 3.9 Collect a sample in a pre-cleaned bottle, fill in the label, and deliver the sample to the Cleaning Lab for analysis. Continue filtering the fluid while awaiting results of the analysis. This analysis shall include the following tests.

<u>Test</u>	<u>Requirement</u>	
	<u>Size Range</u>	<u>Maximum No. per 100 ml</u>
Particle Count	10-25 μ	500
	25-50	300
	50-100	50
	100	15
	Fibers	10
Volume Resistivity (ohm-cm)	Report	
Dielectric Breakdown (Volts/mil)	Report	
Water Content, (PPM),	Report	

Filtering shall be discontinued when a sample meets the above particle count requirement.

- 3.10 Close the air supply valve on the wall.
- 3.11 Close valves (1) and (2). This batch of fluid is now ready for the degassing operation.
4. Dry and degas the capacitors as follows.
 - 4.1 Install the capacitor(s) in the main chamber along with one pre-cleaned, wide mouth sample bottle.
 - 4.2 Attach a thermocouple to one capacitor on an outside surface facing the center of the main chamber.
 - 4.3 Attach feedthrough wires to this capacitor for external monitoring of changes in dissipation factor during the drying operation.
 - 4.4 Secure the dome lid on the main chamber.
 - 4.5 Open the vacuum valve to the main chamber.
 - 4.6 Close the vacuum valve to the side loader and close the bleed and backfill valves.
 - 4.7 Turn on the refrigerator compressor and the vacuum pump.
 - 4.8 Turn on the main chamber heater and set the temperature controller at 225°F .
 - 4.9 Monitor the pressure in the chamber, the chamber wall temperature, and the capacitor can temperature. Read Section 5 below.
 - 4.10 Adjust the temperature controller to maintain the capacitor can temperature at $210 \pm 5^{\circ}\text{F}$.
 - 4.11 Continue the evacuation and heating cycle for approximately 48 hours or until the dissipation factor on the test capacitor (See 4.3) has reached a stable, minimum value.
5. Dry and degas the fluid as follows. This operation should be initiated approximately 24 hours after the capacitor can temperature (See 4.10) has stabilized at $210 \pm 5^{\circ}\text{F}$.
 - 5.1 Close the vacuum valve on the main chamber.
 - 5.2 Open the vacuum valve on the side loader VERY SLOWLY. This is a two man operation to minimize foaming. The first man should observe the fluid through the front viewing port. The second man should control the pressure by adjusting the vacuum valve and/or the side loader bleed valve to keep the fluid from foaming out of the inner can. Gross foaming will cease in approximately fifteen

minutes. As foaming ceases, close the bleed valve and open the vacuum valve slowly to the full open position.

- 5.3 Turn on the side loader heater and adjust the temperature controller to 225°F.
- 5.4 Monitor the pressure in the side loader, the chamber wall temperature, and the inner can fluid temperature.
- 5.5 When the inner can fluid temperature reaches 210°F, adjust the controller to maintain the fluid temperature at $210 \pm 5^\circ\text{F}$. Elapsed time to reach 210°F is ten to twelve hours.
- 5.6 When the pressure in the side loader is reduced to 500 microns, close the vacuum valve on the side loader and open the vacuum valve on the main chamber.
- 5.7 When the pressure in the main chamber is reduced to 500 microns, open the vacuum valve on the side loader. Both the side loader and the main chamber are now being evacuated and heated simultaneously.
- 5.8 Continue to monitor the dissipation factor on the test capacitor, and the pressures and temperatures in both chambers. The elapsed time for this step should be five hours minimum, however, there is no direct method to measure residual dissolved gas or residual water in the fluid. Therefore, the cognizant Program Manager or his designated representative will make the final decision on when to terminate the degassing operation.
6. Impregnate the capacitors as follows.
 - 6.1 Rotate the platform in the main chamber to position a capacitor under the fluid transfer line.
 - 6.2 Crack valve (3) VERY SLOWLY to allow fluid to flow from the side loader into the capacitor at a very slow, almost drop-wise, rate. When this capacitor is completely filled, proceed to fill the remaining units in the same manner.
 - 6.3 Fill the sample bottle in the same manner. Bottle must be filled to within 1/4 inch of the top.
 - 6.4 Close the vacuum valve on the side loader. Shut off the side loader heater.
 - 6.5 Close the vacuum valve on the main chamber.
 - 6.6 Shut off the refrigerator compressor and the vacuum pump.

- 6.7 Backfill the main chamber with dry gaseous nitrogen by connecting the gas bottle to the backfill port, setting the regulator to 15-30 psig, and opening the backfill valve. The nitrogen shall be per MIL-P-27401B, Type I, or per BB-N411b, Type I, Class I, Grade A or B.
- 6.8 When the pressure in the main chamber reaches one atmosphere, shut off the nitrogen and open the cover.
- 6.9 Immediately replace the mylar seal and the cap on the sample bottle and remove same from the chamber. Fill in the level and forward sample to the Cleaning Lab for analysis.
- 6.10 Immediately seal the capacitors.
- 6.11 The analytical tests on the fluid sample shall be as follows.

Test

Particle Count
Water Content (ppm)
Volume Resistivity (ohm-cm)
Breakdown Strength (V/mil)

- 6.12 Open the bleed valve on the side loader when the inner can fluid temperature has decayed to 100°F.
- 6.13 Verify that all electrical devices and all pressurizing gases are shut off and secure.

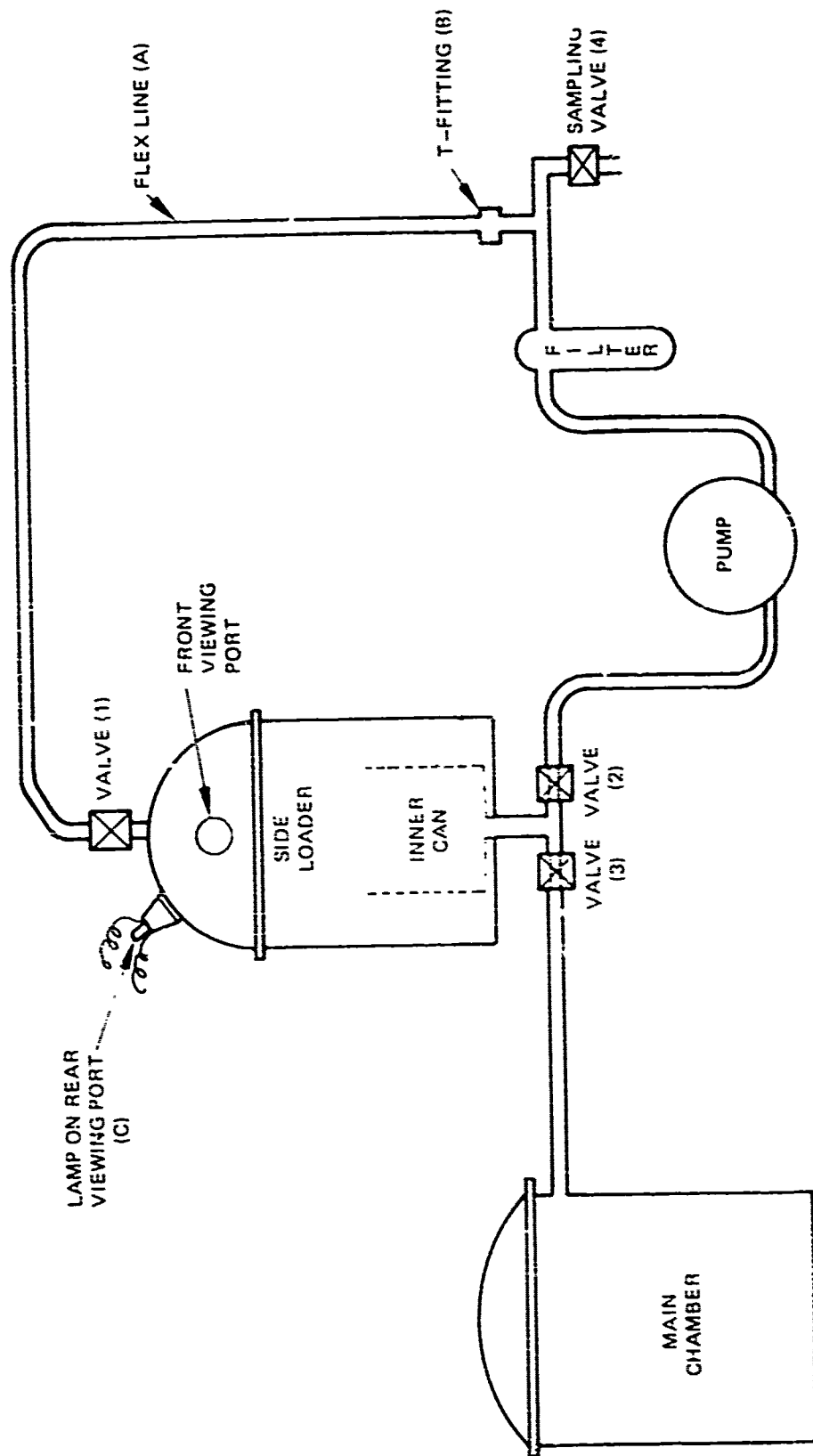


Figure 115. SCHEMATIC
OIL IMPREGINATION SYSTEM